CLIMAAX
climate ready regions

Deliverable Phase 2 – Climate risk assessment

Climate Resilient crETE (CRETE)

Greece, Region of Crete

Version Final | January 2026

HORIZON-MISS-2021-CLIMA-02-01 - Development of climate change risk assessments in European regions and communities based on a transparent and harmonised Climate Risk Assessment approach

Funded by the European Union

This project has received funding from the European Union's Horizon Europe research and innovation programme under grant agreement No 101093864. Views and opinions expressed are however those of the author(s) only and do not necessarily reflect those of the European Union or the European Climate, Infrastructure and Environment Executive Agency (CINEA). Neither the European Union nor the granting authority can be held responsible for them.

Document Information

Deliverable Title	Phase 2 – Climate risk assessment
Brief Description	
Project name	Climate Resilient crETE (CRETE)
Country	Greece
Region/Municipality	Region of Crete
Leading Institution	Technical University of Crete
Author(s)	Marinos Kritsotakis (Region of Crete) Maria Stratigaki (Region of Crete) Eleni Kargaki (Region of Crete) Evgenia Stylianou (Region of Crete) Mikaela Papa (Technical University of Crete) Aristeidis Koutroulis (Technical University of Crete)
Deliverable submission date	08/01/2026
Final version delivery date	08/01/2026
Nature of the Deliverable	R – Report
Dissemination Level	PU - Public

Version	Date	Change editors	Changes
1.0	4/11/2025	Technical University of Crete	Draft Deliverable sent to Region of Crete
2.0	17/11/2025	Technical University of Crete	Flood risk assessment added
	1/12/2025	Technical University of Crete	Final accompanying detailed **flood** risk assessment report sent to Region of Crete
	25/12/2025	Technical University of Crete	Final accompanying detailed **drought** risk assessment report sent to Region of Crete
3.0	26/12/2025	Region of Crete	Updated Scoping and Risk exploration
4.0	26/12/2025	Technical University of Crete	Drought risk assessment added; Key risk assessment findings added
5.0	29/12/2025	Region of Crete	Final Scoping and Risk exploration
Final	07/01/2026	Region of Crete	Final version to be submitted

Table of Contents

Document Information 2
Table of Contents 3
List of figures 4
List of tables 5
Abbreviations and acronyms 6
2. Executive summary 7
1 Introduction 9
1.1 Background 9
1.2 Main objectives of the project 10
1.3 Project team 10
1.4 Outline of the document's structure 11
2 Climate risk assessment – phase 2 12
2.1 Scoping 12
2.1.1 Objectives 12
2.1.2 Context 12
2.1.3 Participation and risk ownership 14
2.1.4 Application of principles 15
2.1.5 Stakeholder engagement 16
2.2 Risk Exploration 19
2.2.2 Screen risks (selection of main hazards) 19
2.2.3 Choose Scenario 22
2.3 Regionalized Risk Analysis 23
2.3.1 Drought - fine-tuning to local context 23
2.3.2 Flood - finetuning to local context 30
2.4 Key Risk Assessment Findings 39
2.4.1 Mode of engagement for participation 39
2.4.2 Gather output from Risk Analysis step 40
2.4.3 Assess Severity 40
2.4.4 Assess Urgency 41
2.4.5 Understand Resilience Capacity 41
2.4.6 Decide on Risk Priority 42
2.5 Monitoring and Evaluation 43
2.6 Work plan Phase 3 44
3 Conclusions Phase 2- Climate risk assessment 45

4 Progress evaluation and contribution to future phases 47
4.1 Key Performance Indicators and Milestones 47
5 Supporting documentation 48
6 References 49

List of figures

Figure 1-1: Olive cultivation zones across Crete Island (Grillakis et al., 2022) 9
Figure 2-1: Trends in (a) average annual temperature (°C), (b) average annual precipitation (mm), and (c) Standardized Precipitation Index (SPI) for Crete indicating periods of drought (negative SPI) and wetness (positive SPI), from 1950 to 2025. 20
Figure 2-2: Relative drought hazard index at sub-basin (basin–municipality unit) scale for the baseline period (1981–2010) (top) and change in hazard category for three future periods (represented by 2030, 2055 and 2085) under SSP1-2.6, SSP3-7.0 and SSP5-8.5. 24
Figure 2-3: Multi-model mean olive yield loss (%) from precipitation deficit in Crete for four future periods (rows) and three emission scenarios (columns: RCP2.6, RCP4.5, RCP8.5). 25
Figure 2-4: Spatial distribution of average olive oil production trends in Greece for the period 2011–2022 (tons year^{-1}). Asterisks mark statistically significant trends at a level of p-value lower than 0.05. 26
Figure 2-5: Relative drought risk index aggregated at municipality level. The top panel presents baseline (2020) risk values; the lower panels show changes relative to baseline for 2011–2040, 2041–2070 and 2071–2100 under SSP1-2.6, SSP3-7.0 and SSP5-8.5. 28
Figure 2-6: Multi-model mean annual revenue loss from absence of irrigation for olive production in Crete (kEUR per grid cell) for four future periods (rows: 2026–2045, 2046–2065, 2066–2085, 2086–2100) and three emission scenarios (columns: RCP2.6, RCP4.5, RCP8.5). Colors show mean revenue loss; stippling and cross-hatching indicate the 2020 share of irrigated cropland from GAEZ v5, highlighting where high potential losses coincide with low or high irrigation coverage. 28
Figure 2-7: Projected change [%] in olive oil yield for Crete between 2005–2085 under RCP4.5 and RCP8.5 29
Figure 2-8: Location of the ten focus areas (1–10) used in the second-phase flood risk assessment in Crete. 31
Figure 2-9: Example of refinement from Phase-1 (left) to Phase-2 (right) river-flood hazard mapping in one of the focus areas (Giofiros). Phase-1 used coarse flood hazard maps (JRC), while Phase-2 applies 2 m-resolution depth grids from the EL13 Flood Risk Management Plan, resolving detailed inundation patterns around individual buildings. 31
Figure 2-10: Building-level flood hazard-exposure in Heraklion for the 50-year (RP50, top) and 500-year (RP500, bottom) design floods. Blue shading shows 2 m–resolution flood depth from the EL13 Flood Risk Management Plan overlaid with Microsoft Global Building Footprints, which provide almost complete coverage of the local building stock. This Phase-2 set-up represents a major improvement over Phase-1, which relied on coarser JRC global flood hazard maps (~100 m) and the incomplete OpenStreetMap building layer, and therefore allows much more detailed and reliable estimates of exposed buildings and associated. 32
Figure 2-11: Spatial distribution of the multi-model mean 24-hour precipitation return level for a 50-year event (left) and its relative change with respect to the 1976–2005 baseline (right) under the RCP8.5 scenario for 2011–2040, 2041–2070, and 2071–2100. 33

Figure 2-12 Location of the Giofiros (right) and Keritis (left) basins in Crete and the corresponding E-HYPEcatch units (shaded) used in the CLIMAAX river discharge workflow. 34
Figure 2-13 Spatial distribution of land-use based flood damage for RP100 in the ten areas of interest. 35
Figure 2-14 Estimated mean direct damage to individual buildings in Heraklion for RP50 and RP100. Colored polygons show the spatial distribution of mean damage per building (in 10^6 €), overlaid on the corresponding flood-depth maps; zoomed panels highlight critical hotspots along the main urban torrents. 36
Figure 2-15 Top panels: relative change (%) in 24-hour precipitation associated with the medium-impact rainfall threshold of 200 mm/day over Crete, for three future periods (2011–2040, 2041–2070, 2071–2100) under RCP4.5 (left column) and RCP8.5 (right column), expressed as a percentage shift with respect to the 1976–2005 baseline. Bottom panels: equivalent return period (years) of exceeding the 200 mm/day severe-impact rainfall threshold over Crete, for the same periods and scenarios 38
Figure 2-16 Relative change (%) in 10-year and 50-year extreme river discharges for Giofiros (left) and Keritis (right) for the future periods 2011–2040, 2041–2070 and 2071–2100 under RCP4.5 and RCP8.5, compared to the historical baseline; dots show individual GCM–RCM combinations and large symbols the ensemble medians. 39
Figure 2-17: Key Risk Assessment dashboard for Crete, showing stakeholder-derived scores of current (C) and future (F) severity, urgency of action, and resilience/climate-risk-management capacity for river flooding and drought. 40
Figure 2-18: Phase-3 work plan for Climate Resilient crETE – CRETE. 44

List of tables

Table 2-1 Data overview of Drought workflows 23
Table 2-2: Relative changes in specific climatic indices on yearly basis compared to the historical period for Crete. 26
Table 2-3 Data overview Flood workflows 30
Table 2-4: Total mean and maximum damage to buildings per region, of a 50, 100, and 1000 return period flood event, based on current climatic conditions. 36
Table 2-5: Total estimated exposed and displaced number of inhabitants per region, of a 50, 100, and 1000 return period flood event, based on current climatic conditions. 37
Table 2-6: Median and standard deviations from stakeholder scoring of severity, urgency and capacity for river flooding and drought. 43
Table 4-1: Overview key performance indicators 47
Table 4-2: Overview milestones 48

Abbreviations and acronyms

Abbreviation / acronym	Description
APSFR	Area of Potential Significant Flood Risk
CHELSA	Climatologies at High resolution for the Earth's Land Surface Areas (high-resolution climate dataset)
CLIMAAX	Climate Change Risk Assessment project under Horizon Europe (framework used in this study)
CORDEX	Coordinated Regional Climate Downscaling Experiment (regional climate model ensemble)
CRA	Climate Risk Assessment
CRETE-CLIMAAX	"Climate Resilient crETE" CLIMAAX pilot for the Region of Crete
DEM	Digital Elevation Model
EDO	European Drought Observatory
E-HYPE	European configuration of the HYPE hydrological model (E-HYPEcatch)
E-OBS	Gridded European daily observational climate dataset
FRMP	Flood Risk Management Plan (2nd Revision, Water District EL13 – Crete)
GAEZ	Global Agro-Ecological Zones database
GCAM	Global Change Analysis Model (global socio-economic and land-use model)
GCM	Global Climate Model
GHS-POP	Global Human Settlement – Population grid dataset
ISIMIP	Inter-Sectoral Impact Model Intercomparison Project (global bias-corrected climate data)
LLRO	Local Land Reclamation Organizations
LUISA	Land-Use based Integrated Sustainability Assessment model (EU land-use projections)
RAAP	Regional Adaptation Action Plan of Crete
RCM	Regional Climate Model
RCP	Representative Concentration Pathway (greenhouse-gas concentration scenario, e.g. RCP4.5, RCP8.5)
RP	Return period of an extreme event (e.g. RP50, RP100)
SPI	Standardized Precipitation Index
SSP	Shared Socioeconomic Pathway (e.g. SSP1-2.6, SSP3-7.0, SSP5-8.5)
TUC	Technical University of Crete
WASP	Weighted Anomaly Standardized Precipitation index

2. Executive summary

This deliverable presents the second-phase climate risk assessment for the Region of Crete within the CLIMAAX project. It refines and regionalizes the Phase-1 analysis of drought and river flooding, making systematic use of the CLIMAAX workflows, local datasets and targeted stakeholder engagement. Together with the detailed technical reports on drought and flood risk (Deliverables 2a and 2b) and the Phase-1 assessment, it provides a coherent evidence base to support the forthcoming revision of the Regional Adaptation Action Plan (RAAP), the update of the Action Plan for Combating Drought and Water Scarcity, and the design of the Regional Climate Change Observatory.

The report applies three drought-related workflows and four flood-related workflows. Relative drought risk is assessed for 244 basin-municipality units using composite indicators of climatic hazard, socio-economic exposure and vulnerability. Agricultural drought is analyzed through an olive-specific workflow that links climate projections to irrigation deficits and revenue loss from rainfed olive groves. An independent empirical analysis for the yield-climate impacts provides an external check on the CLIMAAX agricultural workflow and offers a longer perspective on yield-climate relationships.

For flooding, high-resolution (2m) inundation maps from the River Basin Management Plans are combined with LUISA land-cover data to derive land-use based flood damage for ten flood-prone areas. A second workflow overlays the same inundation maps with the new Microsoft Global Building Footprints to estimate direct damage and population exposure at building level, greatly improving on Phase-1 results that relied on coarser JRC flood maps and incomplete OpenStreetMap building data. In the absence of flood hazard projections, two additional workflows quantify future changes in extreme precipitation and extreme river discharge using EURO-CORDEX climate projections and hydrological modelling for representative basins.

Key findings indicate that drought hazard is already highest in central and eastern Crete and is projected to intensify and spread under higher end scenarios, particularly after mid-century. When combined with exposure (cropland, population, tourism) and vulnerability (GDP, groundwater access, irrigated area, planned infrastructure), this yields high relative drought risk for several municipalities in Heraklion, Rethymno and parts of Chania and Lasithi, with some areas showing risk category increases. The agricultural workflow shows that, under the assumption of unmet irrigation demand, potential revenue losses from olive production can reach several hundred €/ha in central and eastern Crete, with hotspots where losses approach 10,000 €/ha. The empirical yield-climate analysis confirms that precipitation deficits during key phenological stages are strongly associated with reduced yields, supporting the direction of the CLIMAAX impact estimates even if magnitudes remain uncertain.

For floods, the refined analysis confirms very high concentration of damage potential in a limited number of hotspots. Heraklion, Ierapetra and parts of Messara and northern Chania combine dense building stock, critical infrastructure and substantial inundation depths. For Heraklion alone, mean direct building damage is estimated at around €265 million for a 50-year event, €314 million for a 100-year event and nearly €590 million for a 1000-year event, with tens of thousands of residents exposed and several thousand potentially displaced across the ten study areas. Extreme-precipitation projections show increasing intensity and/or decreasing return periods for 24-hour heavy rainfall, particularly under RCP8.5 after mid-century, while extreme-discharge analyses

suggest higher peaks in some catchments and altered seasonality, reinforcing concern about future flood pressures.

Stakeholder workshops and an online Key Risk Assessment survey, involving 33 representatives from regional directorates and agencies, translated these quantitative results into qualitative risk judgments. River flooding and drought were both assigned a High risk priority. Flooding was rated as having substantial severity now and, in the future, with “more action needed” on urgency and medium resilience capacity. Drought was rated moderate today from an impact perspective but substantial in the future, with higher urgency (“immediate action needed”) reflecting recent multi-year droughts, expected growth in water demand and the systemic nature of water scarcity across sectors.

The assessment also highlights important limitations: coarse and globally derived land-use and socio-economic scenarios that do not fully reflect local development pathways, limited crop-yield statistics at sub-regional level, the absence of future high-resolution flood-inundation maps, and incomplete information on building use and social vulnerability. The report identifies clear directions for improvement, including the development of locally grounded land-use and water-demand scenarios, exploitation of new high-resolution climate datasets (such as CLIMADAT-GRID) and systematic use of open monitoring products (e.g. European Drought Observatory) in the planned Regional Climate Change Observatory.

In conclusion, Phase-2 confirms that river flooding and drought are both high-priority risks for Crete, with impacts concentrated in identifiable hotspots but with system-wide implications for water security, agriculture, tourism and urban development. At the same time, the phase demonstrates that combining the CLIMAAX framework with local data and models can substantially increase the credibility and usefulness of regional risk assessments. Phase-3 will build on these results to explore adaptation capacity, co-design drought related measures with stakeholders, and outline a feasible pathway for a regional climate-risk monitoring system that can directly support the RAAP update and operational decision-making in Crete.

1 Introduction

1.1 Background

Crete, the largest island in Greece, lies at the climatic transition between the eastern Mediterranean and North Africa and is increasingly exposed to climate-related stresses. The island has a typical Mediterranean regime, with warm–hot dry summers and mild, wet winters, but long-term observations show a steady rise in mean temperature, a shortening of the wet season and more frequent meteorological droughts (Koutroulis et al., 2011; Tramblay et al., 2020). Pronounced interannual rainfall variability, together with steep topography and shallow soils, favors both rapid onset drought and intense runoff responses. As a result, Crete is simultaneously vulnerable to multi-year water scarcity and to damaging flash floods, especially along urbanized and low-lying coastal zones (Diakakis et al., 2012; Koutroulis et al., 2010a).

The island's economy is dominated by climate-sensitive sectors. Agriculture remains a core pillar, with olive cultivation covering most lowland and mid-altitude zones (Figure 1-1) and providing income for a large share of rural households (Grillakis et al., 2022). Olive production, horticulture and viticulture depend heavily on increasingly stressed surface and groundwater resources and are directly affected by heat and water-deficit extremes. Tourism, concentrated in the dry summer period, further amplifies seasonal water demand, often in the same coastal areas where water availability is most constrained. Recent hydrological years have included consecutive droughts, depleted reservoirs and local supply restrictions, while past flood events have caused substantial damage to infrastructure, housing, agricultural land and transport networks (Koutroulis et al., 2010b; Kreibich et al., 2022; Perdiou et al., 2017; Tichavský et al., 2020). Together, these trends underline that drought, water scarcity and flash flooding are central climate risks for Crete.

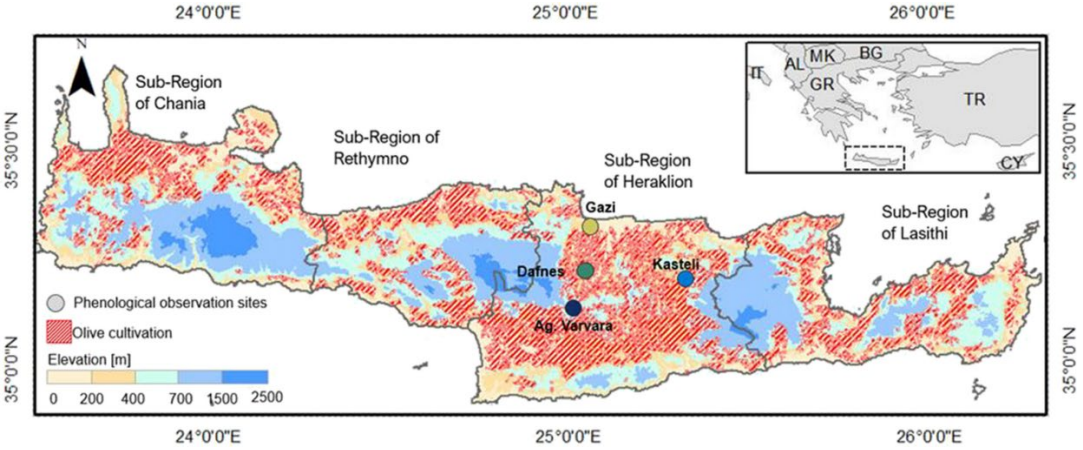

Figure 1-1: Olive cultivation zones across Crete Island (Grillakis et al., 2022)

Within this context, the CLIMAAX project provides the Region of Crete and the Technical University of Crete with a common, evidence-based framework for assessing climate risk. Phase 1 established initial drought and flood risk baselines; Phase 2 refines these assessments with higher-resolution data, olive-specific impact analysis and stakeholder-based risk prioritization. The results are intended to directly support upcoming policy processes: the update of the Regional Plan for Adaptation to Climate Change (RAAP), the revision and extension of the Action Plan for Combating Drought and Water Scarcity, and the design of the new Regional Climate Change Observatory, which will act as a long-term hub for monitoring key climate indicators and risks. Phase 3 of CLIMAAX-CRETE will build on the current assessment to explore adaptation capacity, co-develop monitoring

pathways with stakeholders and further embed climate-risk information in sectoral and regional planning.

1.2 Main objectives of the project

Phase-2 of CLIMAAX-CRETE aims to move from a first, largely exploratory multi-risk screening (Phase-1) to a regionalized, decision-ready assessment for droughts and river floods, the two hazards identified as highest priority for Crete. The core objective is to refine the CLIMAAX workflows using high-resolution local datasets and sector-specific information, so that risk estimates better reflect the island's hydro-climatic conditions, land-use patterns and socio-economic structure. For drought, Phase-2 develops a Crete-tailored relative drought index, an agricultural drought workflow focused on olive production, and an independent climate-yield analysis for olives. For floods, it upgrades the analysis from global hazard layers to detailed 2-m inundation maps, building-level exposure and updated extreme-precipitation and discharge indicators. These advances are designed to produce risk metrics that can directly inform water-resources management, agricultural planning, spatial planning and civil protection.

A second key objective is to embed these refined risk insights in regional policy processes. Phase-2 explicitly supports the upcoming update of the Regional Adaptation Action Plan (RAAP) and the extension of the Action Plan for Combating Drought and Water Scarcity, and feeds into the emerging initiative to establish a Regional Climate Change Observatory. To this end, the project has organized a series of structured engagements as consultation meetings, stakeholder workshops, a joint event with the Pathways2Resilience Path4PDE project, and a dedicated workshop with an online Key Risk Assessment survey to ensure that technical advances are co-interpreted with regional services and that Phase-2 results provide a shared evidence base for Phase 3, where adaptation options, monitoring pathways and concrete contributions to sectoral and regional plans will be developed.

The CLIMAAX risk assessment workflows have been essential for structuring this second-phase work. They provided a common, transparent framework for defining hazards, exposure and vulnerability, selecting scenarios and documenting assumptions, so that the updated analyses are tailored to Crete and remain comparable with other CLIMAAX. At the same time, Phase-2 has demonstrated the value of enriching the standard workflows with local data and models: high-resolution inundation maps from the River Basin Management Plans, detailed building footprints, local river-discharge assessment, olive production and phenology data, and regional socio-economic information. The combination of a shared European methodology with locally specific datasets and modelling tools greatly improves the realism and credibility of the risk estimates, makes the results more directly usable by regional services, and creates a solid technical foundation for the adaptation planning and monitoring activities foreseen in Phase 3.

1.3 Project team

The CRETE CLIMAAX project is a collaborative effort between the Region of Crete and the Technical University of Crete (TUC), combining regional governance expertise with climate risk assessment. The Region of Crete, structured into six General Directorates and 37 Directorates, is responsible for the economic, social, and cultural development of the island. TUC provides external services, bringing extensive experience in the areas of climate risk assessment, hydrology, and adaptation planning.

Partner	Name	Role in CLIMAAX-CRETE	Main expertise / responsibilities
Region of Crete	Dr. Marinos Kritsotakis	Project Lead, Director-General of Sustainable Development	Strategic oversight, alignment with regional policies and RAAP, coordination across directorates (Water, Civil Protection, Environment, Infrastructure).
	Eleni Kargaki	Deputy Head Directorate of Environment & Spatial Planning	Climate and energy policy, integration of CRA results into regional planning and spatial / land-use policies.
	Evgenia Stylianou	Coordinator, Regional Climate Change Adaptation Plan Team	Coordination of adaptation planning, liaison with sectoral directorates, use of CLIMAAX outputs in RAAP and drought–water scarcity action plan.
	Dr. Maria Stratigaki	Project Management Support	Day-to-day project management, scheduling and reporting, support to stakeholder engagement and link with the emerging Regional Climate Change Observatory.
Technical University of Crete (TUC)	Assoc. Prof. Aristeidis Koutroulis	Scientific Lead	Overall design of drought and flood risk analyses, supervision of workflows, synthesis of results and scientific quality control.
	Mikaela Papa	Climate Risk Analyst	Implementation of CLIMAAX workflows, climate hazard modelling, development of drought and flood indicators and maps.
	Eirini Koutrogiannaki	Researcher	Support to drought risk assessment, contribution to stakeholder material and reporting.
	Evgenia Galanopoulou	Researcher	Support to drought risk assessment and Phase-3 planning.

1.4 Outline of the document's structure

This document is structured to follow the CLIMAAX framework and to clearly distinguish between Phase-1 and Phase-2 work.

- Section 1 introduces the regional context for Crete, summarizes the objectives of the Phase-2 assessment and explains how it builds on and refines the first-phase deliverable.
- Section 2 presents the core climate risk assessment. It first describes the risk exploration and scenario choices, then details the regionalized drought and flood workflows (hazard, exposure, vulnerability and risk), including key maps and indicators. It concludes with the Key Risk Assessment, where stakeholders evaluate severity, urgency and resilience capacity using the CLIMAAX dashboard.
- Section 3 summarizes the main conclusions of Phase-2 and highlights implications for adaptation planning in Crete.
- Section 4 reports on progress, key performance indicators and milestones, and explains how this phase contributes to Phase-3 activities.
- Section 5 lists the supporting technical reports, communication outputs and workshop material that complement the main text.

2 Climate risk assessment – phase 2

2.1 Scoping

2.1.1 Objectives

The Climate Risk Assessment (CRA) for Crete is intended to assess and quantify climate-related hazards by exploiting the CLIMAAX framework. In this region, the primary concerns are droughts and floods; therefore, the present assessment is being used to identify vulnerabilities, exposure levels, and potential impacts on critical sectors. These concerns pertain to diverse domains, including agriculture, water resources, infrastructure, and urban settlements. The CRA's objective is thus to support evidence-based decision-making and policy development to enhance climate resilience in Crete by leveraging scientific methodologies and high-resolution data.

A comprehensive evaluation of vulnerabilities to climate hazards and their ramifications for pivotal sectors has previously been formulated within the framework of the present Regional Adaptation Action Plan (RAAP) of Crete. This plan constitutes a component of the overarching framework of the National Strategy for Adaptation to Climate Change under the National Climate Law. However, a comprehensive climate risk analysis has not been incorporated into RAAP, despite its urgent necessity for the region and given the climatic projections for the future. In order to address this limitation, a more systematic approach for the identification and prioritization of high-risk areas and sectors is required. The implementation of the CLIMAAX CRA methodology will facilitate this objective, as it will enable a quantitative evaluation of climate risks. This is of particular significance, given that the RAAP serves as a strategic guide for the Region of Crete, supporting the preparation and maturity of climate adaptation projects, and ensuring their successful integration into funding opportunities in the new programming period.

The findings of the project will be used to address a range of issues and topics by generating climate risk assessment outputs. Of particular significance is the role that this project will play in informing the revision process of the second cycle of the Regional Climate Adaptation Plan of Crete, scheduled for 2026+, by providing data and analysis. In view of this, the adaptation planning will be aligned with the latest climate projections, sectoral risks, and policy priorities.

The outputs of the CRA will also play a vital role in the establishment of a novel Regional Climate Adaptation Support Mechanism for Crete. This mechanism is envisaged not only as a Climate Change Observatory for the island, but more as a comprehensive structure that extends beyond climate monitoring and evaluation. The primary objective of this initiative is to assess the risks associated with climate change in Crete's primary sectors and regions. Furthermore, the provision of scientific and technical assistance for the development and implementation of policy constitutes a primary function of the support mechanism. The project will further facilitate communication and dissemination of the results of related climate change projects; it will function as an information hub for professionals and raise awareness of climate-related issues among citizens.

It is anticipated that these contributions will enhance climate adaptation governance on the island of Crete, ensuring that risk assessments translate into actionable strategies and informed decision-making at both regional and local levels.

2.1.2 Context

Climate hazards, impacts, and risks have been evaluated to date through the Regional Adaptation Action Plan for Climate Change (RAAP) of the Region of Crete. This plan systematically identifies

key climate threats and vulnerabilities and outlines sector-specific adaptation measures pertaining to areas such as agriculture, tourism, water resources, infrastructure, and health. The RAAP of Crete serves as a critical planning instrument for the integration of climate adaptation into local policies and initiatives, and acts as a strategic foundation for safeguarding the natural environment and enhancing the resilience of infrastructure within a climate-sensitive region. Furthermore, it is also important to note that this plan aligns with the National Adaptation Strategy and functions as a principal reference for planning, awareness-raising, and decision-making at the regional level.

The RAAP provides a comprehensive assessment of the current situation, including vulnerability analysis, selection and prioritization of adaptation measures, timelines, and related considerations across 11 key areas. The evaluated sectors encompass agricultural and livestock production, forests and reforested regions, biodiversity and ecosystems, fisheries and aquaculture, water resource availability, river and flood events, coastal zones, tourism, energy demand and infrastructure, transportation infrastructure (including road networks, ports, and airports), health, the built environment, and cultural heritage.

The island of Crete is currently experiencing a series of escalating climate-related challenges, including prolonged periods of drought, a consequence of increased climate variability. The increasing frequency of extreme weather events — such as flash floods, heatwaves, and water scarcity — highlights the imperative for the development of enhanced climate risk management strategies. While the current RAAP establishes a foundational framework for adaptation, the absence of comprehensive quantitative risk assessments hampers the effective prioritization of interventions and the efficient allocation of resources. This concern remains closely aligned with both national and European adaptation objectives.

The Region of Crete's climate resilience strategy must be aligned with established plans at the regional, national, and European levels. These include the Crete 2030 Development Plan, the Flood Risk Management Plan for Crete, the Action Plan for Combating Drought and Water Scarcity in Crete, the EU Adaptation Strategy, and the National Climate Law. The overarching objective of these frameworks is to facilitate systematic adaptation planning at the regional level, thereby ensuring coherence with European climate resilience policies. Additionally, they provide guidance on major infrastructure investments that underpin sustainable development, as well as informed flood mitigation and emergency response actions.

Accordingly, the principal governance mechanisms comprise (i) the RAAP, which details adaptation priorities across critical sectors; (ii) Water Resource Management and Flood Management Plans, aimed at mitigating drought and flood risks and promoting sustainable water use; and (iii) national and EU funding programmes that facilitate infrastructure development, resilience initiatives, and research projects.

The anticipated impacts of climate change in Crete include:

- Sea level rise, which may result in seawater intrusion into coastal aquifers, degradation of water quality, challenges to coastal infrastructure, and increased erosion of sandy beaches.
- Reduced precipitation, which could lead to decreased availability of water resources, potential infrastructure failures, drought conditions, and advancing desertification.
- Alterations in precipitation and evaporation patterns, potentially increasing agricultural water demand, elevating the risk of flooding in coastal areas, threatening the integrity of water wells, and contributing to land degradation.

- Rising temperatures and more frequent heatwaves, presenting health risks to residents and vulnerable populations, as well as posing threats to summer tourism.

These effects tend to disproportionately impact lower-income social groups and other vulnerable or susceptible populations.

Effective management of climate risks requires the implementation of targeted adaptation measures. These include initiatives to enhance water allocation, optimize irrigation practices, and minimize water loss, as well as flood risk mitigation through improved drainage infrastructure and nature-based solutions. In the context of agriculture, adaptation strategies may involve the relocation of crop cultivation to higher elevations, the adaptation of drought-resistant crop varieties, the implementation of soil conservation methodologies, and, in the long term, the transition to indoor cultivation systems utilizing advanced technology for the creation of controlled environments. Additional actions comprise the expansion of afforestation, the permeabilization of urban surfaces, and techniques for the reduction of urban heat, such as the increase of green spaces and the design of buildings that are resilient to heat.

2.1.3 Participation and risk ownership

The organizational structure of the Region of Crete comprises four Regional Units: Chania, Rethymnon, Heraklion, and Lasithi, each managing its respective local services. The framework incorporates specialized Directorates and Departments dedicated to Health Services, Administrative Services, Agriculture and Rural Development, as well as Culture, Tourism, and Infrastructure.

To optimize the value of the diverse knowledge and expertise present, the stakeholder engagement profile incorporated a broad spectrum of entities, including governmental bodies, research institutions, private sector organizations, and community groups. The mapping process was guided by each stakeholder's relevance to climate risk assessment, management, and adaptation in Crete, resulting in multi-level participation and involvement of the following:

- The Region of Crete plays an instrumental role in the formulation of regional strategies, the establishment of priorities, the coordination of adaptation plans, and the incorporation of the effects of climate change into its decision-making processes. The entities involved are the Directorate of Technical Works, the Directorate of Environment & Spatial Planning, and the Department of Civil Protection.
- At the national level, the Greek State is responsible for setting regulatory frameworks, allocating resources, and overseeing large-scale prevention measures such as wildfire management conducted in collaboration with local services. These responsibilities are overseen by the Ministry of Civil Protection, the Ministry of Environment and Energy, and the Ministry of Rural Development.
- The Decentralized Administration of Crete.
- Local authorities, such as the Municipalities (including Technical and Civil Protection Services), are especially relevant in areas susceptible to flooding and drought. The Municipal Water and Sewerage Companies are also important in this regard, as they oversee water resource management and implement flood mitigation strategies. The Crete Development Organization is also involved in supporting regional economic planning and infrastructure investment initiatives.
- Research and academic institutions make significant contributions through targeted risk assessments, the provision of data and technical expertise, and policy advice. The Hellenic

Centre for Marine Research (HCMR) offers hydrological and flood modelling expertise, while the Foundation for Research and Technology – Hellas (FORTH) specializes in assessing flood risks within coastal regions.

- Local stakeholders and citizens engage in a collaborative process by identifying specific needs, contributing grassroots insights, and executing preventive measures. These activities are supported by EU directives and research initiatives, with a focus on addressing key risk areas.

The allocation of risk ownership among the national, regional, and local levels of governance represents a fundamental component of effective climate risk management, with each level assuming responsibility for distinct elements of this process. Responsibility is collectively exercised: the Region of Crete offers strategic direction on regional adaptation, while national frameworks provide overarching support and local entities engage directly with specific risks. Each organization operates within the parameters of its own distinct regulatory framework, which clearly defines its mandate regarding climate risk mitigation, preparedness, and response. For example, national ministries are responsible for developing the legal and regulatory frameworks governing climate adaptation. The Region of Crete manages the implementation of adaptation strategies on the island, the oversight of major infrastructure projects, and the provision of coordination and support for municipal risk reduction initiatives. Similarly, municipalities are charged with the management of local risk mitigation, emergency response, and water resource administration.

The primary vulnerable groups exposed to key climate risks and threats span various sectors, including:

- The agricultural sector, confronted with a substantial water shortage and subsequent detrimental effect on crops and livestock. Agricultural communities are especially vulnerable to water scarcity and drought conditions. Notable examples of impacted groups include associations representing olive producers, winemakers, farmers, livestock breeders, and beekeepers.
- The tourism and business sectors, where hotel associations and technical and commercial chambers are increasingly affected by the growing frequency and intensity of heatwaves.

Elderly populations and individuals residing in densely constructed urban environments are particularly vulnerable to the impacts of severe heatwaves, especially in areas with limited vegetation and inadequate green infrastructure. Urban and coastal communities face heightened risks due to rising sea levels and an increased frequency of extreme weather events such as floods and wildfires. These communities are also at increasing risk from flash flooding and soil erosion.

2.1.4 Application of principles

Our analysis was guided by the application of several fundamental principles, aimed at developing and formulating a climate action planning framework defined by justice, equity, and inclusivity. The effective implementation of these principles necessitates adherence to certain specific requirements.

It is imperative to advocate for the utilization of structured methodologies to ensure the engagement of diverse groups throughout the project's lifecycle. This approach targets active involvement from citizens, stakeholders, local officials and the community at key project points, such as decision-making, planning and problem-solving. This tactic approach ensures that outcomes reflect real needs, builds trust and fosters shared ownership. For the purposes of this project, a range of

activities were used, including surveys, workshops and meetings that enabled open dialogue among participants. The objective of these activities was to gather input and co-create solutions for public policy, community projects or organizational strategies.

In order to achieve climate justice and foster inclusivity and participation, it is essential to take into account the various socio-economic parameters and status variations. In pursuit of this objective, we are dedicated to the organization of open events and visits to the local community, extending beyond the confines of the urban fabric, during the third phase of the CLIMAAX project. We are committed to inclusivity, seeking to ensure that representatives of vulnerable and marginalized social groups are included to reflect their perspectives, realities and needs.

In terms of transparency, the objective was to facilitate data sharing and open reporting. Furthermore, presentations, results and research data were always made available to interested parties. In particular, the outputs produced in the first phase – including the main climate risk assessment deliverables, the technical reports, and the communication and dissemination materials – were all uploaded to the Zenodo repository for open access. Analogous measures and actions will be implemented for the subsequent second phase and deliverable D2.

In accordance with the precautionary principle, the United Nations Framework Convention on Climate Change (UNFCCC) acknowledges that parties should "take precautionary measures to anticipate, prevent or minimize the causes of climate change and mitigate its adverse effects. Where there are threats of serious or irreversible damage, lack of full scientific certainty should not be used as a reason for postponing such measures...". In pursuit of this principle, it is vital that mitigation and adaptation measures be implemented prior to the availability of full information and the resolution of uncertainties regarding the scope and timing of climate change.

Consequently, we do not permit uncertainty regarding potential damage to serve as a justification for postponing action. Conversely, we are committed to furthering our dialogue, by organizing events, meetings and workshops, and promoting proactive and reactive responses to future climatic changes. In order to serve this purpose, even in the absence of sufficiently certain scientific evaluation of potential damage, measures are taken and the updating of the RAAP of Crete as well as the establishment of the observatory are prioritized. The decision-making process and the management of risk with adaptational responses, which limit the time lag between action and reaction, are therefore strongly supported, despite the uncertainty present in both natural and socioeconomic systems.

2.1.5 Stakeholder engagement

In accordance with the initial vision of the CLIMAAX project to ensure robust stakeholder involvement throughout its duration, stakeholder engagement was further enhanced during the project's second phase.

- A joint workshop was convened on ***22 October 2025,*** in person, between the Region of Crete and the Region of Western Greece, at the Region of Crete headquarters in Heraklion, with the participation of 27 individuals. The event focused on climate resilience actions and received recognition on the CLIMAAX website's "Region Updates" dashboard, featured under the heading "Greek Regions Collaborate to Strengthen Climate Resilience."
  In the course of this technical session, our region provided a progress update on the CLIMAAX-crETE project, with specific reference to the challenges of drought and flood risk management.

The region of Western Greece was also found to present important areas of vulnerability and funding action tools, supported by Path4PDE – Pathways2Resilience Horizon.
The event served as a platform for the two regions to present their respective updates and major achievements, culminating in the development of a unified roadmap for resilient, climate-ready territories. The results of these discussions will guide, in the forthcoming future, revisions to regional strategies and investment pipelines. Additionally, the agenda placed significant emphasis on the alignment of adaptation measures and the enhancement of inter-regional collaboration, alongside fostering of cross-program synergies.
Participants included regional leaders, governors, members, professors, and scientists from academic and research institutions, all convened to engage in a comprehensive multi-risk assessment, to foster active participation, raise awareness, and gather expert input. By conducting coordinated assessments and facilitating knowledge exchange, regional authorities are collaborating to harmonize strategies and strengthen preparedness for climate-related impacts.
Various regional directorates and administrative units encompassed a range of domains, including (i) Sustainable Development, Energy, Spatial Planning and Environment, (ii) Climate Change and Sustainable Urban Mobility, (iii) Environment, Climate Resilience and Spatial Planning, (iv) Independent Civil Protection Service, (v) Infrastructure and Rural Development, and (vi) Technical Projects and Services. Their participation offered specialized perspectives on climate risks, thereby enabling a coordinated and comprehensive approach to climate adaptation at the regional level.

- Insights into flood risk assessment, with a focus on extreme precipitation events in Crete, were presented through a poster at the 11th International Conference on Civil Protection & New Technologies, hosted at the facilities of the Hellenic Mediterranean University in Heraklion on ***24 October 2025.*** SafeHeraklion2025 brought together civil protection stakeholders from academia, local governments, central administration, private sector and voluntary organizations, both domestic and international. It provided the framework for the implementation of fruitful discussions and the development of synergies in the domain of Civil Protection, with a long-term potential.
- The findings demonstrated significant variation in potential flood damage across the island, and projections of future climate conditions indicated an anticipated increase in both the intensity and frequency of extreme precipitation events. The session emphasized the applicability of CLIMAAX results for Greek regions, enabling alignment of risk assessments with investment strategies and informing forthcoming policy revisions. Additionally, it provided valuable support to local decision-makers in identifying vulnerable areas and enhancing risk management approaches in response to evolving climate challenges. The team also placed significant emphasis on data sharing, transparent methodologies, and well-defined implementation pathways, which are fundamental elements of the CLIMAAX approach.
-
- The first round of stakeholder meetings was conducted online on ***18 December 2025***. Following the session, participants were invited to complete a survey regarding the Risk Evaluation Protocol for Key Risk Assessment, focusing on severity, capacity, and urgency. Stakeholders included Director Generals, the Directorate of Environment and Spatial Planning, the Independent Civil Protection Directorate, the Rural Development Directorate, as well as representatives from Technical Projects and Services. The insights derived from both the meeting discussions and

the survey are instrumental in supporting ongoing improvement and ensuring the quality of the project process.

- The results presented on the enhanced workflows incorporating local data for flood and drought risk assessment were positively received and regarded as highly valuable, particularly due to the increased resolution and specificity compared to those shown during the project's initial phase. The progress of the project was met with positive feedback, accompanied by constructive suggestions and proposals that contributed to enhancing the overall process. Variations in the interpretation of results, regarding both current conditions and future projections, were effectively communicated through insightful observations. This facilitated a constructive discussion and encouraged open dialogue among participants.
- Concerns have been expressed regarding the risks of desertification on the island, attributed to the combined impacts of climate change and human activities. These factors pose a significant threat to biodiversity in general, and specifically to olive tree productivity.
- With regard to agricultural activity, the crops currently being considered (corn, wheat, soybean, cotton, rice) are more representative of other regions of Greece rather than Crete. The existing universal data on various crop types do not adequately reflect local conditions, thus highlighting the need for an alternative scenario for future agricultural activity on the island. This is particularly pertinent given Crete's reliance on its primary sector and arable land. However, developing such a scenario is complex due to the involvement of numerous factors; therefore, it is essential to develop a tailored socioeconomic approach and involve agronomists to accurately identify both local needs and the suitability of these crops compared to those that are realistic for the island of Crete.
- The open discussion also stressed the issue of land use which remains insufficiently addressed. This finding emphasizes the need for more robust data and comprehensive local information to enhance accuracy, particularly regarding adjustments to exposure categories. This concern was identified during the project's first phase, where limitations in the resolution of global datasets hindered detailed vulnerability assessments, resulting in imprecise socio-economic exposure and vulnerability indicators.
- The discussion also covered anticipated shifts in mapping population displacement and density due to projected climatic variations, alongside adjustments and changes in vulnerability categories associated with planned water infrastructure.
- Several stakeholders emphasized the essential role of accurately monitoring flash flood dynamics, as well as clearly communicating emergency protocols to enable and support more informed risk management decisions. This approach also contributed to identifying infrastructure vulnerabilities and revealed the necessity for cross-sectoral prioritization.
- These findings serve to confirm the sensitivity of the indicators and highlight the multiparametric nature of the project. For example, certain trends were less pronounced when analyzed at the municipal level, as risk is distributed across a broader area. This approach enables the identification of intra-municipal inequalities, which are effectively represented in the maps. Additionally, the disparities between eastern and western Crete contribute to substantial variations, resulting in shifts in indicator categories such as the hazard index associated with annual precipitation.

The project outcomes will continue to benefit the members and employees of the Region of Crete as they engage with these scientific and research data. The implementation of the CLIMAAX workflow fosters productive collaboration between research institutions, in this case the Technical University of Crete, and the Region of Crete through consistent interaction and scheduled meetings

throughout the project's duration. The project data will be utilized in two distinct ways. Firstly, it will inform the upcoming update of the RAAP of Crete. Secondly, it will contribute to the regional observatory platform. This approach delivers significant added value, as evidenced by the research team at the Technical University of Crete, who have substantiated the needs of the local community and the wider region of Crete.

In relation to the scheduled meetings for the implementation of the third phase of the project, the second round of stakeholder meetings is scheduled to take place in Heraklion during March 2026 and will be conducted in person. In addition to the one-day event, preparations are underway to host two to three regional gatherings throughout Crete, including venues such as Chania, Heraklion, and possibly an additional location. The objective of these events is twofold: firstly, to disseminate project outcomes more widely, and secondly, to facilitate engagement with policymakers and decision makers in the region. By taking this approach, we will be able to gain insights into the authentic needs of local communities and formulate practical solutions that are aligned with existing circumstances.

2.2 Risk Exploration

2.2.2 Screen risks (selection of main hazards)

In Phase-1, the initial screening already identified drought (meteorological, agricultural and hydrological) and river flooding as the dominant climate-related hazards for Crete, based on past impacts, stakeholder consultation and the Regional Adaptation Action Plan. Phase-2 keeps this focus but refines the understanding of where and how these hazards manifest and how they may evolve.

Relevant hazards and current situation

For drought, the second consecutive very dry hydrological years 2022–2023 and 2023–2024, followed by a still-deficit year 2024–2025 (Figure 2-1). Multi-year water scarcity **is now a recurrent feature** rather than an exceptional event. Central and eastern Crete repeatedly register below-average precipitation and above-average temperatures, with low reservoir levels and high pressure on aquifers and irrigation schemes. These conditions particularly affect olive production areas, irrigated horticulture zones and tourism-intensive coastal municipalities.

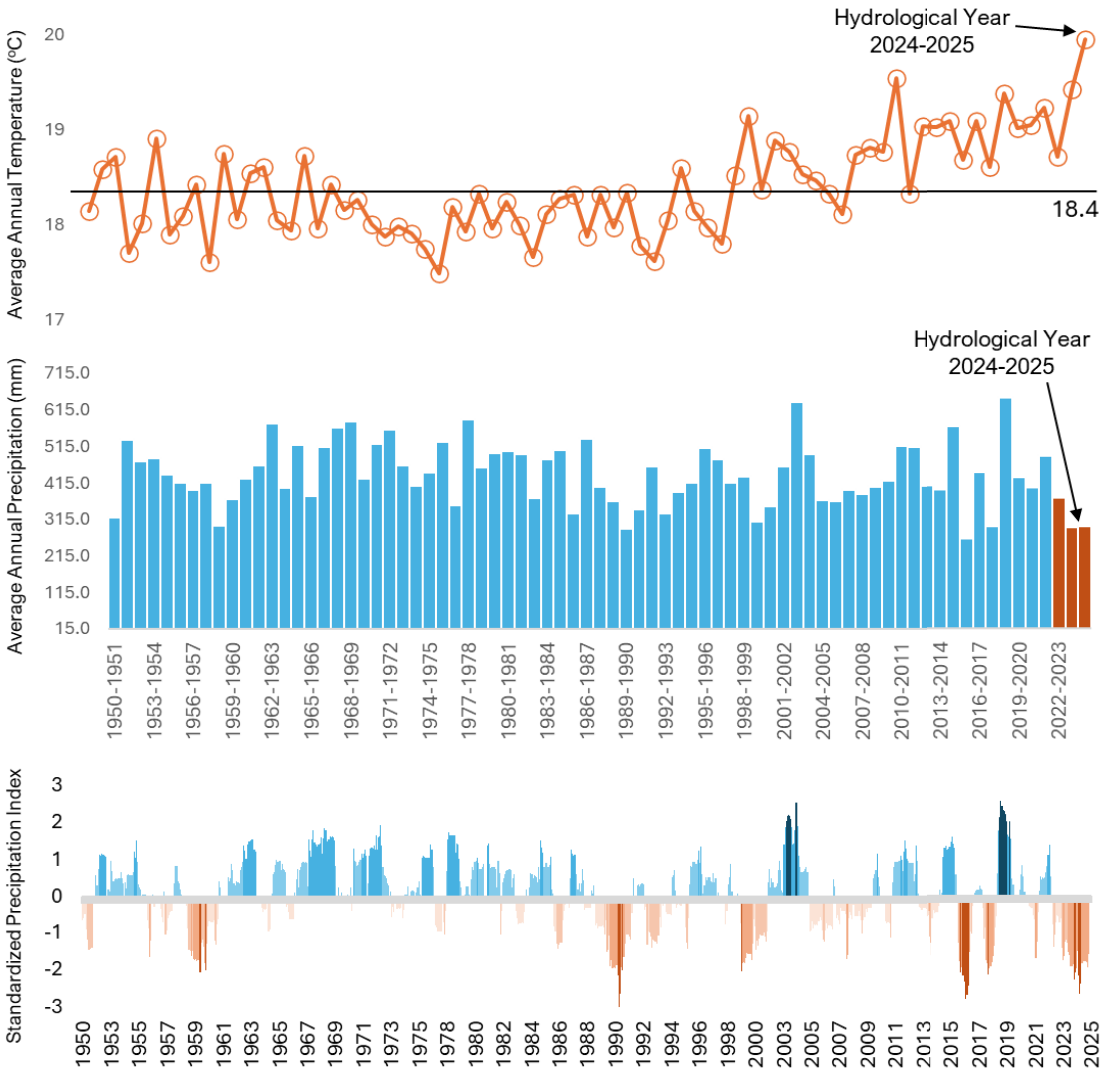

Figure 2-1: Trends in (a) average annual temperature (°C), (b) average annual precipitation (mm), and (c) Standardized Precipitation Index (SPI) for Crete indicating periods of drought (negative SPI) and wetness (positive SPI), from 1950 to 2025.

River flood hazard remains relevant, with damaging events in urbanized and steep catchments, but its exploration and refinement are documented in the dedicated flood technical deliverable (2b).

Insights from the Copernicus Climate Atlas

The Copernicus Climate Atlas provides a Mediterranean-wide, macro-scale picture of climate change, which we use as a contextual backdrop rather than as a direct input to the CLIMAAX-CRETE indicators. Across the Mediterranean basin, the Atlas shows robust warming in all seasons, with the strongest signal in summer. By the end of the century, many Mediterranean land areas are projected to experience several degrees of additional warming relative to 1981–2010, along with more frequent and persistent heatwaves. This implies higher evaporative demand and longer periods of soil-moisture stress, even where annual rainfall does not decrease substantially. For precipitation, the Atlas indicates a general drying tendency in the Mediterranean region, particularly in its southern and eastern sectors. Projections show reductions in mean annual rainfall, more frequent multi-month dry spells and an increase in consecutive dry days, while short-duration heavy rainfall events

may intensify locally. At the macro scale this translates into a higher likelihood of meteorological and hydrological drought, compounded by greater variability between years.

Although the spatial resolution of the Copernicus Atlas cannot resolve the complex topography and coastal gradients of Crete, its regional messages are consistent with the island-scale picture as a warmer, drier, and more variable climate with increasing pressure on water resources. We therefore use the Atlas primarily as a consistency and plausibility check for the locally derived hazard indicators, confirming that the Cretan-scale projections for temperature, precipitation and drought lie within, and often at the drier end of, the broader Mediterranean climate change signal.

Hazards covered in this assessment

In Phase 2 we retain drought and floods as the two priority climate hazards for Crete, but with a much richer set of workflows than in Phase 1. On the drought side, we:

(i) apply a refined Relative Drought Risk workflow, using locally tailored hazard, exposure and vulnerability indicators at sub-basin and municipal scale.

(ii) run the CLIMAAX Agricultural Drought workflow for olive groves, linking climatic water stress to spatially explicit revenue-loss estimates and

(iii) complement these with an independent olive yield–climate impact analysis (Karkou study), based on long yield records and local climate data.

On the flood side, we:

(i) implement a River Flood Risk workflow driven by the new 2 m national flood-hazard maps for RP50, RP100 and RP1000, combined with land use and damage functions at basin scale;

(ii) apply the Flood Damage and Population Exposure workflow using Microsoft Global Building Footprints and GHS-POP to derive building-level Expected Annual Damage and Expected Annual Exposed/Displaced Population

(iii) use the Extreme Precipitation workflow to analyze changes in heavy 24-hour rainfall against locally derived impact thresholds (100 and 200 mm/day) and

(iv) apply the River Discharge Statistics workflow to the Giofiros and Keritis basins, exploring climate-driven changes in high-flow regimes.

Available data and remaining needs

Droughts – available data and remaining needs

For drought, Phase-2 we used CHELSA BIOCLIM+ and ISIMIP3b (WASP) for climatic hazard, EURO-CORDEX projections in the CLIMAAX agricultural workflow, GCAM/Demeter land-use with LUISA cross-checks, gridded population and tourism projections, and vulnerability layers (LitPop GDP per capita, irrigated-area fractions, groundwater wells/aquifers, planned water works). These support relative drought mapping and olive yield/revenue-loss estimates at sub-basin and municipal level.

Key gaps concern: (i) the need for a unified, locally optimized climate basis (CLIMADAT-GRID, Varotsos et al., 2025) for all hazard indicators; (ii) explicitly downscaled, locally credible land-use scenarios, since exposure is dominated (~86 %) by agricultural water demand and GCAM alone is too coarse; (iii) systematic sensitivity tests of the chosen indicator weights; and (iv) more reliable,

spatially resolved crop-yield statistics to better calibrate agricultural drought impacts, especially for olives.

Floods – available data and remaining needs

For floods, the study already relies on 2-m national flood-hazard maps (RP50/100/1000), detailed Microsoft building footprints, GHS-POP population grids, land-use data and local flow records for key rivers, allowing a robust first appraisal of current river-flood risk.

The main gaps are: (i) lack of high-resolution future flood-hazard maps consistent with climate scenarios and (ii) limited attribute data for exposed assets. Building footprints rarely distinguish use type or occupancy. Enriched inventories (residential vs commercial vs critical facilities, typical occupants and age structure) are needed to move from generic damage estimates to detailed, socially differentiated flood-risk assessment.

2.2.3 Choose Scenario

In Phase-2 we continued to frame risk in a scenario setting that combines future climate trajectories with socio-economic change but refined the choices in discussion with the Region of Crete and stakeholders.

For time horizons, stakeholders expressed strongest interest in the next 10–20 years, while also asking for a view towards mid-century and the end of the century. Accordingly, all workflows use three time horizons broadly considering near-term, mid-term and long-term climatic and socioeconomic settings.

In terms of future climate scenarios and for drought, we used the SSP1-2.6, SSP3-7.0, SSP5-8.5 combinations embedded in CHELSA/ISIMIP3b for the relative drought indicators and the RCP4.5 and RCP8.5 ensemble available from the EURO-CORDEX forcing of the agricultural workflow and the olive-yield climate impact analysis, based on empirically derived climate-yield relationships. For floods, future precipitation extremes and river discharge conditions are taken from the EUROCORDEX RCP4.5 and RCP8.5 products used in the CLIMAAX workflows for a consistent intermediate and high forcing envelope. During stakeholder discussions, low end pathways were generally perceived as increasingly unlikely given recent trends, while very high-end pathways (RCP8.5/SSP5-8.5) were treated mainly as stress test scenarios rather than central expectations. Intermediate pathways (around RCP4.5 / SSP2-4.5–SSP4-6.0) were considered most plausible for planning, but are not available consistently across all datasets, which constrains full harmonization of scenarios between workflows.

Socioeconomic evolution is represented through the SSP based projections of population, GDP, land use and tourism that drive the exposure and vulnerability indicators in the relative drought analysis. These projections provide internally consistent macro-scale narratives. In the Phase-2 assessment, climate and socio-economic scenarios are combined by evaluating hazard indicators under the relevant RCP/SSP combinations and overlaying them with SSP-consistent exposure and vulnerability fields for the same time slices.

Stakeholders repeatedly stressed that global SSP/GCAM products only provide a broad envelope of plausible futures and may not capture local land-use change, water-infrastructure implementation or demographic shifts in high-risk areas. Therefore, while the current scenario set is adequate for island-wide screening and for identifying robust hotspots across sectors, a key conclusion for next steps is the need to develop locally downscaled, co-designed socio-economic and land-use

scenarios for selected priority areas (e.g. the Heraklion coastal zone for floods, central-eastern olive plains for drought), which can then be combined with higher-resolution climate and impact models for planning.

2.3 Regionalized Risk Analysis

In Phase 2, the climate risk assessment for Crete moves from a coarse macroscale to a regionalized, workflow-specific analysis that is better aligned with local decision scales. Each workflow uses its own exposure and analysis units, chosen to match the nature of the hazard and the available data. Indirect and cross-sectoral impacts are only partly captured, mainly through exposure and vulnerability proxies such as agricultural land use, population and tourism density, GDP per capita, groundwater and irrigation indicators, and planned water-infrastructure capacity. Subsequent subsections describe how each workflow has been fine-tuned to the local context, which datasets have been used, and which new impact and risk metrics have been derived. The fundamental datasets used in updated drought and flood risk workflows are listed in Table 2-1 and Table 2-, respectively, and detailed information is included in the accompanying Technical Deliverables.

2.3.1 Drought - fine-tuning to local context

The updated drought risk assessment workflows applied are (a) relative drought risk, (b) agricultural drought for olives and (c) an empirical olive-yield analysis as an additional assessment based on local models and data.

Table 2-1 Data overview of Drought workflows

Hazard data	*Vulnerability data*	*Exposure data*	*Impact metrics/Risk output*
Relative Drought: CHELSA BIOCLIM+ BIO1, BIO5, BIO12 (1981–2100, SSP1-2.6, SSP3-7.0, SSP5-8.5). Basin scale ISIMIP3b precipitation (WASP index).	GDP per capita ((Wang and Sun, 2022)). Groundwater-access indicator (borehole-aquifer, local data). Irrigated area fraction (AQUASTAT GAEZ v5). Planned water-infrastructure per SSP (Koutroulis et al., 2016).	GCAM/Demeter cropland fractions SSP1/3/5 (Calvin et al., 2019). Population projections (Wang et al., 2022) SSP-based gridded population. Tourism exposure derived from tourism projections (Koutroulis et al., 2018) + population distribution.	Relative drought hazard index, exposure index, vulnerability indices. Composite relative drought risk index at basin and municipality level.
Agricultural drought: EURO-CORDEX climate (T, RH, wind, Rs), ET_0 via FAO Penman–Monteith, ETc and water-stress driven yield loss for olives (RCP4.5/8.5, three time slices).	GAEZ v5 irrigated cropland fraction (all crops) as irrigation proxy.	SPAM 2010 olive production. GAEZ v5 (2020) aggregated crop value for Crete.	% yield loss of rainfed olives. Absolute and relative revenue loss per grid cell.
Empirical olive-yield analysis: E-OBS indices (seasonal rainfall, May–June precipitation, high summer Tmax, SPEI, chill) and their EURO-CORDEX projections for RCP4.5/8.5 (three future periods)	Not explicit	ELSTAT olive area and production (2011–2022) per regional unit. Corine Land Cover 2018 for olive groves extent.	Observed climate–yield regression coefficients per prefecture. Projected % change in olive yield for Crete and other macro-regions.

2.3.1.1 Drought Hazard assessment

Relative drought

The relative drought hazard index reveals a clear and persistent spatial gradient across Crete. In the baseline period (Figure 2-2), most basins in central and eastern Crete already fall into elevated hazard classes (categories 3–5), reflecting the combined influence of higher temperatures, lower annual precipitation and more pronounced warm-season deficits. Western Crete is generally classified in lower categories (1–2), with a few intermediate-hazard units along the central north coast and parts of the southern slopes.

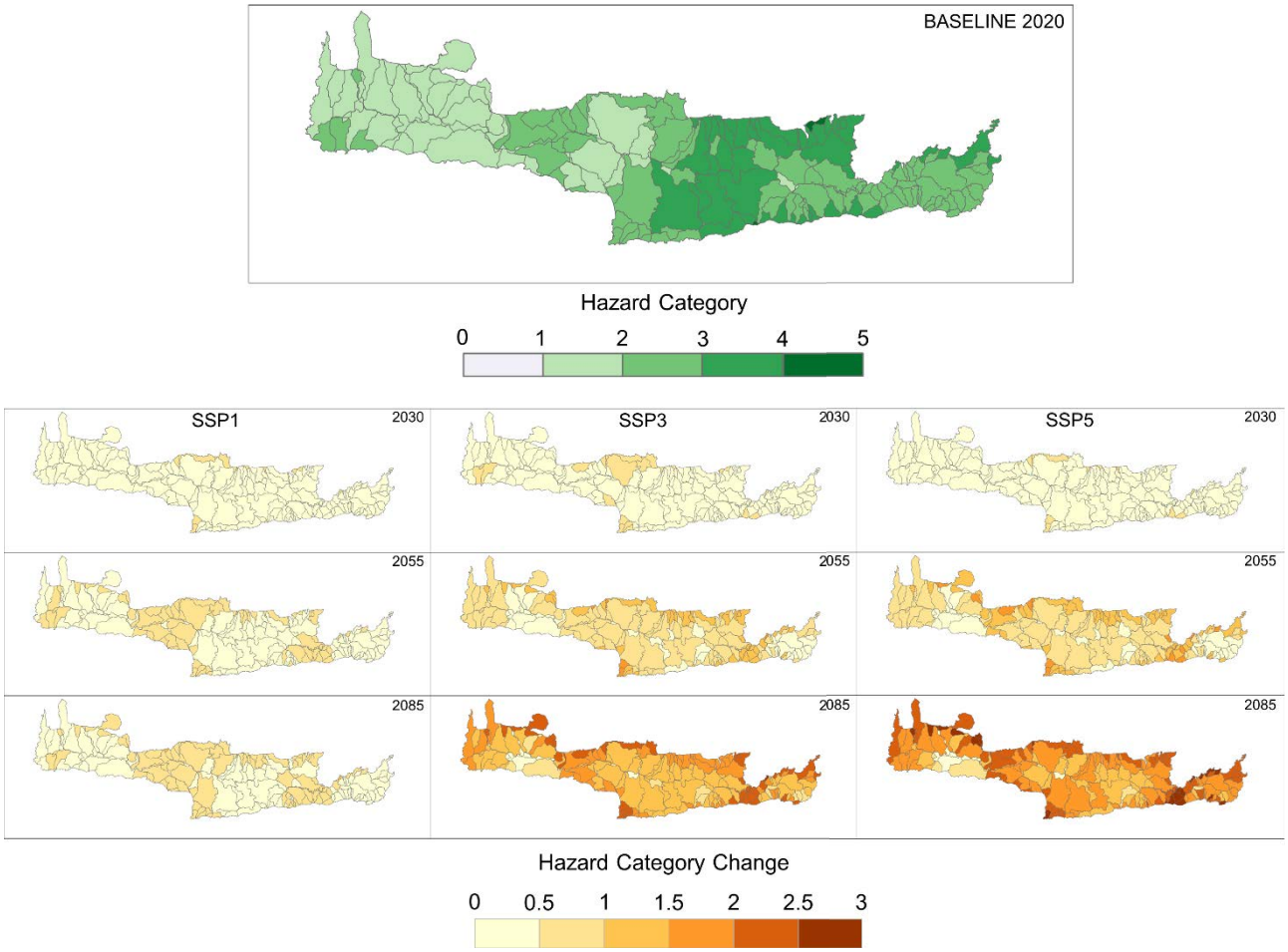

Figure 2-2: Relative drought hazard index at sub-basin (basin–municipality unit) scale for the baseline period (1981–2010) (top) and change in hazard category for three future periods (represented by 2030, 2055 and 2085) under SSP1-2.6, SSP3-7.0 and SSP5-8.5.

Projections are expressed as changes in hazard category relative to this pooled, island-wide baseline. Under SSP1-2.6, changes remain modest and spatially mixed: by near and mid future most basins shift by at most one category, with scattered increases in central Crete partly offset by small decreases in some western and eastern units. By 2085, a larger fraction of central and southern basins move into higher categories, but widespread, strong intensification is still limited.

Under SSP3-7.0 and SSP5-8.5, the signal becomes progressively stronger and more coherent. By mid-century, many basins across central and western Crete exhibit category increases of +1 to +2, indicating that they move upward within the island-wide hazard ranking. By far future, large contiguous areas in western and especially central Crete show shifts of +2 to +3 categories, while parts of eastern Crete display smaller increases or near-stable classes. Given that categories are

defined from a single pooled distribution over all periods and scenarios, these patterns indicate that the most pronounced future intensification of drought-relevant climate conditions is concentrated in central and western basins, while eastern Crete tends to maintain its already high relative hazard rather than experiencing a comparable further escalation.

Agricultural drought

Agricultural drought hazard for olives is assessed with the CLIMAAX agricultural drought workflow, which converts climate-driven soil water deficits into percentage yield losses for rainfed olive groves. The workflow is driven by bias-corrected EURO-CORDEX projections (RCP2.6, RCP4.5, RCP8.5) and computes, for each grid cell over Crete, a multi-model mean yield loss relative to a historical reference, based on seasonal precipitation, evapotranspiration demand and a simplified water-stress response function for olives.

Figure 2-3 summarizes how the overall exposure of Cretan olive groves to water-stress-induced yield loss shifts over time. Under all scenarios, the distribution gradually moves from low to higher loss classes in the mid- and late-century slices, with the strongest right-shift under RCP4.5 and especially RCP8.5. By 2086–2100 in RCP8.5, a large share of the olive area falls in classes exceeding 10 % mean yield loss, whereas in the near-term slices a much larger fraction remains below that threshold. The agricultural drought hazard is interpreted as an island-scale intensification of water-stress risk for olives, expressed through the changing proportion of cultivated area affected by moderate and severe yield reductions.

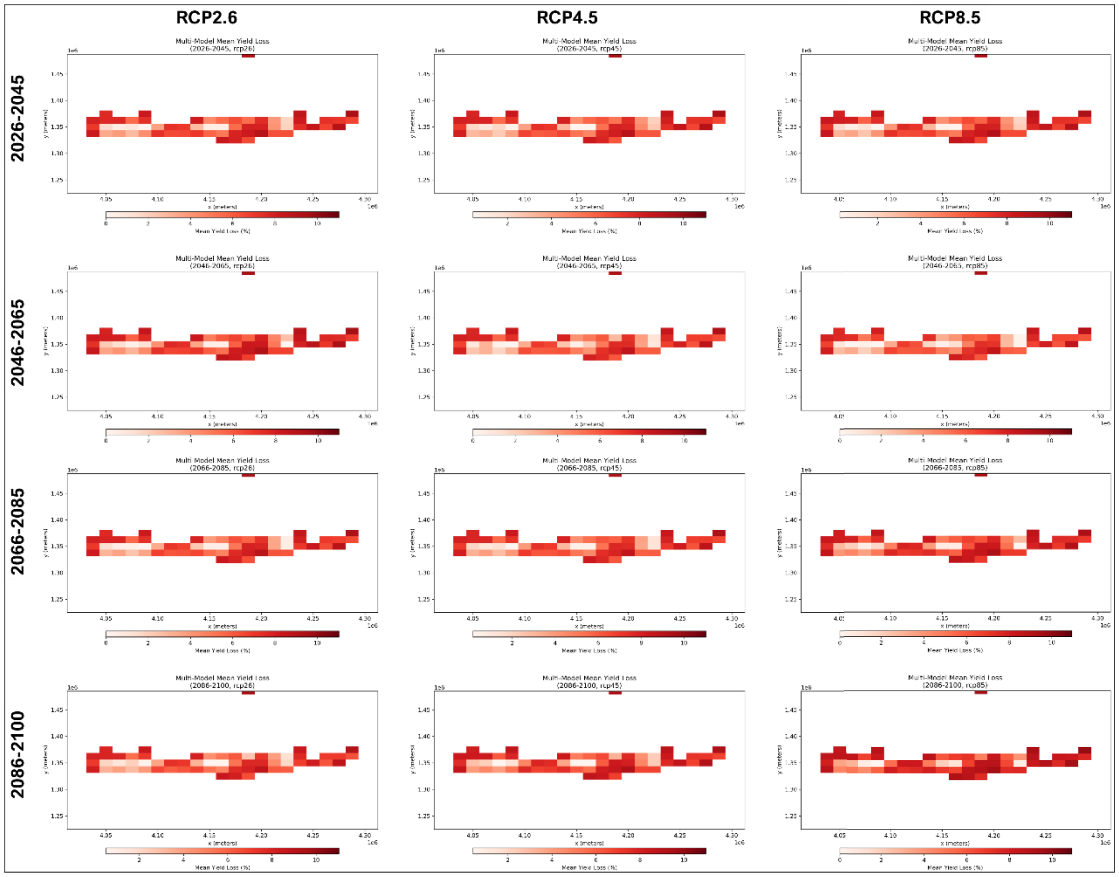

Figure 2-3: Multi-model mean olive yield loss (%) from precipitation deficit in Crete for four future periods (rows) and three emission scenarios (columns: RCP2.6, RCP4.5, RCP8.5).

Climate Change Impacts on Olive Oil Yield

The olive-yield analysis translates projected climate change into shifts in agroclimatic hazards that directly affect tree physiology and production. Table 2-2 summarizes the relative changes in a set of temperature- and moisture-related indices for Crete, comparing three future periods (2026–2045, 2046–2065, 2066–2085) under RCP4.5 and RCP8.5 with the historical baseline. Across all periods and both scenarios, mean annual temperature increases by about +0.7 to +1.4 °C, while maximum daily temperature during the growing season and key phenological windows similarly rises. These warming signals are accompanied by small changes in annual precipitation totals, but more systematic reductions in summer–early-autumn rainfall and in indices reflecting effective water availability (e.g. number of dry days). In practice, this translates into a higher frequency and duration of hot, dry spells during flowering, fruit set and oil accumulation periods when olive trees are particularly sensitive to water stress and thermal extremes.

Table 2-2: Relative changes in specific climatic indices on yearly basis compared to the historical period for Crete.

	Future period	Tmax_MARAPR	DTR_MARAPR	Tmax_APRMAY	DTR_MAYJUN	SPEI_MAYJUN	Tmin_JULAUG-	Tmax_AUGSEP	DTR_SEPOCT
RCP 45	**2026-2045**	+0.7°C	+0.1°C	+0.5°C	0.0°C	−0.1	+0.5°C	+0.4°C	−0.1°C
	2046-2065	+0.9°C	0.0°C	+0.5°C	0.0°C	−0.1	+0.9°C	+0.9°C	−0.1°C
	2066-2085	+1.4°C	+0.1°C	+1.3°C	0.0°C	−0.1	+1.3°C	+1.2°C	−0.1°C
RCP 85	**2026-2045**	+0.7°C	0.0°C	+0.5°C	−0.1°C	−0.1	+0.5°C	+0.4°C	−0.1°C
	2046-2065	+0.9°C	0.0°C	+0.5°C	−0.1°C	−0.1	+0.9°C	+0.9°C	−0.1°C
	2066-2085	+1.4°C	0.0°C	+1.3°C	−0.1°C	−0.1	+1.3°C	+1.2°C	−0.1°C

Figure 24 maps observed trends in annual olive-oil output across Greece for 2011–2022. Several major producing regions, including parts of Crete and the southern mainland, exhibit statistically significant negative trends in production, despite no evidence of a systematic decline in planted area over the same period. This pattern is consistent with an emerging signal of climate-driven yield instability as years with concurrent precipitation deficits and heat anomalies lead to sharp production drops, while “favorable” years only partly compensate. The projected intensification of warm-dry conditions and the recent tendency towards more frequent poor harvests indicate a rising hazard of climate-induced yield loss for olive groves in Crete, even before considering changes in management or irrigation.

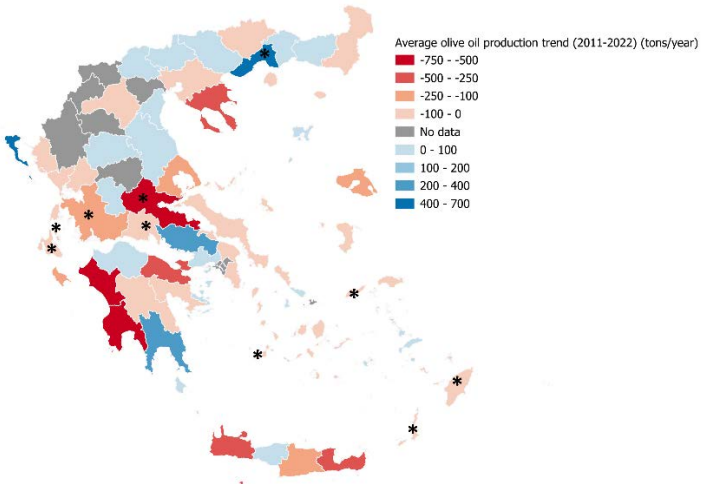

Figure 2-4: Spatial distribution of average olive oil production trends in Greece for the period 2011–2022 (tons year⁻¹). Asterisks mark statistically significant trends at a level of p-value lower than 0.05.

2.3.1.2 Drought Risk assessment

Relative drought

The relative drought risk index combines the basin-scale hazard results with the composite exposure and vulnerability indicators and is then aggregated to municipality level (Figure 2-5). The baseline map (2020) shows a clear south-central risk corridor. These high scores reflect the coincidence of relatively elevated climatic hazard with intensive agricultural water demand and comparatively constrained groundwater and infrastructure buffers. In contrast, much of eastern Crete and some northern coastal municipalities show lower risk categories (0–2), despite non-negligible hazard, because of lower combined exposure and vulnerability.

Future changes in risk category (Figure 2-5) indicate that the spatial pattern of drought sensitivity is persistent, but its intensity is scenario dependent. Under SSP1-2.6, most municipalities experience small negative or near-zero shifts, implying modest risk reduction from a relative perspective. The largest decreases are seen in western mountainous municipalities where exposure and vulnerability are projected to ease. Under SSP3-7.0, several already high-risk municipalities in central and western Crete move up by one to two categories by the end of the century, driven by higher hazard and sustained or increasing exposure with only limited adaptation in water infrastructure. SSP5-8.5 shows a more mixed pattern: in the near and mid-term some western and central municipalities reduce risk thanks to stronger infrastructure pathways and economic capacity, while some eastern and southern municipal units experience relative increases linked to growing exposure under intensifying hazard.

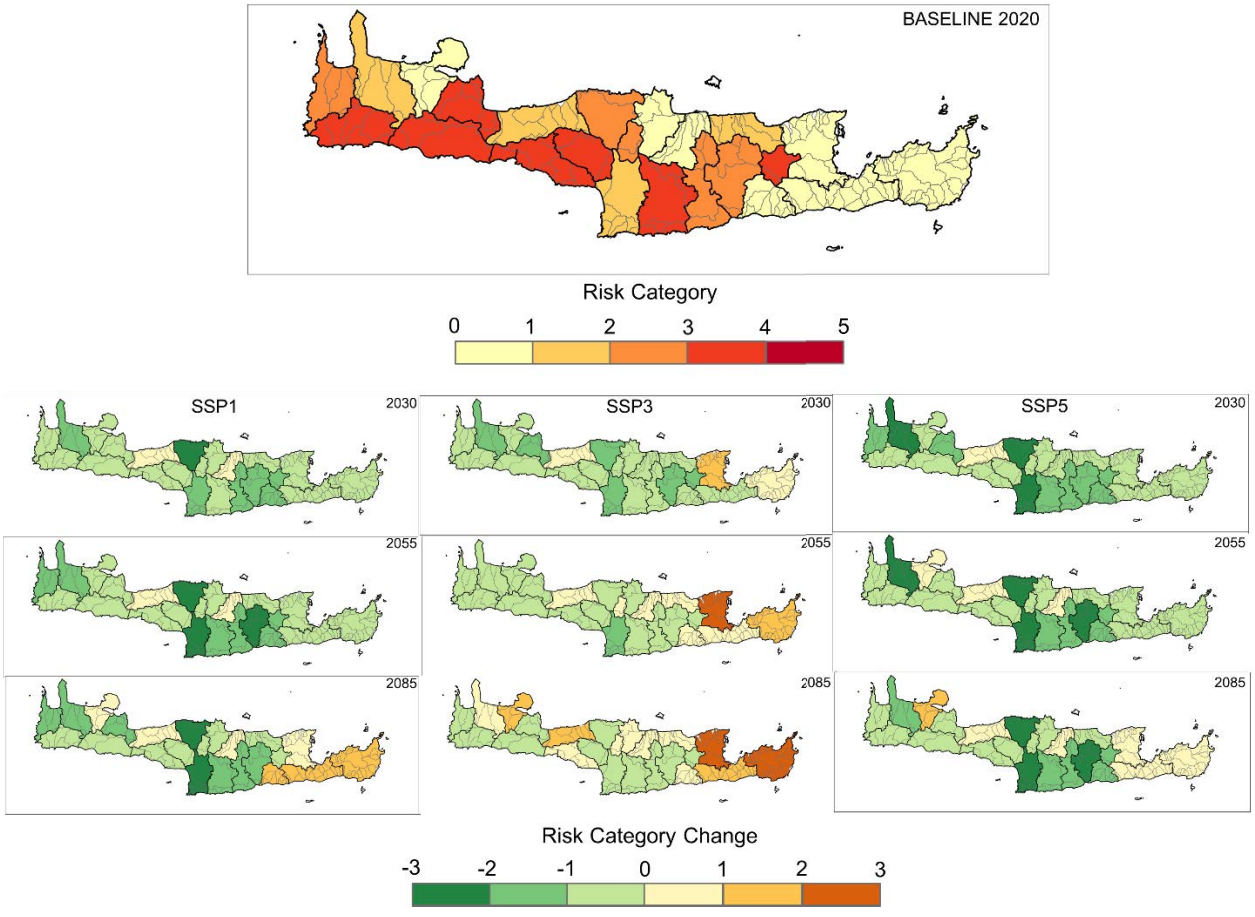

Figure 2-5: Relative drought risk index aggregated at municipality level. The top panel presents baseline (2020) risk values; the lower panels show changes relative to baseline for 2011–2040, 2041–2070 and 2071–2100 under SSP1-2.6, SSP3-7.0 and SSP5-8.5.

Agricultural drought

The agricultural drought risk assessment translates the olive-yield loss projections into an economic metric by estimating annual revenue loss under a "no irrigation available" assumption for each 0.25° grid cell. Figure 2-6 synthesizes these results for four future periods and three RCPs. Across all scenarios, the spatial pattern of revenue loss is remarkably stable: the largest modelled losses (often >60–80 kEUR yr^{-1} per grid cell) cluster in the main olive-producing belts of central Crete, extending from the northern foothills of Psiloritis towards the Messara plain and parts of eastern Crete. Peripheral and higher-elevation areas with smaller cultivated areas show consistently lower losses, not because climatic stress is weaker, but because the underlying production volume, and thus the exposed economic value, is smaller.

The risk interpretation is refined by overlaying current irrigation coverage. This combination highlights two distinct risk configurations. In several central-Cretan cells, high potential revenue losses coincide with substantial irrigation infrastructure, implying that sustained drought or supply failures in these systems would translate into large absolute economic impacts and pressure on water resources. Conversely, some cells along the central–eastern axis and in parts of eastern Crete show sizeable rainfed revenue losses with only limited irrigation coverage. Here, the scope for buffering drought through additional irrigation is structurally constrained, pointing to higher residual risk for farmers even under adaptation.

Temporally, the median multi-model losses do not explode over time but tend to persist at elevated levels across all periods, with modest upward shifts under RCP4.5 and especially RCP8.5 in the later time slices. This persistence indicates that agricultural drought risk for olives is not confined to isolated extreme years, but represents a chronic economic pressure that accumulates over successive decades unless production systems, water management and crop choices are adapted.

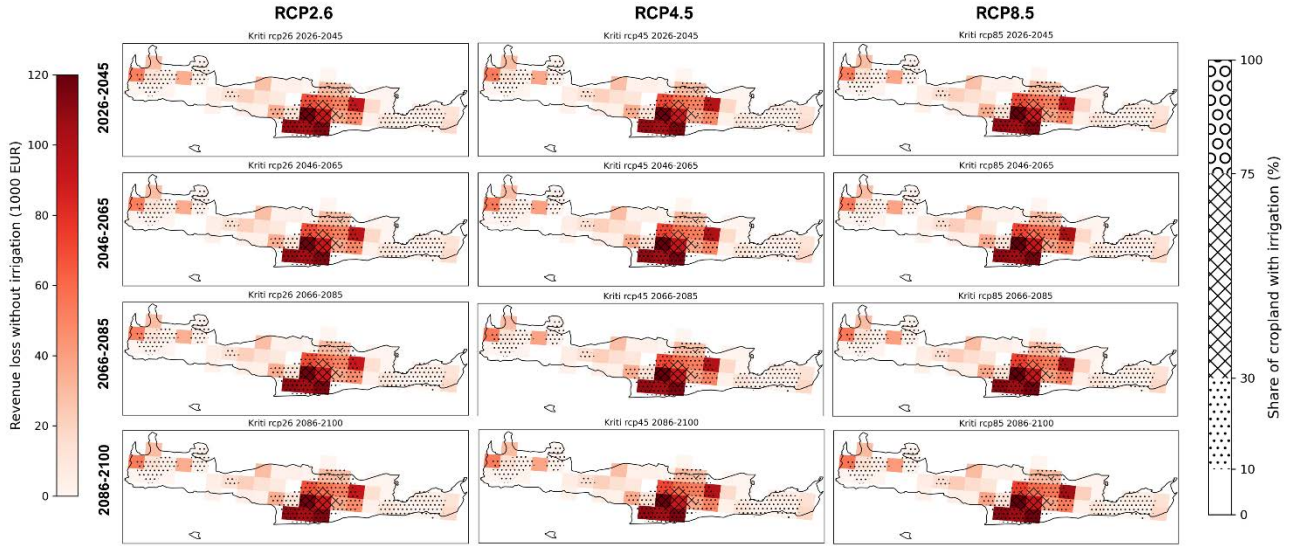

Figure 2-6: Multi-model mean annual revenue loss from absence of irrigation for olive production in Crete (kEUR per grid cell) for four future periods (rows: 2026–2045, 2046–2065, 2066–2085, 2086–2100) and three emission scenarios (columns: RCP2.6, RCP4.5, RCP8.5). Colors show mean revenue loss; stippling and cross-hatching indicate the 2020 share of irrigated cropland from GAEZ v5, highlighting where high potential losses coincide with low or high irrigation coverage.

Climate Change Impacts on Olive Oil Yield

The empirical olive-yield analysis translates projected climate change into percentage deviations of island-wide olive production, using a regression model calibrated on 2011–2022 ELSTAT yields and a set of physically-based climate indices. Applying this model to EURO-CORDEX simulations for RCP4.5 and RCP8.5 yields the time series shown in Figure 2-7, expressing annual yield anomalies for Crete as % change relative to the 2005 baseline.

Across both scenarios, the central tendency of projected yield change remains close to zero, with most years falling within a ±10–15 % band. This indicates that, at the scale of the whole island and under the climatic signal represented by the current model, climate change does not drive a systematic collapse of average olive production. However, the uncertainty bands and the year-to-year excursions highlight substantial interannual volatility, with more frequent years of moderate negative anomalies (e.g. −20 % or lower) in the latter half of the century, especially under RCP8.5. In practice, this means that while mean yields may remain broadly comparable to recent decades, the probability of sequences of poor harvests increases, raising the risk of income instability for producers and local supply chains.

Because the model is calibrated at regional scale and does not resolve irrigation, soil water holding capacity or cultivar differences, the results should be viewed as a complementary, macro-level risk signal rather than a replacement for the more detailed agricultural-drought workflow. Taken together, the two analyses suggest that: (i) spatially concentrated hotspots of high revenue loss emerge where irrigation is limited and precipitation deficits are strongest, and (ii) at island scale, climate change primarily amplifies the frequency of bad years rather than inducing a uniform downward shift in average yield. This combination of localized structural risk and increased temporal variability underscores the need for risk-spreading strategies (e.g. irrigation loss reduction, waste water reuse, diversification) in olive-dependent areas of Crete.

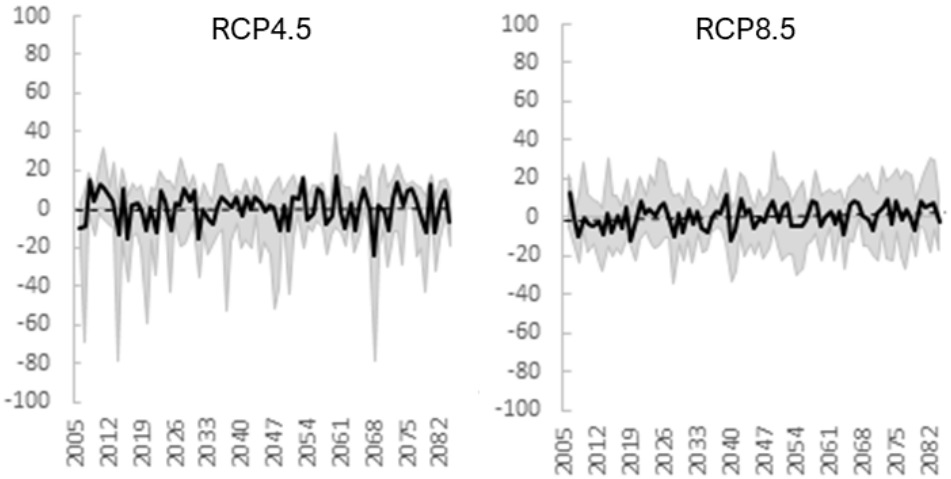

Figure 2-7: Projected change [%] in olive oil yield for Crete between 2005–2085 under RCP4.5 and RCP8.5

2.3.2 Flood - finetuning to local context

Multiple flood-related workflows were applied in Phase-2: (a) river flood risk, (b) flood damage and population exposure, (c) extreme precipitation and (d) discharge. These are summarized in Table 2-3.

Table 2-3 Data overview Flood workflows

Hazard data	*Vulnerability data*	*Exposure data*	*Impact metrics/Risk output*
River flood hazard: 2 m-resolution flood depth and extent rasters for RP50, RP100 and RP1000 from the EL13 Flood Risk Management Plan, derived using SCS–CN runoff estimates, HEC-HMS design hydrographs and 1D/2D HEC-RAS routing.	Depth-damage relationships for different land-use categories (Huizinga et al., 2017).	LUISA land-cover dataset for Crete, used to mask/interpret inundated areas.	Maps and basic statistics of inundated area and depth classes per APSFR zones.
Flood Damage and Population Exposure: same as **River flood hazard workflow**	Depth-damage curves for buildings, with linked maximum economic damage (Huizinga et al., 2017) and depth thresholds for exposed-displaced population.	Microsoft Global Building Footprints; derived building-based population layer (residents per 100 m²) Critical infrastructure within APSFRs.	Direct economic damage for RP50, RP100 and RP1000; Number of exposed and displaced inhabitants Expected Annual Impact indicators per APSFR
Extreme precipitation: Bias-corrected EURO-CORDEX daily precipitation (multiple GCM–RCM pairs) processed with the CLIMAAX Extreme Precipitation workflow to obtain GEV-based return levels under RCP4.5/8.5.	Not explicit	Macro-scale – Crete level	Changes in magnitude for fixed return periods and changes in return periods for 1-day rainfall thresholds (100 and 200 mm).
Extreme discharge: HCII river-discharge time series from the E-HYPEcatch model forced by EURO-CORDEX climate projections under RCP4.5/8.5.	Not explicit	Giofiros and Keritis river basins	Flow quantiles and return levels for baseline and future periods, expressed as relative changes

2.3.2.1 Flood, Extreme Precipitation and Discharge Hazard assessment

River Flood Hazard

River flood hazard was re-evaluated in Phase 2 using the high-resolution hydraulic products of the 2nd River Basin Management Plan/Flood Risk Management Plan for the Water District of Crete (EL13). Instead of screening the whole island with coarse DEMs as in Phase 1, the analysis focuses on ten flood-prone areas distributed along the north and south coasts and in key inland valleys (Figure 2-8). These focus areas (APSFRs) were selected because they concentrate existing assets and documented flood problems and coincide with the main river systems for which detailed hydraulic studies are already available. For each focus area, flood extent and depth rasters at 2 m resolution were used for three return periods (RP50, RP100 and RP1000). The maps are based on design events derived from SCS–CN runoff estimates and HEC-HMS hydrographs, routed through coupled 1D/2D HEC-RAS models. This represents a substantial refinement relative to Phase 1, where flood hazard was approximated using JRC global river flood hazard dataset. The new products capture flow paths, local depressions, protection works and urban micro-topography and thus provide a much more realistic basis for overlaying building footprints, land use and population.

Figure 2-9 illustrates this improvement for one of the focus areas. These enhanced hazard layers underpin the subsequent damage and population-exposure calculations.

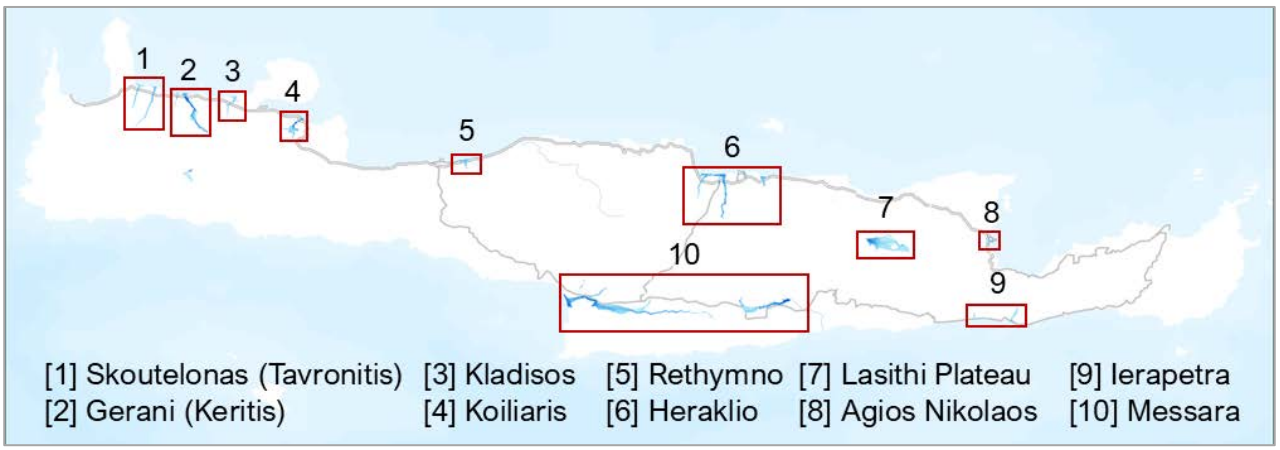

Figure 2-8: Location of the ten focus areas (1–10) used in the second-phase flood risk assessment in Crete.

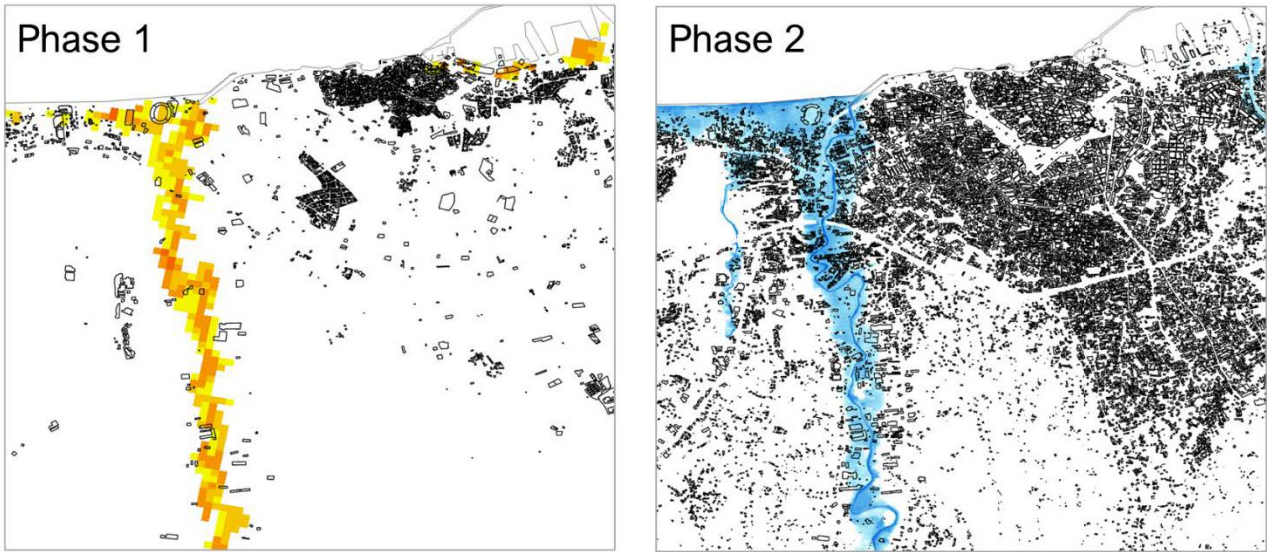

Figure 2-9: Example of refinement from Phase-1 (left) to Phase-2 (right) river-flood hazard mapping in one of the focus areas (Giofiros). Phase-1 used coarse flood hazard maps (JRC), while Phase-2 applies 2 m-resolution depth grids from the EL13 Flood Risk Management Plan, resolving detailed inundation patterns around individual buildings.

Flood building damage and population exposure

For the building-damage and population-exposure workflow, Phase 2 moves from coarse, global exposure layers to a fully building-level representation for selected APSFRs, with Heraklion used as the main demonstrator. Flood hazard is provided by the 2 m–resolution EL13 design-event maps (RP50, RP100, RP1000), giving detailed flood depth and extent within the urban fabric. These depth rasters are intersected with the Microsoft Global Building Footprints, which offer near-complete coverage of individual structures and reliable footprint areas.

Compared with Phase-1, which relied on JRC global flood hazard maps (~100 m resolution) and the incomplete OpenStreetMap building layer, this setup substantially sharpens the exposure picture. Figure 2-10 illustrates this improvement for Heraklion: at RP50, dense clusters of residential and commercial buildings along the main river corridor are shown as directly intersected by inundation, while the RP500 case emphasizes the additional, more dispersed assets affected only in very rare events. Population exposure is estimated by combining the building layer with a gridded population dataset, allocating residents to buildings in proportion to footprint area within each grid cell. This

enables calculation of the number of potentially affected inhabitants by return period and APSFR, and the derivation of summary indicators such as exposed residents per hectare or per unit of river length.

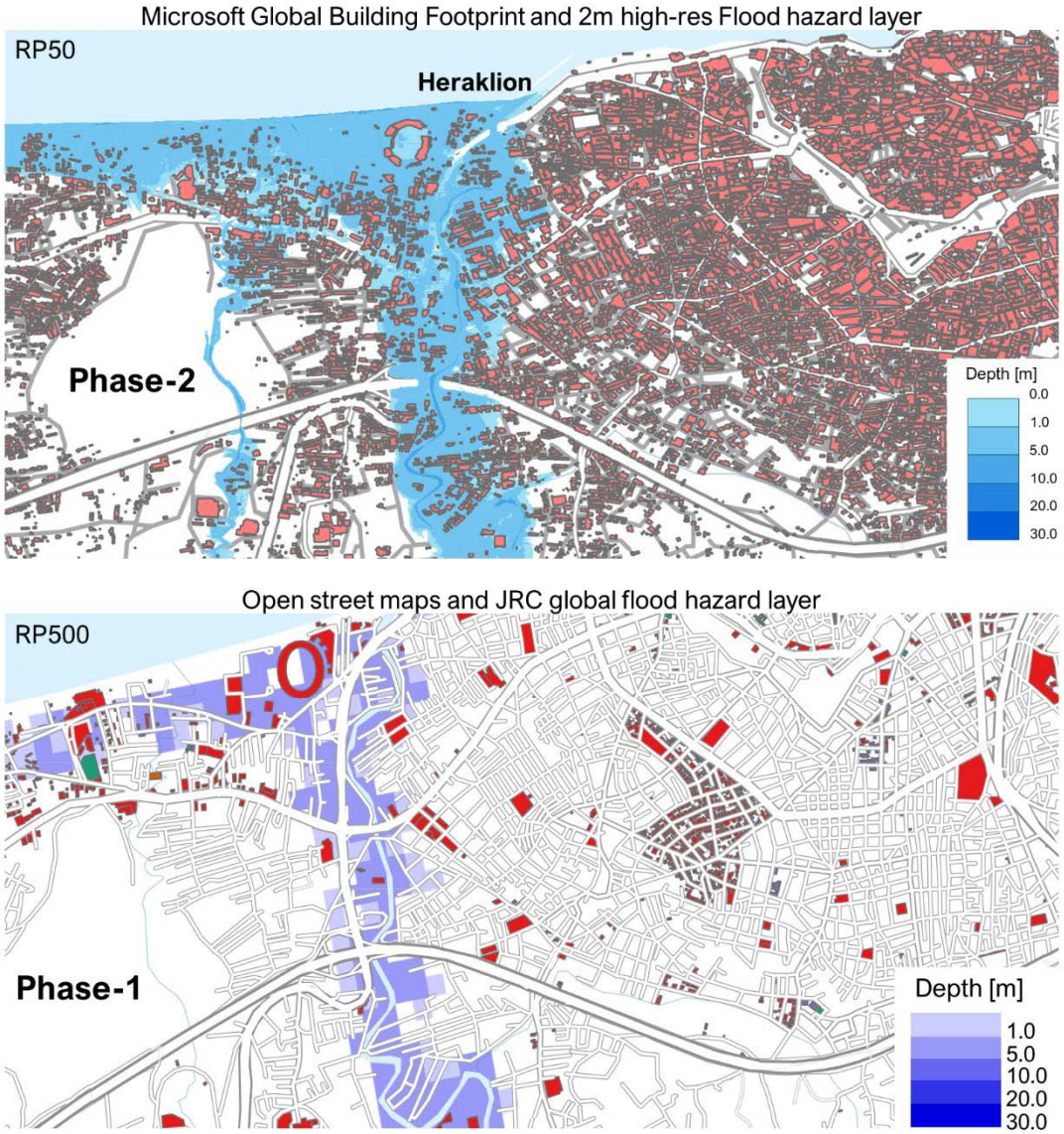

Figure 2-10: Building-level flood hazard-exposure in Heraklion for the 50-year (RP50, top) and 500-year (RP500, bottom) design floods. Blue shading shows 2 m–resolution flood depth from the EL13 Flood Risk Management Plan overlaid with Microsoft Global Building Footprints, which provide almost complete coverage of the local building stock. This Phase-2 set-up represents a major improvement over Phase-1, which relied on coarser JRC global flood hazard maps (~100 m) and the incomplete OpenStreetMap building layer, and therefore allows much more detailed and reliable estimates of exposed buildings and associated.

Extreme precipitation

In the absence of high-resolution flood hazard maps for future scenarios, the extreme-precipitation hazard assessment complements the river-flood analysis by examining how short-duration, high-intensity rainfall events may evolve over Crete. Using the CLIMAAX extreme-precipitation workflow, bias-corrected EURO-CORDEX daily precipitation for RCP8.5 was fitted with a GEV distribution and used to derive multi-model mean 24-hour return levels for different return periods (e.g. for 50-year return period shown in Figure 211). In the baseline, 50-year 24-h rainfall amounts are highest over

the western and central mountainous massifs, where return levels exceed ~200–220 mm, and lower over eastern and leeward coastal areas. Under RCP8.5, the spatial pattern of extremes remains broadly similar, but return levels increase over most of the island, particularly in southern and eastern Crete and along parts of the north coast. By late century (2071–2100), many grid cells exhibit increases on the order of +20-40%, with local hotspots exceeding +50%. Detailed information for additional return periods and RCP4.5 is contained in the accompanying detailed Flood risk assessment Report.

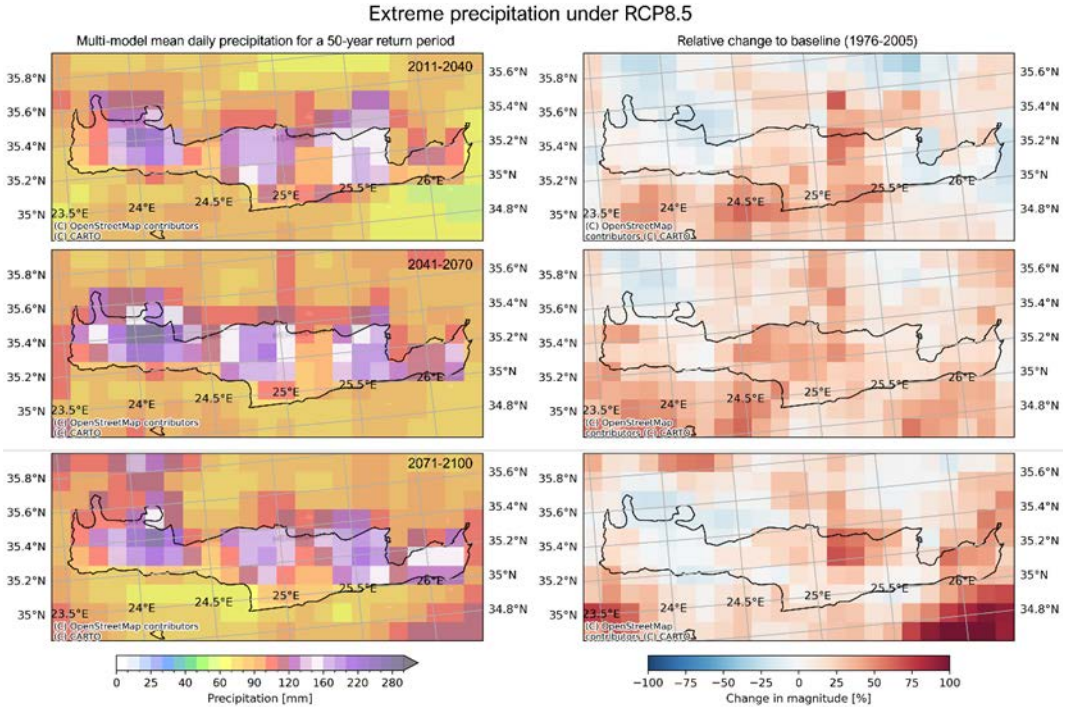

Figure 2-11: Spatial distribution of the multi-model mean 24-hour precipitation return level for a 50-year event (left) and its relative change with respect to the 1976–2005 baseline (right) under the RCP8.5 scenario for 2011–2040, 2041–2070, and 2071–2100.

Extreme discharge

To complement the map-based hazard assessment, we applied the CLIMAAX hazard assessment for river flooding using river discharge statistics workflow to two of the most flood-prone basins in Crete with high observed impacts: Giofyros (Heraklio) and Keritis (Gerani/Chania). The workflow uses the Hydrological Climate Impact Indicators (HCII) dataset produced by SMHI and distributed via the Copernicus Climate Data Store, which provides catchment-scale river discharge simulations from the E-HYPEcatch hydrological model forced by EURO-CORDEX climate projections at ~0.11° resolution. For each of the two basins we:

- selected the corresponding E-HYPE catchments from the HCII dataset (Figure 2-12) extracted historical daily discharges to characterize variability and derive flow-duration curves
- obtained HCII indicators of extreme river discharges and their relative changes for multiple return periods and time slices (early-, mid-, end-century) under different RCP scenarios.

The discharge statistics were used to explore how climate change may alter high-flow regimes in Giofiros and Keritis, and to provide a hydrological context for the flood hazard information derived from the flood hazard maps and the extreme-precipitation workflow.

Figure 2-12 Location of the Giofiros (right) and Keritis (left) basins in Crete and the corresponding E-HYPEcatch units (shaded) used in the CLIMAAX river discharge workflow.

2.3.2.2 Flood Risk assessment

River Flood Risk

The land-use based river flood risk assessment combines the 2 m FRMP depth maps with the LUISA land-cover dataset and depth-damage functions to estimate direct economic losses for each of the ten focus areas. Figure 2-13 maps the spatial distribution of damage for an RP100 event. High and very high damage cells concentrate in two types of environments:

- Coastal and river-mouth urban areas, e.g., Heraklion, Rethymno, Agios Nikolaos and Ierapetra, where dense residential, commercial and industrial fabric lies directly within the inundation footprint.
- Intensively cultivated floodplains in particular the Messara plain, the Lasithi Plateau and the lower reaches of Keritis and Koiliaris, where extensive cropland and greenhouses are affected by shallow but widespread flooding.

Event-based losses for RP100 range from about €55-80 million in the smaller urban catchments (Kladisos, Koiliaris, Rethymno, Agios Nikolaos, Ierapetra) to €247 million in the Lasithi Plateau and €615-744 million in Heraklion and Messara, respectively. Messara alone accounts for roughly one quarter of total RP100 damages across all study areas, reflecting the combination of a large agricultural plain. Comparison with RP50 and RP1000 (not shown here) indicates a strong non-linear increase of damage with return period in most basins, especially where small floodplains host dense urban development. In Heraklion, the increase between RP50 and RP1000 is more modest, suggesting that highly exposed districts are already largely inundated for RP50-100 events.

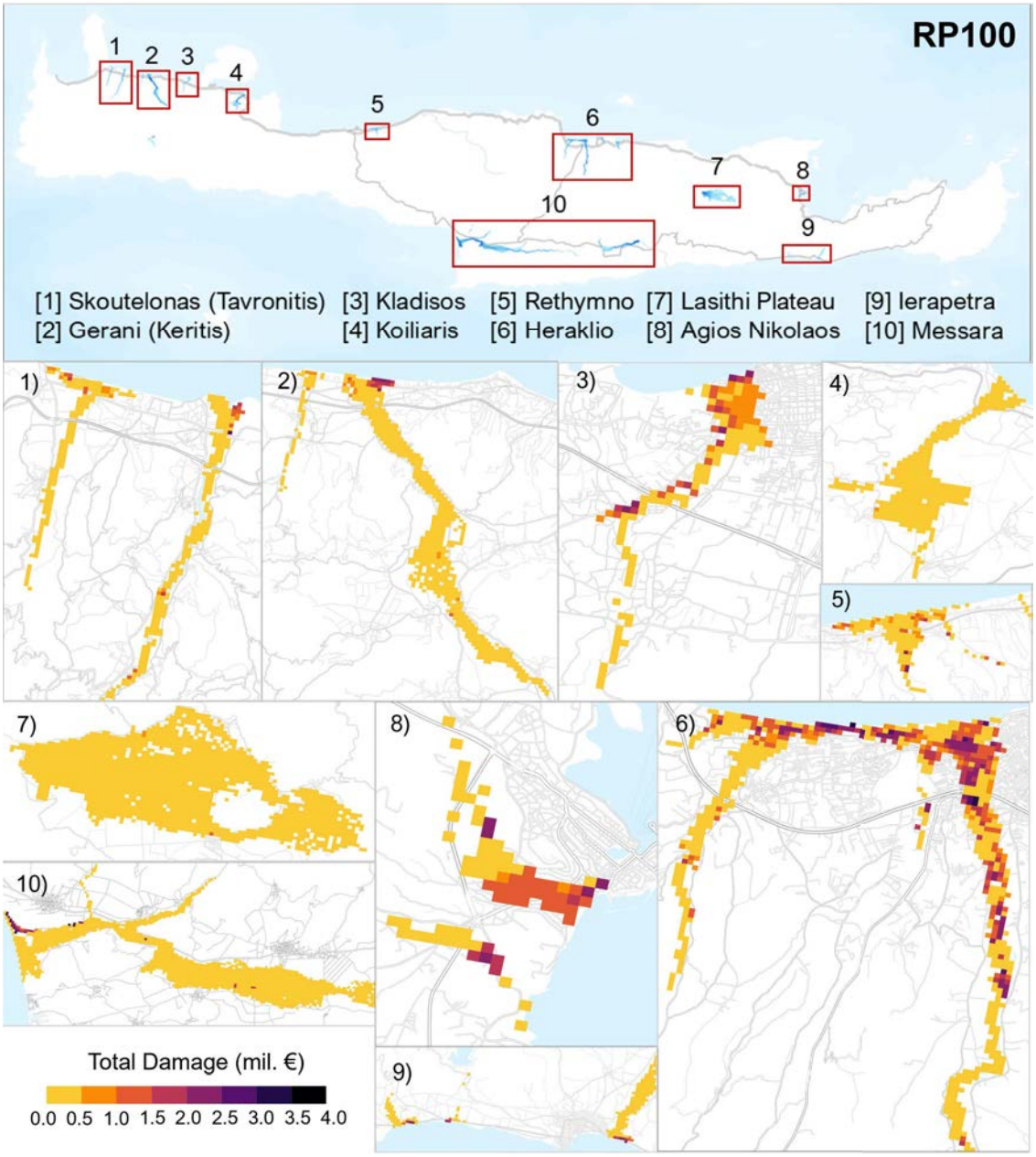

Figure 2-13 Spatial distribution of land-use based flood damage for RP100 in the ten areas of interest.

Flood building damage and population exposure

For the building-level flood risk and population exposure analysis, the refined workflow was applied consistently to all ten flood-prone areas (Figure 2-8). The accompanying Figure 2-14 focuses on Heraklion as the most exposed urban hotspot, while Table 2-4 and Table 2-5 summarize results for all areas.

In Heraklion, mean direct damage to buildings is estimated at about €265 million for a 1-in-50-year flood (RP50), rising to €314 million for RP100 and almost €590 million for RP1000, with maximum realizations reaching €732 million in the most severe scenario. Other areas show substantially lower absolute losses: for RP100, mean damages range from about €9–13 million in Koiliaris and Lasithi Plateau to €60–88 million in Rethymno and €59–80 million in Messara and Ierapetra. This confirms that, although flooding is a distributed problem along the north and south coasts, large, urbanized deltas and coastal plains concentrate the bulk of expected economic losses.

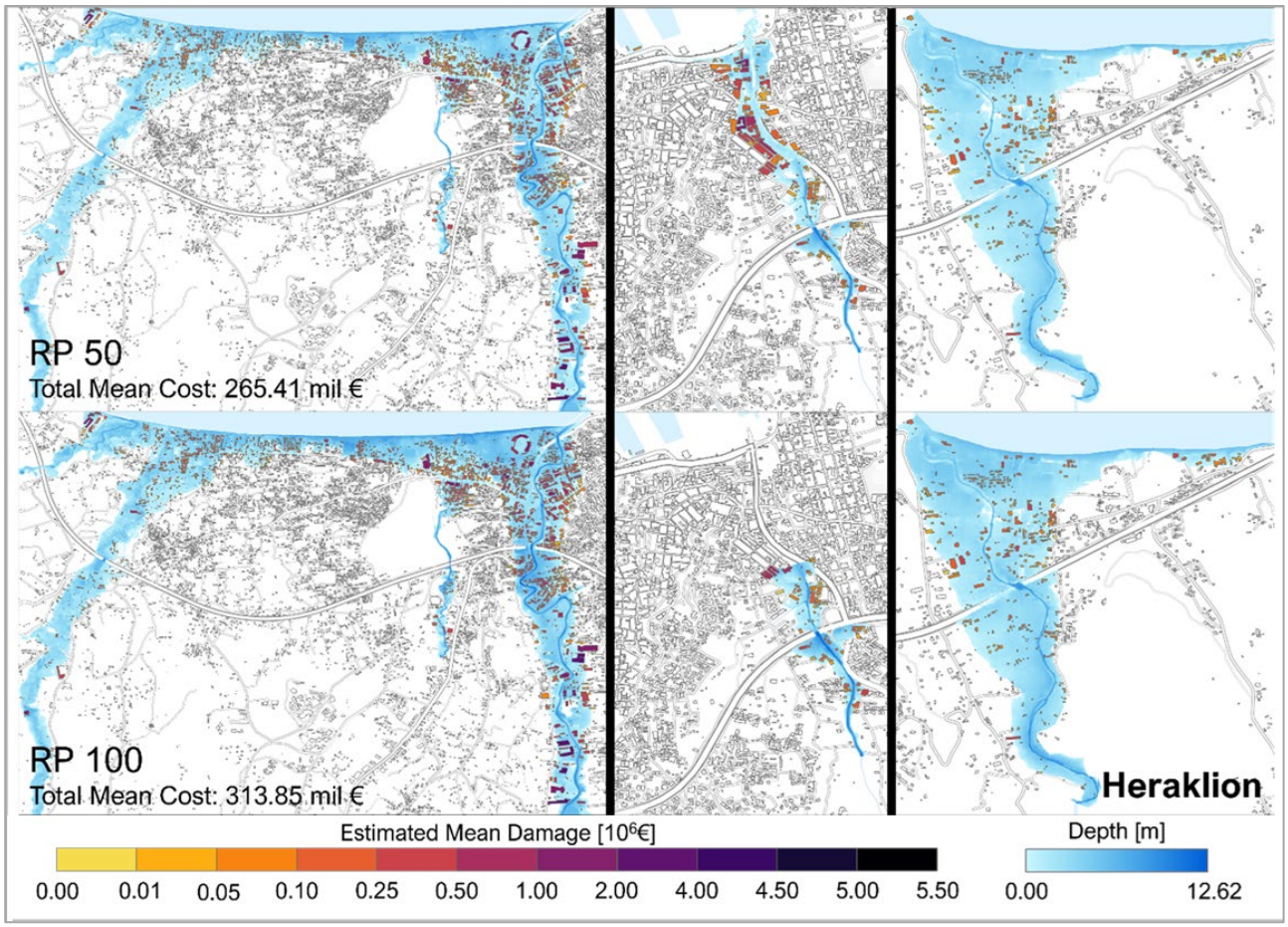

Figure 2-14 Estimated mean direct damage to individual buildings in Heraklion for RP50 and RP100. Colored polygons show the spatial distribution of mean damage per building (in 10^6 €), overlaid on the corresponding flood-depth maps; zoomed panels highlight critical hotspots along the main urban torrents.

Table 2-4: Total mean and maximum damage to buildings per region, of a 50, 100, and 1000 return period flood event, based on current climatic conditions.

	Total maximum damage [10^6€]					
	RP50		**RP100**		**RP1000**	
Region	***Mean***	***Max***	***Mean***	***Max***	***Mean***	***Max***
Tavronitis Skoutelonas	22.8	19.0	31.2	23.0	85.3	35.6
Keritis Maleme	16.0	22.6	26.8	37.2	48.6	60.8
Kladisos	30.9	46.6	44.0	63.0	99.3	124.2
Koiliaris	7.6	9.8	9.7	12.4	19.3	23.2
Rethymno	60.2	34.2	87.6	46.3	176.0	105.7
Heraklion	265.4	378.9	313.8	427.5	589.2	731.5
Lasithi Plateau	8.5	12.9	8.6	13.0	14.2	19.8
Agios Nikolaos	26.0	36.1	31.1	41.8	55.2	66.2
Ierapetra	68.5	135.2	80.0	152.3	133.9	229.4
Messara	52.5	70.5	59.3	79.0	99.3	117.2

The population exposure analysis shows a similar hierarchy. Under current climate, total exposed number of inhabitants across the ten areas range from roughly 1,000-3,000 people for small coastal plains (Koiliaris, Tavronitis–Skoutelonas, Keritis, Lasithi Plateau) up to 7,000-13,000 in Messara, Kladisos and Ierapetra. Heraklion again dominates, with around 30,000 people exposed for RP50 and more than 42,000 for RP1000. The number of potentially displaced inhabitants (buildings experiencing depths above the displacement threshold) reaches 16,000, 19,000 and 34,000 people

for RP50, RP100 and RP1000 respectively in Heraklion, compared with a few hundred to several thousand in the other areas.

Table 2-5: Total estimated exposed and displaced number of inhabitants per region, of a 50, 100, and 1000 return period flood event, based on current climatic conditions.

	Total Exposed | Displaced Population					
Region	**RP50**		**RP100**		**RP1000**	
Tavronitis Skoutelonas	2274	591	2486	832	3050	1723
Keritis Maleme	2070	762	3301	1582	4360	2879
Kladisos	7205	897	8247	1545	11260	6877
Koiliaris	944	425	1073	575	1553	1098
Rethymno	3753	964	4933	1490	7956	5766
Heraklion Town	29947	16397	31306	19940	42490	34137
Lasithi Plateau	1750	252	1753	247	2228	659
Agios Nikolaos	2697	1711	2850	2112	3470	3020
Ierapetra	12253	2337	13257	2887	17033	6238
Messara	6976	3414	7472	3832	7314	5863

Extreme precipitation

The extreme-precipitation workflow translates EURO-CORDEX daily rainfall projections into return levels and changes in frequency for very intense 24-hour events over Crete. Figure 2-15 summarizes results for the selected 200 mm day^{-1} threshold, which is representative of high-impact episodes linked to flash flooding and fluvial interactions. The upper panels show the relative change in the 50-year return level of 24-hour precipitation, while the lower panels express the same information as changes in the return period (years) for exceeding the 200 mm day^{-1} threshold, comparing three future time slices (2011–2040, 2041–2070, 2071–2100) to the 1976–2005 baseline under RCP4.5 and RCP8.5.

Under RCP4.5, the multi-model mean indicates modest but spatially coherent increases in event magnitude across much of Crete by mid-century, with the strongest signal appearing in southern and eastern sectors. The corresponding return-period maps show a shortening of return times for 200 mm day^{-1} events, particularly along windward slopes and in parts of north-central and eastern Crete, suggesting that what is currently an event rarer than once in 50 years may become substantially more frequent. Under RCP8.5, both the intensity and frequency shifts are amplified: large parts of the island exhibit marked increases in 24-hour extremes and pronounced reductions in return periods by the end of the century, especially in southern and eastern grid cells. Although individual model spread remains considerable, the multi-model signal consistently points towards a more hazardous regime of short-duration, high-intensity rainfall, with implications for flash-flood risk in small catchments, urban drainage exceedance, and compound flooding when such events coincide with saturated soils.

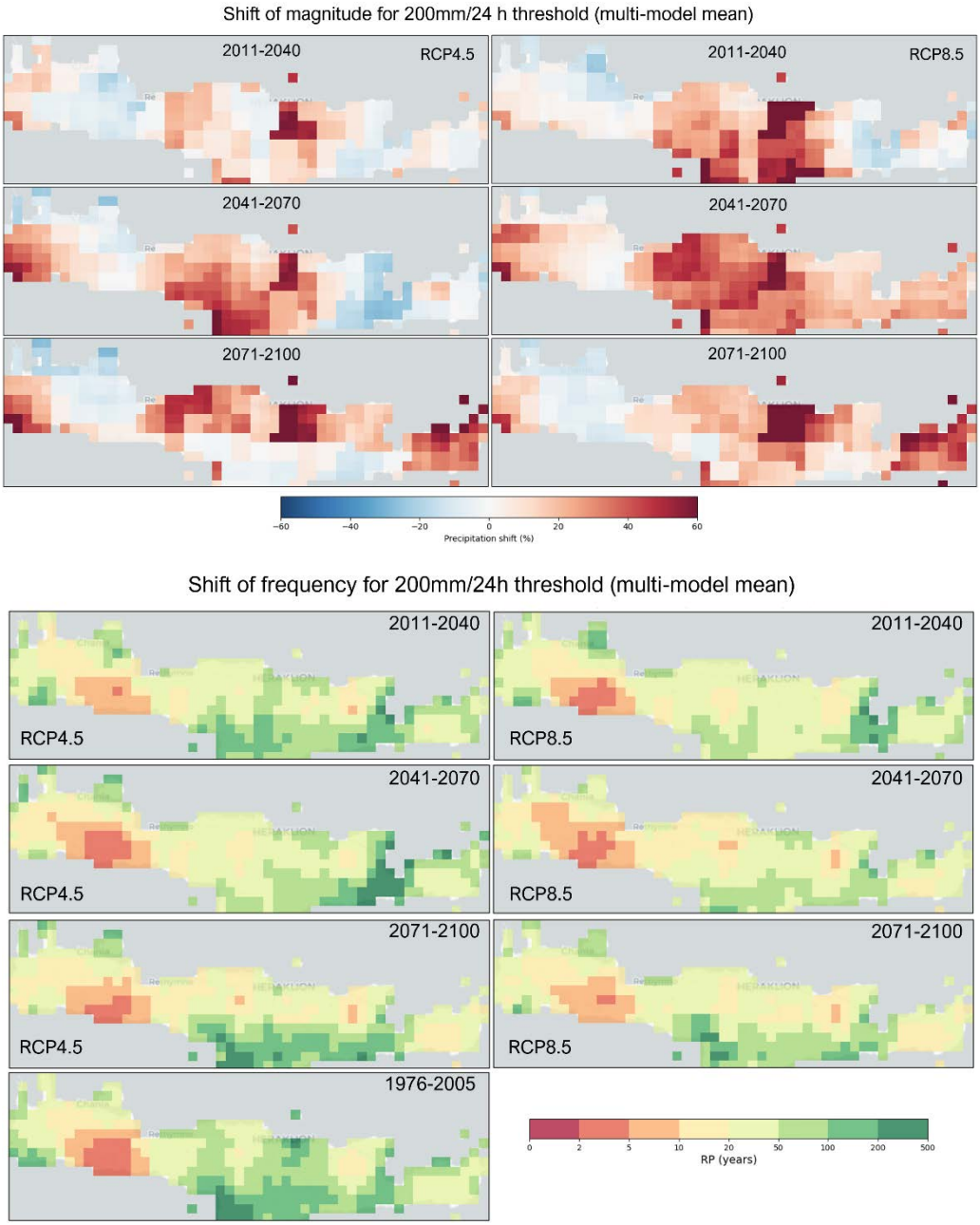

Figure 2-15 Top panels: relative change (%) in 24-hour precipitation associated with the medium-impact rainfall threshold of 200 mm/day over Crete, for three future periods (2011–2040, 2041–2070, 2071–2100) under RCP4.5 (left column) and RCP8.5 (right column), expressed as a percentage shift with respect to the 1976–2005 baseline. Bottom panels: equivalent return period (years) of exceeding the 200 mm/day severe-impact rainfall threshold over Crete, for the same periods and scenarios

Extreme discharge

Figure 2-16 summarizes projected changes in extreme river discharges for the Giofiros (Heraklion) and Keritis (Chania) basins, expressed as relative change (%) in 10-year (RP10) and 50-year (RP50) peak flows for three future periods (2011–2040, 2041–2070, 2071–2100) under RCP4.5 and RCP8.5. For both basins and return periods, the ensemble indicates predominantly positive changes relative to the historical baseline, with increases generally growing from the near-term to the end of the century and being larger under RCP8.5 than under RCP4.5. The spread across GCM-RCM members is substantial, particularly for the longer return period RP50, with some models showing

only small changes or even slight decreases in extremes, and others suggesting pronounced amplification of peak flows. This spread highlights that, while a tendency towards higher extreme discharges is plausible, especially for Giofiros in the mid- and late-century and for Keritis under RCP8.5, the magnitude of change remains highly uncertain. In risk terms, these results support a precautionary approach for design and reinforcement of flood-protection measures in the two basins, while also emphasizing the need to consider a range of plausible futures rather than a single deterministic estimate.

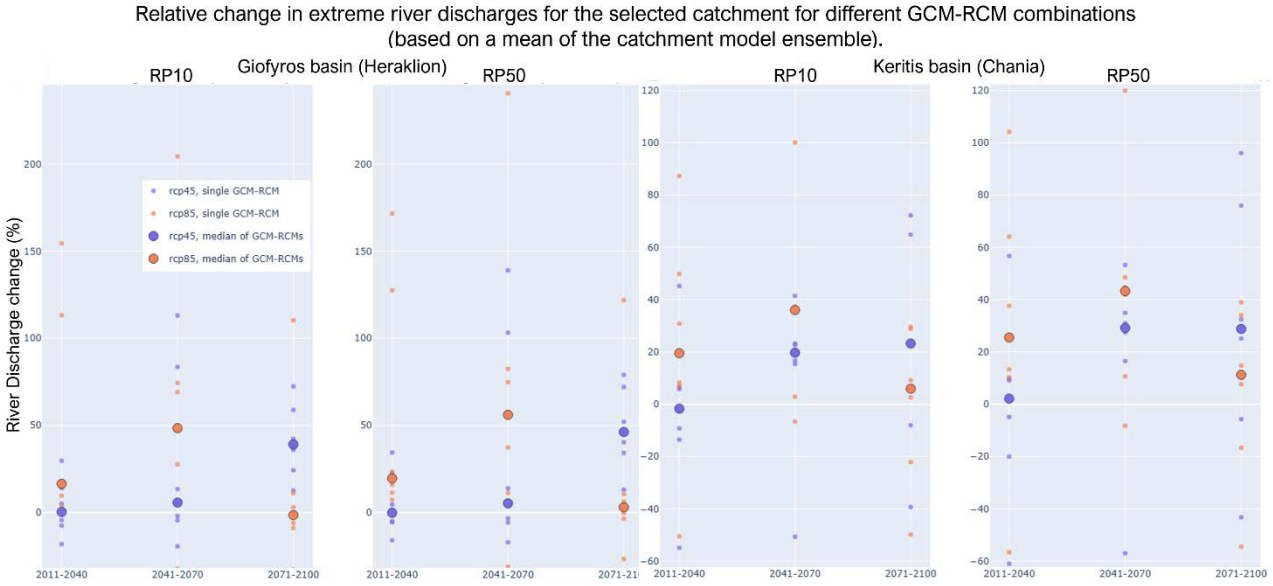

Figure 2-16 Relative change (%) in 10-year and 50-year extreme river discharges for Giofiros (left) and Keritis (right) for the future periods 2011–2040, 2041–2070 and 2071–2100 under RCP4.5 and RCP8.5, compared to the historical baseline; dots show individual GCM–RCM combinations and large symbols the ensemble medians.

2.4 Key Risk Assessment Findings

2.4.1 Mode of engagement for participation

The Key Risk Assessment was carried out through an online survey combined with a dedicated stakeholder workshop on 18 December 2025. Thirty-three (33) representatives of the Region of Crete and sectoral directorates (water resources, civil protection, environment and spatial planning, rural development, tourism) participated.

After presenting the refined drought and flood assessments, participants were guided through the CLIMAAX Key Risk Assessment protocol and the simplified online dashboard. Each participant independently scored, for river flooding and drought, (i) current and future severity, (ii) urgency of action and (iii) existing resilience/climate-risk-management (CRM) capacity. Scores were then aggregated (median values) and discussed in plenary, with participants able to adjust their ratings considering the model results and peers' arguments. The final dashboard (Figure 2-17) reflects this combined quantitative and inclusive process.

During the discussion, stakeholders also commented explicitly on limitations of the underlying risk analyses. For example, for drought assessment, water and agricultural services stressed that the exposure and vulnerability patterns are plausible at regional scale, but that the SSP-based projections of land use are too coarse to capture local realities and planned developments. They requested more locally co-developed socio-economic scenarios in future work. For floods, civil

protection and planning departments welcomed the move to high-resolution hazard and exposure data for the current climate but highlighted that the absence of future high-resolution flood maps and the limited information on building use and occupancy restrict the depth of risk evaluation.

Risk Workflow	Severity C	Severity F	Urgency	Capacity Resilience/ CRM	Risk Priority
River flooding	3	3	3	2	High
Drought	2	3	4	2	High

Severity	Urgency	Resilience Capacity	Risk Ranking
Critical	Immediate action needed	High	Very high
Substantial	More action needed	Substantial	High
Moderate	Watching brief	Medium	Moderate
Limited	No action needed	Low	Low

Figure 2-17: Key Risk Assessment dashboard for Crete, showing stakeholder-derived scores of current (C) and future (F) severity, urgency of action, and resilience/climate-risk-management capacity for river flooding and drought.

2.4.2 Gather output from Risk Analysis step

Risk assessment outputs were condensed into a short briefing and used as the evidence base for stakeholder scoring.

For drought, the evaluation used:

- Municipal and basin-scale relative drought risk categories and their projected changes in the form of maps and tables (risk ranking of municipalities).
- Maps of agricultural drought revenue losses for rainfed olives.
- The olive yield-climate analysis summarizing projected percentage yield changes.

For floods, the evaluation used:

- High-resolution river-flood depth and damage maps (RP50, RP100, RP1000) for ten hotspot areas.
- Estimates of direct building damage and displaced population by return period and region.
- Island-wide projections of extreme precipitation, shifts in intensity and frequency, and river discharge projected changes for two key basins.

2.4.3 Assess Severity

Participants rated river flooding severity as substantial (score 3) for both current and future conditions. This reflects past destructive events (e.g. the 2019 Chania floods), the large, expected damages in several hotspots (Heraklion, Messara, northern Chania) and the potential for casualties and major disruption to transport, housing and tourism infrastructure, even though events are episodic. At the same time, some stakeholders stressed that the modelled economic damages to agricultural areas, especially in the Messara plain, appear exaggerated, because they are derived from generic land-use based vulnerability curves. In the Cretan context, floods are predominantly fluvial, water usually drains quickly from fields, and perennial crops such as olive trees are relatively

resistant to short-lived inundation and as a result, depth-damage relationships for agricultural land may overestimate real losses.

For drought, current severity was rated moderate (2) but future severity substantial (3). Stakeholders linked this to: (i) the documented upward trend in temperature and recent multi-year drought; (ii) the concentration of relative drought risk and agricultural losses in Heraklion, central plains and parts of Lasithi; and (iii) the strong dependence of agriculture, tourism and domestic supply on finite surface and groundwater resources. They also emphasized that water demand is expected to rise, particularly in areas with intense tourism activity, so even if climate conditions only moderately worsen, the combination of higher demand and limited resources is likely to amplify future water scarcity.

Feedback from the workshop suggests that regional decision makers have an overall basic to moderate level of understanding of climate risks, but this knowledge is uneven across departments and often focused on past events rather than forward-looking, scenario-based risk. Staff working on water resources and civil protection are generally more familiar with drought and flood concepts, whereas other sectors expressed a need for clearer guidance on interpreting model outputs, uncertainties and risk indicators.

2.4.4 Assess Urgency

For each risk, stakeholders were asked to rate when major impacts are expected, whether conditions are likely to worsen in the near term, and how persistent the hazard is. Scores were given for “now” and for the next 10–20 years, consistent with a realistic planning horizon.

River flooding was assigned an urgency score of 3 (more action needed). Stakeholders recognized that severity is already substantial and that damaging events (e.g. 2019 storms) can occur at any time, driven by intense storms. However, they also noted that: (i) no strong, systematic near-term increase in fluvial flood hazard emerges from the climate projections and (ii) some structural and organizational measures are already in place. This combination led to the view that action cannot be postponed, but the situation does not yet warrant the “immediate action needed” category at least at an island scale, but for specific locations.

Drought received a higher urgency score of 4 (immediate action needed). Participants emphasized that severity is projected to increase from moderate to substantial. They also stressed that the process is already unfolding as recent multi-year droughts, steadily rising temperatures, and recurrent water-supply tensions in Heraklion, eastern Lasithi, and tourism hotspots were repeatedly cited and as slow-onset hazard impacts accumulate over several years on local aquifers, reservoirs, ecosystems and perennial crops. Stakeholders also stressed that water demand is expected to rise further through tourism growth, localized urban expansion and pressure for more irrigation, so that even moderate additional climatic drying could rapidly push some systems beyond safe operating margins.

Across both risks, the discussion of methodological limitations (e.g. coarse and uncertain land-use projections for drought, lack of future high-resolution flood maps and detailed building attributes) did not reduce urgency scores but rather reinforced the message that adaptation planning and data and monitoring improvements must proceed in parallel.

2.4.5 Understand Resilience Capacity

Participants were asked to consider financial, human, institutional, physical, and natural capacities, as well as existing and planned measures. The majority view placed Crete in the medium-substantial

range for both hazards, with the responses reflecting an overall “substantial but not sufficient” level of climate-risk management capacity.

For drought, stakeholders highlighted a number of positive elements: the existence of a Regional Adaptation Action Plan and the Drought Water Scarcity Action Plan which together provide a formal framework for water management and adaptation. On the physical side, large multi-purpose dams (e.g. Aposelemis, Faneromeni) and an extensive, though imperfect, irrigation network already support part of the agricultural and domestic demand, while groundwater still offers an important buffer in several basins. Human and institutional capacity is supported by active regional water management authorities. At the same time, weak spots were clearly recognized: absence of an operational drought-monitoring system, limited observations, fragmented governance of irrigation, and constrained staff and time for systematic climate-risk integration into everyday decisions. Financial capacity exists through national and EU funds, but competition among sectors and the effort required to prepare mature, climate-robust projects were seen as significant bottlenecks.

For floods, resilience is strengthened by established civil-protection procedures, and some implemented or planned structural measures in major flood prone areas and along key river reaches. Early-warning systems based on meteorological forecasts and emergency protocols were viewed as functional, though not always sufficiently tailored to small catchments and flash flooding. Social capacity was generally rated as moderate. Awareness is high immediately after major events but tends to fade, and risk information is not yet systematically embedded in spatial planning, but for specific location.

Participants agreed that Crete has an important base of plans, infrastructure and expertise, but these are not yet adequate to fully cope with the projected evolution of drought and flood risk. Increasing resilience will require institutionalizing climate-risk monitoring especially for drought, improving data and information flows, upgrading and adapting water infrastructure, and strengthening cross-sectoral coordination so that climate-risk considerations become routine in regional planning and investment decisions.

2.4.6 Decide on Risk Priority

Risk priority was derived directly from the stakeholder scores summarized in Table 2-6. For river flooding, both current and future severity medians are substantial (3), with relatively low spread (StDev = 0.85). Urgency is also scored 3 (“more action needed”), while resilience capacity is only medium (2). For drought, the median current severity is moderate (2), but future severity rises to substantial (3) and urgency reaches 4 (“immediate action needed”), reflecting concerns about multi-year drought, growing water demand and structural pressures on agriculture and supply. Resilience capacity again scores only 2 (medium).

The aggregated scores were then discussed linked to the quantitative risk results confirming that:

- Drought should be treated as a High-priority risk, with increasing severity, immediate action needed, and only medium-substantial current resilience capacity.
- River flooding should also be treated as a High-priority risk, with substantial severity and more action needed, especially in a limited number of well-defined hotspots.

Table 2-6: Median and standard deviations from stakeholder scoring of severity, urgency and capacity for river flooding and drought.

Risk Workflow	Severity				Urgency		Capacity Resilience/CR		Risk Priorit
	C		F						
	Median	StDev	Median	StDev	Median	StDev	Median	StDev	
River flooding	3	0.85	3	0.83	3	0.76	2	0.62	**High**
Drought	2	0.76	3	0.83	4	0.91	2	0.36	**High**

2.5 Monitoring and Evaluation

Phase-2 provided a much clearer and more spatially detailed picture of drought and flood risk in Crete but also exposed where the evidence base is still weak. The main technical advances were:

- (i) using locally relevant indicators for relative drought risk (e.g. groundwater access, irrigated area, tourism exposure),
- (ii) high-resolution river-flood hazard data and building footprints for 10 flood-prone areas, and
- (iii) independent olive-yield impact analysis to cross-check agricultural drought results.

The most important difficulties were the absence of locally downscaled future land-use cropping scenarios, the lack of high-resolution future flood hazard maps, and the limited information on building function and occupancy, which constrain the realism of socio-economic impact estimates.

Stakeholders were involved throughout (consultation meetings, thematic workshops, online survey) and played a central role in interpreting results and scoring severity, urgency and capacity. Their feedback was broadly positive on the usefulness of spatial risk maps and hotspot identification, but they stressed the need for: (i) more realistic local socio-economic scenarios, and (ii) operational products that can feed directly into the drought-water-scarcity action plan.

Learning is ensured by documenting all Phase-2 methods in technical deliverables, sharing data, and importantly by the Region of Crete's new initiative to establish a Regional Climate Change Observatory in collaboration with scientific institutions. The Observatory is envisaged as the long-term home for climate-risk indicators and monitoring.

New data assembled in Phase-2 will support the update of the next Regional Plan for Adaptation to Climate Change (RAAP) of Crete (e.g., Microsoft building footprints, and regionalized climate indices for extremes). Further improvements will require better local crop-yield data, locally developed land-use and water-demand scenarios, high-resolution flood hazard projections models, and richer attributes for buildings for hot-spot regions.

Communication of the final outcomes will rely on: (i) the main CLIMAAX Phase-2 report, (ii) sector-specific summaries for water, agriculture and civil protection, and (iii) continued media and workshop activities by the Region of Crete and the Technical University of Crete, including at least two co-organized targeted events in the next project phase to engage local, on-the-ground stakeholders.

Throughout Phase 2, resources were used efficiently and in a clearly complementary way. The Technical University of Crete concentrated on the technical core of the risk assessment, implementing the updated CLIMAAX workflows, processing the drought and flood analyses, participating in the Barcelona CLIMAAX meeting, and supporting the presentation and interpretation of results in stakeholder workshops and meetings. The Region of Crete ensured that this work was

well anchored locally by providing access to key regional datasets, leading the organization of local events, and maintaining continuous interaction with TUC during all stages of the assessment. In parallel, the Region of Crete co-organized a joint event with the Pathways2Resilience Path4PDE project, allowing experience exchange and leveraging synergies with other EU initiatives on adaptation to climate change.

The CRA from both phases has had a clear positive impact on understanding climate risk in Crete. At institutional level, it has strengthened the Region's capacity to interpret climate information, and link it to concrete hotspots (basins, municipalities, APSFRs). At stakeholder level, the workshops, survey and maps improved awareness of how risks vary within the island and how they may evolve under different futures, moving discussion from general concern to specific areas, sectors and thresholds. The work will be fed into the ongoing update of the RAAP and the Drought-Water Scarcity Action Plan and is expected to support future initiatives (e.g., the Regional Climate Change Observatory) by providing a robust, spatially explicit evidence base for prioritizing investments.

2.6 Work plan Phase 3

Phase 3 will support the improvement of risk management within the local context, and in specific the update and extension of the Action Plan for Combating Drought and Water Scarcity in the Region of Crete, in collaboration with the Section of Hydroeconomy of the Decentralized Administration of Crete and the Directorate of Sustainable Development of the Region of Crete.

Phase 3 will co-design a drought-monitoring pathway for Crete. This pathway will show how existing open datasets (primarily the European Drought Observatory) together with future local information can be combined into a practical monitoring system that underpins the updated drought-water scarcity plan and the emerging Regional Climate Change Observatory.

Work will start by reviewing how the current drought-water scarcity plan defines stages and triggers (indicators, thresholds) and what information the competent services actually use. On this basis we will outline how EDO indicators (e.g. CDI, SPI, soil-moisture and vegetation anomalies) can be systematically used to characterize conditions in these sub-basins and linked to the existing four drought stages. Phase 3 will then test and document example workflows (conceptual data flows, indicative maps/graphs, simple calculation sheets) that illustrate how such indicators could be updated regularly and reported to decision makers, and where local data streams (reservoir levels, abstractions, crop conditions) could be plugged in as they become available.

Analytical work, adaptation-capacity exploration and a second round of stakeholder discussions are scheduled mainly between February 2026 and May 2026 (Figure 2-18), with synthesis into Deliverable 3 by July 2026 and participation in the final CLIMAAX workshop in Brussels at the end of 2026.

Climate Resilient crETE - CRETE	Aug-25	Sep-25	Oct-25	Nov-25	Dec-25	Jan-26	Feb-26	Mar-26	Apr-26	May-26	Jun-26	Jul-26
Phase 3												
Adaptation capacity exploration			M3.1							M3.4		
Stakeholders discussions					M3.2			M3.3			M3.5	
D3 Elaboration												**D3**

Figure 2-18: Phase-3 work plan for Climate Resilient crETE – CRETE.

3 Conclusions Phase 2- Climate risk assessment

Phase-2 consolidated and refined the climate-risk picture for Crete by updating the CLIMAAX drought and flood workflows with higher-resolution data, improved methods and targeted stakeholder input. Compared with Phase 1, the analyses now provide a more spatially detailed and sector-specific understanding of where and how climate hazards interact with exposure and vulnerability, and where the main uncertainties remain.

Drought: The updated relative drought analysis confirms that drought pressure on Crete is not a transient anomaly but a structural risk. Using basin-municipality units and revised hazard, exposure and vulnerability indicators, the assessment shows that:

- Present-day drought risk is highest in southern and central municipalities where relatively high climatic stress coincides with intensive agriculture and limited groundwater availability.
- Under SSP3-7.0 and SSP5-8.5, these high-risk zones persist and expand, with several municipalities moving up in risk classes by the end of the century. Even under SSP1-2.6, pockets of elevated risk remain where agricultural and tourism water demand is concentrated.
- Stakeholders highlighted that these results are broadly consistent with recent multi-year drought experience, reservoir stress and local observations, while also revealing inland hotspots that receive less public attention than coastal tourism centers.

The agricultural drought workflow and the olive-yield impact analysis provide a complementary view focused on rainfed and irrigated olive groves (the main pillar of agricultural activity in Crete):

- The CLIMAAX agricultural workflow indicates substantial revenue losses if irrigation cannot be guaranteed, with multi-model mean losses exceeding several hundred €/ha in high-value olive zones under dry years and potentially reaching around 10,000€/ha in intensively cultivated areas under persistent precipitation deficits.
- The independent olive-yield study, based on observed production and CORDEX climate indices, suggests no robust long-term trend in yields at island scale, but a growing influence of heat and water-stress indicators on interannual variability.

Together, these findings point to a risk profile characterized less by gradual yield decline and more by increasing frequency of very bad years, especially when drought coincides with management or market constraints.

Across workflows, stakeholders recognized that future water demand is likely to increase, particularly due to tourism, higher irrigation expectations and possible changes in crop mix. This reinforces the message that even if climatic drought intensification were moderate, water-scarcity risk would still grow without demand-side measures and stricter allocation rules.

Floods: Phase-2 shifted from global JRC products to local 2 m flood-depth maps from the EL13 Flood Risk Management Plan, combined with detailed Microsoft building footprints. The analysis of ten flood-prone areas shows that:

- Heraklion, Ierapetra and Messara stand out with the highest potential building damage, with mean direct damages for Heraklion alone ranging from ≈265 M€ (RP50) to ≈590 M€ (RP1000).
- Estimated exposed and displaced population is also highest in these areas, with smaller though still significant numbers in Rethymno, Ierapetra and Messara.

- Comparison with OpenStreetMap demonstrates that using near-complete Microsoft building footprints greatly improves the credibility of exposure estimates and highlights dense built-up corridors that were partially missed in Phase 1.

The extreme precipitation and extreme discharge analyses add a climatic perspective:

- EURO-CORDEX ensembles under RCP4.5 and RCP8.5 indicate increases in 24-h heavy rainfall intensity and/or frequency, particularly in western and central Crete by mid- and late-century.
- Catchment-scale hydrological simulations for Giofiros and Keritis suggest higher high-flow discharges in future decades, though with substantial model spread. This supports the view that existing flood-risk estimates are likely conservative under continued warming.

Challenges addressed and remaining gaps

Phase 2 successfully addressed several Phase-1 limitations:

- Replaced coarse global layers with higher-resolution hazard, exposure and vulnerability datasets (e.g. CHELSA/ISIMIP3b at basin scale, Microsoft buildings, refined agricultural and tourism indicators).
- Introduced new impact-oriented metrics, such as olive-specific revenue loss due to irrigation failure, building-level flood damage and displaced population.
- Strengthened stakeholder engagement, using the Key Risk Assessment protocol and survey to co-evaluate severity, urgency and resilience capacity, leading to a shared conclusion that both drought and river flooding merit high priority.

At the same time, important challenges remain unresolved and motivate future and Phase-3 work:

- Drought results still rely on global land-use projections (GCAM/Detemer, SPAM 2010) and simplified vulnerability proxies and stakeholders questioned their realism for local crops and irrigation expansion.
- Flood analysis, while much improved, is limited to current-climate hazard maps; fully consistent future flood scenarios would require new local hydrodynamic modelling.

Despite these limitations, Phase 2 substantially deepens the understanding of climate-related drought and flood risks in Crete, providing a robust analytical foundation and shared stakeholder framing for Phase-3 work on adaptation capacity, monitoring pathways and integration into regional risk-management plans. Building on these results, the analyses are expected to directly support the next update of the Regional Plan for Adaptation to Climate Change (RAAP), to feed into the design of the new Regional Climate Change Observatory being initiated by the Region of Crete with scientific partners, and to inform the revision and extension of the Action Plan for Combating Drought and Water Scarcity, ensuring that forthcoming measures are evidence-based, spatially targeted and aligned with Crete's long-term resilience strategy.

4 Progress evaluation and contribution to future phases

This deliverable covers the 2nd phase of climate-related drought and flood risk assessment for Crete. Building on the first-phase screening, it refines the CLIMAAX workflows with local datasets, higher spatial resolution and sector-specific analyses. The results provide a more realistic picture of where and why risk is concentrated, both at sub-basin and municipal level, and under a range of future socio-economic and climate pathways.

Phase-2 work has also strengthened the interface with regional policy. The revised indicators, maps and statistics are now structured so they can be directly linked to the Regional Adaptation Action Plan, the River Basin Management Plan and the Drought Water Scarcity Action Plan of Crete. Communication and stakeholder activities ensured that methods and findings were discussed in detail with regional authorities and sectoral actors. Progress against the project Key Performance Indicators and Milestones is summarized in Section 4.1. All methodological milestones and the majority of communication targets have been already achieved.

The insights from this phase feed directly into the third phase of CLIMAAX-CRETE, which will focus on translating the risk assessment into guidelines for development of operational drought monitoring and early-warning concept for the island, based on open data services (e.g. EDO), and on co-designing concrete adaptation options and monitoring metrics with the Region of Crete.

4.1 Key Performance Indicators and Milestones

The progress made in this phase is summarized in the tables below, highlighting achievements and pending actions:

Table 4-1: Overview key performance indicators

Key performance indicators	***Target until the end of the project***	***Progress***
KPI1 - Number of workflows successfully applied on Deliverable 1	2	2 + wildfires still resolving issues
KPI2 - Number of stakeholders involved in the activities of the project	25+	• 31 stakeholders during the 1st consultation meeting (15/01/2025) and 1st Workshop (19/03/2025) – 33 stakeholders during the 1st round of Stakeholders meeting on 18 Dec 2025 • Additionally, one joint workshop (27 attendees) of CLIMAAX-CRETE and Pathways2Resilience Path4PDE projects on 22 Oct 2025
KPI3 - Number of communication actions taken to share results with your stakeholders	4	• 1st consultation meeting and 1st Workshop (19/03/2025) • 1 joint workshop with Pathways2Resilience Path4PDE (22/10/2025) • 1st round of Stakeholders meeting on (18/12/2025)
KPI4 - Number of publications and dissemination actions	2 - (M3.5)	• Poster presentation at 1st FutureMed Workshop & Training School 29th September to 3rd October – Chania • Oral presentation and short publication at SafeHeraklion. Assessing Flood Risk and Extreme Precipitation in Crete. 22 to 24 October 2025.
KPI5 - Number of reports available for policy makers	3 - (D1, D2, D3)	• 1 (D1) + 2 technical reports for drought and floods (see sup. doc.)

Key performance indicators	*Target until the end of the project*	*Progress*
		• 2 (D2) + 2 technical reports for drought and floods
KPI6 - Number of articles in regional media mentioning the project	3	Various project activities like workshops and stakeholder meetings resulted to **over 20** regional media posts (up to 24/12/025). More information in D2 and accompanying sub-deliverables.

Table 4-2: Overview milestones

Milestones	*Completion Date*	*Progress*
M2.1 Local datasets for Drought Risk Workflow refinement defined	31/05/2025	Successfully completed
M2.2 Local datasets for Flood Risk Workflow refinement defined	31/05/2025	Successfully completed
M 2.3 Attend the CLIMAAX workshop held in Barcelona	10/06/2025	CRETE-CLIMAAX representative and poster
M2.4 Refined Drought Risk Workflow tested	07/12/2025	New relative locally tailored Drought Risk Assessment defined and tested.
M2.5 Refined Flood Risk Workflow tested	30/06/2025	Successfully tested several workflows related to flood hazard
M2.7 Refined Flood Risk Workflow successfully applied	27/11/2025	3 Refined Drought Risk Workflows successfully applied (Relative Drought Risk, Agricultural (olive) Drought Risk, Empirical olive yield impact analysis)
M2.6 Refined Drought Risk Workflow successfully applied	06/10/2025	Updated local river flood maps + flood buildings and population exposed + River flood discharges for Giofiros basin + heavy rainfall workflow
M2.8 Comparison of results between Phases 1 and 2 done	24/12/2025	Comparison of results between Phases 1 and 2 done for Flood and Drought Risks and reported in D2 and in 2 Detailed Technical Deliverables
M3.2 Round 1 of Stakeholders meeting done	04/11/2025	Key relevant studies defined: [1] Second Revision of the River Basin Management Plan for the Water District of Crete (EL13) – May 2024 [2] Preparation of the Regional Plan for Adaptation to Climate Change (RAAP) of Crete – December 2021 [3] Action Plan for Drought and Water Scarcity Management in the Region of Crete – April 2021
M3.1 Previous studies on existing management plans defined	18/12/2025	33 stakeholders during the 1st round of Stakeholders meeting on (18 Dec 2025). Additionally, one joint workshop (25 attendees) of CLIMAAX-CRETE and Pathways2Resilience Path4PDE projects on 22 Oct 2025.

5 Supporting documentation

The outputs generated in this 2nd phase of CLIMAAX-CRETE include this (D2) main Climate risk assessment deliverable, two detailed technical reports and updated communication and dissemination material. All documents are uploaded to the Zenodo repository.

1. Main report

- Deliverable 2: updated Climate Risk Assessment for Crete (PDF), presenting the refined methodologies, updated datasets and key findings for both drought and flood risk, together with their implications for regional adaptation planning.

2. Technical reports

- *2a. updated Drought Hazard and Risk Assessment for Crete* – Technical Report (PDF) – a stand-alone technical documentation of the updated drought workflows, covering the relative drought index, the refined agricultural drought assessment for olives and the linkage with the independent olive-yield impact analysis.
- *2b. updated Flood Hazard and Risk Assessment for Crete* – Technical Report (PDF) – a technical report describing the refined river-flood workflows, including use of local hydrological data, updated exposure layers and impact estimates for assets and population.

3. Communication and dissemination outputs

3.Communication Outputs CLIMAAX CRETE – 2nd Phase (PDF). A consolidated record of institutional press releases, regional and national media coverage, web posts, the SafeHeraklion 2025 oral presentation and abstract, and the CLIMAAX poster contribution to the Barcelona workshop, documenting how project results are communicated to stakeholders and the wider public.

4. Workshop and meeting material

4.CRETE-CLIMAAX workshop and meeting Agendas (PDF). Agendas and brief descriptions for the Phase 2 consultation and stakeholder workshops in Crete and the joint CLIMAAX–Path4PDE meeting in Barcelona, which were used to present interim findings, gather feedback and discuss links with regional planning instruments.

6 References

Calvin, K., Patel, P., Clarke, L., Asrar, G., Bond-Lamberty, B., Cui, R.Y., Di Vittorio, A., Dorheim, K., Edmonds, J., Hartin, C., Hejazi, M., Horowitz, R., Iyer, G., Kyle, P., Kim, S., Link, R., McJeon, H., Smith, S.J., Snyder, A., Waldhoff, S., Wise, M., 2019. GCAM v5.1: representing the linkages between energy, water, land, climate, and economic systems. Geoscientific Model Development 12, 677–698. https://doi.org/10.5194/gmd-12-677-2019

Diakakis, M., Mavroulis, S., Deligiannakis, G., 2012. Floods in Greece, a statistical and spatial approach. Nat Hazards 62, 485–500. https://doi.org/10.1007/s11069-012-0090-z

Grillakis, M.G., Kapetanakis, E.G., Goumenaki, E., 2022. Climate change implications for olive flowering in Crete, Greece: projections based on historical data. Climatic Change 175, 1–18. https://doi.org/10.1007/s10584-022-03462-4

Huizinga, J., De, M.H., Szewczyk, W., 2017. Global flood depth-damage functions: Methodology and the database with guidelines [WWW Document]. JRC Publications Repository. https://doi.org/10.2760/16510

Koutroulis, A.G., Grillakis, M.G., Daliakopoulos, I.N., Tsanis, I.K., Jacob, D., 2016. Cross sectoral impacts on water availability at +2 °C and +3 °C for east Mediterranean island states: The case of Crete. Journal of Hydrology 532, 16–28. https://doi.org/10.1016/j.jhydrol.2015.11.015

Koutroulis, A.G., Grillakis, M.G., Tsanis, I.K., Jacob, D., 2018. Mapping the vulnerability of European summer tourism under 2 °C global warming. Climatic Change 151, 157–171. https://doi.org/10.1007/s10584-018-2298-8

Koutroulis, A.G., Tsanis, I.K., Daliakopoulos, I.N., 2010a. Seasonality of floods and their hydrometeorologic characteristics in the island of Crete. Journal of Hydrology 394, 90–100. https://doi.org/10.1016/J.JHYDROL.2010.04.025

Koutroulis, A.G., Tsanis, I.K., Daliakopoulos, I.N., 2010b. Seasonality of floods and their hydrometeorologic characteristics in the island of Crete. Journal of Hydrology, Flash Floods: Observations and Analysis of Hydrometeorological Controls 394, 90–100. https://doi.org/10.1016/j.jhydrol.2010.04.025

Koutroulis, A.G., Vrohidou, A.-E.K., Tsanis, I.K., 2011. Spatiotemporal Characteristics of Meteorological Drought for the Island of Crete. https://doi.org/10.1175/2010JHM1252.1

Kreibich, H., Van Loon, A.F., Schröter, K., Ward, P.J., Mazzoleni, M., Sairam, N., Abeshu, G.W., Agafonova, S., AghaKouchak, A., Aksoy, H., Alvarez-Garreton, C., Aznar, B., Balkhi, L., Barendrecht, M.H., Biancamaria, S., Bos-Burgering, L., Bradley, C., Budiyono, Y., Buytaert, W., Capewell, L., Carlson, H., Cavus, Y., Couasnon, A., Coxon, G., Daliakopoulos, I., de Ruiter, M.C., Delus, C., Erfurt, M., Esposito, G., François, D., Frappart, F., Freer, J., Frolova, N., Gain, A.K., Grillakis, M., Grima, J.O., Guzmán, D.A., Huning, L.S., Ionita, M., Kharlamov, M., Khoi, D.N., Kieboom, N., Kireeva, M., Koutroulis, A., Lavado-Casimiro, W., Li, H.Y., LLasat, M.C., Macdonald, D., Mård, J., Mathew-Richards, H., McKenzie, A., Mejia, A., Mendiondo, E.M., Mens, M., Mobini, S., Mohor, G.S., Nagavciuc, V., Ngo-Duc, T., Thao Nguyen Huynh, T., Nhi, P.T.T., Petrucci, O., Nguyen, H.Q., Quintana-Seguí, P., Razavi, S., Ridolfi, E., Riegel, J., Sadik, M.S., Savelli, E., Sazonov, A., Sharma, S., Sörensen, J., Arguello Souza, F.A., Stahl, K., Steinhausen, M., Stoelzle, M., Szalińska, W., Tang, Q., Tian, F., Tokarczyk, T., Tovar, C., Tran, T.V.T., Van Huijgevoort, M.H.J., van Vliet, M.T.H., Vorogushyn, S., Wagener, T., Wang, Y., Wendt, D.E., Wickham, E., Yang, L., Zambrano-Bigiarini, M., Blöschl, G., Di Baldassarre, G., 2022. The challenge of unprecedented floods and droughts in risk management. Nature 2022 608:7921 608, 80–86. https://doi.org/10.1038/s41586-022-04917-5

Perdiou, A., Tsitoura, P., Aggelidis, I., Michailidou, E., Hatziparaskevas, K., 2017. Flood risk management plan for the River Basins of the Water District of Crete. HELLENIC REPUBLIC, MINISTRY OF ENVIRONMENT AND ENERGY, SPECIAL SECRETARIAT OF WATER.

Tichavský, R., Koutroulis, A., Chalupová, O., Chalupa, V., Šilhán, K., 2020. Flash flood reconstruction in the Eastern Mediterranean: Regional tree ring-based chronology and assessment of climate triggers on the island of Crete. Journal of Arid Environments 177, 104135. https://doi.org/10.1016/j.jaridenv.2020.104135

Tramblay, Y., Koutroulis, A., Samaniego, L., Vicente-Serrano, S.M., Volaire, F., Boone, A., Le Page, M., Llasat, M.C., Albergel, C., Burak, S., Cailleret, M., Kalin, K.C., Davi, H., Dupuy, J.-L., Greve, P., Grillakis, M., Hanich, L., Jarlan, L., Martin-StPaul, N., Martínez-Vilalta, J., Mouillot, F., Pulido-Velazquez, D., Quintana-Seguí, P., Renard, D., Turco, M., Türkeş, M., Trigo, R., Vidal, J.-P., Vilagrosa, A., Zribi, M., Polcher, J., 2020. Challenges for drought assessment in the Mediterranean region under future climate scenarios. Earth-Science Reviews 210, 103348. https://doi.org/10.1016/j.earscirev.2020.103348

Varotsos, K.V., Katavoutas, G., Kitsara, G., Karali, A., Lemesios, I., Patlakas, P., Hatzaki, M., Tenentes, V., Sarantopoulos, A., Psiloglou, B., Koutroulis, A.G., Grillakis, M.G., Giannakopoulos, C., 2025. CLIMADAT-GRid: a high-resolution daily gridded precipitation and temperature dataset for Greece. Earth System Science Data 17, 4455–4477. https://doi.org/10.5194/essd-17-4455-2025

Wang, T., Sun, F., 2022. Gross domestic product (GDP) downscaling: a global gridded dataset consistent with the Shared Socioeconomic Pathways. https://doi.org/10.5281/ZENODO.5880037

Wang, X., Meng, X., Long, Y., 2022. Projecting 1 km-grid population distributions from 2020 to 2100 globally under shared socioeconomic pathways. Sci Data 9, 563. https://doi.org/10.1038/s41597-022-01675-x

Funded by the European Union

CLIMAAX climate ready regions

Drought Hazard and Risk Assessment for Crete

2nd Phase

**Aposelemis reservoir, the main domestic water source of Heraklion town at its lower historical level Nov 2025*

Authors: Aristeidis Koutroulis, Technical University of Crete

Mikaela Papa, Technical University of Crete

Prepared for: The Region of Crete
Project Title: Climate Resilient Crete (CRETE)
Cascade Funded by: The European Union's Horizon Europe Climate Programme
Grant Agreement No.: 101093864 – CLIMAAX

Contents

1 Executive Summary 5
2 Introduction 7
2.1 Background and context 7
2.2 From Phase-1 to Phase-2 8
2.3 Objectives of the Phase-2 assessment 9
3 Methodological Framework 10
3.1 New Relative Drought Methodology for Crete 10
3.1.1 Conceptual framework 10
3.1.2 Hazard indicators 12
3.1.3 Exposure indicators 13
3.1.4 Vulnerability indicators and sub-indices 14
3.2 Updated Agricultural Drought Risk Assessment 16
3.2.1 Conceptual approach 16
3.2.2 Workflow updates relative to Phase-1 16
3.2.3 Hazard - Agricultural drought 17
3.2.4 Exposure - Agricultural drought 19
3.2.5 Vulnerability - Agricultural drought 20
3.2.6 Uncertainty considerations 21
3.3 Climate Change Impacts on Olive Oil Yield 22
3.3.1 Study overview 22
3.3.2 Data 22
3.3.3 Methodological approach for climate-yield relationships 25
4 Results 29
4.1 New Relative Drought Methodology for Crete 29
4.1.1 Relative drought Hazard maps 29
4.1.2 Relative drought Exposure maps 33
4.1.3 Relative drought Vulnerability maps 37
4.1.4 Relative drought Risk maps 41
4.1.5 Uncertainties and robustness of results - Relative Drought Risk 45
4.2 Updated Agricultural Drought Risk in Crete 45
4.2.1 Hazard patterns - Agricultural Drought 45

4.2.2 Risk maps and revenue losses - Agricultural Drought 49
4.2.3 Uncertainties and robustness of results - Agricultural Drought 52
4.3 Climate Change Impact on Olive Oil Yield 53
4.3.1 Baseline olive oil production and yield (2011–2022) 53
4.3.2 Observed climate-yield relationships (hazard-risk link) 56
4.3.3 Projected changes in climatic hazard indices 62
4.3.4 Projected changes in olive oil yield (risk) 63
4.3.5 Uncertainties and robustness of results 64
4.3.6 Comparison Agricultural drought workflow with olive-yield impact projections 65
5 Discussion 66
5.1 Synthesis across methods 66
5.2 Sectoral implications 67
5.2.1 Agriculture (with emphasis on olives) 67
5.2.2 Water resources 68
5.2.3 Tourism 68
5.2.4 Environment and ecosystems 68
5.3 Alignment with Crete's Regional Adaptation Action Plan of Crete (RAAP) 69
5.4 Limitations and Future Work 70
5.4.1 Relative drought Risk assessment 70
5.4.2 Agricultural drought workflow (olive revenue loss) 71
5.4.3 Olive-yield climate impact study 72
6 Conclusions and recommendations 72
6.1 Key conclusions 72
6.1.1 Relative drought risk 72
6.1.2 Agricultural drought (olive revenue loss) 73
6.1.3 Olive yield projections 73
6.2 Recommendations 73
6.2.1 Water management and irrigation 73
6.2.2 Agricultural practices and diversification 74
6.2.3 Monitoring and data needs 74
6.2.4 Policy and planning 74

References 75
7 Appendix 77

Disclaimer: In the preparation of this work, generative Artificial Intelligence (ChatGPT) was used as an assisting tool in specific parts of the text, primarily to improve grammar, sentence structure, and overall clarity, and to help shorten certain sections.

1 Executive Summary

This report presents the Phase-2 assessment of drought risk in Crete within the CLIMAAX-CRETE project, with emphasis on (i) a new, Crete-tailored relative drought risk index, (ii) agricultural drought impacts on olive groves and (iii) independent climate–olive yield projections. All components combine hazard, exposure and vulnerability to produce spatially explicit information at sub-basin and municipal level, designed to support the Regional Adaptation Action Plan and the forthcoming Drought & Water Scarcity Action Plan.

The updated relative drought analysis shows that drought risk is strongly structured within the island and is not uniform across the four regional units. A belt spanning central and south-eastern Crete systematically emerges in the higher risk classes, where relatively adverse climatic conditions coincide with intensive agriculture, tourism pressures and more constrained water resources. Western Crete appears generally in lower-intermediate risk categories, though with local hotspots. Across future scenarios, risk increases are moderate under low end scenarios, but become more marked and spatially extensive under SSP3-7.0 and SSP5-8.5, with many basins shifting to increased risk classes by the end of the century.

The agricultural drought workflow for olive production, re-run with the corrected CLIMAAX methodology and updated GAEZ-v5 crop value and irrigation information, confirms that central and eastern Crete are particularly vulnerable to precipitation-driven water deficits. Under scenarios with stronger drying and limited ability to satisfy irrigation requirements, potential economic losses for intensive olive groves can locally approach ~1,000 €/stremma. Where reliable irrigation and infrastructure are in place, impacts are substantially reduced but not eliminated, especially in already water-stressed systems.

The olive-yield climate impact study based on statistically derived climate–yield relationships provides an independent line of evidence that is broadly consistent with the CLIMAAX results. It indicates an increasing frequency and magnitude of negative yield anomalies as late-spring rainfall decreases and high summer temperatures become more common, with the strongest adverse signals again concentrated in central and eastern production zones. The convergence of findings across three different methods underlines that drought in Crete represents a systemic, structurally embedded risk for the primary sector and water resources, rather than a sequence of isolated dry years.

Despite these advances, important limitations remain. Agricultural exposure still relies on SPAM 2010 (for crop distribution) and on GCAM/Demeter land-use projections, which provide only a broad scenario-consistent picture and may deviate from recent local trends, a critical issue given that agriculture accounts for roughly 86% of total water demand. Hazard indicators are based on bias-corrected but imperfect global/regional climate datasets (CHELSA, ISIMIP3b), while vulnerability layers (GDP per capita, groundwater access, irrigated area, infrastructure portfolios) come from heterogeneous

sources and involve expert-judgement weighting choices. These factors mean that absolute index values are uncertain and results should be interpreted primarily as relative contrasts and robust spatial patterns within the modelling framework.

On the basis of the Phase-2 findings, the report recommends that the Region of Crete:

- Prioritise central and south-eastern basins as drought-risk hotspots for storage, conveyance, groundwater protection and efficiency measures; integrate drought-risk information in permits for water-intensive uses and in reservoir and groundwater operating rules.
- Promote efficient irrigation, soil-moisture conservation, drought-tolerant varieties and diversification of cropping systems in high-risk municipalities; explore economic-risk instruments for olive growers in structurally exposed areas.
- Develop an operational drought-monitoring system for Crete (combining CLIMADAT-Grid, EDO and local observations), improve local datasets on crop yield, irrigation and groundwater, and periodically update indicators as new data and climate projections become available.
- Embed the drought-risk maps and indicators into the next Regional Adaptation Action Plan of Crete revision and the dedicated Drought and Water Scarcity Action Plan, using them as the spatial basis for prioritizing adaptation measures, investments and cross-sector coordination.

2 Introduction

2.1 Background and context

Crete, the largest island in Greece, lies at the southern margin of Europe where Mediterranean climate systems interact with North African and mid-latitude circulation. The island is characterised by warm, dry summers and mild, wetter winters, but this regime has been progressively modified by climate change. Observed trends show increasing mean temperatures, shifts in the seasonality of precipitation and more frequent and persistent drought episodes (Koutroulis et al., 2011; Tramblay et al., 2020; Tsanis et al., 2011). These changes amplify pressures on already stressed water resources and on climate-sensitive sectors such as agriculture, ecosystems and tourism (Koutroulis et al., 2016).

Updated hydroclimatic data for Crete, summarised in Figure 2-1 , shows a long-term warming tendency in annual mean temperature since the 1950s, together with highly variable but, on average, declining annual precipitation. The lower panel, showing the Standardized Precipitation Index (SPI), highlights an increasing occurrence of multi-month dry episodes, especially in recent decades. The most recent sequence of hydrological years up to 2024–2025 is marked by repeated negative SPI values and below-normal rainfall, indicating a persistent water-deficit situation rather than isolated dry years. In parallel, regional records document critically low storage levels in major reservoirs such as Aposelemis and Faneromeni, reduced groundwater recharge, and widespread stress on rainfed and irrigated agriculture. These deficits are particularly damaging because they coincide with peak irrigation demand and the tourist season, intensifying competition among agricultural, domestic and tourism uses of water.

Against this backdrop, Crete's exposure and sensitivity to drought are of strategic concern. Agriculture, especially olive cultivation, remains a cornerstone of the regional economy and a dominant water user, while rapidly evolving tourism and urban development increase baseline water demand and introduce new vulnerabilities along coastal zones. Ecosystems, including high-elevation habitats and coastal wetlands, are simultaneously affected by reduced freshwater availability and increasing temperatures.

The CLIMAAX-CRETE project is framed within this evolving climatic and socio-economic context. It seeks to provide a robust, quantitative assessment of drought risk for the island, building on state-of-the-art European workflows and progressively refining them with high-resolution, Cretan-specific information. Subsequent sections present the Phase-2 analyses, which combine a newly developed relative drought methodology at basin and municipal scale, an updated agricultural drought workflow for olives and an independent climate-olive yield study. Together, these components aim to support evidence-based planning for water resources and climate adaptation in Crete.

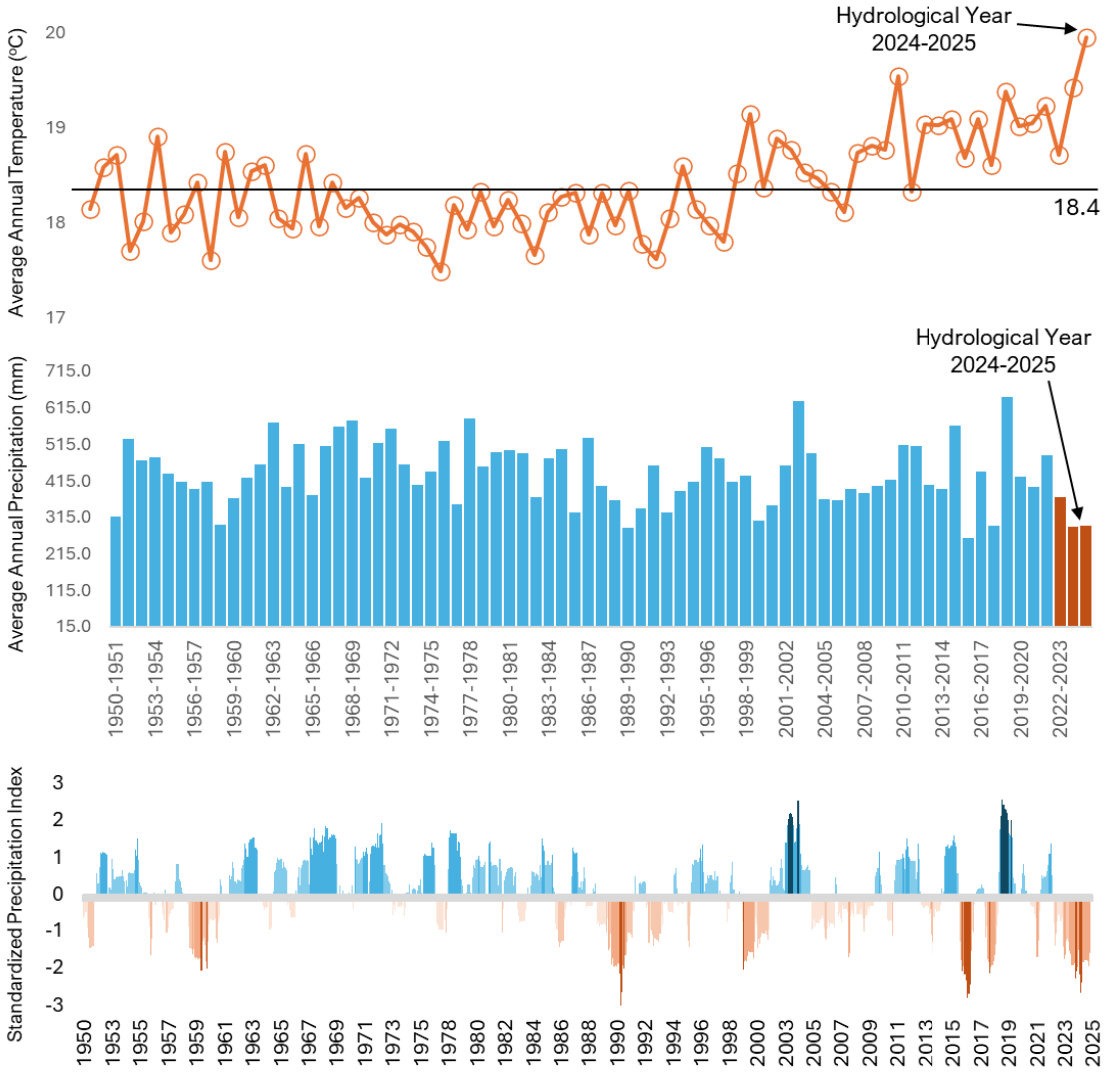

Figure 2-1: Trends in (a) average annual temperature (°C), (b) average annual precipitation (mm), and (c) Standardized Precipitation Index (SPI) for Crete indicating periods of drought (negative SPI) and wetness (positive SPI), from 1950 to 2025.

2.2 From Phase-1 to Phase-2

In Phase-1, drought risk in Crete was assessed using two CLIMAAX workflows applied largely "as-is" at European scale. The relative drought workflow followed Carrão et al. (2016), computing a composite risk index at NUTS-3 level with global/EU datasets (CHELSA climate, GCAM land use, SSP population, generic socio-economic indicators). The output was a relative risk score for the four Cretan regional units, comparable with the rest of Greece and Europe but too coarse for basin-scale or municipal planning. In parallel, the agricultural drought workflow estimated yield and revenue losses from precipitation-driven water deficits for olives, again using global inputs: SPAM 2010 crop production and area, GAEZ-based values and irrigated fractions, and regional climate

projections driving a simple ET-based yield response. This provided a first map of potential economic impacts on olive production under future drought conditions.

The Phase-1 results were useful to highlight that Crete is systematically exposed to drought in a national context and that olives are a key vulnerable sector, but they also revealed important limitations that motivated the Phase-2 refinements. For the relative drought analysis, the use of NUTS-3 units and globally normalised indices masked the strong intra-island contrasts and made it difficult to use the maps directly in local decision-making. Indicator values were scaled against pan-European ranges, so small differences within Crete could be compressed, and local exposure and vulnerability patterns were driven by coarse global datasets that do not fully reflect Cretan land use, tourism structure or water-system characteristics.

Phase-2 therefore focuses on downscaling and refinement. The relative drought assessment is implemented at sub-basin and municipality-intersection scale, using Cretan-specific indicator definitions, pooled normalisation within the island and updated exposure/vulnerability datasets. The agricultural drought workflow is re-run with the corrected CLIMAAX implementation, enriched with updated value and irrigation information from GAEZ v5 and interpreted alongside an independent climate-yield study for olives. Together, these refinements move the analysis from a broad screening towards a Cretan-tailored risk picture that can directly inform regional planning and the forthcoming Drought & Water Scarcity Action Plan.

2.3 Objectives of the Phase-2 assessment

The Phase-2 assessment has three main, complementary objectives.

- First, to develop a Crete-tailored relative drought methodology, redefining hazard, exposure and vulnerability indicators at sub-basin and municipality level, using high-resolution, regionally relevant data and island-wide normalization. The goal is to capture the strong intra-island contrasts in drought conditions and water stress in a way that is directly usable for regional planning and prioritization.
- Second, to refine the agricultural drought risk for olive groves in Crete by re-running the CLIMAAX agricultural workflow with the corrected revenue-loss formulation and updated datasets (e.g. GAEZ v5 crop values, improved irrigation information).
- Third, to integrate an independent olive-yield - climate change impact analysis alongside the CLIMAAX workflows, using the statistically derived climate-yield relationships as an external line of evidence to support, cross-check and interpret the CLIMAAX results.

3 Methodological Framework

3.1 New Relative Drought Methodology for Crete

[Limitations of Phase-1 relative drought workflow (national-scale normalization, difficulty with temporal comparison of risk).]

3.1.1 Conceptual framework

The Phase 2 relative drought assessment adopts the same hazard–exposure–vulnerability risk framework used in Phase 1 and in Carrão et al., (2016) but is fully, contextually redesigned for the specific scales of Crete. Drought risk is expressed as a dimensionless composite index, which combines climatic hazard, the spatial distribution of population and activities exposed to water scarcity, and their socio-economic ability to cope with drought. The index is interpreted as relative drought risk rather than absolute economic loss, or physical damage, and it allows for regional comparisons across Crete, as well as assessment periods and climate scenarios, but not direct conversion into monetary terms or infrastructure design thresholds.

Unlike the national Phase 1 application, which operated at NUTS-3 prefecture level, the Phase-2 assessment is carried out at a hydrologically meaningful and policy-relevant sub-municipal scale. First, 130 river basins larger than 5 km² were delineated across Crete. These basins were then intersected with the boundaries of the 23 municipalities of the island, yielding 244 distinct basin–municipality units. All hazard, exposure, vulnerability and risk indicators are calculated for these 244 units (Figure 3-1). This design enables (i) diagnostics and prioritisation at the river-basin scale, which is appropriate for water-resources and drought-management planning, and (ii) aggregation to the municipality level, which is the primary administrative level for local adaptation measures and policy implementation.

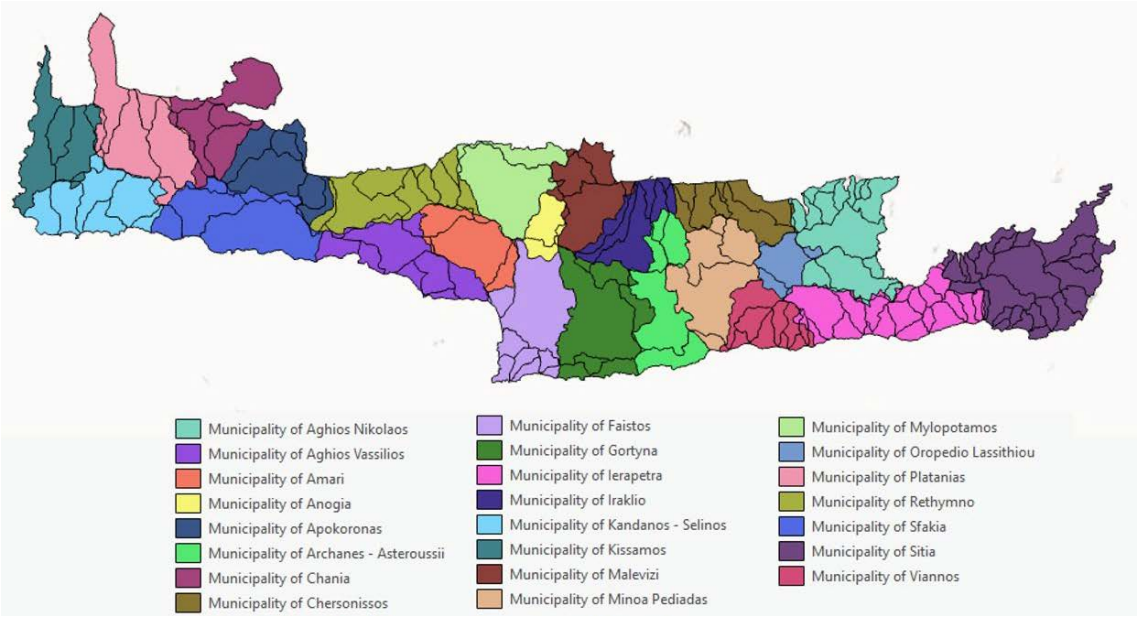

Figure 3-1: Administrative map of Crete showing the 23 municipalities used in the Phase 2 relative drought assessment. River basins larger than 5 km² are intersected with these municipal boundaries to form 244 basin–municipality units, which constitute the basic spatial units for calculating drought hazard, exposure, vulnerability, and composite risk.

The temporal dimension of the assessment is represented by a historical baseline and three future periods: 2015–2040, 2041–2070 and 2071–2100. For each of these time slices we consider three socio-climatic scenarios—SSP1-2.6, SSP3-7.0 and SSP5-8.5—which span a wide range of possible futures in terms of greenhouse-gas forcing and socio-economic development. All datasets used in the analysis are processed consistently for these periods and scenarios.

Given the complex geomorphology of the island, which results in many small river basins, and its pronounced socio-economic heterogeneity, the methodology systematically uses the best available high-resolution datasets for each component (e.g. 3-arcsecond hazard datasets, ~1 km land-use and irrigation data, downscaled socio-economic projections) wherever possible. Indicators are normalised and combined within the Crete domain, rather than at national scale as in Phase 1, therefore the resulting risk index reflects contrasts within Crete and preserves comparability across time slices. The outcome is a set of hazard, exposure, vulnerability and composite risk maps at basin and municipal level that are directly usable for regional planning, prioritisation of measures and integration into Crete's Climate Adaptation Plan. Finally, for all hazard, exposure and vulnerability sub-indicators, classes were assigned using percentile thresholds derived from a single pooled distribution that includes the baseline and all future periods and scenarios, ensuring that all time slices and SSPs are directly comparable on a common relative scale.

3.1.2 Hazard indicators

Four hazard indicators were selected to assess relative drought hazard within the study area. Three of these correspond to the bioclimatic variables Annual Mean Temperature, Maximum Temperature of the Warmest Month, and Annual Precipitation from the CHELSA-BIOCLIM+ dataset (Brun et al., 2022), covering the period 1981–2100, under the SSP1-2.6, SSP3-7.0, and SSP5-8.5 climate scenarios, at a spatial resolution of 3 arcseconds.

Following the methodology developed by Carrão et al., (2016) and applied in Phase 1 of the Drought Hazard Assessment, the Weighted Anomaly of Standardized Precipitation (WASP) index was additionally computed at the 244 sub-municipal scale for Crete. The WASP index represents the probability of exceeding the median severe precipitation deficit for a given region, based on historical conditions or future projections. The index was calculated separately at sub municipality-basin level using aggregated monthly precipitation data of four CMIP6 global climate models (GFDL-ESM4, IPSL-CM6A-LR, MPI-ESM1-2-HR, MRI-ESM2-0) from the ISIMIP3b bias-adjusted climate dataset (Lange and Büchner, 2021), for the same period (1981–2100) and climate scenarios (SSP1-2.6, SSP3-7.0, SSP5-8.5). An overview of the datasets used in the hazard assessment is provided in Table 3-1.

Table 3-1 Summary information of hazard variables and corresponding references.

Variable	Assessment Period	Model	Resolution
CHELSA-BIOCLIM+ · Annual Mean Temperature (bio1) · Maximum Temperature of the Warmest Month (bio5) · Annual Precipitation (bio12)	Historical · 1981–2010 SSP126, 370, 585 · 2011–2040 · 2041–2070 · 2071–2100	GFDL-ESM4 IPSL-CM6A-LR MPI-ESM1-2-HR MRI-ESM2-0	1km x 1km
ISIMIP3b Daily Precipitation (WASP index)	Historical · 1981–2014 SSP126, 370, 585 · 2015–2040 · 2041–2070 · 2071–2100	GFDL-ESM4 IPSL-CM6A-LR MPI-ESM1-2-HR MRI-ESM2-0	0.5°x0.5°

To ensure comparability across climate scenarios and periods and compatibility across assessments, all hazard indicators were normalised to a common 0–1 scale using their respective global percentile distributions. The final drought hazard indicator (dH) was computed as a weighted linear combination of four normalized climatic sub-indicators at the sub-municipal level. To reflect the dominant role of water availability in shaping

drought conditions, the two precipitation- and drought-related indicators — the WASP index and annual precipitation (BIO12) were each assigned a weight of 1/3. The two temperature-related indicators, annual mean temperature (BIO1) and maximum temperature of the warmest month (BIO5), were each assigned a weight of 1/6. The resulting hazard index is therefore given by

$$dH = \frac{1}{3}\,\mathrm{WASP} + \frac{1}{3}\,\mathrm{BIO12} + \frac{1}{6}\,\mathrm{BIO1} + \frac{1}{6}\,\mathrm{BIO5},$$

after all sub-indicators have been normalized to the 0–1 range so that they are directly comparable. The chosen weights express that precipitation deficits and drought episodes exert the strongest direct control on hazard in Crete, while temperature is included as an amplifying factor.

3.1.3 Exposure indicators

Exposure was defined as the spatial concentration of drought-sensitive socio-economic activity within each basin-municipality analysis unit, with emphasis on the sectors that dominate water use and therefore drive potential impacts under constrained water availability. A cross-sectoral perspective is particularly relevant for Crete, where agriculture is the main water-consuming sector, while domestic and tourism-related demands add additional pressure-especially during the dry season. The exposure assessment incorporates three complementary components: Agricultural Land Use (irrigation demand), Population Density (domestic water demand), and Tourism Activity (tourism water demand).

1. Agricultural exposure was quantified using the GCAM-projected land-use dataset, downscaled with Demeter (Chen et al., 2020), to estimate the fraction of agricultural land per analysis unit under SSP1, SSP3 and SSP5 for the period 2015–2100. The LUISA (2018) basemap was used as a consistency check on the spatial extent of agricultural areas produced by the downscaling (e.g., ensuring that high projected fractions are not assigned to clearly non-agricultural land).
2. Population exposure was derived from the 1 × 1 km population projections dataset (Wang et al., 2022) available under SSP1, SSP3 and SSP5 for 2020–2100. For each assessment period, the median year was used, and population counts were aggregated to the basin-municipality units (sum over grid cells intersecting each unit) to preserve totals.
3. Tourism exposure was estimated by combining (i) projected tourism activity at NUTS-3 level (SSP-consistent projections) from Koutroulis et al., (2018) with (ii) the 1 km population distribution for the same periods and scenarios. The downscaling assumption is that, within each NUTS-3 region, tourism activity is preferentially concentrated in populated places (coastal settlements and urban centers), so projected NUTS-3 tourism totals were distributed proportionally to the fine-scale population field to derive sub-municipal tourism fractions.

To ensure comparability across indicators with different units and ranges, each exposure component was transformed into a relative score using its (global) percentile distribution and then aggregated to a composite exposure index using water-demand-informed weights. Specifically, the weighting was designed to reflect the sectoral structure of water use in Crete, where agriculture accounts for the dominant share of total consumption (around 86% in sectoral breakdowns), while domestic and other uses constitute substantially smaller shares.

In the Phase 2, weights were derived from indicative annual water-demand volumes for Crete: agricultural water demand (~450 Mm^3), domestic demand estimated from resident population using a per-capita consumption assumption (e.g., 240 L/person/day), and tourism demand estimated from total overnight stays using a per-overnight water-use assumption (commonly 400 L per overnight stay). Based on these reference volumes, the composite exposure index was calculated as a weighted sum of the three normalised sub-indices (86% Agriculture, 10.5% Domestic, and 3.5% Tourism), providing an exposure metric that is both spatially explicit and consistent with the cross-sectoral dominance of irrigation demand in Crete.

3.1.4 Vulnerability indicators and sub-indices

Vulnerability in this Phase 2 captures the degree to which people and economic activities within each basin-municipality unit can withstand, absorb and recover from drought pressure, given their socio-economic capacity and the availability of water-related infrastructure. In contrast to the exposure component, vulnerability is designed to represent the coping and adaptation capacity of each unit. For this reason, all selected indicators are formulated so that improved capacity (e.g., higher income, stronger irrigation coverage, better access to groundwater or improved supply infrastructure) corresponds to lower vulnerability. Four vulnerability indicators were used, combining both scenario-dependent and static components.

1. Economic adaptive capacity is represented through GDP per capita (SSP-dependent), expressed on 1-km grids based on the LitPop approach (Wang and Sun, 2022), and interpreted as a proxy for investment capacity and institutional ability to implement adaptation actions. In the vulnerability formulation, higher GDP per capita implies lower vulnerability; therefore, a complementary linear transformation was applied to reverse the direction of the normalized indicator.
2. A second vulnerability-reducing component is the extent of irrigated agricultural land, derived from the global 1-km irrigated area product from GAEZ v5 (2020) “Share of irrigated land” dataset at ~1 km resolution (see Figure 3-7). This indicator reflects the degree to which agricultural systems can buffer precipitation deficits through managed water supply and thus reduces sensitivity of production to drought. It is treated as largely static over the assessment horizon, acknowledging that local irrigation development is possible but not consistently available as a spatially explicit, SSP-consistent dataset at the scale of Crete.

3. Third, physical access to groundwater is represented through the spatial extent of active groundwater abstraction points linked to aquifers (borehole/well abstraction). This indicator is used as a proxy for the presence of alternative water sources during dry conditions. It is again formulated as a vulnerability-reducing factor (greater groundwater access corresponds to lower vulnerability). The groundwater indicator is included as a structural component and is treated as static within the assessment, while recognizing that groundwater availability itself may be affected by long-term overexploitation, here it is used strictly as an "access" proxy rather than a sustainability metric.
4. Finally, to reflect differences in system-level adaptation capacity under different socio-economic pathways, the assessment includes an SSP-dependent indicator for water infrastructure capacity. This indicator is derived from a portfolio of 68 candidate water engineering works (e.g., dams/reservoirs, conveyance and irrigation networks, borehole interventions, rehabilitation measures), which was screened for plausibility under SSP1, SSP3 and SSP5 in collaboration with the regional water authority. The screening translates SSP narratives into a pragmatic feasibility logic: SSP1 emphasizes efficiency and environmentally compatible interventions, SSP3 assumes constrained investment and coordination, limiting feasible projects, SSP5 assumes strong growth and engineering deployment, enabling a broader and more capital-intensive portfolio.

All vulnerability indicators are processed at 1-km (or point scale) and aggregated to the 244 basin-municipality units using area-weighted statistics. To enable combination across variables with different units and ranges, each sub-indicator is normalized to a 0–1 scale within the Crete domain for the broader set of time slices and scenarios. The vulnerability sub-indices were combined into a single composite index using a fixed weighting scheme. Specifically, vulnerability V was defined as the average of two equally weighted components: (i) economic adaptive capacity, represented by normalized GDP per capita, and (ii) water-availability–related capacity, which groups the water-system indicators. The second component was calculated as

$$\frac{1}{2}\left[(\text{Groundwater access} + \text{Irrigated area} + \text{Water infrastructure}) \times \frac{1}{1 + \Delta\text{BIO12}}\right]$$

where all indicators and the precipitation change ΔBIO12 were first normalized to the 0–1 range. In this formulation, GDP per capita receives 50% of the total weight, while the combined water-availability indicators receive the remaining 50%, adjusted by the factor $1/(1 + \Delta\text{BIO12})$ so that projected reductions in annual precipitation increase overall vulnerability.

3.2 Updated Agricultural Drought Risk Assessment

3.2.1 Conceptual approach

The updated agricultural drought risk assessment follows the CLIMAAX hazard-exposure-vulnerability framework (Figure 3-2), with a focus on olive groves as the dominant crop in Crete and on revenue loss as the risk metric. Agricultural drought hazard is defined as the fractional yield loss of rainfed olive groves due to water deficit during the growing season, derived from ET-based crop water balance and a yield-water response model. Exposure represents the economic value of olive production potentially affected by this hazard. It is quantified using spatially explicit olive production and crop value layers, which provide, for each grid cell, the tonnage of olive production and the associated crop value in constant 2010 prices. Vulnerability is represented by the availability of irrigation infrastructure, expressed as the percentage of cropland equipped with irrigation systems. In the workflow, irrigated area is assumed to be effectively protected against precipitation-driven yield losses, while non-irrigated area is fully exposed. Risk is finally expressed as potential revenue loss ("lost opportunity cost") under a hypothetical fully rainfed situation. The output is a set of maps of revenue loss per grid cell (in 2010 EUR), together with the spatial distribution of irrigation coverage.

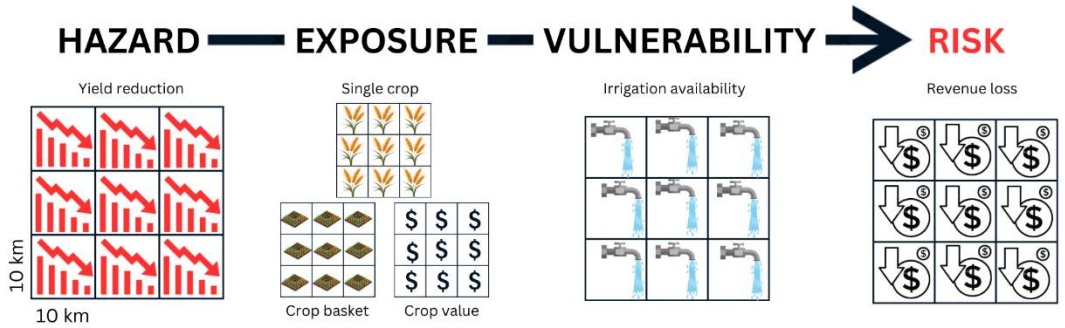

Figure 3-2: Framework for agricultural drought risk assessment, showing the components of risk-Hazard (yield reduction), Exposure (crop type, crop value, and crop basket), and Vulnerability (irrigation availability) resulting in the estimation of revenue loss as the overall risk.

3.2.2 Workflow updates relative to Phase-1

In Phase 2, the agricultural drought workflow for Crete was re-run using the updated CLIMAAX agriculture workflow from the Handbook, keeping the same spatial domain (Crete), crop selection (olives), climate scenario configuration and olive crop parameters as in Phase 1. Relative to the first application, three methodological updates are important:

A. Correction of revenue loss calculation

In the original implementation, total crop revenue per cell was effectively multiplied twice by the crop production fraction (crop_prod_fraction), which led to a systematic

underestimation of revenue losses. In the updated workflow, the revenue loss is computed by first deriving the total crop revenue per cell, and then applying the single crop_prod_fraction factor only once to obtain the revenue attributable to olives, before multiplying by the yield-loss fraction, removing the previous underestimation bias.

B. Explicit treatment of fractional land use in each cell

In Phase 1, revenue-loss values were sometimes interpreted as if the whole grid cell were covered by olives. In the updated workflow, the interpretation explicitly follows the CLIMAAX implementation: SPAM production and GAEZ value are already fractional at cell level, and the revenue loss natively reflects the fact that olives occupy only a share of the cell's agricultural area. Comparisons with external per-hectare estimates are made only after normalizing by the actual olive area per cell.

C. Use of updated CLIMAAX code with unchanged 2010 baseline data

For Crete, SPAM 2020 does not provide complete coverage for crops as shown in Figure 3-3, so the updated workflow is still run with SPAM 2010 crop production as in Phase 1. However, the original GAEZ 2010 layers for aggregated crop value and irrigated cropland share are replaced by GAEZ v5 (2020) products.

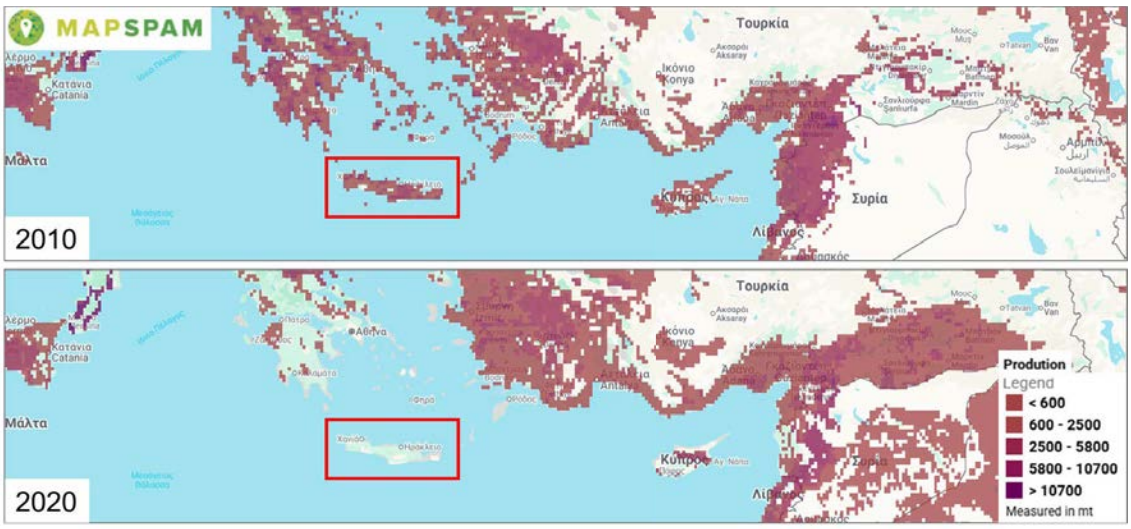

Figure 3-3: Spatial distribution of crop production for "other oil crops" (olive crop) according to 2010 and 2020 MapSPAM repository.

3.2.3 Hazard - Agricultural drought

The agricultural drought hazard is quantified as percentage yield loss of rainfed olive groves due to water deficit during the olive growing season. The hazard module follows the CLIMAAX agricultural drought hazard workflow as applied in Phase 1, with the same crop parameterization for olives.

Standard evapotranspiration (ET_0) is first computed using the FAO Penman-Monteith equation based on daily time series of maximum and minimum temperature, relative

humidity, wind speed and solar radiation from EURO-CORDEX regional climate model simulations, together with elevation and thermal climate zone information. ET_0 is then converted to crop evapotranspiration under non-limiting water conditions (ETc) using olive-specific crop coefficients (Kc) and crop development fractions (Lgp_f1–f4) defined by thermal climate zone, as specified in the CLIMAAX crop table for olive trees (see Table 3-2).

Table 3-2.: Parameters, specific to olive tree crops, used for the calculation of ET0 (FAO).

Previous Code	**2.2.2.3**	**Lgp_f2**	**0.246575**
Group	4	Lgp_f3	0.164384
Class	44	Lgp_f4	0.246575
Subclass	442	Season start	(90) April
Crop	Olive	Season End	(300) November
Clim	3	RD1	1.2
Kc_in	0.65	RD2	1.7
Kc_mid	0.7	DF	0.65
Kc_end	0.7	Type	2
Lgp_f1	0.082192	Ky	0.2

Actual evapotranspiration (ETa) under rainfed conditions is derived by combining ETc with daily precipitation and soil water holding capacity, following the FAO I&D Paper 33 (Doorenbos and Kassam, 1979). water-balance approach. Yield loss is then computed as a function of the relative reduction in evapotranspiration (1 − ETa/ETc) and the crop-specific yield response factor Ky, again using the FAO formulation. Figure 3-4 illustrates the spatial distribution of available water capacity (AWC) across Crete representing the capacity of soil to retain water, which is a critical factor in determining the resilience of agricultural systems to drought.

Elevation data (Figure 3-5) derived from the USGS GDTEM 2010 digital elevation model (Danielson and Gesch, 2011). While this dataset has a coarser resolution compared to newer DEMs, it is sufficient for the resolution requirements of this assessment.

The agricultural drought hazard was assessed using four future time slices (2026-2045, 2046-2065, 2066-2085 and 2086-2100) and three emission scenarios (RCP2.6, RCP4.5 and RCP8.5), consistent with the climate projections used elsewhere in this study. For each combination of scenario and period, the workflow was forced with an ensemble of EURO-CORDEX regional climate models (CM5-CNRM-ALADIN, CM5-KNMI-RACMO, MPI-ESM-SMHI-RCA4, NORESM1-REMO2015 and NORESM1-SMHI-RCA4), from which daily meteorological variables and derived ET_0 were obtained.

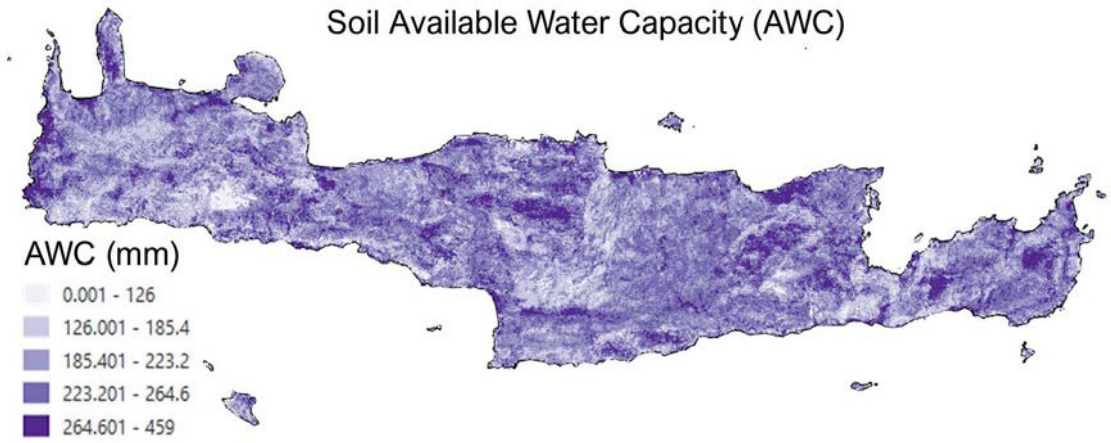

Figure 3-4: Available Water Capacity (AWC) for Crete (in mm).

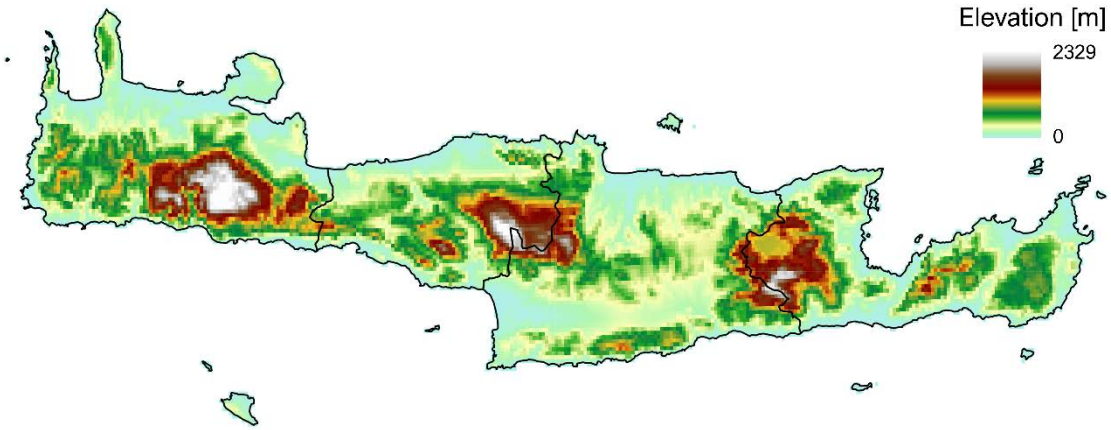

Figure 3-5: Elevation map of Crete derived from the USGS GDTEM 2010 digital elevation model.

3.2.4 Exposure - Agricultural drought

In the updated agricultural drought risk assessment, exposure represents the economic value of olive production that is potentially affected by water-related yield losses. For Crete, exposure is derived by combining spatially explicit information on olive production from MapSPAM 2010 with aggregated crop value data from GAEZ v5 (2020).

Olive production is taken from the 2010 MapSPAM dataset, which provides crop-specific production at 5-arc-minute resolution. Because MapSPAM 2020 does not include reliable information for Crete, the 2010 layer is retained as the most recent consistent source for spatial patterns of olive production.

The economic value of crops is obtained from the GAEZ v5 (2020) Aggregated crop value product at approximately 11 km resolution. This layer supplies the total value of agricultural production per grid cell under 2015 conditions (Figure 3-6). It is resampled

to the same grid as the hazard outputs and then combined with the MapSPAM information: for each grid cell, the total agricultural value from GAEZ v5 is multiplied by the MapSPAM-derived olive production fraction, yielding an estimate of olive-specific revenue per cell.

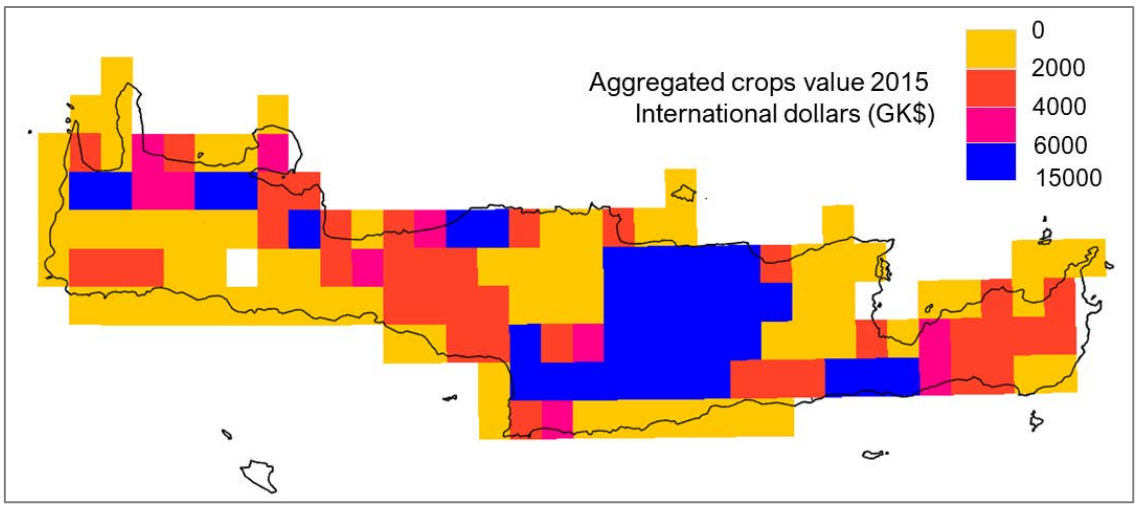

Figure 3-6: Aggregated crop value for Crete in 2015, expressed in international dollars (GK$) per 11 km resolution, based on data from the FAO Global Agro-Ecological Zones (GAEZ).

3.2.5 Vulnerability - Agricultural drought

vulnerability represents the structural capacity of agriculture in Crete to cope with precipitation deficits, expressed through the spatial distribution of irrigation infrastructure. We use the GAEZ v5 (2020) "Share of irrigated land" dataset at ~1 km resolution, which provides for each grid cell the percentage of cropland that is equipped for irrigation (Figure 3-7).

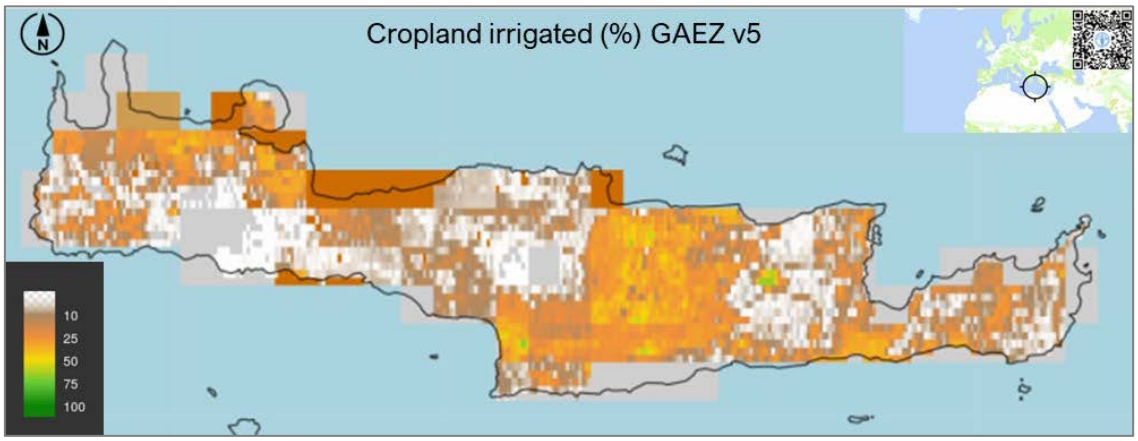

Figure 3-7: Percentage of cropland equipped with irrigation systems across Crete (GAEZv5).

3.2.6 Uncertainty considerations

The updated agricultural drought risk assessment for olives in Crete is affected by several sources of uncertainty that need to be considered when interpreting the results. On the hazard side, the yield-loss calculation relies on globally defined crop parameters (crop coefficients, growing-period fractions and yield response factors) assigned per thermal climate zone. These parameters have not been calibrated specifically for Cretan varieties and management practices and may not fully reflect local responses to water stress, heat, or combined stress. In addition, the hazard is driven by EURO-CORDEX regional climate simulations at relatively coarse resolution. Biases in precipitation and ET_0 and differences between models and RCPs propagate into ETc, ETa and the derived yield-loss fraction, so grid-cell values should be regarded as indicative rather than exact.

Exposure estimates combine MapSPAM 2010 olive production with GAEZ v5 (2020) aggregated crop value. This introduces both temporal and methodological inconsistencies: crop distribution and productivity may have changed between 2010 and 2020, and neither dataset is based on detailed Cretan statistics at field scale. MapSPAM provides modelled production at 5-arc-minute resolution and may misrepresent absolute production in some cells, while GAEZ v5 expresses value in harmonised units that do not directly reflect current local prices. As a result, the absolute monetary values of exposure and revenue loss are uncertain; the main strength of the workflow is in capturing the spatial pattern of relatively higher and lower exposure across the island.

The vulnerability layer derived from the GAEZ v5 share of irrigated land also has limitations. The dataset reports the fraction of irrigated cropland for all crops combined, not specifically for olives; it does not account for the reliability of water supply, inter-annual restrictions, or differences in irrigation technology and efficiency. Furthermore, any irrigation development after 2020 is not represented. Hence, areas mapped as poorly irrigated may in reality have more infrastructure than shown, and vice versa.

These uncertainties mean that the magnitude of modelled yield losses and revenue losses should be interpreted with caution, especially at the level of individual grid cells. The assessment is more robust in terms of relative patterns: identifying which parts of Crete consistently exhibit higher agricultural drought hazard, higher olive-related exposure and lower irrigation coverage.

3.3 Climate Change Impacts on Olive Oil Yield

3.3.1 Study overview

This part of the study investigates how climate variability and change affect olive oil production and yield across Greece with a focus in Crete, by attempting a link of observed production statistics with a suite of climatic indices and then using these relationships to project future yield under climate change scenarios.

The spatial domain covers the 21 most productive regional units (prefectures) of Greece, including all four prefectures of Crete, which together account for about 93% of national olive oil production. Olive oil production and olive tree area data are taken from the Hellenic Statistical Authority (ELSTAT) for the period 2011-2022, from which annual olive oil yield is derived as production (kg) divided by olive tree area (ha).

Climatic drivers are represented through a set of temperature, precipitation, wind and composite-based indices, selected after a literature review of Mediterranean olive-climate studies. These indices are calculated from daily E-OBS gridded observations of temperature, precipitation and wind, aggregated mainly to bimonthly values (e.g. Jan/Feb, May/Jun) and including indices such as maximum summer temperature thresholds, seasonal rainfall totals, the Standardized Precipitation Evapotranspiration Index (SPEI) and winter chill.

For each of the 21 regional units, the study first performs simple linear regressions between olive oil yield (2011-2022) and each climatic index, retaining only statistically significant relationships ($p < 0.1$). It then constructs a two-predictor multiple linear model per regional unit using the two most influential indices, providing a compact statistical description of how local yield responds to climate variability.

Future climate impacts are assessed by driving these regional two-predictor models with projections from five bias-adjusted EURO-CORDEX Regional Climate Models under RCP4.5 and RCP8.5 at 12.5 km resolution. The models provide minimum, mean and maximum temperature and precipitation for three future periods, near future (2026-2045), mid-century (2046-2065), and far future (2066-2085), which are compared against a historical baseline 2006–2025. Olive oil yield changes are then derived per prefecture and aggregated using production-weighted percentiles at the national scale and for three macro-regions: Peloponnese, Crete and the rest of Greece.

3.3.2 Data

The analysis of climate-yield relationships and future impacts is based on data from national and international databases, covering both olive oil production and relevant climatic variables for all regional units of Greece, including the four regional units of Crete.

Olive grove and production data:

Information on olive groves and production was obtained from the *Annual Agricultural Statistical Surveys* of the Hellenic Statistical Authority (ELSTAT) for the period 2011-2022. The datasets include, for each regional unit of Greece:

- area of total compact plantations (sum of citrus, fruit, nuts and dried fruit trees, and olive trees),
- area of olive trees,
- total number of olive trees and total number of trees in compact plantations,
- number of trees for edible olive production and for olive oil production,
- irrigated area under trees in compact plantations,
- annual olive oil production (tons).

From these variables, olive oil yield was calculated as olive oil production (kg) divided by olive tree area (ha). For quality control, regional-unit time series with more than three missing values for a given variable were excluded from trend estimation, and evident inconsistencies or outliers in production and yield were also removed prior to analysis. Descriptive statistics (minimum, mean, maximum and national share) and linear trends were then derived for each dataset.

To map the spatial distribution of olive groves, the CORINE Land Cover 2018 dataset at 100 m resolution (Europe, 6-yearly) was used to identify areas classified as olive groves across Greece.

Observed climate data:

For the calculation of climatic indices (predictors), daily gridded data of:

- mean wind speed,
- total precipitation,
- mean temperature,
- minimum temperature,
- maximum temperature,

were extracted from the E-OBS dataset (E-OBS, 2020) for all regional units of Greece for the period 2011-2022. The variables were aggregated to bimonthly values (Jan/Feb, Mar/Apr, May/Jun, Jul/Aug, Sep/Oct), excluding Nov/Dec due to the olive harvest period. From these, a set of temperature, precipitation, wind and composite-based climatic indices were computed, as summarized in Table 3.1 of the original study (e.g. bimonthly average and maximum temperature, diurnal temperature range, number of hot days, seasonal rainfall indices, SPEI). The olive oil yield data and all climatic indices, except mean wind speed, were standardized using z-scores to allow consistent comparison and correlation analysis, following the approach of Di Paola et al., (2023). Drought conditions were additionally characterized using the Standardized Precipitation Evapotranspiration Index (SPEI), with classification thresholds following Vicente-Serrano et al., (2010).

Table 3-3. Summary of temperature, precipitation, wind and composite-based climatic indices used as predictors of olive oil yield.

Climatic index	Symbol	Unit	Description
Bimonthly diurnal temperature range	DTRavg	°C	Average DTR within 2 months (Jan/Feb, Mar/Apr, May/Jun, Jul/Aug, Sep/Oct)
Bimonthly average temperature	Tavg	°C	Average temperature within 2 months (Jan/Feb, Mar/Apr, May/Jun, Jul/Aug, Sep/Oct)
Bimonthly maximum temperature	Tmax	°C	Moving average maximum temperature within 2 months (Jan/Feb, Mar/Apr, May/Jun, Jul/Aug, Sep/Oct) for 5 days
			Moving average maximum temperature within 2 months (Feb/Mar, Apr/May, Jun/Jul, Aug/Sep, Oct/Nov, Dec/Jan) for 5 days
Bimonthly minimum temperature	Tmin	°C	Moving average minimum temperature within 2 months (Jan/Feb, Mar/Apr, May/Jun, Jul/Aug, Sep/Oct) for 5 days
Monthly maximum temperature over 32°C during April-October	Tmax_32	days	The number of days with temperatures over 32°C in Apr, May, Jun, Jul, Aug, Sep, Oct.
Monthly maximum temperature over 35°C during April-October	Tmax_35	days	The number of days with temperatures over 35°C in Apr, May, Jun, Jul, Aug, Sep, Oct.
Bimonthly total rainfall	WINRR	mm	Total rainfall within 2 months (Jan/Feb, Mar/Apr, May/Jun, Jul/Aug, Sep/Oct)
Total rainfall during winter	WinterRain	mm	Total rainfall during November-April
Total rainfall during summer	SummerRain	mm	Total rainfall during June-November
Winter chill	WinterChill	h	Chilling units based on maximum and minimum temperatures, where optimum efficiency for chilling unit accumulation is within 2.5 °C and 9.1 °C.
Bimonthly maximum standardized precipitation evapotranspiration index (SPEI)	SPEImax	—	Maximum SPEI within 2 months (Jan/Feb, Mar/Apr, May/Jun, Jul/Aug, Sep/Oct)
Wind speed	Wind	m/s	90th percentile of daily mean wind speed

Climate projection data:

Future climate conditions were derived from outputs of five bias-adjusted Regional Climate Models (RCMs) from the EURO-CORDEX experiment (EUR-11, 12.5 km resolution): ECEARTH_CLMcom, ECEARTH_RCA, ECEARTH_RACMO2, IPSL_WRF and

MPILR_REMO09. These simulations provide daily minimum, mean and maximum temperature and precipitation for:

– a historical/reference period 2006–2025, and
– three future periods: 2026–2045 (near future), 2046–2065 (mid-future) and 2066–2085 (far future),

under the RCP4.5 and RCP8.5 scenarios.

The bias correction of temperature fields was based on the method described by Vautard et al., (2013), while total precipitation was bias-corrected following Vrac et al., (2016)**)**. The overall EURO-CORDEX simulation framework and reference period are consistent with Jacob et al., (2014).

For each RCM and scenario, the same set of climatic indices used in the observational analysis was computed and aggregated at regional-unit level. These projected indices served as inputs to the empirical climate–yield models to estimate changes in olive oil yield between 2025 and 2085 for each regional unit, including the four units of Crete.

3.3.3 Methodological approach for climate-yield relationships

In this study, climatic indices are treated as proxies of the drought-related hazard, while olive oil yield represents the impact (and thus the risk) arising from this hazard. The objective of this methodological step is to quantify how variations in the climatic indices translate into variations in olive oil yield at the level of each regional unit, including the four regional units of Crete. The procedures described here correspond to the third phase of the overall framework shown in Figure 3-8.

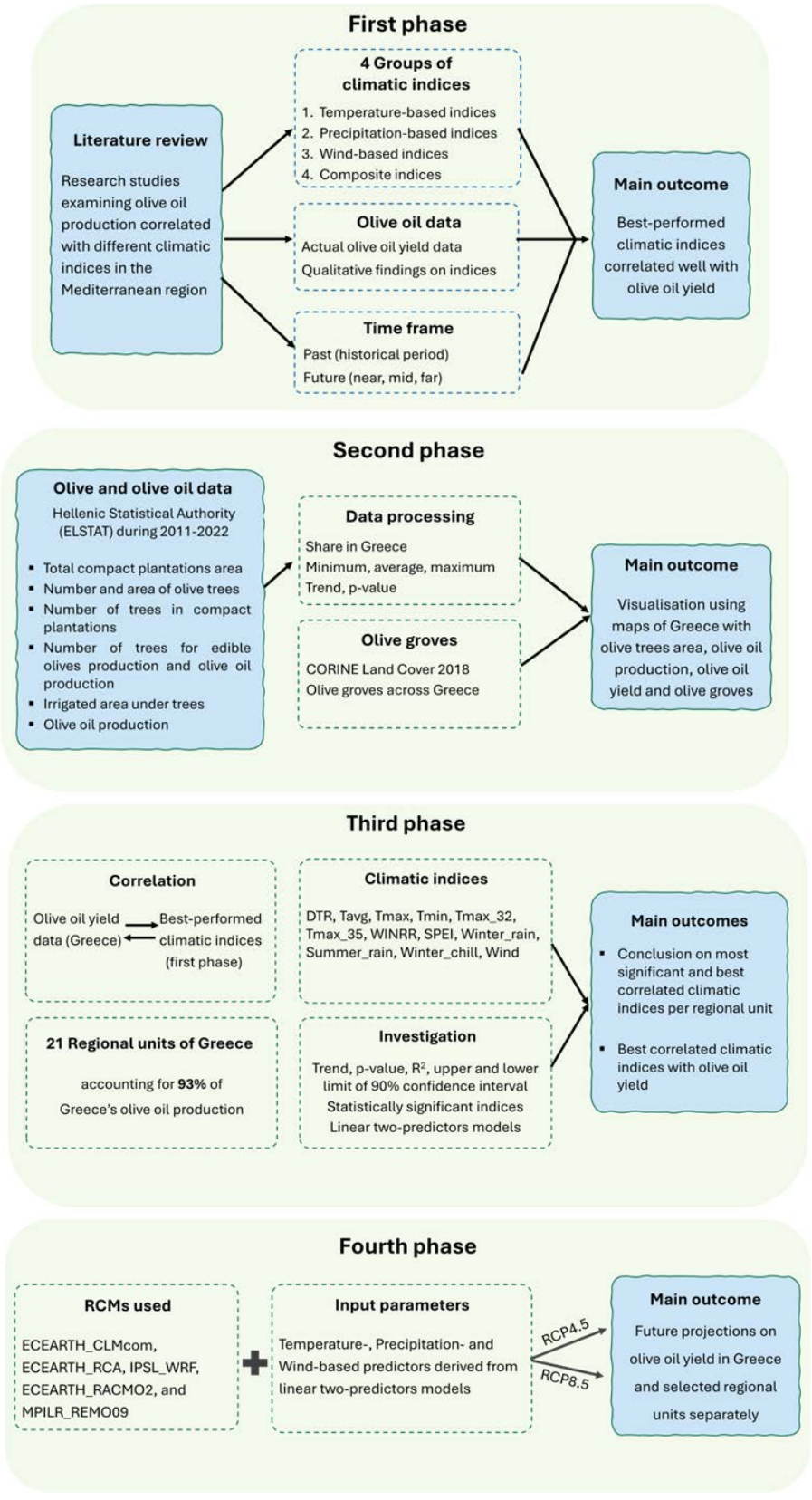

Figure 3-8 Schematic overview of the methodological framework used to analyse climate–olive oil yield relationships and project future yield changes in Greece.

(a) Preparation of time series

For each of the 21 regional units considered, two sets of annual time series were prepared for the period 2011–2022:

– Olive oil yield (impact variable), obtained by dividing annual olive oil production by olive tree area, and
– Climatic indices (hazard descriptors), derived from daily temperature, precipitation and wind data and aggregated to bimonthly or seasonal indices as summarised in Table 3-3 (e.g. temperature-based, precipitation-based, wind-based and composite indices).

To make the variables comparable and to avoid scale effects, olive oil yield and all climatic indices (except wind speed) were standardised using z-scores before statistical analysis.

(b) Simple regression between climate indices and yield

As a first step, the relationship between each individual climatic index and olive oil yield was examined with simple linear regression. For every regional unit and for every climatic index, a model of the form:

$$Y = \alpha_0 + \alpha_1 X$$

was fitted, where Y is the standardised olive oil yield and $X$is the standardised climatic index. This procedure was repeated for all indices and all regional units.

For each regression, the following diagnostics were computed and stored for later synthesis:

– regression coefficients (α_0, α_1),
– coefficient of determination (R^2) and adjusted R^2,
– p-value of the slope, and
– confidence interval of the slope at a chosen confidence level (e.g. 90%).

Only those climate-yield relationships where the slope was statistically significant (p-value below the predefined 0.1 threshold) were retained as candidate hazard-impact links.

(c) Selection of key climatic predictors

The next step consisted in identifying, for each regional unit, the most relevant climatic indices to describe yield variability. This was done by:

1. Reviewing the set of significant simple regressions per regional unit;
2. Considering physical plausibility (e.g. indices that refer to sensitive periods of the olive annual cycle); and
3. Prioritising indices that showed relatively robust statistical performance across units (based on R^2 and significance).

On this basis, two indices were selected as key climatic predictors for each regional unit. These indices represent the dominant aspects of the drought-related hazard (e.g. hot conditions, reduced rainfall, seasonal water imbalance) that are most strongly associated with yield variability in that unit.

(d) Two-predictor climate–yield model per regional unit

For each regional unit, the two selected climatic indices were then combined in a multiple linear regression model, which formally links the hazard descriptors to the impact on yield. The general form of the model is:

$$Y = \beta_0 + \beta_1 X_1 + \beta_2 X_2 + \beta_3 (X_1 \times X_2),$$

where:

- Y is the standardised olive oil yield,
- X_1 and X_2 are the two selected climatic indices (hazard variables),
- β_0 is the intercept,
- β_1 and β_2 quantify the individual effect of each index on yield, and
- β_3 represents the interaction term, allowing the combined influence of the two indices to be captured when they deviate from their mean simultaneously.

The parameters $\beta_0, \beta_1, \beta_2, \beta_3$ were estimated using ordinary least squares. For each regional unit, model performance was evaluated using R^2, adjusted R^2, p-values of the coefficients and basic residual diagnostics (e.g. inspection of residuals vs. fitted values) to ensure the adequacy of the linear specification.

(e) Role of the models in the hazard–risk assessment

Methodologically, these regional two-predictor models constitute the bridge between climatic hazard and yield-based risk:

- the climatic indices encapsulate the characteristics of drought-related hazard (e.g. intensity, timing and persistence of hot and dry conditions), and
- the regression coefficients express how sensitive olive oil yield is to changes in those indices in each region.

In a subsequent step (fourth phase of the framework), these calibrated climate-yield models are driven by climatic indices computed from Regional Climate Model outputs, allowing the translation of projected changes in hazard into projected changes in yield, which are then used as impact-based indicators of drought risk (described in the next Section).

4 Results

4.1 New Relative Drought Methodology for Crete

4.1.1 Relative drought Hazard maps

Relative drought hazard was mapped at the basin–municipality unit scale using a composite climatic indicator that combines long-term thermal stress with drought-relevant precipitation variability. The index integrates four normalised sub-indicators: the WASP index derived from ISIMIP3b precipitation (Figure 7-1), annual precipitation (BIO12) from CHELSA BIOCLIM+ (Figure 7-2), annual mean temperature (BIO1) (Figure 7-3) and maximum temperature of the warmest month (BIO5) (Figure 7-4). Following the weighting scheme described in Section 3.1, the two precipitation/drought indicators (BIO12, WASP) each contribute one third of the final score, while the two temperature indicators (BIO1, BIO5) each contribute one sixth. All sub-indicators were harmonised on a common grid, aggregated to the 244 basin–municipality units, normalised to the 0–1 range, and combined into a single continuous hazard index. Classes were then assigned using percentile thresholds derived from a single pooled distribution that includes the baseline and all future periods and scenarios, so that all time slices and SSPs are directly comparable on the same relative scale.

Figure 4-1 shows the resulting relative drought hazard for the sub-basin units. In the 2020 baseline, higher hazard values cluster mainly in central and eastern Crete, with lower to intermediate values more frequent in the western part of the island. In the future scenarios, SSP1-2.6 shows limited changes in the spatial pattern and only modest increases in the hazard index by the end of the century. In contrast, SSP3-7.0 and especially SSP5-8.5 exhibit a progressive intensification of hazard, with large parts of the central and southern basins shifting into the upper quantile classes by 2041–2070 and 2071–2100. Under SSP5-8.5, most basins in the central belt of the island reach high hazard scores (>0.5 in the normalised index) by the late-century period, showing a pervasive strengthening of drought-favouring climatic conditions.

To support decision-making at the administrative level, the same hazard index was aggregated to the 23 municipalities by averaging over the sub-basins intersecting each municipality (Figure 4-2). The baseline map shows that municipalities such as Heraklion, Mylopotamos, Anogia, Chania, Apokoronas and Sfakia already exhibit relatively high hazard values, whereas several eastern municipalities (e.g. Ierapetra, Aghios Nikolaos) start from lower baseline relative values. The lower panels of Figure 4.1-2 illustrate how these municipal-scale hazard levels evolve across scenarios and periods. Under SSP1-2.6, most municipalities show small negative or near-zero changes relative to the baseline, consistent with a limited strengthening of climatic drought pressure. Under SSP3-7.0 and SSP5-8.5, however, many central and western municipalities display clear upward shifts in their hazard index, particularly by 2071–2100.

These tendencies are quantified in Table 4-1, which reports the baseline municipal hazard value and the change relative to baseline for each scenario and period. Under SSP1-2.6, changes remain modest and predominantly negative (reductions of about 0.02–0.08 in the index) across almost all municipalities even at the end of the century, suggesting that improved global mitigation would help to stabilise relative drought hazard in Crete. Under SSP3-7.0 and SSP5-8.5, several municipalities experience increases of 0.08–0.15 in the hazard index by 2071–2100. For example, in SSP3-7.0 late-century values increase by around 0.09 in Heraklion and 0.15 in Mylopotamos, while under SSP5-8.5 late-century changes exceed 0.10 in a number of municipalities including Heraklion, Faistos, Mylopotamos and Chania. Taken together, these results indicate that the central and western municipalities are particularly sensitive to the choice of emissions pathway, with substantially higher relative drought hazard emerging under high-forcing scenarios.

Table 4-1: Relative drought hazard index values aggregated at municipality level for the baseline period (1981–2010) (top) and changes in hazard category for three future periods under SSP1-2.6, SSP3-7.0 and SSP5-8.5.

		SSP126			SSP370			SSP585		
Municipality	Baseline	2011–2040	2041–2070	2071–2100	2011–2040	2041–2070	2071–2100	2011–2040	2041–2070	2071–2100
Iraklio	0.58	-0.05	-0.03	-0.02	-0.06	0.02	0.09	-0.06	0.02	0.11
Archanes - Asteroussia	0.42	-0.05	-0.05	-0.04	-0.05	-0.02	0.01	-0.07	-0.03	0.02
Viannos	0.40	-0.07	-0.06	-0.05	-0.06	-0.03	0.02	-0.07	-0.04	0.04
Gortyna	0.32	-0.03	-0.02	-0.01	-0.03	-0.01	0.04	-0.03	0.00	0.05
Malevizi	0.39	-0.01	0.00	0.01	-0.01	0.05	0.11	-0.02	0.05	0.13
Minoa Pediadas	0.47	-0.06	-0.04	-0.03	-0.05	0.00	0.07	-0.05	0.00	0.08
Faistos	0.46	-0.07	-0.06	-0.04	-0.06	-0.01	0.05	-0.07	-0.01	0.08
Chersonissos	0.50	-0.05	-0.04	-0.02	-0.05	0.02	0.11	-0.06	0.03	0.13
Aghios Nikolaos	0.38	-0.03	-0.01	0.00	-0.02	0.03	0.08	-0.03	0.03	0.09
Ierapetra	0.29	-0.03	-0.02	-0.01	-0.03	0.01	0.06	-0.04	0.01	0.07
Oropedio Lassithiou	0.48	-0.06	-0.04	-0.05	-0.05	-0.01	0.05	-0.06	-0.01	0.07
Sitia	0.38	-0.04	-0.03	-0.01	-0.03	0.01	0.07	-0.04	0.01	0.10
Rethymno	0.43	-0.03	-0.01	0.00	-0.01	0.04	0.12	-0.03	0.05	0.13
Aghios Vassilios	0.53	-0.06	-0.05	-0.04	-0.06	0.00	0.07	-0.07	-0.01	0.09
Amari	0.44	-0.09	-0.08	-0.07	-0.09	-0.06	-0.02	-0.10	-0.07	0.00
Anogia	0.55	-0.08	-0.07	-0.05	-0.08	-0.01	0.05	-0.08	0.00	0.06
Mylopotamos	0.49	-0.05	-0.03	-0.02	-0.03	0.03	0.12	-0.05	0.03	0.15
Chania	0.54	-0.04	-0.01	0.01	-0.03	0.06	0.18	-0.03	0.07	0.21
Apokoronas	0.45	-0.02	0.01	0.02	0.00	0.07	0.16	-0.02	0.08	0.17
Kandanos - Selinos	0.41	-0.03	-0.01	0.00	-0.02	0.03	0.11	-0.03	0.04	0.11
Kissamos	0.56	-0.07	-0.04	-0.02	-0.05	0.01	0.10	-0.05	0.01	0.14
Platanias	0.49	-0.05	-0.02	-0.01	-0.04	0.03	0.14	-0.03	0.03	0.18
Sfakia	0.55	-0.08	-0.07	-0.05	-0.08	-0.01	0.08	-0.09	-0.01	0.09

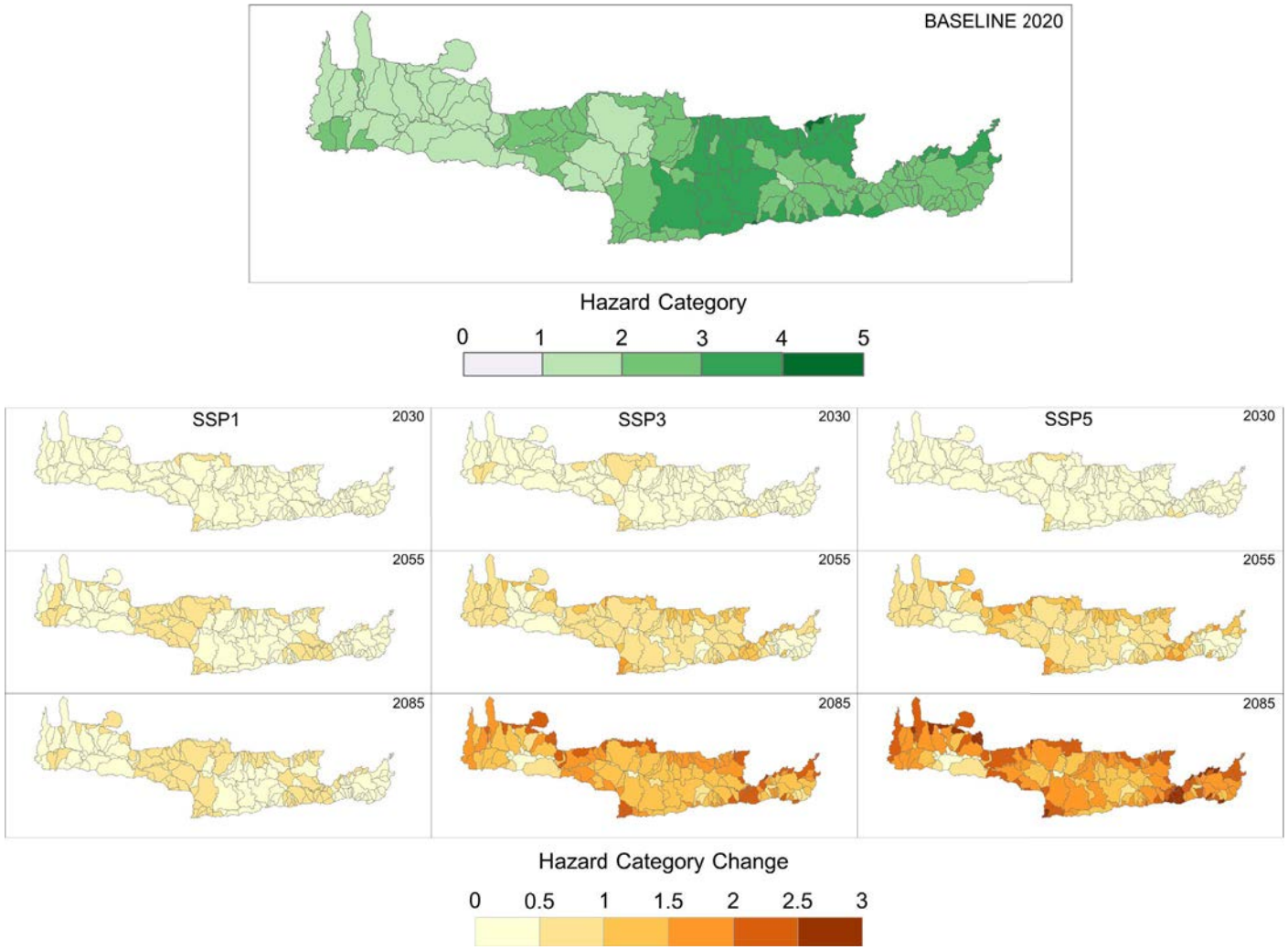

Figure 4-1: Relative drought hazard index at sub-basin (basin–municipality unit) scale for the baseline period (1981–2010) (top) and change in hazard category for three future periods (represented by 2030, 2055 and 2085) under SSP1-2.6, SSP3-7.0 and SSP5-8.5.

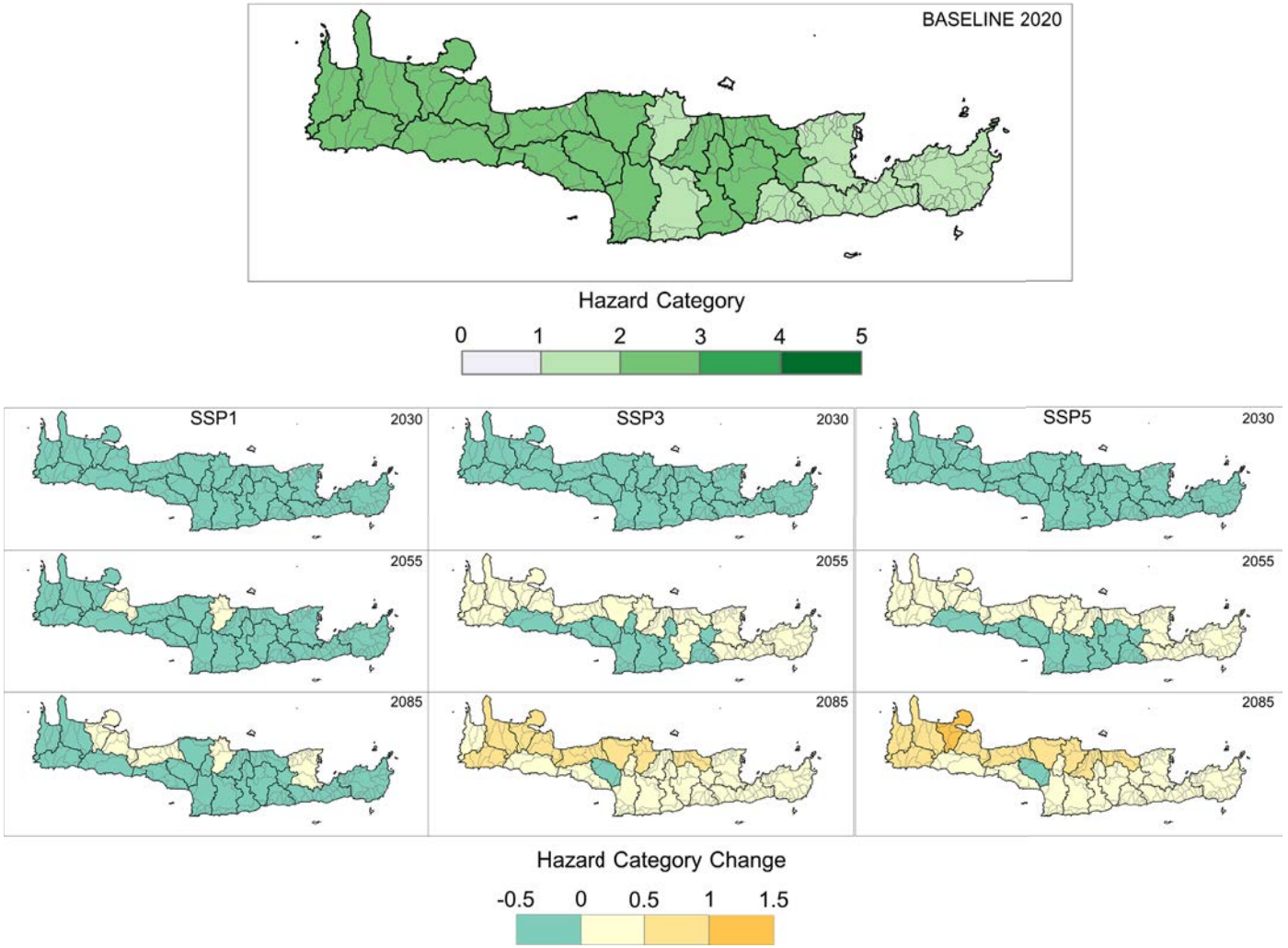

Figure 4-2: Relative drought hazard index aggregated at municipality level for the baseline period (1981–2010) (top) and change in hazard category for three future periods (represented by 2030, 2055 and 2085) under SSP1-2.6, SSP3-7.0 and SSP5-8.5.

4.1.2 Relative drought Exposure maps

The composite exposure index reflects the spatial concentration of water-demanding activities (cropland, population and tourism) within each basin–municipality unit. It combines three normalised sub-indicators – cropland exposure (GCAM/DEMETER), population water-stress exposure (population density) and tourism water-stress exposure – using the demand-based weighting scheme described in Section 3.1.3 (86% agriculture, 10.5% domestic, 3.5% tourism). As for the hazard, all sub-indicators and the composite exposure index are normalised to 0–1 over a pooled distribution that includes the baseline and all future periods and scenarios, so that differences across time slices are directly comparable on a common relative scale.

The baseline (2020) exposure map at sub-basin scale (Figure 4-3, top panel) shows a pronounced north-coast and central-axis footprint: high exposure values are found along the Chania-Rethymno-Heraklion corridor, in parts of the Messara plain and the central uplands, where irrigated agriculture, settlements and tourism co-exist at high densities. Lower values occur in sparsely populated mountainous basins and in parts of eastern Crete. The future maps (Figure 4-3, lower panels) indicate mainly moderate exposure increases in many basins, particularly in the central and eastern parts of the island under SSP3-7.0 and SSP5-8.5 towards mid- and late-century, while changes remain smaller and more mixed under SSP1-2.6. Localised decreases appear where projected cropland or population decline outweighs growth in other sectors.

At municipality level (Figure 4-4), the baseline exposure index is highest in Iraklio, Platanias, Chania, Rethymno, Aghios Vassilios, Anogia and Sfakia (baseline values typically 0.6–0.8), reflecting the combination of extensive cropland and/or dense settlement and tourism activity. Lower exposure values (0.2–0.4) are found in more sparsely populated or less intensively cultivated municipalities such as Viannos, Sitia and Aghios Nikolaos. The scenario maps show that, under SSP1-2.6, municipal-scale exposure remains broadly similar to the baseline, with small positive or negative changes. Under SSP3-7.0 and SSP5-8.5, exposure tends to increase in several central and eastern municipalities, while some western and mountainous municipalities show modest reductions or stabilisation, showing a gradual shift in relative pressure across the island.

These patterns are quantified in Table 4-2, which summarises the baseline exposure index and its change for each municipality and scenario/period. Under SSP1-2.6, most municipalities exhibit changes within about ±0.05, indicating limited redistribution of exposure. Under SSP3-7.0, however, several municipalities show increases of 0.15–0.30 by 2071–2100 (e.g. Viannos, Anogia, Ierapetra, Oropedio Lasithiou, Sitia), signalling a marked strengthening of relative exposure in parts of central and eastern Crete. In contrast, some currently highly exposed municipalities (e.g. Aghios Vassilios, Sfakia) show small negative changes under multiple scenarios, consistent with projected reductions in cropland and/or population.

The sub-indicator maps (Figures 7-5 - 7-7) help interpret the composite patterns. Cropland exposure (Figure 7-5) confirms the dominance of the north-coastal agricultural belt and central plains in both GCAM-based and LUISA 2020 data, with future scenarios showing either stabilisation or modest redistribution of agricultural area rather than large expansions. Population water-stress exposure (Figure 7-6) is concentrated around the main urban and peri-urban zones and remains high in these areas in all scenarios, with some gradual intensification under SSP3-7.0 in central and eastern municipalities. Tourism water-stress exposure (Figure 7-7) is highest along the northern coastline and in established tourist hotspots; scenario changes are more modest in absolute terms but reinforce the role of specific coastal basins as multi-sectoral pressure points where agricultural, domestic and tourism demands coincide.

Table 4-2:Baseline municipal exposure index (2020) and changes relative to baseline for three future periods (2011–2040, 2041–2070, 2071–2100) under scenarios SSP1-2.6, SSP3-7.0 and SSP5-8.5.

		SSP126			SSP370			SSP585		
Municipality	Baseline	2011–2040	2041–2070	2071–2100	2011–2040	2041–2070	2071–2100	2011–2040	2041–2070	2071–2100
Iraklio	0.82	-0.01	0.01	0.11	0.04	0.07	0.10	0.02	0.03	0.04
Archanes - Asteroussia	0.61	-0.01	0.00	0.10	0.04	0.08	0.10	0.01	0.02	0.02
Viannos	0.15	-0.01	0.04	0.29	0.06	0.15	0.18	-0.01	0.03	0.06
Gortyna	0.65	0.00	0.02	0.09	0.03	0.05	0.06	0.02	0.03	0.04
Malevizi	0.47	0.02	0.04	0.21	0.09	0.13	0.17	0.02	0.03	0.06
Minoa Pediadas	0.46	0.00	0.02	0.17	0.04	0.10	0.14	0.00	0.03	0.04
Faistos	0.54	0.00	0.01	0.08	0.02	0.05	0.07	0.00	0.01	0.02
Chersonissos	0.53	-0.02	-0.01	0.02	0.01	0.07	0.12	-0.03	-0.01	0.01
Aghios Nikolaos	0.20	0.02	0.04	0.22	0.16	0.23	0.28	0.01	0.05	0.08
Ierapetra	0.33	0.00	0.03	0.20	0.03	0.11	0.14	0.00	0.02	0.04
Oropedio Lassithiou	0.48	-0.06	-0.02	0.18	-0.02	0.09	0.17	-0.09	-0.05	-0.02
Sitia	0.23	0.00	0.02	0.19	0.04	0.10	0.15	-0.01	0.02	0.03
Rethymno	0.64	0.14	0.14	0.14	0.13	0.14	0.12	0.14	0.14	0.13
Aghios Vassilios	0.76	-0.05	-0.04	0.02	-0.05	-0.03	-0.03	-0.05	-0.05	-0.05
Amari	0.54	0.07	0.08	0.18	0.08	0.12	0.15	0.06	0.07	0.08
Anogia	0.34	0.07	0.10	0.21	0.14	0.23	0.29	0.07	0.09	0.10
Mylopotamos	0.45	-0.04	-0.04	0.09	0.04	0.10	0.13	-0.05	-0.04	-0.02
Chania	0.67	-0.03	-0.01	0.10	-0.03	-0.02	0.01	-0.02	-0.02	-0.03
Apokoronas	0.83	0.04	0.04	0.04	0.03	0.02	0.01	0.04	0.03	0.02
Kandanos - Selinos	0.64	0.03	0.03	0.07	0.02	0.04	0.04	0.03	0.02	0.02
Kissamos	0.60	0.00	0.01	0.02	-0.01	0.00	0.01	0.00	0.00	-0.01
Platanias	0.40	0.02	0.02	0.04	0.04	0.07	0.07	0.02	0.03	0.03
Sfakia	0.64	-0.07	-0.06	0.03	-0.06	-0.05	0.00	-0.07	-0.07	-0.07

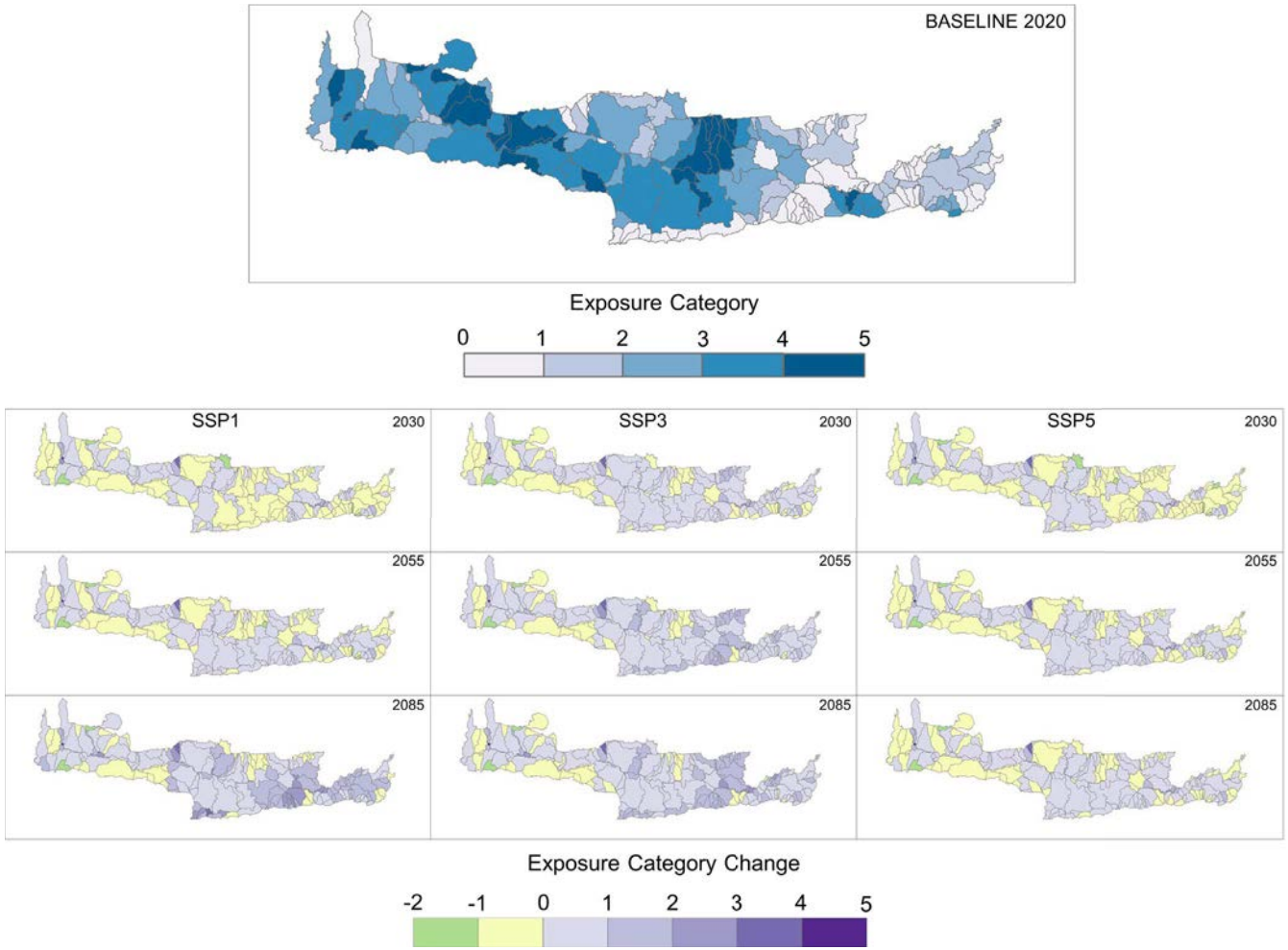

Figure 4-3: Composite exposure index at sub-basin (basin–municipality unit) scale for the baseline year 2020 (top) and for three future periods (2011–2040, 2041–2070, 2071–2100) under SSP1-2.6, SSP3-7.0 and SSP5-8.5.

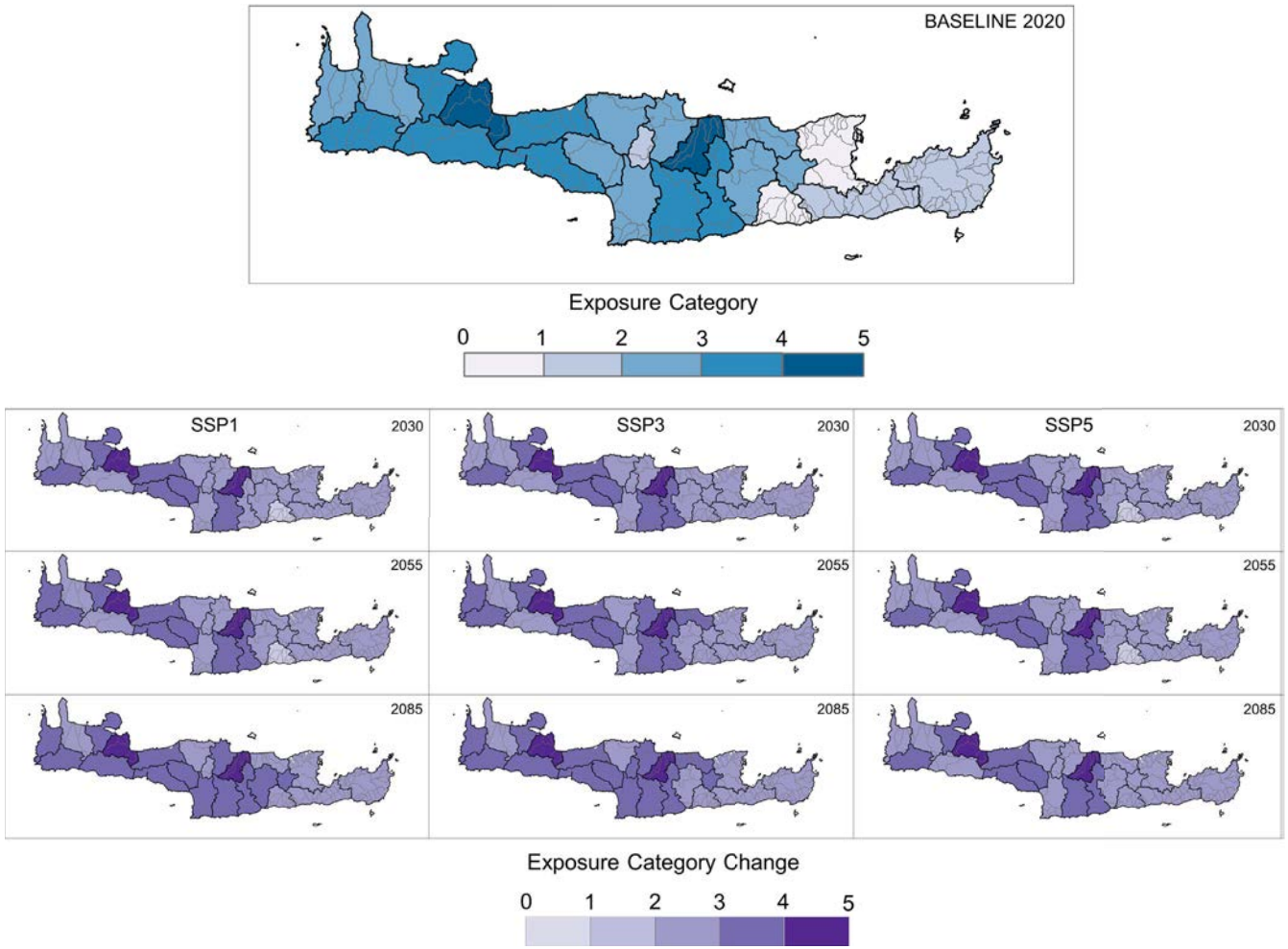

Figure 4-4: Composite exposure index aggregated at municipality level. The top panel shows baseline (2020) values; lower panels show exposure for 2011–2040, 2041–2070 and 2071–2100 under SSP1-2.6, SSP3-7.0 and SSP5-8.5.

4.1.3 Relative drought Vulnerability maps

The composite vulnerability index represents the capacity of each basin-municipality unit to cope with drought, combining socio-economic conditions and water-system characteristics. As described in Section 3.1.4, the index is built from four normalised sub-indicators: GDP per capita, groundwater access, irrigated area fraction and planned water-infrastructure capacity. GDP per capita and the combined water-availability component each account for 50% of the final score. All sub-indicators were transformed so that higher values correspond to higher vulnerability (lower adaptive capacity) and were normalised over a pooled distribution including the baseline and all future periods and scenarios.

The baseline vulnerability map at sub-basin scale (Figure 4-5, top) highlights a corridor of elevated vulnerability in central and south-central Crete, extending from the inland municipalities of Amari, Anogia and Mylopotamos towards parts of Faistos and neighbouring basins. Additional local maxima occur in mountainous areas of western Crete and in selected eastern basins. These zones combine comparatively lower income levels, lower access to groundwater resources and more limited irrigation and storage infrastructure. In contrast, several coastal and urbanised basins around Chania, Heraklion and parts of eastern Crete exhibit lower baseline vulnerability.

Future changes (Figure 4-5, lower panels) point to a general tendency towards reduced vulnerability in many basins, particularly those with currently high scores. Under SSP1-2.6, improvements are moderate but widespread, with many central and southern basins showing reductions of around one vulnerability class by mid-century. Under SSP3-7.0 and especially SSP5-8.5, vulnerability reductions become more pronounced in parts of central and western Crete, reflecting the combined effect of income growth and expanded water-infrastructure capacity in the SSP-consistent pathways. At the same time, a few basins in eastern Crete and selected coastal zones exhibit small increases.

Aggregation to municipality level (Figure 4-6) shows that Amari, Anogia, Aghios Vassilios, Apokoronas, Kandanos–Selinos and Sfakia are among the most vulnerable municipalities in the 2020 baseline (index values around 0.6–0.8), while Iraklio, Chania and several eastern municipalities start from substantially lower vulnerability (≈0.1–0.3). The scenario maps show that, across all SSPs, most municipalities experience declining vulnerability over time, with the strongest improvements in those starting from the highest baseline levels. This behaviour is quantified in Table 4-3, under SSP1-2.6, late-century changes in highly vulnerable municipalities often reach −0.20 to −0.30 in the index (e.g. Anogia, Amari, Sfakia), whereas low-vulnerability municipalities generally exhibit only small changes (within about ±0.05). Under SSP3-7.0 and SSP5-8.5, reductions in the most vulnerable municipalities are of similar or greater magnitude, while a limited number of municipalities with relatively low baseline vulnerability show modest increases (up to about +0.05–0.10).

The sub-indicator maps help interpret these patterns. The GDP per capita indicator (Figure 7-8) shows consistent income growth across the island, strongest in urban and peri-urban municipalities, which generally reduces vulnerability over time in all SSPs. The

groundwater-related indicator (Figure 7-9) captures limited access to exploitable groundwater resources, rather than dependence on existing abstractions. Higher values indicate basins with sparse or low-yield aquifers and fewer productive wells, where there is reduced potential to buffer meteorological drought through groundwater use. In these areas, even moderate climatic drought can translate more quickly into water-supply stress, contributing to higher overall vulnerability. The irrigated area fraction (Figure 7-9) moderates vulnerability in basins with extensive, well-developed irrigation systems, mainly in the northern coastal plains and parts of the Messara. Finally, the planned water-infrastructure sub-indicator (Figure 7-10 and Figure 7-11) shows strong spatial contrasts between SSPs: SSP1 emphasises a smaller set of targeted works, SSP3 a limited portfolio of relatively modest interventions, and SSP5 a much more extensive expansion of storage and conveyance capacity. When aggregated to the basin scale, these differences translate into progressively higher water-system capacity and lower vulnerability in the core agricultural basins under SSP3 and especially SSP5.

Table 4-3: Baseline municipal vulnerability index (2020) and changes relative to baseline for three future periods (2011–2040, 2041–2070, 2071–2100) under SSP1-2.6, SSP3-7.0 and SSP5-8.5.

		SSP126			SSP370			SSP585		
Municipality	Baseline	2011–2040	2041–2070	2071–2100	2011–2040	2041–2070	2071–2100	2011–2040	2041–2070	2071–2100
Iraklio	0.09	0.01	0.01	0.00	-0.01	-0.01	-0.02	-0.01	-0.02	-0.02
Archanes - Asteroussia	0.18	-0.06	-0.08	-0.09	-0.06	-0.07	-0.08	-0.07	-0.10	-0.11
Viannos	0.35	-0.10	-0.15	-0.18	-0.09	-0.13	-0.18	-0.13	-0.20	-0.23
Gortyna	0.29	-0.09	-0.14	-0.16	-0.09	-0.11	-0.15	-0.10	-0.16	-0.19
Malevizi	0.15	-0.04	-0.04	-0.05	-0.05	-0.05	-0.05	-0.05	-0.06	-0.08
Minoa Pediadas	0.29	-0.11	-0.14	-0.16	-0.11	-0.13	-0.15	-0.12	-0.17	-0.18
Faistos	0.15	-0.07	-0.08	-0.09	-0.06	-0.07	-0.08	-0.08	-0.09	-0.10
Chersonissos	0.14	-0.01	-0.03	-0.03	-0.02	-0.02	-0.04	-0.02	-0.03	-0.04
Aghios Nikolaos	0.19	0.02	0.01	-0.01	0.01	0.00	-0.01	0.02	-0.02	-0.03
Ierapetra	0.23	-0.01	-0.03	-0.04	-0.02	-0.04	-0.05	-0.04	-0.07	-0.09
Oropedio Lassithiou	0.55	-0.12	-0.19	-0.24	-0.11	-0.16	-0.23	-0.12	-0.22	-0.27
Sitia	0.27	0.01	-0.01	-0.03	0.01	-0.02	-0.03	-0.01	-0.05	-0.07
Rethymno	0.19	-0.01	-0.02	-0.02	-0.01	-0.02	-0.02	-0.01	-0.02	-0.04
Aghios Vassilios	0.65	-0.11	-0.18	-0.22	-0.10	-0.14	-0.20	-0.11	-0.20	-0.26
Amari	0.60	-0.14	-0.21	-0.26	-0.14	-0.18	-0.25	-0.15	-0.24	-0.29
Anogia	0.61	-0.19	-0.23	-0.25	-0.18	-0.21	-0.25	-0.19	-0.24	-0.28
Mylopotamos	0.40	-0.16	-0.20	-0.22	-0.15	-0.17	-0.20	-0.16	-0.21	-0.24
Chania	0.19	-0.01	-0.01	-0.01	-0.02	-0.02	-0.03	-0.02	-0.02	-0.03
Apokoronas	0.54	-0.24	-0.27	-0.28	-0.26	-0.27	-0.29	-0.26	-0.30	-0.33
Kandanos - Selinos	0.62	-0.09	-0.15	-0.21	-0.08	-0.12	-0.19	-0.09	-0.18	-0.25
Kissamos	0.36	-0.13	-0.17	-0.18	-0.13	-0.15	-0.17	-0.14	-0.18	-0.20
Platanias	0.40	-0.15	-0.18	-0.19	-0.15	-0.16	-0.18	-0.21	-0.24	-0.26
Sfakia	0.82	-0.01	-0.04	-0.07	-0.01	-0.03	-0.07	-0.01	-0.06	-0.11

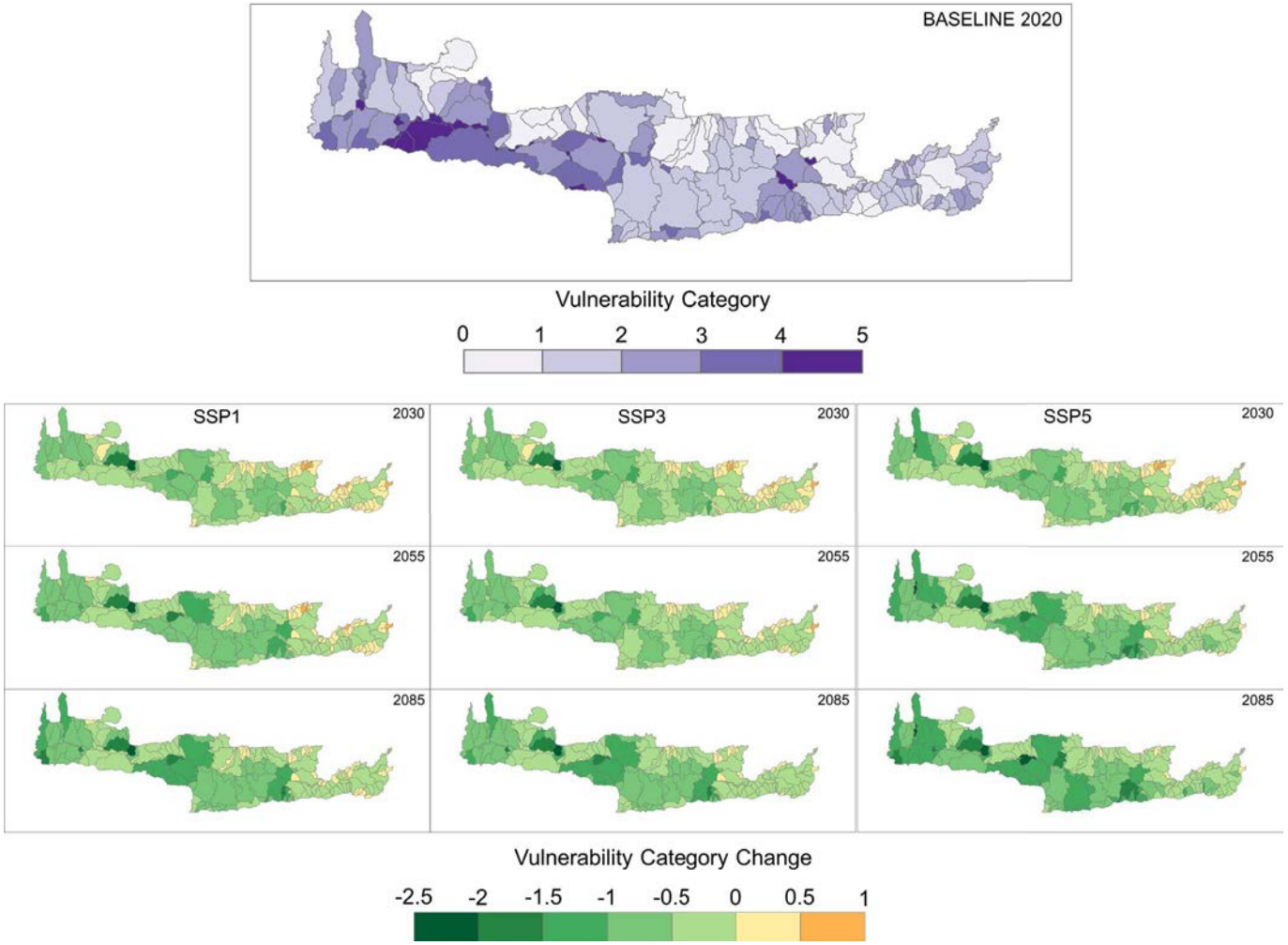

Figure 4-5: Composite drought-vulnerability index at sub-basin (basin–municipality unit) scale for the baseline year 2020 (top) and changes relative to the baseline for three future periods (2011–2040, 2041–2070, 2071–2100) under SSP1-2.6, SSP3-7.0 and SSP5-8.5.

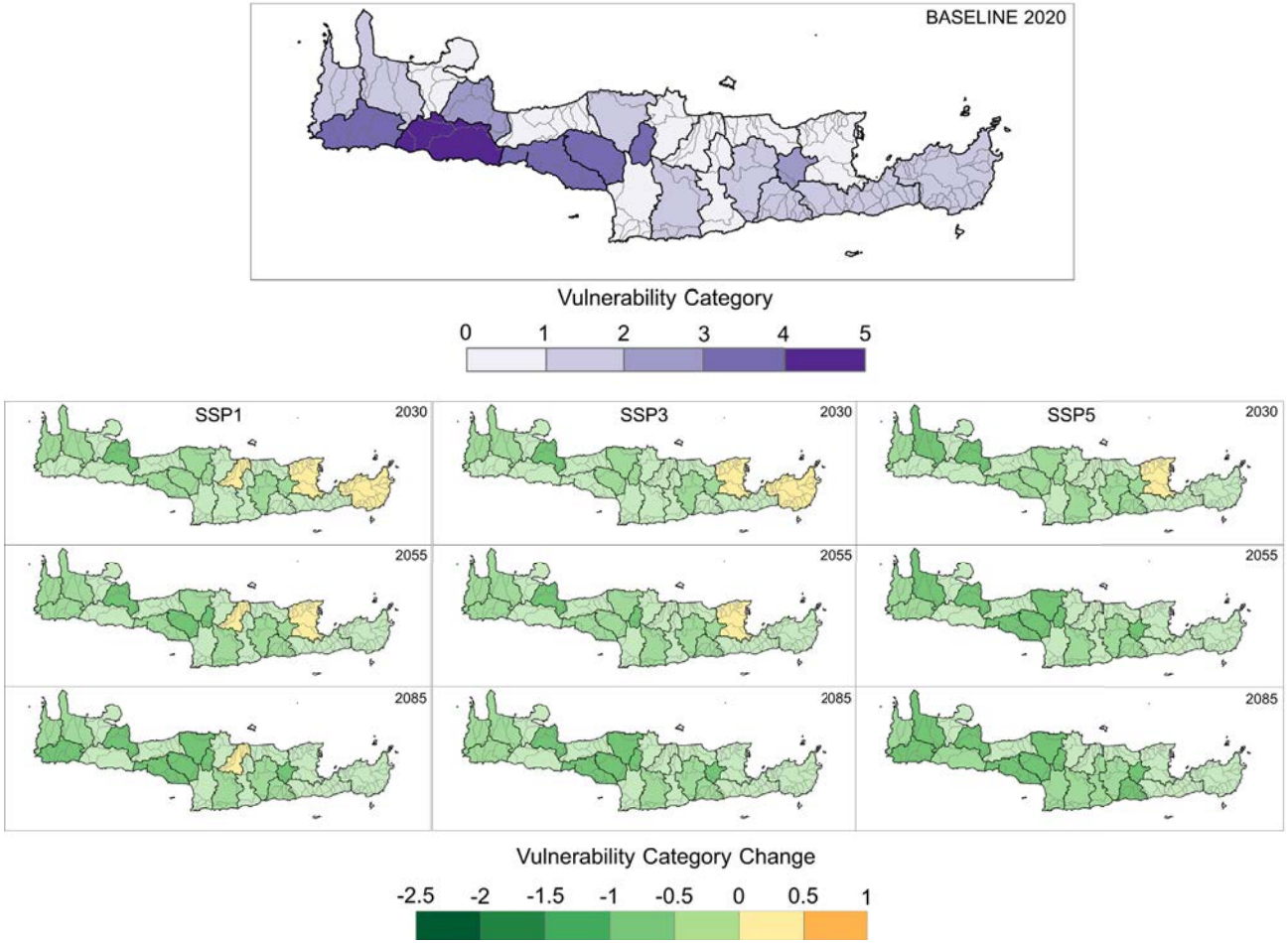

Figure 4-6: Composite drought-vulnerability index aggregated at municipality level. The top panel shows baseline (2020) vulnerability; lower panels show changes relative to baseline for 2011–2040, 2041–2070 and 2071–2100 under SSP1-2.6, SSP3-7.0 and SSP5-8.5.

4.1.4 Relative drought Risk maps

The composite relative drought risk index was derived at the basin-municipality unit scale by combining the normalised hazard, exposure and vulnerability indices described in Sections 4.1.1–4.1.3. The three components were first rescaled to 0–1 on the pooled distribution (baseline plus all time periods and scenarios) and then combined multiplicatively, followed by re-normalisation, so that high risk occurs only where climatic hazard, exposure and vulnerability co-exist. Resulting continuous risk values were finally grouped into classes using pooled percentile thresholds, ensuring full comparability between the baseline and all future periods and SSPs.

The baseline risk map at sub-basin scale (Figure 4-7, top) shows a well-defined central-southern risk belt, extending from western Crete through the Amari-Mylopotamos-Messara region towards parts of Viannos and Ierapetra, with additional hotspots in Apokoronas and Sfakia. These areas combine high relative hazard, dense agricultural and/or domestic water demand, and comparatively high vulnerability due to high agricultural activity or weaker socio-economic conditions. Northern coastal basins east of Heraklion and parts of eastern Crete display lower present-day risk, mainly because of lower hazard and/or stronger adaptive capacity.

Scenario maps (Figure 4-7, lower panels) reveal that, despite the increase in climatic hazard, overall risk tends to stabilise or decrease across much of the island, particularly under SSP1-2.6. In this low-forcing pathway, many of today's highest-risk basins move down by one or more risk classes by mid-century, as reductions in vulnerability (income growth, targeted infrastructure) outweigh modest hazard intensification and exposure changes. Under SSP3-7.0 and SSP5-8.5, the picture is more mixed. For 2030 and 2055, many central and western basins still show risk reductions relative to baseline, but by 2085 some basins in south-central and eastern Crete display small to moderate risk increases, showing that under stronger climate change the hazard signal can begin to offset adaptation gains.

At municipality level (Figure 4-8), the baseline risk index shows Aghios Vassilios, Sfakia, Apokoronas, Kandanos-Selinos and Amari as the highest-risk municipalities (baseline values typically between about 2.0 and 4.0 in the normalised index), while municipalities such as Aghios Nikolaos, Sitia and Malevizi exhibit substantially lower present-day risk (<1). The scenario maps illustrate that, under SSP1-2.6, most municipalities with initially high-risk experience marked decreases by mid- to late-century, whereas low-risk municipalities change little. Under SSP3-7.0 and SSP5-8.5, the largest reductions still occur in some of the present-day hotspots, but several municipalities in eastern and south-eastern Crete (e.g. Viannos, Ierapetra, Sitia) exhibit net risk increases towards the end of the century, reflecting the combination of stronger hazard intensification and rising exposure.

These tendencies are quantified in Table 4-4. In SSP1-2.6, municipalities such as Sfakia, Apokoronas, Aghios Vassilios and Kandanos–Selinos show late-century decreases on the order of −0.8 to −1.8 risk units, while changes in low-risk municipalities remain small and sometimes slightly positive. Under SSP3-7.0 and SSP5-8.5, some central–southern

municipalities (e.g. Gortyna, Sitia, Viannos) exhibit positive changes up to about +1.0–1.5 by 2071–2100, indicating a shift into higher risk classes despite reductions in vulnerability elsewhere. Overall, the risk analysis suggests that adaptation and socio-economic development can substantially lower drought risk in several current hotspots, especially under a mitigation-consistent pathway (SSP1-2.6), but that under higher-forcing scenarios a number of basins in central and eastern Crete remain or become priority areas for drought-risk management.

Table 4-4: Baseline municipal relative drought risk index (2020) and changes relative to baseline for three future periods (2011–2040, 2041–2070, 2071–2100) under SSP1-2.6, SSP3-7.0 and SSP5-8.5.

		SSP126			SSP370			SSP585		
Municipality	Baseline	2011–2040	2041–2070	2071–2100	2011–2040	2041–2070	2071–2100	2011–2040	2041–2070	2071–2100
Iraklio	0.81	0.18	0.18	0.13	-0.16	-0.11	-0.02	-0.16	-0.11	-0.02
Archanes - Asteroussia	1.85	-0.13	-0.78	-0.78	-0.13	0.01	0.01	-0.78	-0.78	-0.78
Viannos	0.64	-0.17	0.11	1.04	0.22	0.76	0.76	-0.48	-0.48	-0.37
Gortyna	2.63	-0.75	-0.83	-0.83	0.00	0.02	0.02	-0.75	-0.92	-0.91
Malevizi	0.12	0.00	0.21	0.26	0.26	0.30	0.53	-0.01	0.00	0.26
Minoa Pediadas	1.78	-0.59	-0.96	-0.79	-0.59	0.17	0.17	-0.76	-0.96	-0.79
Faistos	1.45	-0.72	-0.72	-0.72	-0.72	-0.65	0.00	-0.72	-0.72	-0.72
Chersonissos	0.91	-0.11	-0.17	-0.10	-0.10	0.70	0.84	-0.18	-0.04	-0.01
Aghios Nikolaos	0.11	0.23	0.23	0.66	0.74	1.04	1.74	0.23	0.28	0.50
Ierapetra	0.76	-0.06	0.07	0.54	0.11	0.47	0.96	-0.09	0.15	0.19
Oropedio Lassithiou	1.94	-0.10	0.14	0.40	0.14	0.40	0.40	-0.17	-0.67	-0.60
Sitia	0.37	0.03	0.17	0.85	0.32	0.56	1.18	-0.01	0.28	0.47
Rethymno	0.78	0.42	0.82	0.54	0.54	1.17	1.44	0.42	1.17	1.22
Aghios Vassilios	3.81	-0.34	-0.34	-0.17	-0.34	0.17	0.17	-0.34	-0.34	-0.17
Amari	2.97	-0.04	-0.65	0.04	0.00	0.15	0.18	-0.04	-0.03	0.00
Anogia	1.58	0.05	0.05	0.10	0.05	0.78	1.05	0.05	0.05	0.10
Mylopotamos	1.95	-0.97	-1.76	-0.74	-0.78	-0.55	-0.55	-0.97	-1.76	-1.57
Chania	1.01	-0.38	-0.38	0.03	-0.38	0.11	0.70	-0.38	0.11	0.35
Apokoronas	3.31	-1.37	-1.28	-1.37	-1.37	-0.67	-0.47	-1.37	-1.29	-0.47
Kandanos - Selinos	2.75	0.49	0.03	0.29	0.49	0.63	0.77	0.49	0.29	0.29
Kissamos	1.76	-0.60	-0.60	-0.60	-0.60	-0.44	0.32	-0.60	-0.60	-0.16
Platanias	0.92	-0.56	-0.56	-0.56	-0.56	0.35	0.40	-0.62	-0.56	-0.52
Sfakia	3.92	-0.85	-0.85	-0.57	-0.60	-0.52	0.08	-0.85	-0.77	-0.21

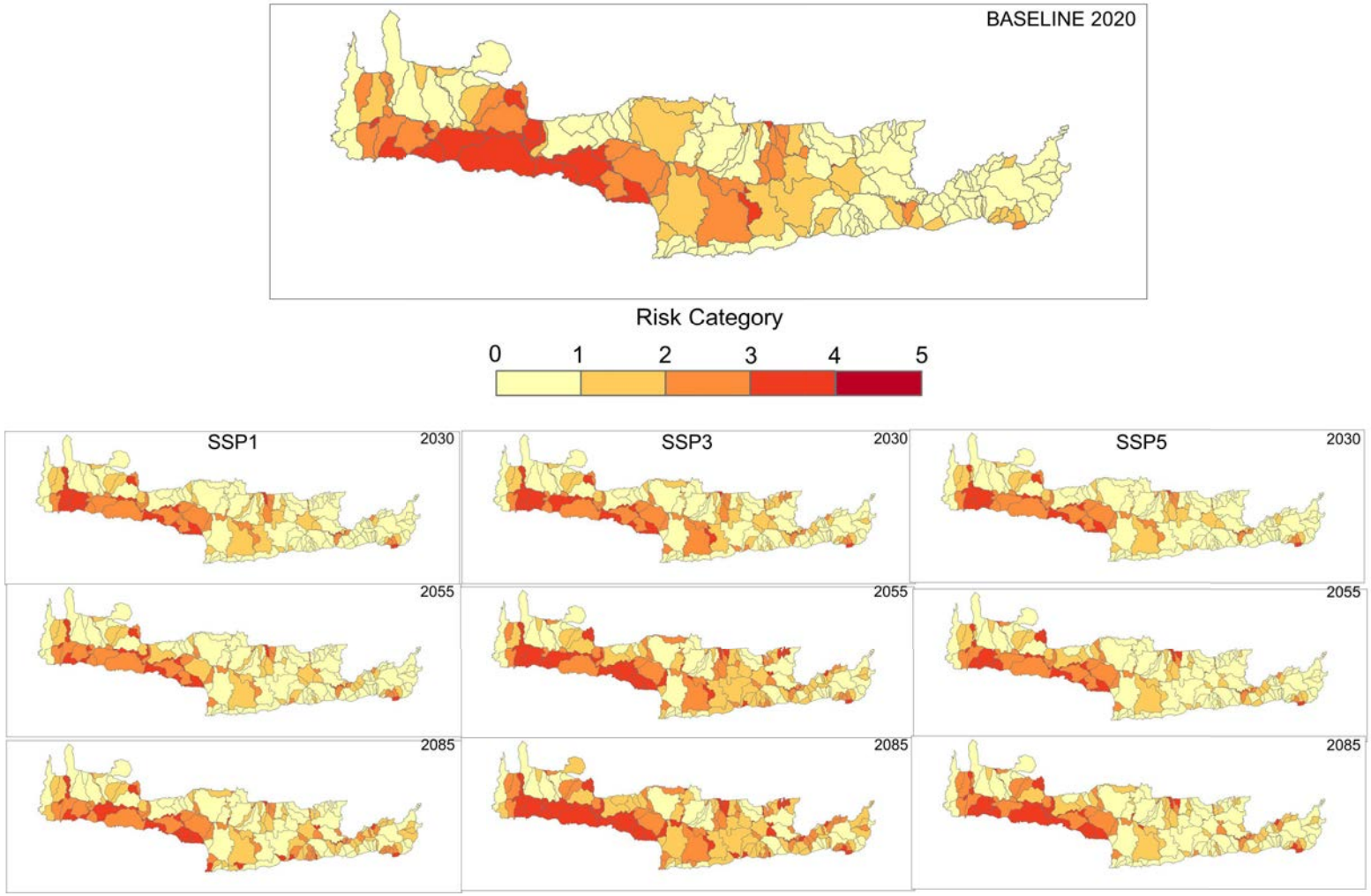

Figure 4-7: Relative drought risk index at sub-basin (basin–municipality unit) scale for the baseline year 2020 (top) and changes relative to baseline for three future periods (2011–2040, 2041–2070, 2071–2100) under SSP1-2.6, SSP3-7.0 and SSP5-8.5 (bottom panels).

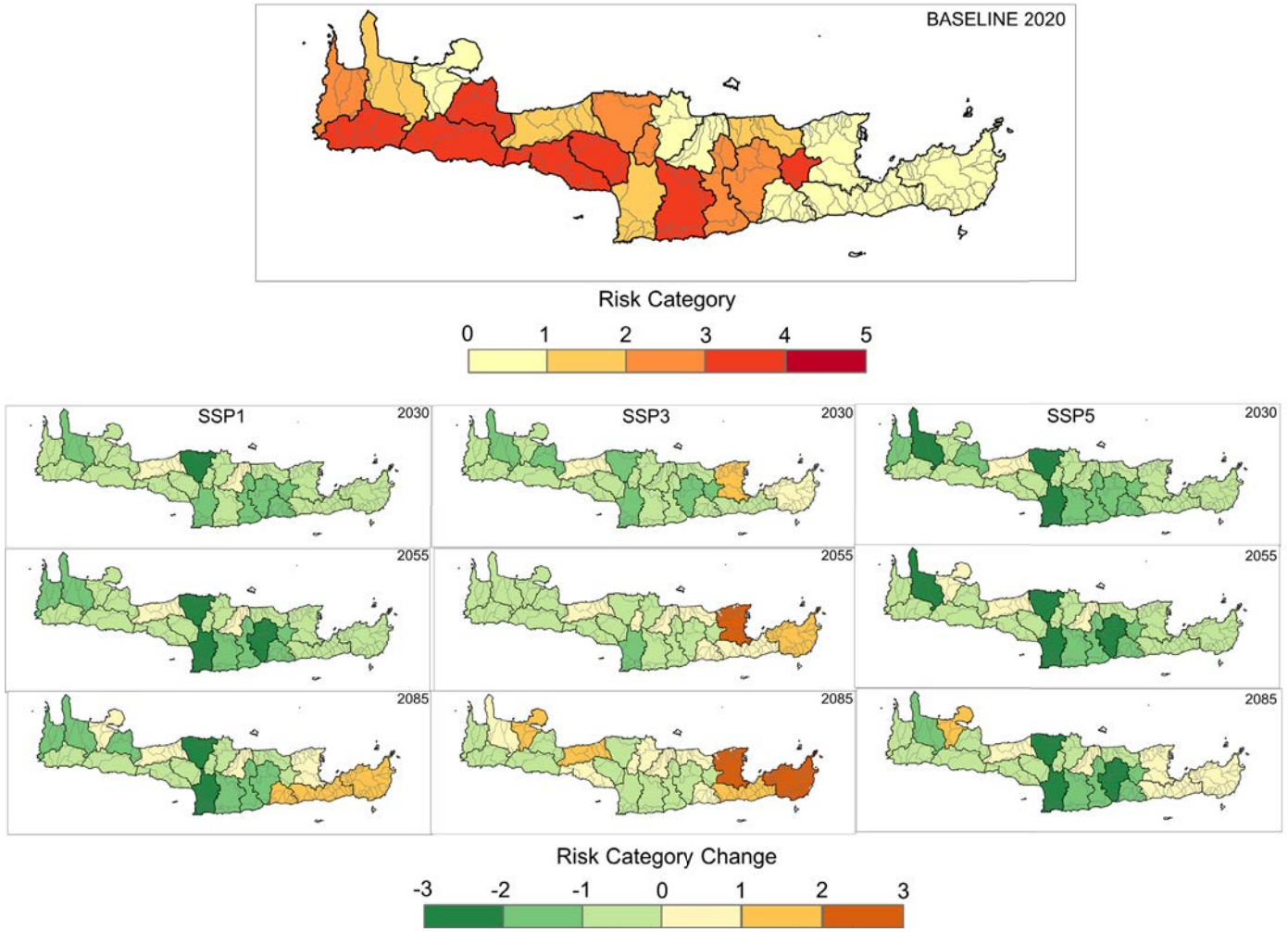

Figure 4-8: Relative drought risk index aggregated at municipality level. The top panel presents baseline (2020) risk values; the lower panels show changes relative to baseline for 2011–2040, 2041–2070 and 2071–2100 under SSP1-2.6, SSP3-7.0 and SSP5-8.5.

4.1.5 Uncertainties and robustness of results - Relative Drought Risk

The relative drought risk index inherits uncertainties from all three of its components. On the hazard side, the CHELSA and ISIMIP3b climate datasets are bias-corrected but remain uncertain in their representation of mean precipitation and its variability over the complex Cretan topography, especially in orographic rain-shadow areas and along coastal gradients. The SSP1-2.6, SSP3-7.0 and SSP5-8.5 projections further introduce scenario spread in both temperature and precipitation trajectories. Because the hazard metric is constructed from pooled percentiles of BIO1, BIO5, BIO12 and the WASP index across all periods and scenarios, any biases or systematic drifts in these driving datasets propagate into the relative ranking of units. Results should therefore be interpreted as internally consistent, scenario-conditioned contrasts within the modelling framework, rather than as precise quantitative probabilities of drought occurrence. A key avenue for future improvement is the use of the recently developed CLIMADAT-Grid dataset as the primary climate forcing, in order to derive hazard indicators that are more closely tailored to the Cretan climate and to reduce structural and bias uncertainties in the hazard component.

Uncertainty is also present in the exposure and vulnerability components. Agricultural exposure is derived from GCAM/Demeter land-use projections, which provide only a broad, scenario-consistent picture of crop extent and may diverge from locally observed trends in cropping patterns, intensification or shifts between rainfed and irrigated systems. This is particularly important in Crete, where agriculture accounts for about 86% of total water demand and therefore dominates the composite exposure index and any mismatch between GCAM land use and actual agricultural extent can directly bias the spatial pattern of exposure. Finally, the fixed weighting scheme used to combine sub-indicators reflects expert judgment and has not been formally optimised. Alternative weight choices could modify absolute index values and, in some cases, the relative ranking of units. These points underline the need in future work for locally downscaled and policy-relevant land-use and water-use scenarios that can better anchor the exposure and vulnerability components in Cretan realities.

Despite these limitations, several aspects of the results appear robust. High-risk basins and municipalities tend to occur where independent information confirms the coexistence of strong climatic stress, intensive water-demand sectors and constrained water resources.

4.2 Updated Agricultural Drought Risk in Crete

4.2.1 Hazard patterns - Agricultural Drought

For the updated assessment, the agricultural drought hazard for olives in Crete is expressed through three climate-driven fields: cumulative standard evapotranspiration (ET_0) over the growing season, cumulative precipitation, and the resulting percentage yield loss from precipitation deficit. In the main text we focus on the RCP4.5 scenario for

three future time slices (2026–2045, 2046–2065, 2066–2085), using the ensemble of five EURO-CORDEX RCMs (CNRM-ALADIN, KNMI-RACMO, MPI-ESM–SMHI-RCA4, NORESM1-REMO2015 and NORESM1–SMHI-RCA4); corresponding maps for RCP2.6 and RCP8.5 are provided in the Appendix (from Figure 7-12 to Figure 7-17).

The ET_0 maps under RCP4.5 (Figure 4-9) similarly reproduce the pattern identified in Phase 1: lower atmospheric water demand over higher elevations and higher ET_0 in the warmer eastern and southern lowlands. Across the three future periods, most models show a gradual increase in ET_0, reflecting the warming climate, while preserving the spatial structure of higher demand in the east and along the southern coastal plains. The atypical behaviour of NORESM1-REMO2015 noted in Phase 1, with relatively high ET_0 over some elevated areas, is still visible and continues to be treated as a model-specific bias rather than a physical signal.

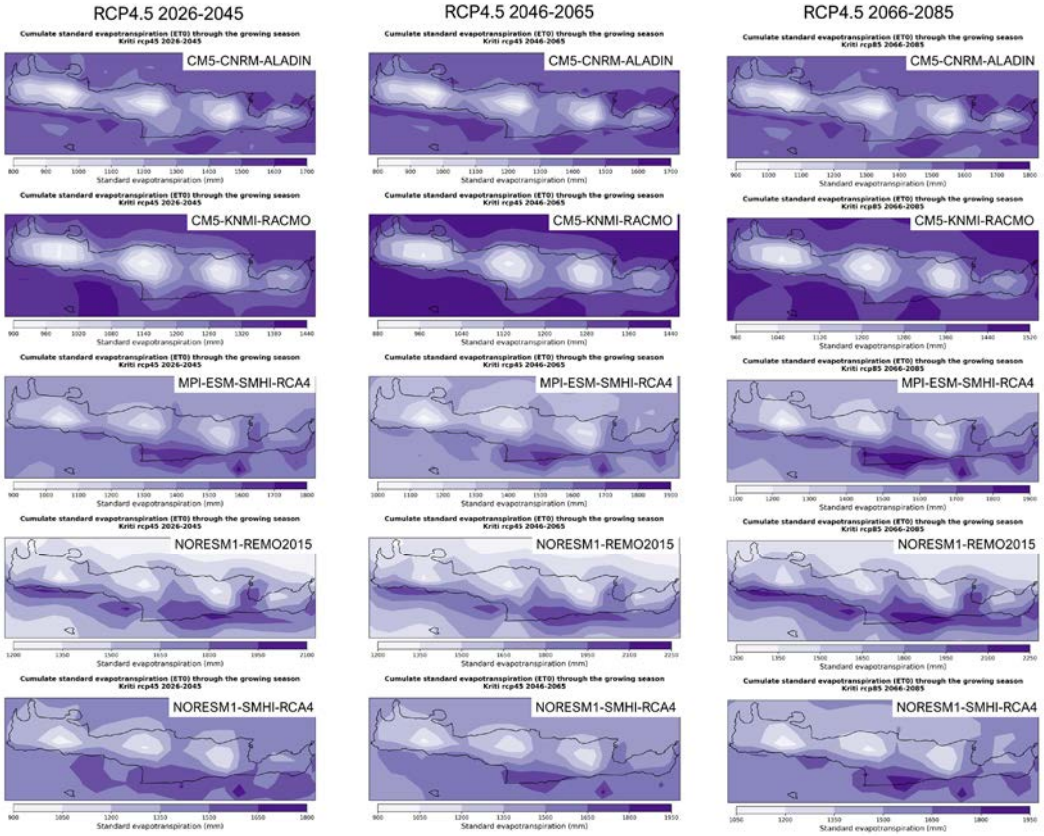

Figure 4-9: Cumulative standard evapotranspiration (ET_0) in Crete for RCP4.5, for three future periods (2026–2045, 2046–2065, 2066–2085) and five EURO-CORDEX RCMs.

The precipitation maps for RCP4.5 (Figure 4-10) show a consistent west-east gradient across all periods and models, with higher cumulative rainfall over the western and mountainous parts of Crete and substantially lower totals over the eastern and lowland areas. This pattern is already evident in the near-future slice and persists into mid- and far-future projections, although individual models differ in the absolute amounts and the sharpness of the gradient. These results are fully consistent with the Phase-1 analysis,

where the 2046–2050 RCP4.5 projections also indicated wetter conditions in western Crete and drier conditions in the east.

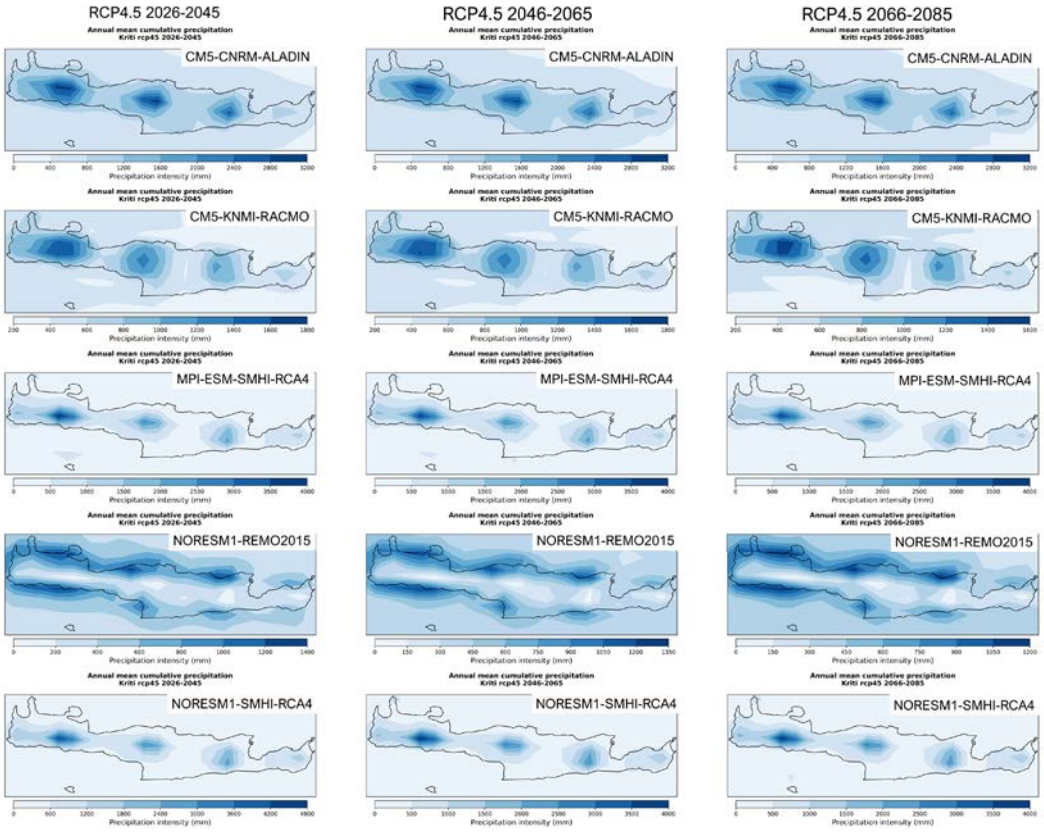

Figure 4-10: Annual mean cumulative precipitation in Crete for RCP4.5, for three future periods (2026–2045, 2046–2065, 2066–2085) and five EURO-CORDEX RCMs. Note that the colour ramps are of different scale among models.

Combining precipitation and ET_0 in the FAO yield-water response formulation yields the olive yield-loss maps for RCP4.5. The updated results confirm the Phase-1 finding that central and eastern Crete systematically experience the highest yield losses under rainfed conditions, while western Crete shows lower losses with some pockets of moderate impact. In the near-future period, typical yield losses in the central-eastern belt are already several percent and increase slightly towards mid- and far-future slices in most models. The spatial pattern, with a core of higher losses spanning the central plateau and eastern lowlands and lower losses in the wetter west, is robust across models and time slices and closely matches the 2046–2050 RCP4.5 pattern reported in the first-phase deliverable.

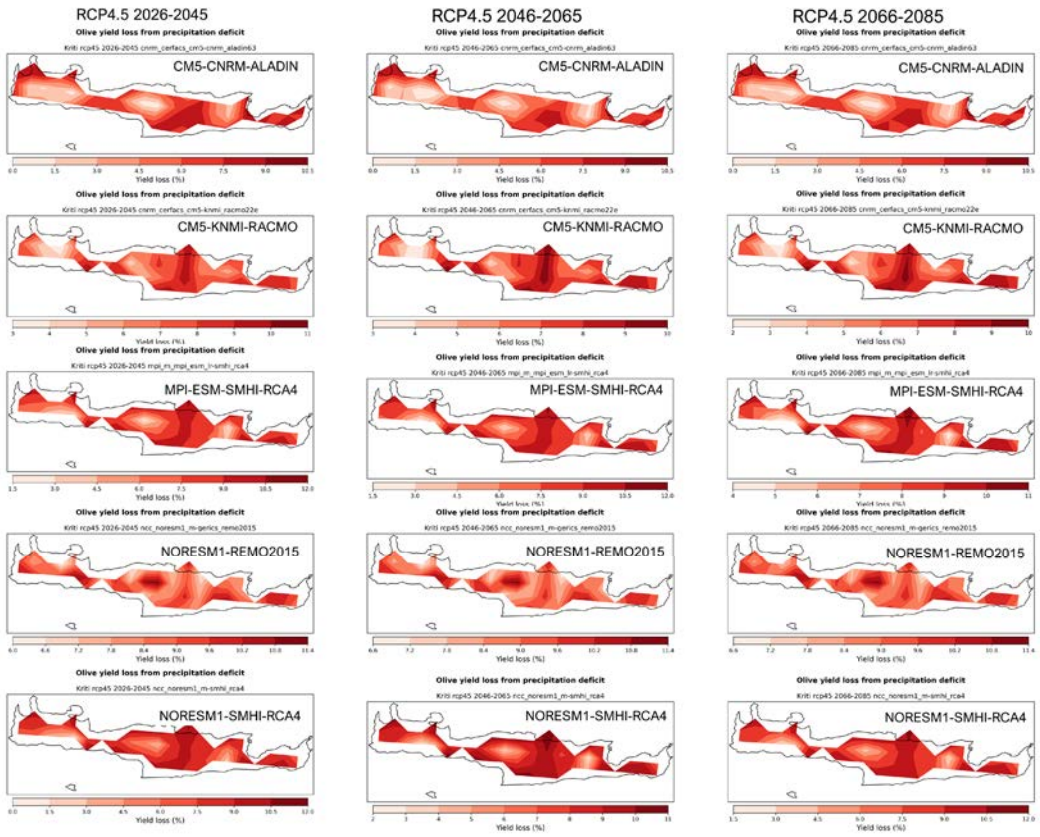

Figure 4-11: Olive yield loss (%) from precipitation deficit under rainfed conditions in Crete for RCP4.5, for three future periods (2026–2045, 2046–2065, 2066–2085) and five EURO-CORDEX RCMs, as computed by the CLIMAAX agricultural drought hazard workflow.

Figure 4-12 synthesises the hazard information from the five EURO-CORDEX RCMs into a single field for each scenario-period combination. Focussing on the RCP4.5 column, the figure shows a very robust west-east gradient in drought hazard: the lowest mean yield losses occur in western Crete and along parts of the northern coastal zone, while a continuous band of higher losses extends from the central plateau towards the eastern lowlands. This pattern is already established in 2026-2045 and is essentially preserved through 2046–2065 and 2066–2085, with only a modest increase in mean loss magnitude in the core hotspot. In all three periods, the multi-model mean yield loss in central-eastern Crete reaches values of the order of 9-11%, whereas most western grid cells remain below about 6-7%. This indicates that, under RCP4.5, agricultural drought hazard for rainfed olives is not characterised by a progressive spatial shift, but by a persistent intensification of an existing hotspot linked to the combination of lower rainfall and higher atmospheric demand in the east. Under RCP2.6, the same spatial structure appears but with slightly lower mean losses in the central-eastern belt and a weaker contrast with the west, consistent with a more moderate warming and ET_0 increase. Under RCP8.5, the hotspot intensifies and expands marginally, with central-eastern grid cells exhibiting the highest multi-model mean losses across all scenarios and periods while western Crete remains the least affected area.

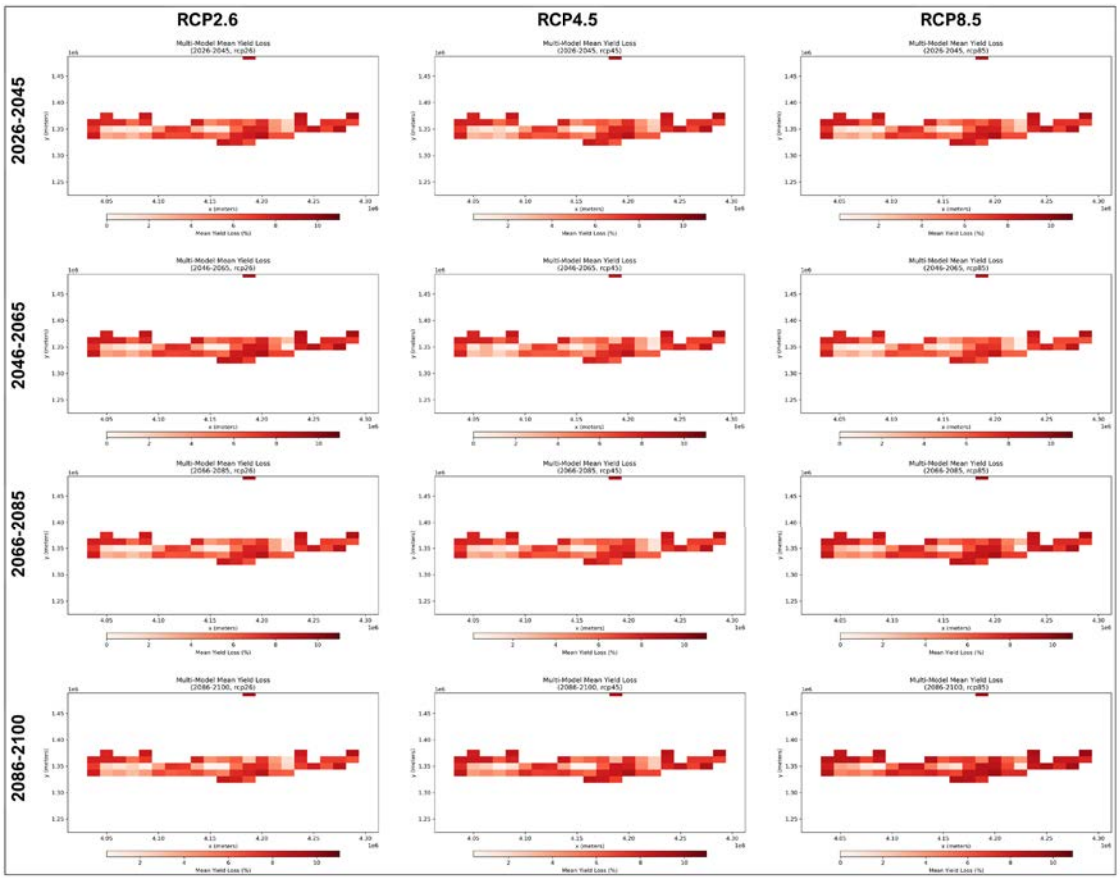

Figure 4-12: Multi-model mean olive yield loss (%) from precipitation deficit in Crete for four future periods (rows) and three emission scenarios (columns: RCP2.6, RCP4.5, RCP8.5). Each panel shows the spatial pattern of average yield loss across the five EURO-CORDEX RCMs.

4.2.2 Risk maps and revenue losses - Agricultural Drought

The revenue-loss maps aggregate the agricultural drought hazard and exposure components into a single impact-based risk indicator, the average annual loss of olive revenue per grid cell (kEUR) under a hypothetical situation with no irrigation.

Across all scenarios (Figure 4-13), the dominant feature is a persistent central-eastern hotspot of revenue loss. Under RCP4.5 this band, roughly from the central plateau to the eastern lowlands, concentrates the largest losses in all periods, with individual cells exceeding 80–100 kEUR yr^{-1} in the mid-century slices. The magnitude of losses there reflects the coincidence of (i) relatively high yield-loss fractions from the hazard workflow and (ii) high olive revenue according to the updated GAEZ v5 value layer. Western Crete, by contrast, shows substantially lower losses per cell, typically below about 40 kEUR even in the higher-forcing scenarios.

The comparison between scenarios mainly affects the amplitude rather than the location of risk. Under RCP2.6 the same central-eastern band appears but with smaller losses and a weaker contrast relative to the west. Under RCP8.5 the hotspot intensifies and

slightly expands, with high-loss cells appearing more frequently and persisting into the far-future slices, whereas RCP4.5 tends to peak around 2046-2065 and stabilise or slightly decline thereafter. This behaviour is consistent with the evolution of the underlying hazard fields, i.e., stronger ET_0 increases and slightly lower precipitation under RCP8.5 increase the multi-model mean yield loss, which is then amplified in revenue terms where exposure is high.

The irrigation overlay adds an important vulnerability dimension. Many of the highest-loss cells in central Crete coincide with large current irrigation shares, indicating that the present economic importance of olives in these areas is already sustained by irrigation. The maps therefore quantify the "lost opportunity cost" if that irrigation were not available. Conversely, several parts of western and north-eastern Crete show moderate revenue loss but very low irrigated share, pointing to zones where production is structurally dependent on rainfall and where even moderate increases in hazard may translate into substantial year-to-year income variability.

Compared with the Phase-1 assessment (single slice, RCP4.5, 2046-2050), the spatial structure of risk is essentially unchanged: both the Phase-1 single-model maps and the Phase-2 multi-model mean under RCP4.5 show a contiguous hotspot of high revenue loss in central to eastern Crete, with much lower losses in the western part of the island. The Phase-2 workflow, however, produces systematically higher loss amplitudes in the hotspot cells and a clearer contrast with the west. This reflects (i) the correction of the revenue-loss calculation (removal of the double crop_prod_fraction application), which increases cell-level losses where olives occupy a substantial share of agricultural output, and (ii) the use of GAEZ v5 (2020) aggregated crop value and irrigated-land share, which assign greater economic weight to high-productivity olive zones than the older 2010 layers. The extension to multiple scenarios (RCP2.6, 4.5, 8.5) and time slices confirms that this central-eastern band of elevated revenue loss is not an artefact of the original model configuration or period choice, but a robust feature of the agricultural drought risk profile for olives in Crete.

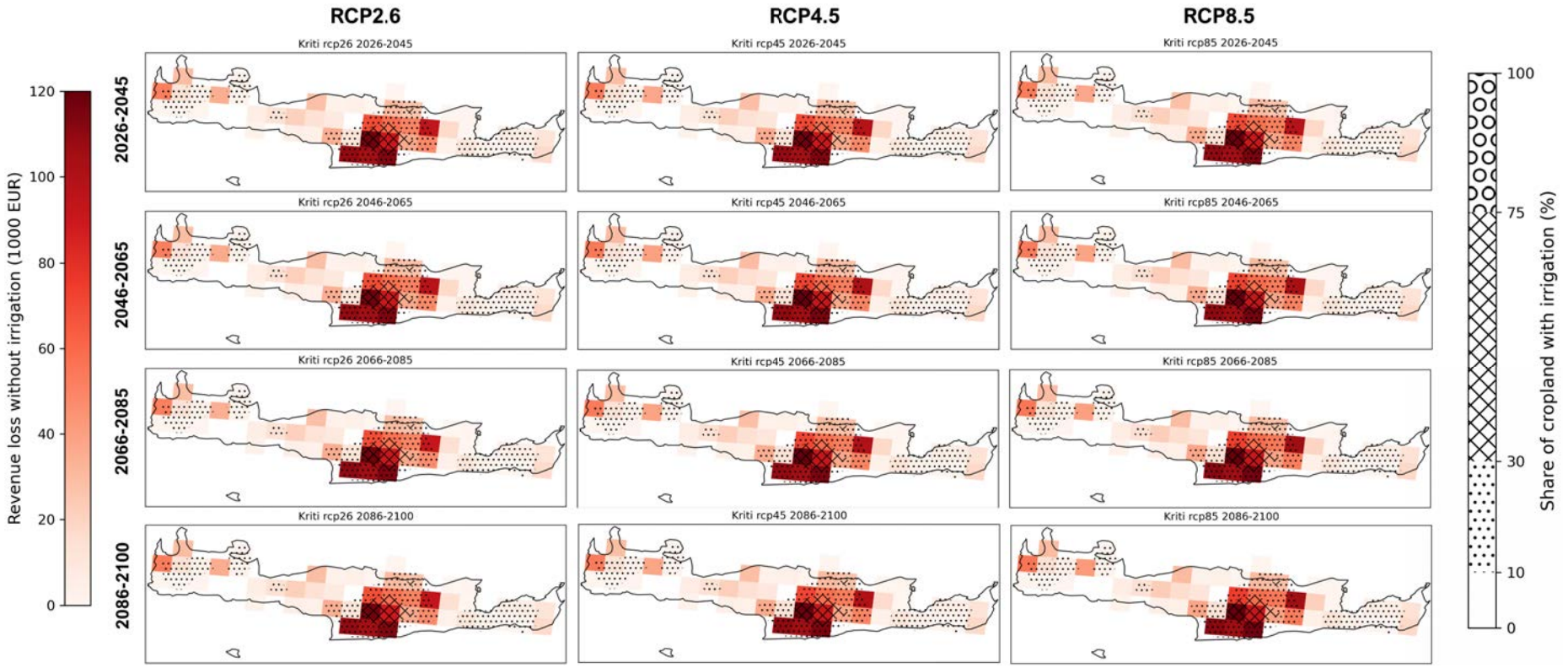

Figure 4-13: Multi-model mean annual revenue loss from absence of irrigation for olive production in Crete (kEUR per grid cell) for four future periods (rows: 2026–2045, 2046–2065, 2066–2085, 2086–2100) and three emission scenarios (columns: RCP2.6, RCP4.5, RCP8.5). Colours show mean revenue loss; stippling and cross-hatching indicate the 2020 share of irrigated cropland from GAEZ v5, highlighting where high potential losses coincide with low or high irrigation coverage.

4.2.3 Uncertainties and robustness of results - Agricultural Drought

The revenue-loss maps inherit uncertainty from all components of the workflow. On the hazard side, yield loss is driven by ET_0 and precipitation from five EURO-CORDEX RCMs. These models differ in their representation of circulation, rainfall intensity and temperature, and some show clear artefacts over Crete (e.g. anomalous ET_0 patterns in NORESM1–REMO2015). As a result, the magnitude of yield loss in a given cell can vary by several percentage points between models and scenarios. The multi-model mean used in the risk maps smooths this spread and emphasises the common signal, but it also hides the possibility of more extreme losses in individual models and years. Grid resolution is another limitation: at ~10–12 km, the climate fields and hazard outputs cannot fully resolve coastal gradients, elevation bands or local wind systems that affect olive water stress.

Uncertainty in exposure and vulnerability arises from the input datasets. Olive production is taken from MapSPAM 2010, while economic value and irrigated-land share come from GAEZ v5 (2020). This temporal mismatch, together with the fact that both products are modelled rather than purely observed, means that absolute levels of olive revenue per cell are approximate, and recent changes in planting patterns, varietal mix and irrigation expansion may not be captured. Furthermore, the irrigation layer represents share of irrigated cropland for all crops, not specifically olives, and does not account for water-availability constraints or interannual restrictions. The “revenue loss without irrigation” metric therefore reflects a stylised counterfactual (removal of irrigation everywhere), not the actual current risk under existing water-management practices.

Despite these limitations, several aspects of the results are robust across models, scenarios and time slices. All RCMs reproduce the same west–east gradient in precipitation and ET_0, and all yield-loss fields show a persistent band of higher hazard in central and eastern Crete. When combined with the updated exposure layer, this translates into a central-eastern revenue loss hotspot in every scenario and period, while western Crete consistently exhibits lower losses. The Phase-2 corrections to the revenue-loss calculation change the magnitude of losses but not the location of the hotspot, and the use of different RCPs confirms that emissions forcing primarily modulates the amplitude of risk rather than its spatial pattern. For these reasons, the maps should be used primarily to interpret relative differences in drought risk within Crete (e.g. central/east vs west, high-value vs low-value zones), whereas absolute monetary loss values at grid-cell level should be treated as indicative rather than precise.

4.3 Climate Change Impact on Olive Oil Yield

4.3.1 Baseline olive oil production and yield (2011–2022)

The baseline period 2011-2022 provides the reference against which the projected climate-driven changes in olive oil yield are assessed. Using ELSTAT agricultural statistics, the analysis first quantified the spatial distribution of olive trees and olive oil production across all regional units of Greece and then derived average yields (kg/ha) for the same period.

At national scale (Figure 4-14), olive cultivation is highly concentrated in Peloponnese and Crete, followed by Central Greece. The average olive trees area during 2011-2022 reaches 2,073,050 stremmas in Peloponnese and 1,899,049 stremmas in Crete, corresponding to 26.18% and 24.01% of the total olive trees area of Greece (7,917,956 stremmas), respectively (Table 4-5). Within Crete, Heraklion stands out as the largest olive-growing regional unit in the country, with an average of 903,238 stremmas of olive trees, followed by high values in Messenia and Lakonia in Peloponnese.

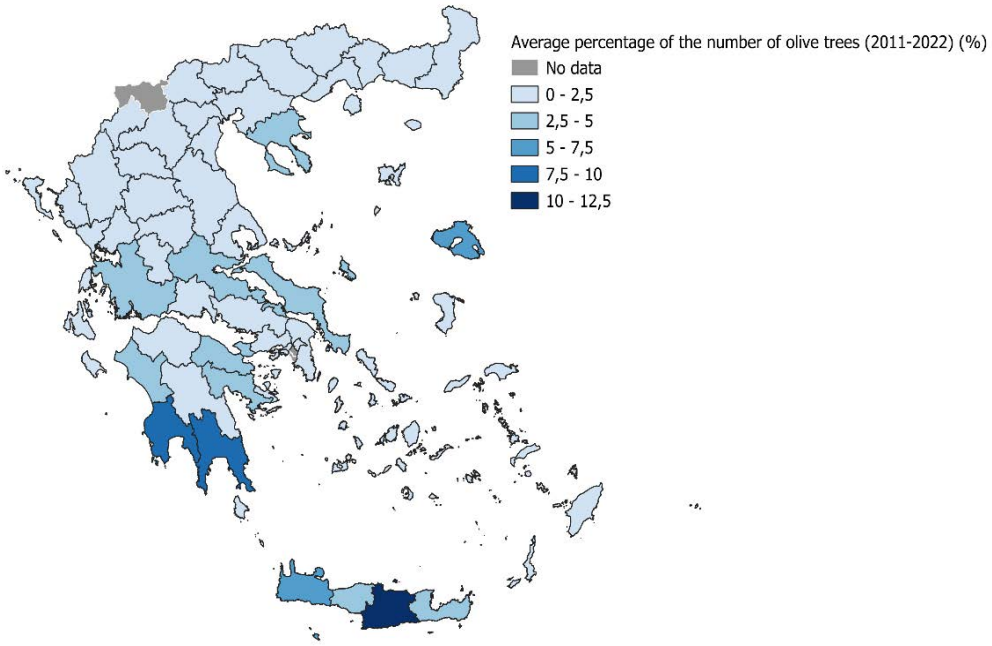

Figure 4-14: Average percentage of olive trees area across Greece during 2011-2022 (Source: ELSTAT)

Table 4-5. Regional units with the highest share in olive oil production (%) during 2011-2022

Regional Unit	Percentage (%)	Regional Unit	Percentage (%)	Regional Unit	Percentage (%)
Messenia	18.43	Corfu	3.68	Boeotia	1.76
Heraklion	10.97	Pthiotida	3.36	Zakynthos	1.59
Ilia	8.84	Korinthia	2.74	Kavala	1.42
Lakonia	8.77	Lesbos	2.52	Euboea	1.34
Chania	8.16	Argolida	2.46	Arkadia	1.20
Lasithi	4.89	Rethymno	2.19	Magnesia	1.18
Achaia	4.65	Chalkidiki	2.12	Preveza	1.00

The same concentration pattern is observed for olive oil production (Figure 4-15). Average production maps show that the highest tonnages over 2011-2022 occur in Messenia (52,079 t), Heraklion (37,310 t) and Ilia (25,387 t). When expressed as share of national production, only 21 out of 74 regional units account for 93.3% of total Greek olive oil output. Among them, the four regional units of Crete occupy a particularly important position: Heraklion contributes 10.97%, Chania 8.16%, Lasithi 4.89% and Rethymno 2.19% of national production. Together, Cretan regional units thus provide more than a quarter of Greek olive oil production, similar in magnitude to Peloponnese.

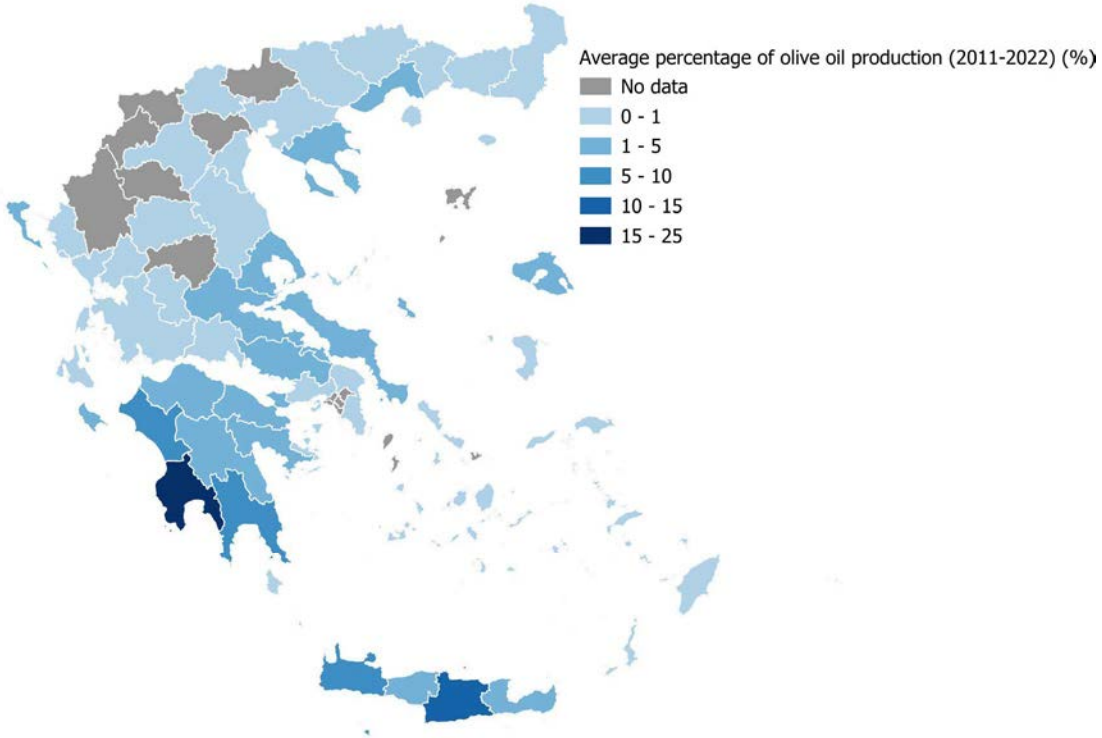

Figure 4-15: Average percentage of olive oil production (%) across Greece during 2011-2022 (Source: ELSTAT)

Average olive oil yield (kg/ha) further shows the importance of Crete and Peloponnese as highly productive areas (Figure 4-16). The yield map for 2011-2022 shows that these two macro-regions host many of the regional units with yields in the 500-1000 kg/ha range. Within Crete, Chania (566 kg/ha) and Lasithi (524 kg/ha) fall in this high-yield class, while Heraklion (409 kg/ha) and Rethymno (240 kg/ha) show intermediate yields compared to other Greek regions. When yield is expressed per stremma of olive trees, the 21 most productive regional units, including all four units of Crete, are again clearly distinguished, with Heraklion, Chania, Lasithi and Rethymno all classified as highly productive in terms of kg olive oil per stremma and per kg of fruit.

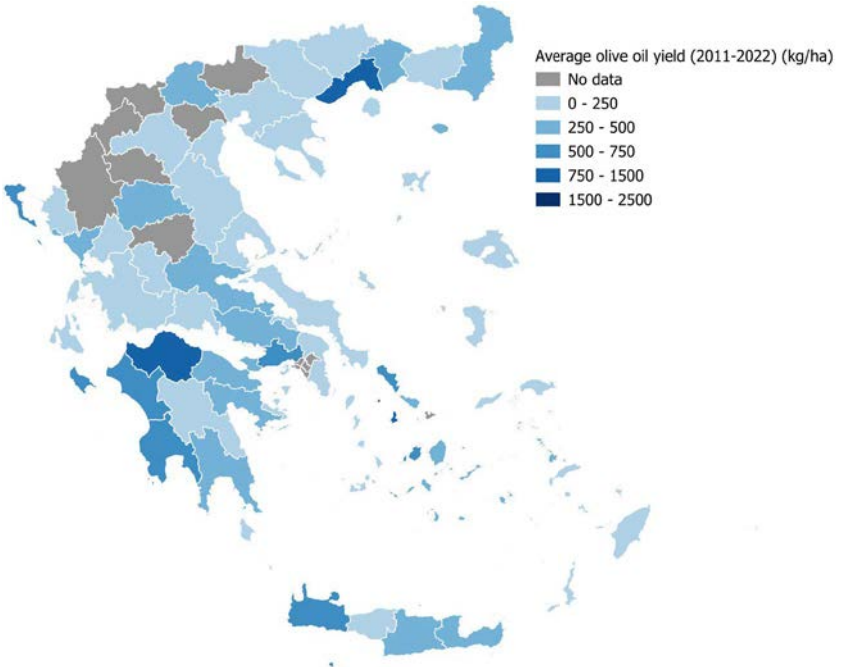

Figure 4-16: Average olive oil yield (kg/ha) across Greece during 2011–2022 (Source: ELSTAT)

Trend analyses for 2011-2022 reveal that, despite their high baseline productivity, many key producing regions have experienced declining production over the period (Figure 4-17). The majority of regional units in Greece show a negative production trend, with particularly strong decreases in several high-output areas, including Chania (−499 t/year), Lasithi (−419 t/year) and Heraklion (−166 t/year). For Crete as a whole, a more nuanced picture emerges when trends in trees, production and yield are combined: Heraklion shows a strong increase in olive trees and a slight increase in yield despite decreasing production, Chania and Lasithi exhibit decreasing trees, production and yield, while Rethymno presents increasing trees, production and yield.

Baseline analysis confirms that Crete is both a major producer and a high-yield region for olive oil in Greece, with substantial planted area and strong dependence on the sector in all four regional units. This baseline production and yield pattern forms the reference

for interpreting the climate-driven yield projections and the associated drought-related risk presented in the following subsections.

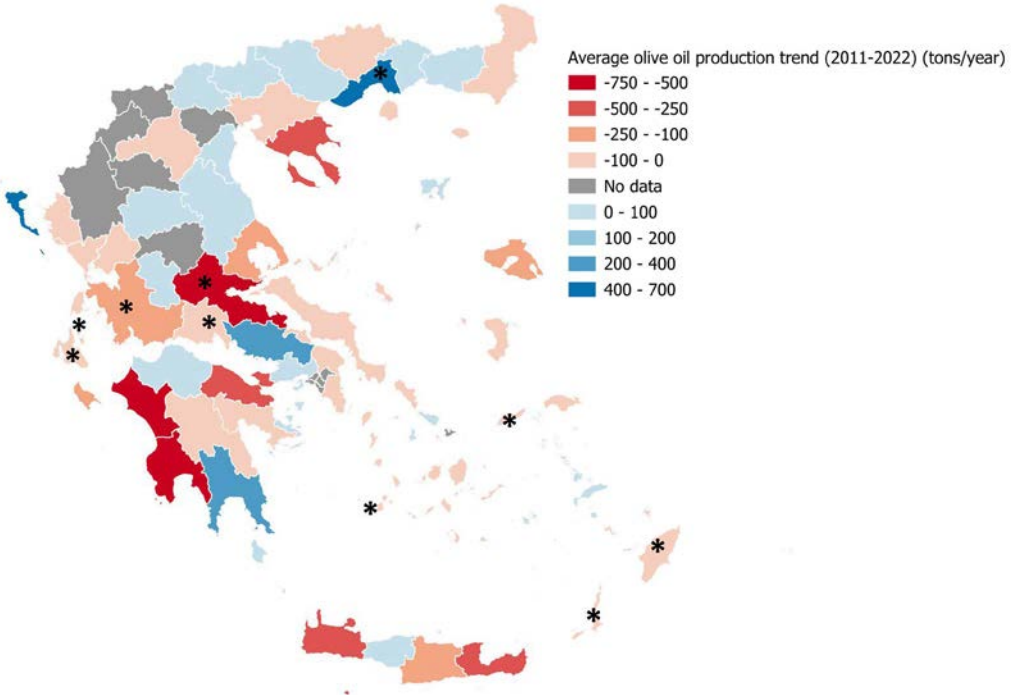

Figure 4-17: Spatial distribution of average olive oil production trends in Greece for the period 2011–2022 (tons year $^{-1}$). Asterisks mark statistically significant trends at a level of p-value lower than 0.05.

4.3.2 Observed climate-yield relationships (hazard-risk link)

The climatic indices are interpreted as proxies of drought-related hazard, while the observed response of olive oil yield is used to characterise the associated risk at regional level. The results summarise how sensitive olive oil yield is to different aspects of temperature and precipitation across Greece, with emphasis on the four regional units of Crete.

National-scale patterns

Across the 21 regional units that together account for 93% of national olive oil production, several climatic indices show statistically significant linear correlations ($p < 0.1$) with per-tree olive oil yield. Table 4-6 provides an overview of these relationships, indicating for each index the number of regional units where it is significant, together with average and median slopes and average R^2. The indices that most frequently correlate with yield are:

– Rainfall_MAYJUN (significant in 6 regional units, with positive median slope)
– Rainfall_JANFEB, Tavg_MARAPR, Tmax_MAYJUN, Tmax_SEPOCT, Tmax_over35_JUL and WinterRain (each significant in 4 regional units)

Table 4-6 Overview of predictors' effect on olive oil yield across the 21 regional units of Greece accounting for 93% of olive oil production. The count refers to the frequency that each predictor or climate variable correlated to the olive yield with a p-value<0.1. Average and median slope is estimated among the different regional units. The R^2 is the average among the respective regional units.

Predictor	Count	Average Slope	Median Slope	R^2
Rainfall_MAYJUN	6	0.1826	0.5214	0.2953
Rainfall_JANFEB	4	0.3561	0.5886	0.3921
Tavg_MARAPR	4	0.5435	0.5365	0.3018
Tmax_MAYJUN	4	-0.2690	-0.5238	0.3334
Tmax_SEPOCT	4	0.5524	0.5288	0.3089
Tmax_over35_JUL	4	-0.2954	-0.5300	0.3405
WinterRain	4	-0.1233	-0.1241	0.4526
DTR_JULAUG	3	-0.3391	-0.6079	0.3716
DTR_JANFEB	3	-0.1736	-0.5001	0.3147
DTR_MARAPR	3	0.6399	0.6382	0.4209
SPEImax_JANFEB	3	0.2571	0.5490	0.3885
Tmax_JANFEB	3	-0.6009	-0.5424	0.3688
Tmax_MARAPR	3	0.6009	0.6098	0.3559
Tmax_over32_AUG	3	-0.6096	-0.6019	0.3793
Tmin_MARAPR	3	0.1595	0.4998	0.3051
Tmin_MAYJUN	3	0.1431	0.5451	0.3686
Tmax_JUNJUL	2	-0.5095	-0.5050	0.2596
WinterChill	2	-0.5130	-0.5072	0.2633
Rainfall_SEPOCT	2	0.1977	0.5649	0.3250
SPEImax_SEPOCT	2	0.1451	0.5112	0.2907
DTR_MAYJUN	2	-0.0761	-0.0761	0.5224
SummerRain	2	-0.6281	-0.6281	0.4213
Tmax_APRMAY	2	-0.5567	-0.5567	0.3100
Tmax_AUGSEP	2	0.5688	0.5688	0.3392
Tmax_FEBMAR	2	-0.0679	-0.0679	0.4229
Tmax_OCTNOV	2	-0.0207	-0.0207	0.3333
Tmax_over32_JUN	2	-0.6166	-0.6166	0.3877
Tmax_over32_SEP	2	0.6140	0.6140	0.3783
Tmax_over35_AUG	2	-0.5828	-0.5828	0.3576
Tmax_over35_JUN	2	-0.5994	-0.5994	0.3657
Tmin_JANFEB	2	0.0251	0.0251	0.3391
Tmin_SEPOCT	2	0.5899	0.5899	0.3480
DTR_SEPOCT	1	-0.6177	-0.6177	0.3816
SPEImax_MAYJUN	1	0.5473	0.5473	0.3237
Tavg_JANFEB	1	-0.6808	-0.6808	0.4635
Tavg_SEPOCT	1	0.6020	0.6020	0.3624
Tmax_JULAUG	1	-0.6991	-0.6991	0.4677
Tmax_over32_JUL	1	-0.6225	-0.6225	0.3298
Tmax_over32_MAY	1	-0.5916	-0.5916	0.3780
Tmin_JULAUG	1	-0.8211	-0.8211	0.6742
Wind_MAY	1	-2.4480	-2.4480	0.4075

Taken together these correlations lead to the following overall picture:

Winter–early spring (Nov–Apr):

- Precipitation during January-February and over the extended cool season (WinterRain) plays a primary role; wetter winters tend to favour higher yields in many regions.
- Temperature (maximum, mean, minimum) and diurnal temperature range (DTR) during January-February also emerge as important, reflecting the role of cool, stable winter conditions and sufficient winter chill.

Spring (Mar–May):

- From early spring, indices based on maximum temperature, frequency of hot days (Tmax_over32), average temperature and DTR become important.
- Tavg_MARAPR typically shows a positive relationship with yield, indicating that moderately warm conditions around flowering and fruit set are beneficial.

Summer (Jun–Aug):

- Summer is dominated by temperature-based hazard: DTR, Tmax, Tmax_over32, Tmax_over35 and Tmin all appear as significant predictors.
- In almost all cases, higher maximum temperatures and more very hot days correlate negatively with yield, signalling strong heat-stress effects on the developing fruit.

Autumn (Sep–Nov):

- During early autumn, maximum, average and minimum temperature and DTR continue to affect yield, especially in September-October when many indices appear; however, the sign of precipitation effects is less consistent across regions, likely reflecting the interplay between late rainfall, irrigation practices and cultivar differences.

The most recurrent hazard signals are (i) high temperatures from June to September, which tend to reduce olive oil yield, and (ii) adequate winter and late-spring rainfall, which generally supports higher yields. The relative importance of the different climatic indices across Greece is further summarised in Table 4-7, which shows how often each index appears as a significant predictor and whether it is also relevant for at least one regional unit of Crete.

Table 4-7. Summary of predictors shown with statistically significant difference.

Predictor	Greece	Individual regional units	Two-predictor model
Tmin_JANFEB	2	Korinthia	Magnesia
		Zakynthos	
Tmax_JANFEB	3	Chalkidiki, Arkadia, Zakynthos	–
Tavg_JANFEB	1	Zakynthos	Arkadia
DTR_JANFEB	3	Magnesia, Korinthia	–
		Kavala	
SPEImax_JANFEB	3	Boeotia	–

		Magnesia Pthiotida	
Rainfall_JANFEB	4	Boeotia, Magnesia, Korinthia Pthiotida	Messenia
Tmax_FEBMAR	2	Zakynthos Pthiotida	Achaia Pthiotida
Tmin_MARAPR	3	Lesbos, Chalkidiki Zakynthos	Lakonia
Tmax_MARAPR	3	Heraklion, Magnesia, Boeotia	Heraklion
Tavg_MARAPR	4	Lesbos, Boeotia, Arkadia, Magnesia	–
DTR_MARAPR	3	Corfu, Kavala, Zakynthos	Corfu, Kavala, Heraklion
SPEImax_MARAPR	–	–	Euboea Zakynthos
Rainfall_MARAPR	–	–	Boeotia, Preveza, Lesbos
Tmax_APRMAY	2	Ilia, Achaia	Magnesia Chania
Tmax_MAYJUN	4	Korinthia, Chania, Achaia Kavala	–
Tmin_MAYJUN	3	Argolida Heraklion, Chalkidiki	Kavala, Arkadia
DTR_MAYJUN	2	Chania Kavala	Chania
SPEImax_MAYJUN	1	Lasithi	Lasithi, Messenia
Rainfall_MAYJUN	6	Magnesia, Boeotia, Arkadia, Lasithi Chania, Rethymno	Boeotia
Tmax_over32_MAY	1	Korinthia	Korinthia
Wind_MAY	1	Boeotia	–
Tmax_over32_JUN	2	Rethymno, Magnesia	Corfu
Tmax_over35_JUN	2	Korinthia, Magnesia	Korinthia
Tmax_JUNJUL	2	Messenia, Chania	–
Tmax_over32_JUL	1	Rethymno	–
Tmax_over35_JUL	4	Chania, Rethymno, Lesbos Lasithi	–
Tmax_JULAUG	1	Lesbos	–
Tmin_JULAUG	1	Ilia	Ilia, Rethymno
DTR_JULAUG	3	Messenia, Lesbos Argolida	Euboea
SPEImax_JULAUG	–	–	Pthiotida, Chalkidiki
Tmax_over32_AUG	3	Arkadia, Rethymno, Chania	–
Tmax_over35_AUG	2	Lesbos, Rethymno	–
Tmax_AUGSEP	2	Lasithi, Zakynthos	Lasithi
SummerRain	2	Heraklion, Zakynthos	Preveza
Tmax_SEPOCT	4	Lakonia, Chalkidiki, Zakynthos, Arkadia	Lakonia
Tmin_SEPOCT	2	Chalkidiki, Arkadia	Argolida
Tavg_SEPOCT	1	Arkadia	Ilia
DTR_SEPOCT	1	Messenia	Rethymno Argolida
Tmax_over32_SEP	2	Ilia and Zakynthos	Zakynthos
SPEImax_SEPOCT	2	Messenia Heraklion	–
Rainfall_SEPOCT	2	Messenia	–

		Heraklion	
Tmax_OCTNOV	2	Chalkidiki	Chalkidiki
		Ilia	
WinterRain	4	Achaia, Pthiotida	Achaia
		Boeotia, Euboea	
WinterChill	2	Messenia, Corfu	Lesbos

Regional climate–yield relationships for Crete

Within this national framework, the four regional units of Crete show distinctive combinations of climatic indices that explain their yield variability. The main climatic indices that exhibit a statistically significant relationship with olive oil yield in the four regional units of Crete are listed in Table 4-8. In specific for:

Heraklion:

- Significant indices include SummerRain (negative slope), Tmax_MARAPR (positive), Tmin_MAYJUN (positive), and SPEImax_SEPOCT and Rainfall_SEPOCT (both negative).
- This suggests that in Heraklion, moderately warm conditions in March–April and higher minimum temperatures in May–June favour yield, while excessive rainfall and wetter conditions in late summer–early autumn tend to be detrimental.

Chania:

- The most important predictors are DTR_MAYJUN, Tmax_MAYJUN, Tmax_JUNJUL, Tmax_over32_AUG, Tmax_over35_JUL and Rainfall_MAYJUN, all with negative slopes.
- Yield in Chania is therefore particularly sensitive to heat stress and large day–night temperature contrasts from late spring through midsummer, as well as to higher rainfall in May–June, which may interfere with flowering and fruit set.

Lasithi

- Key predictors include SPEImax_MAYJUN with a positive slope and Tmax_over35_JUL (also positive in the unit-specific analysis).
- The positive role of SPEImax_MAYJUN indicates that wetter conditions in late spring support fruit development and higher yield, consistent with the positive Rainfall_MAYJUN signal found in several other regions. The behaviour of high July temperatures in Lasithi is more complex and may reflect local conditions and cultivar/management differences noted in the study.

Rethymno

- In the two-predictor model, olive yield is related negatively to DTR_SEPOCT and Tmin_JULAUG, indicating that larger diurnal ranges in early autumn and higher minimum summer temperatures both tend to reduce yield.

– Rethymno also appears among the regional units where Tmax_over32_JUN and Tmax_over35_JUL have significant negative slopes, underlining the vulnerability of its olive groves to early-summer and midsummer heat stress.

When the two-predictor models are considered jointly, Heraklion and Lasithi are among the regional units where both selected predictors have overall positive impact on yield, whereas Rethymno is part of the group where both predictors have negative impact; Chania exhibits predominantly negative temperature-related effects.

Table 4-8. Overview of the most important predictors with statistical difference for 21 regional units of Greece

Predictor	Slope	p-value	R^2	Slope 95% lower	Slope 95% upper
Heraklion					
Summerrain	-0.737	0.011	0.573	-1.155	-0.319
Tmax_MARAPR	0.646	0.050	0.397	0.122	1.169
Tmin_MAYJUN	0.545	0.071	0.351	0.057	1.032
SPEImax_SEPOCT	-0.587	0.071	0.349	-1.113	-0.060
Rainfall_SEPOCT	-0.536	0.078	0.336	-1.031	-0.041
Chania					
DTR_MAYJUN	-0.794	0.002	0.631	-1.142	-0.447
Tmax_over32_AUG	-0.601	0.038	0.362	-1.059	-0.144
Rainfall_MAYJUN	-0.563	0.056	0.318	-1.037	-0.090
Tmax_MAYJUN	-0.526	0.078	0.277	-1.013	-0.039
Tmax_JUNJUL	-0.518	0.084	0.268	-1.008	-0.028
Tmax_over35_JUL	-0.504	0.094	0.254	-0.999	-0.010
Lasithi					
SPEImax_MAYJUN	0.5473	0.0678	0.3237	0.0639	1.0306
Tmax_over35_JUL	0.5459	0.0751	0.3102	0.0484	1.0433
Tmax_AUGSEP	0.5266	0.0781	0.3051	0.0409	1.0124
Rainfall_MAYJUN	0.5361	0.0924	0.2826	0.0141	1.0581
Rethymno					
Tmax_over35_JUL	-0.6675	0.0201	0.4687	-1.1018	-0.2332
Tmax_over32_JUN	-0.6493	0.0274	0.4344	-1.1020	-0.1966
Tmax_over32_AUG	-0.5946	0.0448	0.3761	-1.0626	-0.1266
Tmax_over35_AUG	-0.5933	0.0457	0.3737	-1.0625	-0.1240
Tmax_over32_JUL	-0.6225	0.0646	0.3298	-1.1648	-0.0803
Rainfall_MAYJUN	-0.5133	0.0973	0.2756	-1.0218	-0.0048

Hazard–risk interpretation for Crete

From a drought-risk perspective, these observed relationships imply that the hazard for Cretan olive groves is strongly associated with frequent and intense heat events from late spring through summer (high Tmax, many days above 32–35 °C, large DTR), and in some areas, insufficient or poorly timed rainfall, particularly in late spring. The risk differs between regional units. Chania and Rethymno show a clear negative response to summer heat stress, indicating higher vulnerability under warming conditions. Heraklion

and Lasithi benefit from certain temperature and moisture conditions in spring, and their yield response is more mixed, suggesting comparatively higher resilience, though still sensitive to extreme events and seasonal rainfall anomalies.

These empirical climate-yield relationships, derived from the 2011-2022 period, form the basis for the subsequent projection of future yield changes under climate change scenarios and provide a quantitative link between climatic hazard indicators and olive-yield-based drought risk in Crete.

4.3.3 Projected changes in climatic hazard indices

Future changes in the climatic hazard for olive production were assessed using an ensemble of five regional climate models forced by the RCP4.5 and RCP8.5 scenarios. Projections cover three future time slices, near future (2026-2045), mid-century (2046-2065) and far future (2066-2085), and are expressed as relative changes with respect to the historical reference period 2006–2024.

Spring maximum temperatures (Tmax_MARAPR and Tmax_APRMAY) increase by about 0.7 °C in the near future and up to around 1.3-1.4 °C by the far future under both RCP4.5 and RCP8.5. The diurnal temperature range in spring (DTR_MARAPR) shows changes close to zero, indicating that minimum and maximum temperatures rise at similar rates.

During May-June, DTR_MAYJUN remains essentially unchanged and SPEI_MAYJUN stays around −0.1 in all periods and scenarios, suggesting that, although the climate becomes warmer, there is no strong signal of either pronounced drying or moistening in this specific growth phase.

More pronounced changes emerge in the indices describing peak summer heat. Minimum summer temperature (Tmin_JULAUG) rises by roughly 0.5-0.6 °C in the near future and up to about 1.4-1.5 °C in the far future, while Tmax_AUGSEP increases by approximately 0.4-1.4 °C over the century. The number of very hot days in early autumn, represented by Tmax_32SEP, increases by about 0.7 °C in the near future and up to roughly 2.0-2.3 °C in the far future, again under both emission pathways.

Indices characterising early autumn warmth (Tmin_SEPOCT, Tavg_SEPOCT, Tmax_SEPOCT, Tmax_OCTNOV) also show a gradual warming of around 0.3-0.5 °C in the near future and about 1.3-1.5 °C by the end of the century. The diurnal temperature range in September-October (DTR_SEPOCT) remains close to zero, indicating that both daytime and night-time temperatures increase in tandem.

In summary hazard profile evolves towards hotter summers and early autumns with only mild changes in drought indices, implying stronger thermal stress on olive trees but without a drastic shift in late-spring water availability compared to the historical period. These regional-scale changes are summarised in Table 4-9.

Table 4-9. Relative changes in specific climatic indices on yearly basis compared to the historical period for Crete.

	Future period	Tmax_MARAPR	DTR_MARAPR	Tmax_APRMAY	DTR_MAYJUN	SPEI_MAYJUN	Tmin_JULAUG-	Tmax_AUGSEP	DTR_SEPOCT
RCP45	2026-2045	+0.7°C	+0.1°C	+0.5°C	0.0°C	−0.1	+0.5°C	+0.4°C	−0.1°C
	2046-2065	+0.9°C	0.0°C	+0.5°C	0.0°C	−0.1	+0.9°C	+0.9°C	−0.1°C
	2066-2085	+1.4°C	+0.1°C	+1.3°C	0.0°C	−0.1	+1.3°C	+1.2°C	−0.1°C
RCP85	2026-2045	+0.7°C	0.0°C	+0.5°C	−0.1°C	−0.1	+0.5°C	+0.4°C	−0.1°C
	2046-2065	+0.9°C	0.0°C	+0.5°C	−0.1°C	−0.1	+0.9°C	+0.9°C	−0.1°C
	2066-2085	+1.4°C	0.0°C	+1.3°C	−0.1°C	−0.1	+1.3°C	+1.2°C	−0.1°C

4.3.4 Projected changes in olive oil yield (risk)

For each prefecture of Crete, the calibrated two-predictor model links olive oil yield to two key hazard proxies. These indices were then computed from the ensemble of five EURO-CORDEX RCMs for three future periods and for both RCPs, and fed into the prefecture-specific models. Prefecture-level yield changes were finally aggregated to an island-wide production-weighted median for Crete. The ensemble projections (Figure 4-18) show that Crete is only weakly affected in terms of yield, with changes generally small in magnitude and often close to zero. The detailed median percentage changes for Crete are summarised in Table 4-10.

Across all periods and both scenarios, the projected changes for Crete remain within a narrow band of a few percent around the historical mean, i.e. far from any drastic decline in yield. The RCM spread widens in the far future under RCP8.5, but the ensemble median still points to only modest yield gains rather than substantial losses.

From a drought-risk perspective, the projections imply that the hazard evolves towards warmer springs and hotter summers-early autumns, but without strong deterioration of late-spring moisture at island scale. The risk, expressed as yield impact, remains low to moderate. Under RCP4.5, Crete could experience at most a small yield loss (order of a few percent) and under RCP8.5, after a near-term dip, yields tend to stabilise or slightly increase by the end of the century. In other words, the calibrated climate-yield relationships, when combined with projected changes in hazard indices, suggest that Crete retains suitability for olive cultivation throughout the 21st century, with no substantial climate-driven reduction in olive oil yield at the island scale.

Table 4-10. Median difference in olive oil yield (%) for Crete for three future periods (2026–2045, 2046–2065, 2066–2085) under RCP4.5 and RCP8.5, relative to 2006–2025.

	Period		
	2026-2045	**2046-2065**	**2066-2085**
RCP4.5	−0.5%	−2.3%	−0.5%
RCP8.5	−1.1%	+2.1%	+4.3%

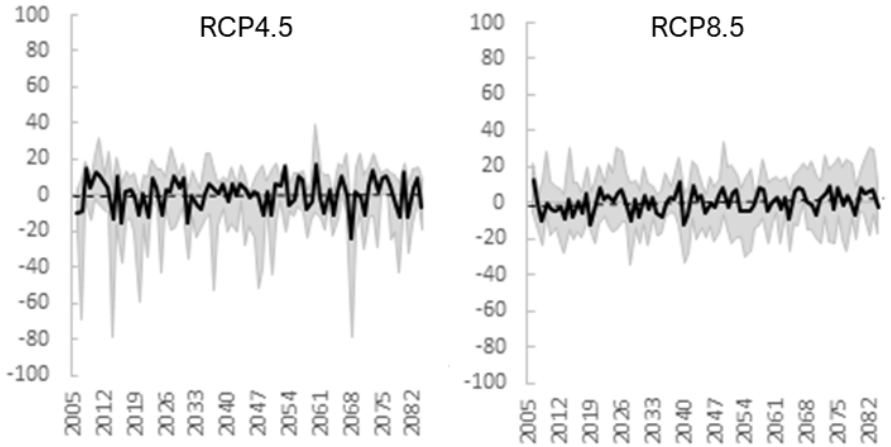

Figure 4-18: Projected change [%] in olive oil yield for Crete between 2005–2085 under RCP4.5 and RCP8.5

4.3.5 Uncertainties and robustness of results

The climate-yield impact assessment for Crete is based on empirical models and therefore subject to several important uncertainties. First, the calibration relies on ELSTAT olive oil production and olive tree area data for the relatively very short period 2011-2022, from which annual yields were derived. This 12-year record may not fully capture multi-decadal climate variability or long alternation cycles in productivity, while any measurement or reporting inconsistency in production and area statistics propagates directly into the yield time series. In addition, the pool of potential climatic predictors is constrained by the availability of E-OBS variables since for several key olive-producing regions, including all four prefectures of Crete, relative humidity is missing, limiting the representation of moisture-related processes.

Uncertainty also arises from the structure of the climate-yield models. The methodology uses simple linear regressions between yield and each climatic index, followed by a two-predictor multiple linear model with an interaction term per regional unit. This implies a linear and stationary response of yield to a small set of indices and assumes that other climatic indices, as well as non-climatic drivers (cultivars, soil conditions, pests and

diseases, fertilisation, pruning, CO_2 effects), either remain constant or are implicitly captured within the short calibration period. As a consequence, the models isolate the effect of selected temperature and precipitation metrics on yield but do not describe the full complexity of the production system.

A third source of uncertainty is the representation of future climate. Projections of the climatic indices are derived from five bias-adjusted EURO-CORDEX regional climate models at 12.5 km resolution under RCP4.5 and RCP8.5, using specific bias-correction methods for temperature and precipitation. This ensemble cannot span the full range of plausible futures, and residual model and bias-correction errors (e.g. altering the transient physical consistency of variables) affect the indices and the resulting yield changes. The spread of projected yield change is large in some cases, with wide bands in the future, even though the ensemble median for Crete remains close to zero or slightly positive. Furthermore, the 12.5 km climate resolution and the prefecture-scale calibration smooth local micro-climates and within-prefecture variability.

4.3.6 Comparison Agricultural drought workflow with olive-yield impact projections

The agricultural drought workflow and the olive-yield impact projections are methodologically distinct but broadly consistent in their implications for Crete. The CLIMAAX agricultural workflow is water-driven as it quantifies olive yield losses as a function of precipitation-driven ET deficits during the growing season and converts these into revenue losses per grid cell after accounting for fractional olive area, crop value and share of irrigated land. It therefore represents a “drought with insufficient irrigation” storyline, in which water supply cannot fully offset the increase in climatic water demand. By contrast, the olive-yield impact analysis is climate-response driven as it uses statistically derived climate-yield relationships at regional scale (21 administrative units for Greece, including Crete), and propagates these through climate projections to estimate shifts in the distribution of olive yields. Irrigation and local water-supply constraints are implicit at best; the focus is on how changes in temperature and rainfall regimes alter the probability of poor yield years.

Despite these differences in framing, both approaches identify central and eastern Crete as the zones of highest climate related pressure on olive production. In the agricultural workflow, these areas show the largest projected yield-loss fractions and revenue losses when irrigation shortfalls are assumed, especially in intensive olive belts of the north-central coast and the Messara-Viannos-Ierapetra corridor. In the olive-yield projections, the same broader region exhibits an increased frequency and magnitude of negative yield anomalies under intermediate and high forcing scenarios, associated with drier late springs and more frequent high temperature episodes. The convergence of spatial signals strengthens confidence that these are genuine hotspots rather than artefacts of any one model or dataset.

Differences between the two lines of evidence are mainly in magnitude and interpretation, not in direction. The agricultural workflow typically yields larger, more

abrupt losses because it explicitly assumes unmet irrigation demand during drought episodes and expresses impacts in monetary terms per unit area. The olive-yield projections give smoother, probabilistic changes in mean yield and interannual variability, reflecting climate stress in a system where some level of water management is implicitly maintained. Interpreted jointly, the two methods suggest that: (i) even with current irrigation practices, climate change alone tends to increase the likelihood of low-yield years in key Cretan olive regions and (ii) under conditions of constrained water supply, these same regions could experience substantial economic losses, especially in high-intensity olive basins. This combined picture is crucial for prioritising adaptation options that simultaneously address water-resource resilience and olive-sector sensitivity in the island's main production zones.

5 Discussion

5.1 Synthesis across methods

The three complementary strands of analysis developed in this deliverable (a) the updated relative drought assessment, (b) the agricultural drought workflow and (c) the olive-yield climate impact study converge on a coherent picture of drought risk in Crete.

The relative drought analysis provides a basin- and municipality-scale overview of how climatic hazard, water-demand exposure and vulnerability combine across the island. It shows that present-day risk is already structured along a central-southern belt (Amari–Mylopotamos-Messara-Viannos-Ierapetra) and in parts of western Crete, with lower relative risk in many eastern and some northern coastal units. Future projections indicate that climatic drought hazard intensifies most under SSP3-7.0 and SSP5-8.5, but that this signal is partly offset by socio-economic development and planned water-infrastructure pathways, especially under SSP1-2.6. The net result is spatially differentiated with current hotspots in central and mountainous municipalities see substantial potential for risk reduction if adaptation pathways materialise, whereas several basins in central and eastern Crete retain or acquire elevated risk where hazard strengthens and exposure remains high.

The updated agricultural drought workflow zooms in on irrigated and rainfed olive production, translating ET-based yield losses into monetary impacts using improved exposure data. This workflow indicates that, under precipitation-driven agricultural drought, the largest potential revenue losses per unit area are concentrated in the intensive olive zones of central and eastern Crete. The correction of the revenue-loss formulation and the use of updated value layers reveal higher absolute losses than in Phase 1, but the spatial pattern is consistent as basins in the central north and the Messara-Viannos-Ierapetra corridor emerge as persistent economic drought hotspots once irrigation shortfalls are assumed. This sector specific perspective is fully compatible with, and nested within, the broader relative risk patterns, by showing where

the aggregated “high-risk” areas correspond to genuinely high economic sensitivity of the primary sector.

The olive-yield climate impact study adds an independent, process-based line of evidence by statistically linking observed regional yields to climate indices (e.g. May-June rainfall, high summer Tmax) and propagating those relationships through regional climate model projections. Although implemented at regional-unit scale for the whole of Greece, its results for Crete are consistent with the CLIMAAX analyses. Under intermediate and high-forcing scenarios, the frequency and magnitude of negative yield anomalies increase, particularly when dry conditions in late spring and high summer temperatures co-occur. Importantly, this study highlights that even without explicit water-management constraints, the changing climate alone is sufficient to raise the probability of poor olive years in Cretan production zones.

Taken together, these three components provide a multi-layered, mutually reinforcing view of drought risk in Crete. The relative assessment frames where drought is most likely to become a systemic management issue. The agricultural drought workflow quantifies how strongly water-supply deficits can translate into economic losses for olive production in those same areas; and the olive yield study demonstrates that projected climate trajectories tend to push olive groves towards more frequent climatic stress. The strong spatial pattern of identified hotspots across methods strengthens confidence in the overall diagnosis and underscores that central and eastern Crete, and particularly the main olive growing basins, should be priority areas for drought risk monitoring, planning and adaptation in the forthcoming implementation phase.

5.2 Sectoral implications

The combined results from the relative drought assessment, the agricultural drought workflow and the olive-yield climate analysis point to differentiated but interconnected implications for key sectors in Crete.

5.2.1 Agriculture (with emphasis on olives)

The primary sector is the most directly exposed to drought in Crete. The relative risk analysis highlights a persistent belt of elevated risk in the central and south-central part of the island, where agricultural exposure is high and vulnerability is only partly compensated by existing irrigation and infrastructure. The agricultural workflow shows that, under precipitation-driven agricultural drought and assuming insufficient irrigation supply, potential revenue losses for intensive olive areas can approach the order of 1,000 €/stremma in the most stressed basins, especially in central and eastern Crete. The olive-yield climate study indicates more frequent and deeper negative yield anomalies under intermediate and high-forcing scenarios. Together, these lines of evidence suggest that olive production in several municipalities will face a structurally higher probability of yield and income instability, and that adaptation in irrigation efficiency,

crop and variety management, and risk-sharing instruments (e.g. insurance) will be critical.

5.2.2 Water resources

From a water-resources perspective, the hazard and vulnerability assessments confirm that many of the current supply systems operate close to stress, particularly where surface storage is limited and access to productive groundwater is poor. Central and south-eastern basins stand out as areas where projected hazard intensification coincides with limited groundwater availability and high consumptive use, implying reduced buffer capacity during multi-year droughts. The infrastructure scenarios used in the vulnerability index show that, under pathways with higher investment capacity, a substantial part of today's vulnerability can be alleviated through a combination of targeted storage works, conveyance upgrades and rehabilitation of existing systems. However, under less favourable socio-economic conditions, these measures remain incomplete, and increased climatic hazard translates more directly into supply deficits. The results therefore underline the importance of coupling infrastructure development with demand management and groundwater protection to maintain flexibility under future drought regimes.

5.2.3 Tourism

Tourism contributes a smaller fraction of total annual water demand than agriculture at island scale, but it is spatially concentrated along the northern coastline and in specific resort areas, which are also exposed in the relative drought analysis. The exposure indicators show that several coastal basins combine high resident population with seasonal tourism peaks, amplifying short-term pressure on local water systems during dry summers. Under scenarios with strong tourism growth, these hotspots remain or become more prominent even when overall vulnerability improves, indicating a need for localised measures e.g., diversification of supply sources, reuse of treated wastewater and efficiency measures in accommodation facilities and integration of tourism demand into drought-management plans. In high-risk coastal municipalities, coordination between tourism, municipal and irrigation operators will be essential to prevent conflict over limited supplies in dry years.

5.2.4 Environment and ecosystems

Although the analyses are centred on human uses, the patterns inferred have direct implications for freshwater and terrestrial ecosystems. Basins with high hazard, exposure and vulnerability typically coincide with areas where environmental flows are already constrained and where over-abstraction from groundwater can exacerbate salinisation risks in coastal aquifers. Under scenarios with stronger hazard intensification, the window for natural recovery of rivers, wetlands and dependent

habitats shrinks, especially in central and eastern Crete where pressure is multi-sectoral. In addition, higher summer temperatures and drier conditions implied by the hazard indicators are consistent with an increased background susceptibility to wildfire, particularly in upland and shrub dominated areas. These findings suggest that drought risk planning for Crete should be linked with ecosystem based adaptation, environmental flow safeguards and landscape-scale fire risk management, rather than treated solely as an issue of water supply for human sectors.

5.3 Alignment with Crete's Regional Adaptation Action Plan of Crete (RAAP)

The current Regional Adaptation Action Plan of Crete (RAAP / ΠΕΣΠΚΑ) identifies droughts and water scarcity as priority climate risks and sets strategic directions for water resources, agriculture, tourism, ecosystems and civil protection, but it does not yet include fully quantitative, high-resolution risk metrics. The CLIMAAX-CRETE drought assessment directly fills this gap by providing spatially explicit indicators of hazard, exposure, vulnerability and composite risk at the basin–municipality scale for both the recent past and alternative future pathways. These outputs can therefore be used as an analytical "backbone" for the second RAAP cycle (2026+) and for the Action Plan for combating drought and water scarcity in Crete.

First, the relative drought risk maps and municipal based results support the RAAP axes on water resources and agriculture by identifying where structural risk is already high (e.g. central and eastern Crete) and where it is projected to intensify under SSP3-7.0 and SSP5-8.5. These patterns can be used to:

- prioritise basins and municipalities for demand-management measures (irrigation efficiency, leak reduction, groundwater protection),
- target the portfolio of planned water works (dams, conveyance networks, wastewater reuse, boreholes, rehabilitations) so that investments coincide with persistently high or rising risk, and
- refine agricultural support measures (diversification, drought-tolerant cultivars, advisory services) in municipalities where agricultural exposure and vulnerability dominate the risk signal.

Second, the exposure indicators for population and tourism are directly relevant to RAAP priorities on urban areas, tourism and public health. Municipalities where rising climatic hazard co-exists with dense permanent or seasonal populations can be flagged in the updated RAAP as hotspots for:

- drinking-water security planning (alternative sources, contingency supply, storage),
- demand-side interventions in tourism (water-saving standards in hotels, reuse schemes), and

- heat–drought combined risk management in cities (green/blue infrastructure, emergency plans).

Third, the vulnerability sub-indices (GDP per capita, groundwater availability, irrigated area, water-infrastructure capacity under each SSP) provide a quantitative basis for the hierarchisation of measures that RAAP already lists qualitatively. Units that combine high hazard with low adaptive capacity (low income, limited groundwater access, sparse or SSP-3 infrastructure pathways) can be tagged as priority recipients for EU and national funding streams, consistent with the RAAP objective of aligning adaptation with the Crete 2030 Development Plan and sectoral plans (water-management plans, drought/scarcity plan, flood-risk plan).

Finally, the CLIMAAX-CRETE products of this phase provide a spatially explicit benchmark of drought hazard, exposure, vulnerability and risk, which can be used in the next RAAP revision as a reference layer for priority setting (baseline for 2015–2040, indicative target ranges for 2041–2070 and alarm conditions for 2071–2100). In the forthcoming third phase of CLIMAAX-CRETE, this analytical basis will be complemented by the design of an operational drought monitoring process for the Region of Crete, building on openly available pan-European services (e.g. the European Drought Observatory) and other routinely updated datasets. The aim is to define a practical set of indicators and procedures that allow the Region to track emerging drought conditions in near-real time and to link predefined management responses to specific alert levels, thereby strengthening the evidence base of the RAAP and the Action Plan for drought and water scarcity.

5.4 Limitations and Future Work

5.4.1 Relative drought Risk assessment

The relative drought risk index inherits uncertainties from all three of its components. On the **hazard** side, the CHELSA and ISIMIP3b climate datasets are bias-corrected but remain uncertain in their representation of mean precipitation and its variability over the complex Cretan topography, especially in orographic rain-shadow areas and along coastal gradients. Because the hazard metric is constructed from pooled percentiles of BIO1, BIO5, BIO12 and the WASP index across all periods and scenarios, any systematic biases or drifts in these drivers propagate into the relative ranking of units. Results should therefore be interpreted as internally consistent, scenario-conditioned contrasts within the modelling framework, rather than as precise probabilities of drought occurrence. A key avenue for improvement is to rebuild the hazard indicators using the recently developed CLIMADAT-Grid dataset as primary climate forcing, in order to derive indices that are more tightly tailored to the Cretan climate and reduce uncertainty in the hazard component.

Uncertainty is also present in exposure and vulnerability. Agricultural exposure is derived from GCAM/Demeter land-use projections, which provide only a broad, scenario-

consistent picture of crop extent and may diverge from locally observed trends in cropping patterns, intensification or shifts between rainfed and irrigated systems. This is critical given that agriculture accounts for about 86% of total water demand and thus dominates the composite exposure index: any mismatch between GCAM land use and actual agricultural extent can directly bias the spatial pattern of exposure. The fixed weighting scheme used to combine sub-indicators reflects expert judgement and has not been formally optimised; alternative weights could shift absolute index values and, in some cases, the relative ranking of units.

Future work on this workflow should therefore focus on: (i) replacing or complementing CHELSA/ISIMIP3b with CLIMADAT-Grid for hazard derivation; (ii) developing locally downscaled and policy-relevant land-use and water-use scenarios (e.g. combining LUISA, regional statistics and GCAM) to better anchor exposure in Cretan realities; (iii) updating groundwater and infrastructure layers as new information becomes available; and (iv) systematically testing alternative indicator sets and weighting schemes (including, potentially, DEA-type formulations for sensitivity analysis) to quantify how methodological choices influence the resulting risk patterns.

5.4.2 Agricultural drought workflow (olive revenue loss)

The agricultural drought workflow for olives is limited primarily by crop and water-use data and by the simplicity of the impact model. Olive production and area are based on MapSPAM 2010, because SPAM 2020 currently lacks coverage for Crete. Spatial patterns of olive intensity therefore reflect conditions around 2010 and may not capture more recent expansion, abandonment or shifts between rainfed and irrigated groves. Crop values and irrigated fractions come from GAEZ v5 and global irrigated-area datasets, which smooth intra-basin heterogeneity and do not encode local price structures, subsidy regimes or network layout. Information on actual irrigation practices (application depths, sources, reliability) is sparse, so the workflow represents a “drought with unmet irrigation demand” rather than a fully explicit water-allocation process.

Methodologically, the workflow uses a single ET-based yield response with fixed crop parameters and growing season, and does not differentiate between cultivars, soil types, tree age or management intensity, nor account for elevated CO_2. Revenue loss is computed under simplified assumptions about which fractions of irrigated and rainfed area are affected, without coupling to a dynamic hydrological or water-resources model. Climate-model uncertainty (choice of RCMs and scenarios) directly affects ET and precipitation deficits and thus the magnitude of yield losses; the four-model ensemble samples, but does not fully span, the range of plausible futures.

Future developments should include: (i) updating exposure once SPAM 2020 (or equivalent regional crop maps) become reliable for Crete; (ii) integrating detailed local crop statistics, olive-grove maps and irrigation-network information from regional authorities; (iii) refining crop-water response functions with soil- and cultivar-specific parameters and, where possible, local experimental data; and (iv) coupling the workflow

to basin-scale hydrological and water-resources models to represent explicit irrigation shortages and allocation decisions. This would allow a more realistic translation of meteorological drought into production and revenue impacts.

5.4.3 Olive-yield climate impact study

The olive-yield climate impact study is constrained by its empirical and regional character. Climate–yield relationships are estimated statistically at the scale of 21 regional units for Greece and thus average over substantial internal variability within Crete. Fine-scale effects of elevation, soil, irrigation and management are only implicitly represented. The model structure assumes that past sensitivities to late-spring rainfall and high summer temperatures remain valid under future climate conditions and that non-climatic drivers (cultivar mix, tree age, technological change, market signals) do not fundamentally alter the response. In reality, adaptation by farmers may either dampen or amplify climate impacts relative to the projections.

Future improvement directions include: (i) assembling more detailed, sub-regional yield and management datasets for Crete, distinguishing explicitly between rainfed and irrigated systems; (ii) exploring non-linear and threshold responses, particularly for extreme heat and combined heat-drought stress; (iii) broadening the climate-model ensemble to include newer, higher-resolution simulations and updated forcing scenarios; and (iv) linking the statistical yield model with the CLIMAAX agricultural drought and water-resources analyses, so that projected climatic stress is evaluated jointly with projected water availability and management options.

6 Conclusions and recommendations

6.1 Key conclusions

6.1.1 Relative drought risk

The relative drought assessment shows that current drought risk is not uniform across Crete. A belt from central to south-eastern Crete concentrates the highest composite risk, driven by the co-location of higher climatic hazard, dominant agricultural and tourism exposure, and limited water-resource robustness. Western Crete generally appears in lower to intermediate risk classes, although local hotspots exist. Looking forward, risk intensifies and spreads under SSP3-7.0 and SSP5-8.5, with more units shifting into higher risk categories by the end of the century, while SSP1-2.6 shows more moderate or locally stabilising trends. The persistence of key hotspots across methods (climatic hazard, exposure, vulnerability indices and agricultural-loss modelling) indicates that drought in Crete is a structural rather than episodic risk.

6.1.2 Agricultural drought (olive revenue loss)

The updated CLIMAAX agricultural workflow confirms that olive production in Crete is highly sensitive to precipitation driven water deficits during the growing season. Central and eastern Crete emerge as persistent hotspots where high olive intensity, limited water buffer and constrained infrastructure combine to produce the largest projected revenue losses. Under scenarios with strong drying and/or reduced irrigation reliability, potential economic losses can locally approach the order of 1,000 €/stremma for intensive olive groves, if irrigation needs cannot be met. Irrigation mitigates impacts where coverage is high and supply is reliable, but does not eliminate risk in systems already operating close to their resource limits.

6.1.3 Olive yield projections

The olive-yield climate impact analysis, based on empirically derived climate-yield relationships, points to increasing frequency and magnitude of negative yield anomalies as late-spring rainfall declines and high summer temperatures become more common. Central and eastern Crete, already important production zones, exhibit the strongest negative signals under intermediate and high forcing. While absolute values are uncertain, the direction and spatial pattern of change agree well with the CLIMAAX agricultural workflow, reinforcing the conclusion that the olive sector in these areas faces elevated medium to long-term drought risk, especially under pathways with limited adaptation.

6.2 Recommendations

6.2.1 Water management and irrigation

- Prioritise central and south-eastern basins as drought-risk hotspots in the forthcoming Drought & Water Scarcity Action Plan and in river-basin management plans.
- Target new storage, conveyance and rehabilitation works where high relative risk overlaps with limited groundwater availability, giving preference to realistic measures (loss reduction, reuse, smart metering, leakage control, managed aquifer recharge).
- Promote high-efficiency irrigation practices and technologies (drip, deficit irrigation strategies) and improved on-farm scheduling, linked to drought early-warning information.
- Strengthen groundwater protection in coastal and over-exploited aquifers through abstraction control, licensing and monitoring, to preserve buffer capacity for multi-year droughts.
- Integrate sectoral demands (irrigation, domestic, tourism) in drought contingency plans with pre-agreed priority rules and restriction levels.

6.2.2 Agricultural practices and diversification

- Support adoption of drought-tolerant olive cultivars and rootstocks, improved canopy management (pruning, shading) and soil-moisture conservation practices (mulching, reduced tillage, cover crops) in high-risk areas.
- Encourage diversification within the primary sector (e.g. mixes of early/late varieties, alternative low-water crops where agronomically feasible, and complementary on-farm activities) to reduce dependence on single-crop income in the most exposed basins.
- Strengthen advisory services and decision-support tools that translate drought indicators into practical recommendations on irrigation timing, fertilisation and harvesting for farmers and cooperatives.
- Explore economic-risk instruments for olive growers in structurally high-risk areas.

6.2.3 Monitoring and data needs

- Develop an operational drought-monitoring system for Crete that blends open pan-European services (e.g. EDO), locally optimised climate products (e.g. CLIMADAT-Grid), in-situ networks and remote sensing (soil moisture, vegetation condition), with outputs at basin and municipal scale.
- Improve spatial datasets for agriculture and water use: high-resolution land-use/land-cover maps for olives and other key crops, up-to-date irrigation-network and reservoir inventories, and harmonised groundwater abstraction and level data.
- Systematically collect and harmonise agricultural statistics (yields, planted area, irrigation status) at sub-regional level to recalibrate both the agricultural drought workflow and the olive-yield models.

6.2.4 Policy and planning

- Embed the CLIMAAX-CRETE drought-risk results directly into the next revision of the Regional Adaptation Action Plan and the dedicated Drought & Water Scarcity Action Plan, as the spatial basis for prioritising measures and investments.
- Use the identified high-risk basins and municipalities to guide zoning and regulation for water-intensive activities (e.g. new irrigated schemes, tourism developments), linking permits and subsidies to water-efficiency and drought-preparedness criteria.
- Institutionalise cross-sector coordination (water, agriculture, tourism, environment, civil protection).
- Plan for iterative revision of both indicators and measures (e.g. every 5 years), so that new data can be assimilated and the regional strategy can adapt to evolving climate and socio-economic conditions.

References

Brun, P., Zimmermann, N.E., Hari, C., Pellissier, L., Karger, D.N., 2022. Global climate-related predictors at kilometer resolution for the past and future. Earth Syst. Sci. Data 14, 5573–5603. https://doi.org/10.5194/essd-14-5573-2022

Carrão, H., Naumann, G., Barbosa, P., 2016. Mapping global patterns of drought risk: An empirical framework based on sub-national estimates of hazard, exposure and vulnerability. Glob. Environ. Change 39, 108–124. https://doi.org/10.1016/j.gloenvcha.2016.04.012

Chen, M., Vernon, C.R., Graham, N.T., Hejazi, M., Huang, M., Cheng, Y., Calvin, K., 2020. Global land use for 2015–2100 at 0.05° resolution under diverse socioeconomic and climate scenarios. Sci. Data 7, 320. https://doi.org/10.1038/s41597-020-00669-x

Danielson, J.J., Gesch, D.B., 2011. Global multi-resolution terrain elevation data 2010 (GMTED2010). US Geological Survey.

Di Paola, A., Di Giuseppe, E., Gutierrez, A.P., Ponti, L., Pasqui, M., 2023. Climate stressors modulate interannual olive yield at province level in Italy: A composite index approach to support crop management. J. Agron. Crop Sci. 209, 475–488. https://doi.org/10.1111/jac.12636

Doorenbos, J., Kassam, A., 1979. FAO Irrigation and Drainage Paper 33, Yield Response to Water.

E-OBS, 2020. E-OBS daily gridded meteorological data for Europe from 1950 to present derived from in-situ observations [WWW Document]. https://doi.org/10.24381/cds.151d3ec6

Jacob, D., Petersen, J., Eggert, B., Alias, A., Christensen, O.B., Bouwer, L.M., Braun, A., Colette, A., Déqué, M., Georgievski, G., Georgopoulou, E., Gobiet, A., Menut, L., Nikulin, G., Haensler, A., Hempelmann, N., Jones, C., Keuler, K., Kovats, S., Kröner, N., Kotlarski, S., Kriegsmann, A., Martin, E., van Meijgaard, E., Moseley, C., Pfeifer, S., Preuschmann, S., Radermacher, C., Radtke, K., Rechid, D., Rounsevell, M., Samuelsson, P., Somot, S., Soussana, J.-F., Teichmann, C., Valentini, R., Vautard, R., Weber, B., Yiou, P., 2014. EURO-CORDEX: new high-resolution climate change projections for European impact research. Reg. Environ. Change 14, 563–578. https://doi.org/10.1007/s10113-013-0499-2

Koutroulis, A.G., Grillakis, M.G., Daliakopoulos, I.N., Tsanis, I.K., Jacob, D., 2016. Cross sectoral impacts on water availability at +2 °C and +3 °C for east Mediterranean island states: The case of Crete. J. Hydrol. 532, 16–28. https://doi.org/10.1016/J.JHYDROL.2015.11.015

Koutroulis, A.G., Vrohidou, A.-E.K., Tsanis, I.K., 2011. Spatiotemporal characteristics of meteorological drought for the Island of Crete. J. Hydrometeorol. 12. https://doi.org/10.1175/2010JHM1252.1

Lange, S., Büchner, M., 2021. ISIMIP3b bias-adjusted atmospheric climate input data. https://doi.org/10.48364/ISIMIP.842396.1

Tramblay, Y., Koutroulis, A., Samaniego, L., Vicente-Serrano, S.M., Volaire, F., Boone, A., Le Page, M., Llasat, M.C., Albergel, C., Burak, S., Cailleret, M., Kalin, K.C., Davi, H., Dupuy, J.L., Greve, P., Grillakis, M., Hanich, L., Jarlan, L., Martin-StPaul, N., Martínez-Vilalta, J., Mouillot, F., Pulido-Velazquez, D., Quintana-Seguí, P., Renard, D., Turco, M., Türkeş, M., Trigo, R., Vidal, J.P., Vilagrosa, A., Zribi, M., Polcher, J., 2020. Challenges for drought assessment in the Mediterranean region under future climate scenarios. Earth-Sci. Rev. 210, 103348. https://doi.org/10.1016/J.EARSCIREV.2020.103348

Tsanis, I.K., Koutroulis, A.G., Daliakopoulos, I.N., Jacob, D., 2011. Severe climate-induced water shortage and extremes in Crete. Clim. Change 106. https://doi.org/10.1007/s10584-011-0048-2

Vautard, R., Gobiet, A., Jacob, D., Belda, M., Colette, A., Déqué, M., Fernández, J., García-Díez, M., Goergen, K., Güttler, I., Halenka, T., Karacostas, T., Katragkou, E., Keuler, K., Kotlarski, S., Mayer, S., van Meijgaard, E., Nikulin, G., Patarčić, M., Scinocca, J., Sobolowski, S., Suklitsch, M., Teichmann, C., Warrach-Sagi, K., Wulfmeyer, V., Yiou, P., 2013. The simulation of European heat waves from an ensemble of regional climate models within the EURO-CORDEX project. Clim. Dyn. 41, 2555–2575. https://doi.org/10.1007/s00382-013-1714-z

Vicente-Serrano, S.M., Beguería, S., López-Moreno, J.I., 2010. A Multiscalar Drought Index Sensitive to Global Warming: The Standardized Precipitation Evapotranspiration Index. J. Clim. 23, 1696–1718. https://doi.org/10.1175/2009JCLI2909.1

Vrac, M., Noël, T., Vautard, R., 2016. Bias correction of precipitation through Singularity Stochastic Removal: Because occurrences matter. J. Geophys. Res. Atmospheres 121, 5237–5258. https://doi.org/10.1002/2015JD024511

7 Appendix

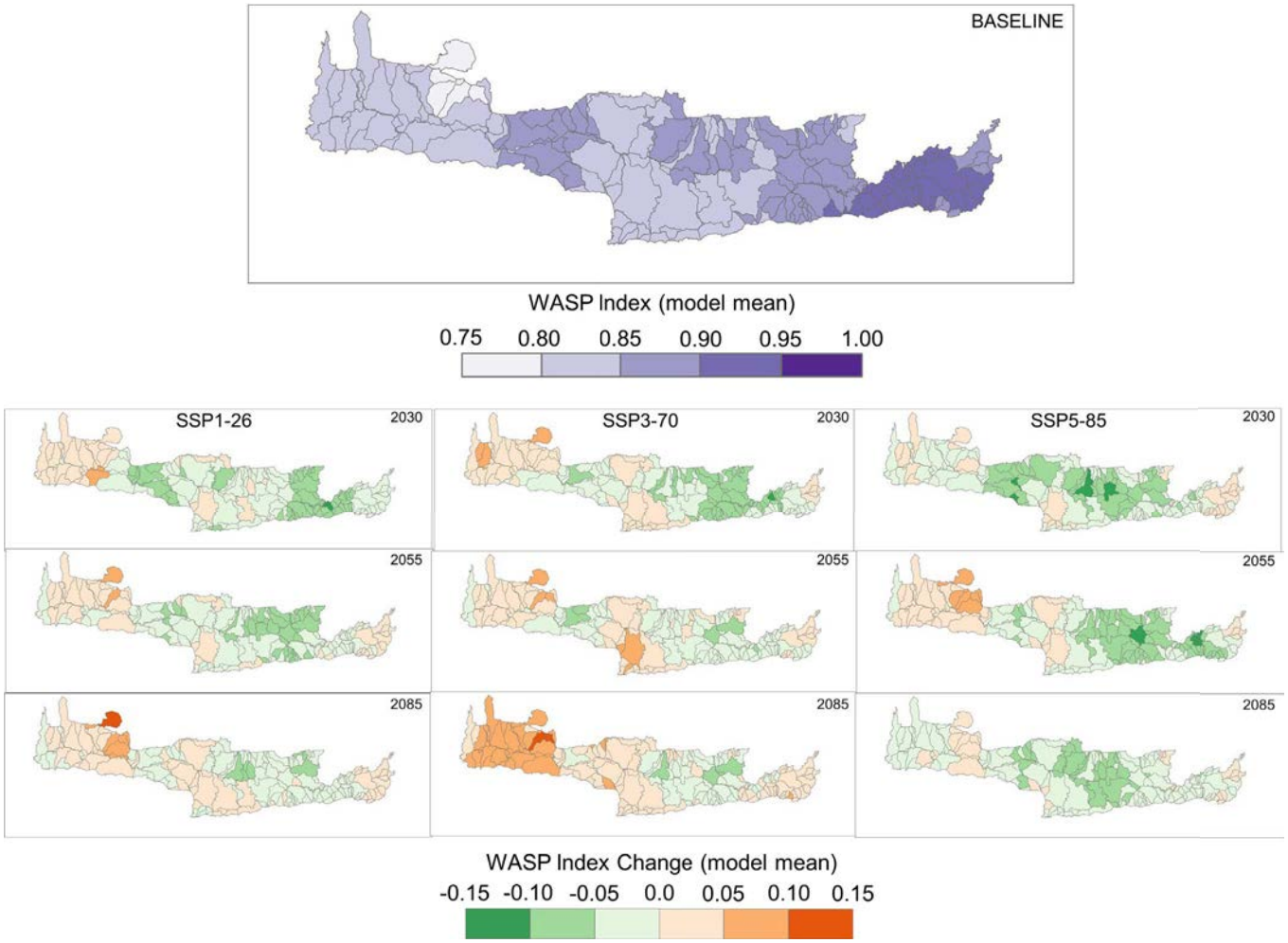

Figure 7-1: Baseline WASP hazard index (2020) at sub-basin scale and changes for 2011–2040, 2041–2070 and 2071–2100 under SSP1-2.6, SSP3-7.0 and SSP5-8.5.

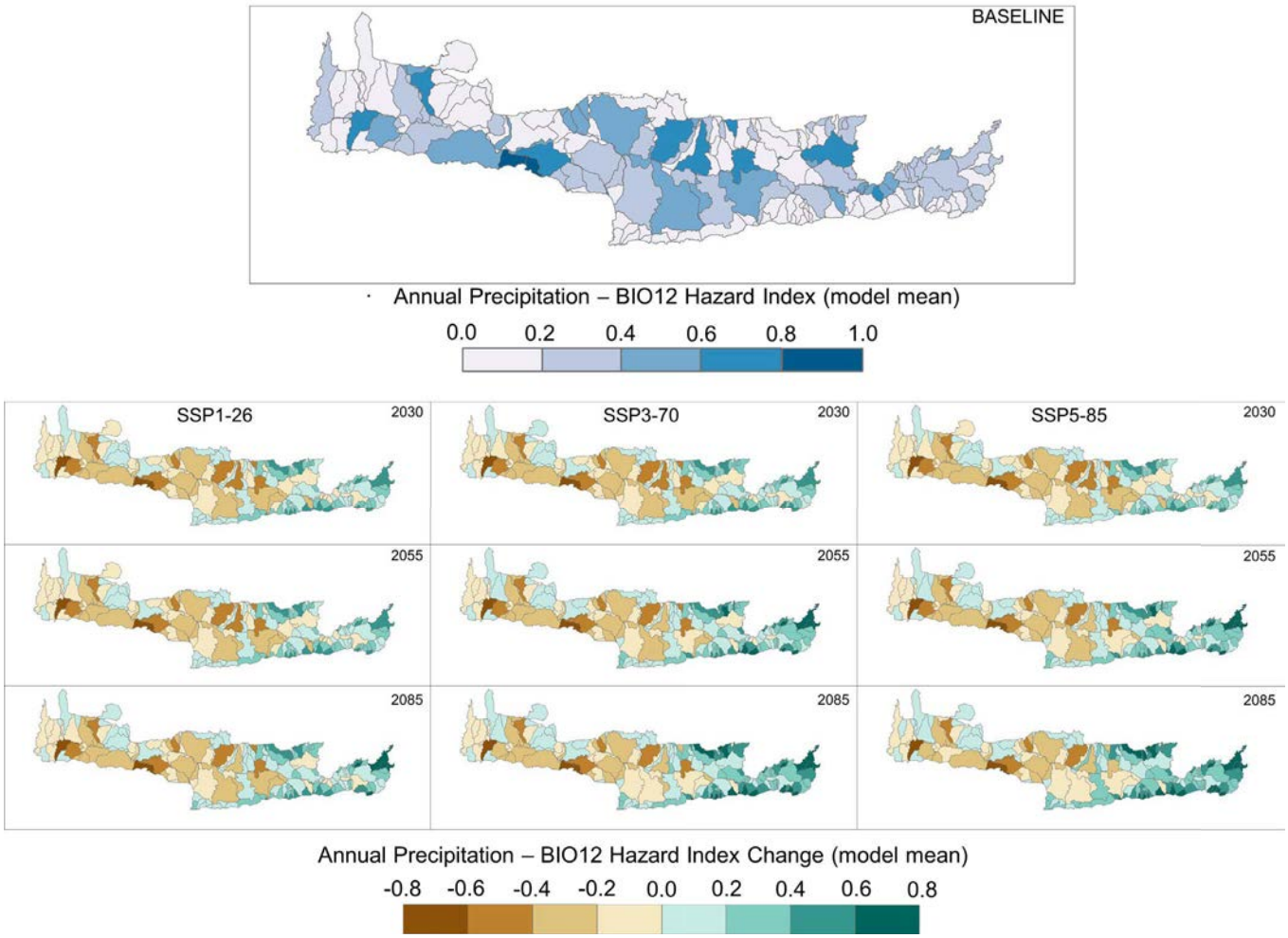

Figure 7-2: Baseline annual precipitation index (2020) at sub-basin scale and changes for 2011–2040, 2041–2070 and 2071–2100 under SSP1-2.6, SSP3-7.0 and SSP5-8.5.

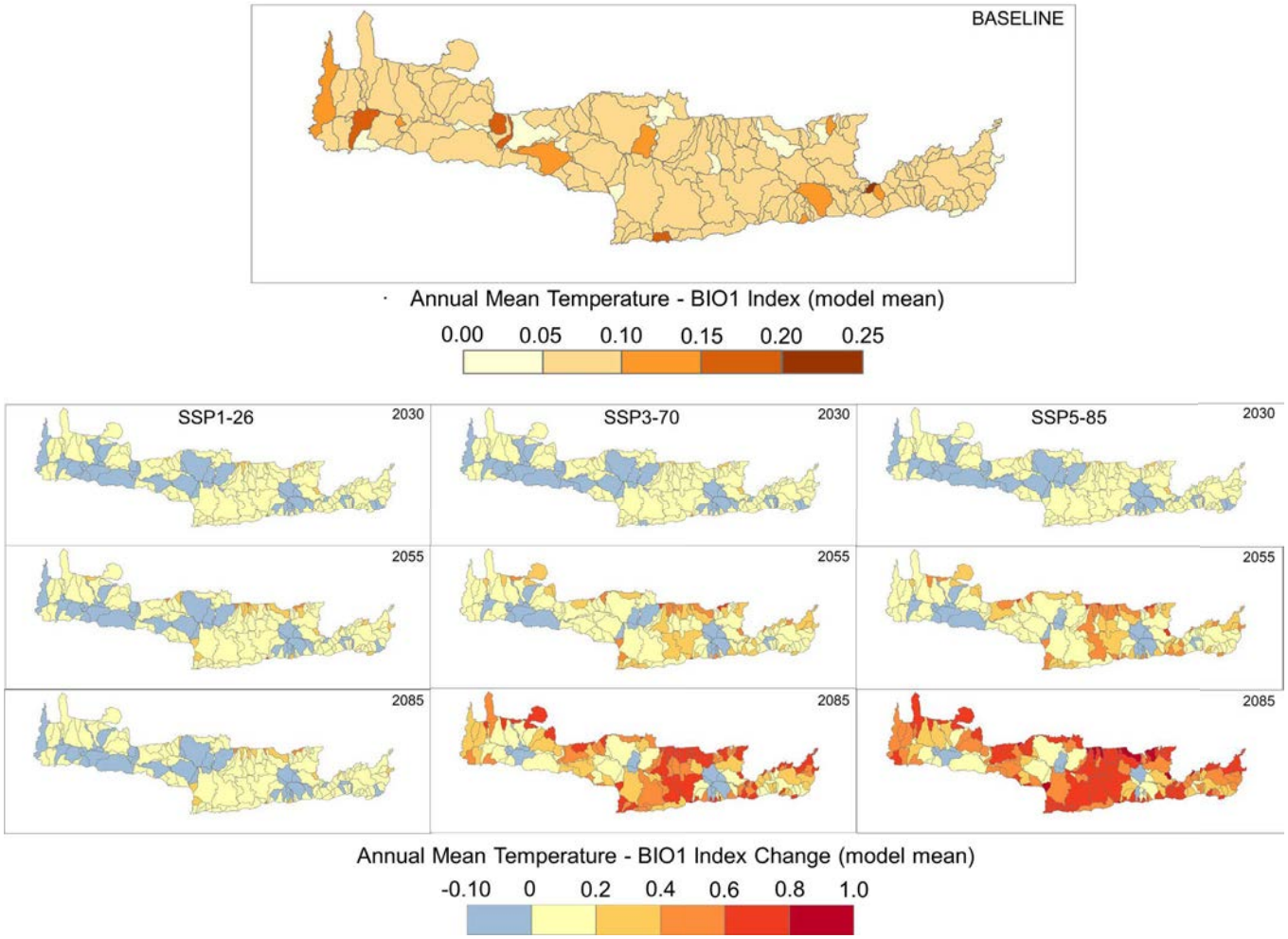

Figure 7-3: Baseline annual mean temperature hazard index (2020) at sub-basin scale and changes for 2011–2040, 2041–2070 and 2071–2100 under SSP1-2.6, SSP3-7.0 and SSP5-8.5.

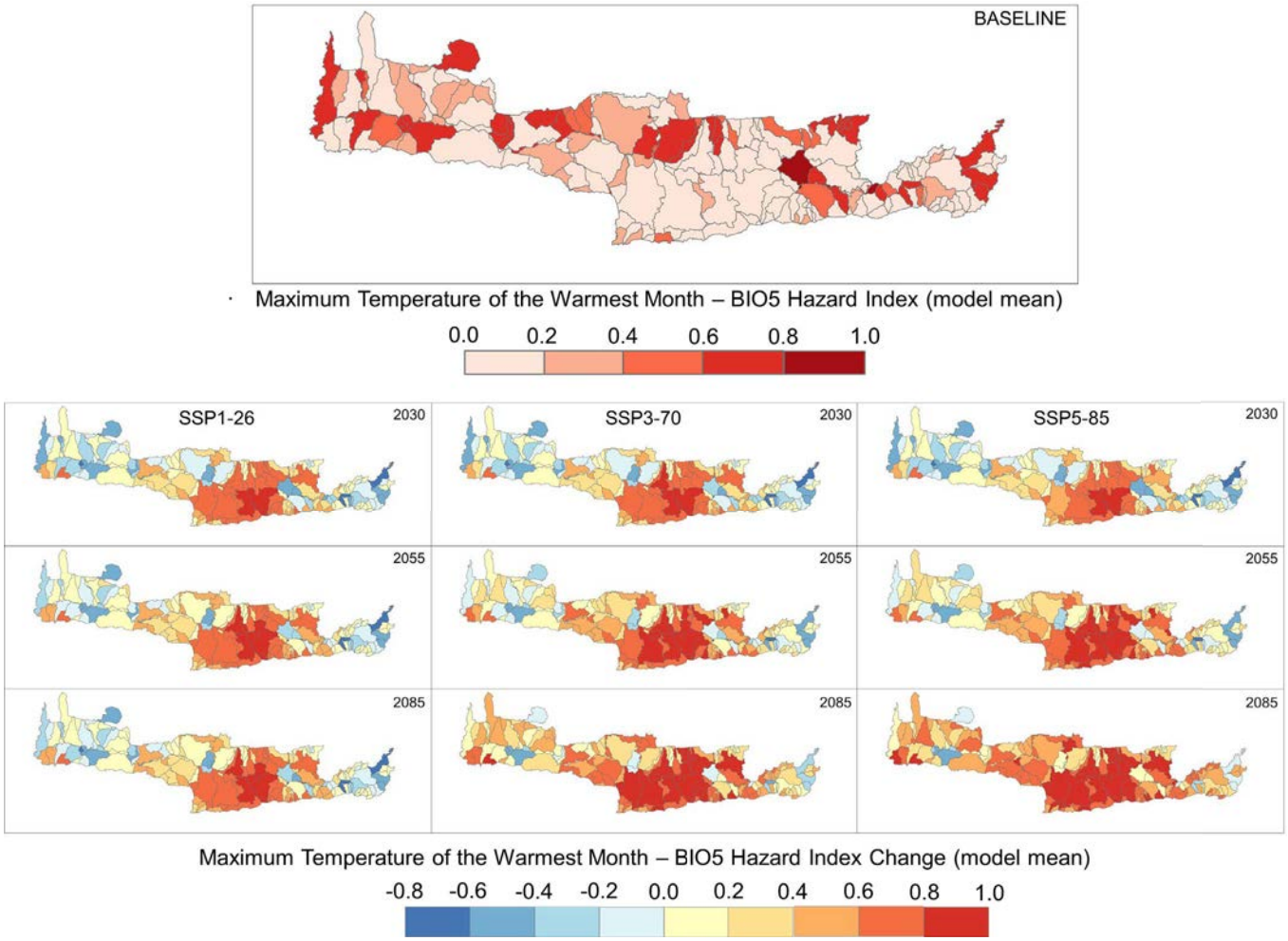

Figure 7-4: Baseline maximum temperature hazard index (2020) at sub-basin scale and changes for 2011–2040, 2041–2070 and 2071–2100 under SSP1-2.6, SSP3-7.0 and SSP5-8.5.

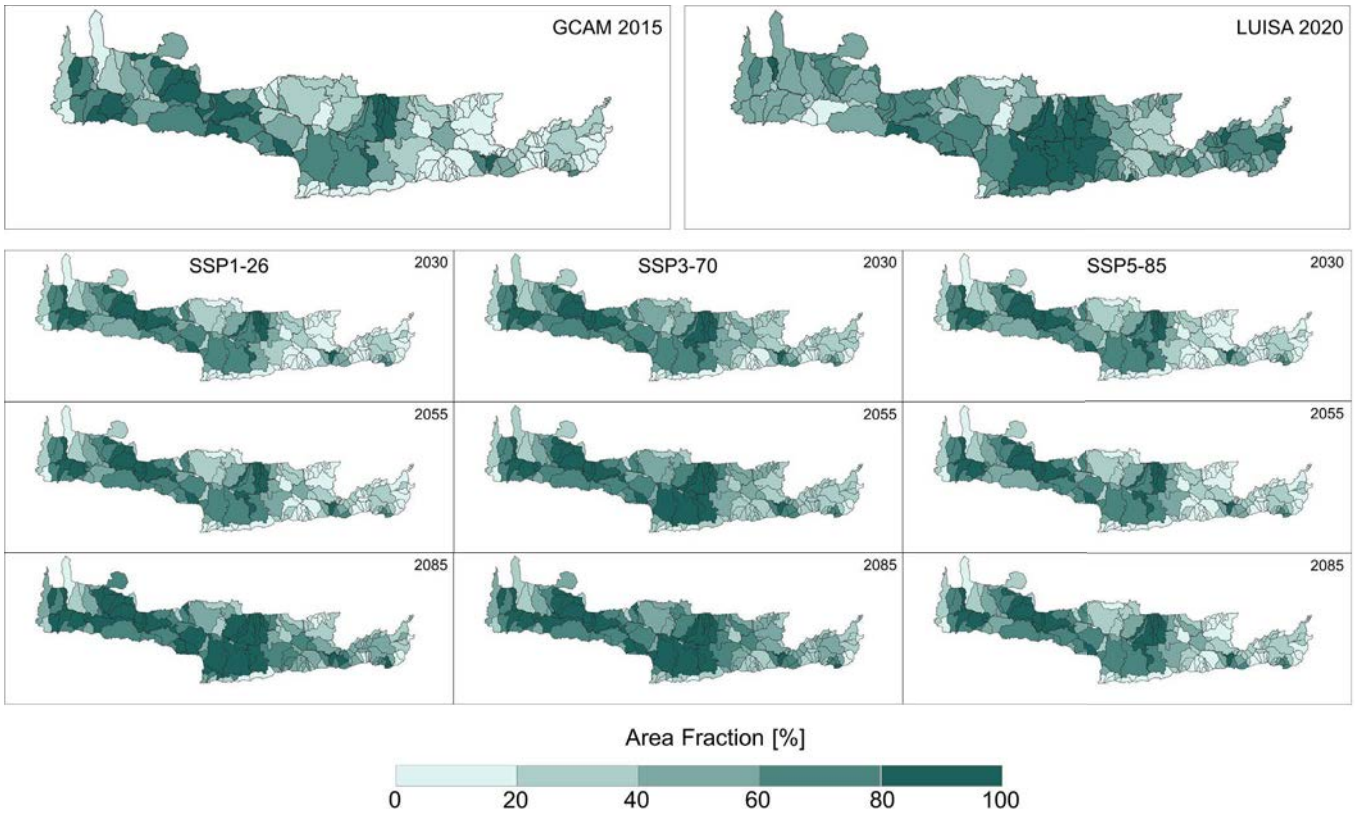

Figure 7-5: Cropland exposure sub-indicator at sub-basin scale. Top panels compare GCAM/DEMETER agricultural area fractions for 2015 (left) with the LUISA 2020 land-use baseline (right). Lower panels show cropland exposure for 2011–2040, 2041–2070 and 2071–2100 under SSP1-2.6, SSP3-7.0 and SSP5-8.5, showing the spatial distribution and evolution of agricultural land use relevant for water demand.

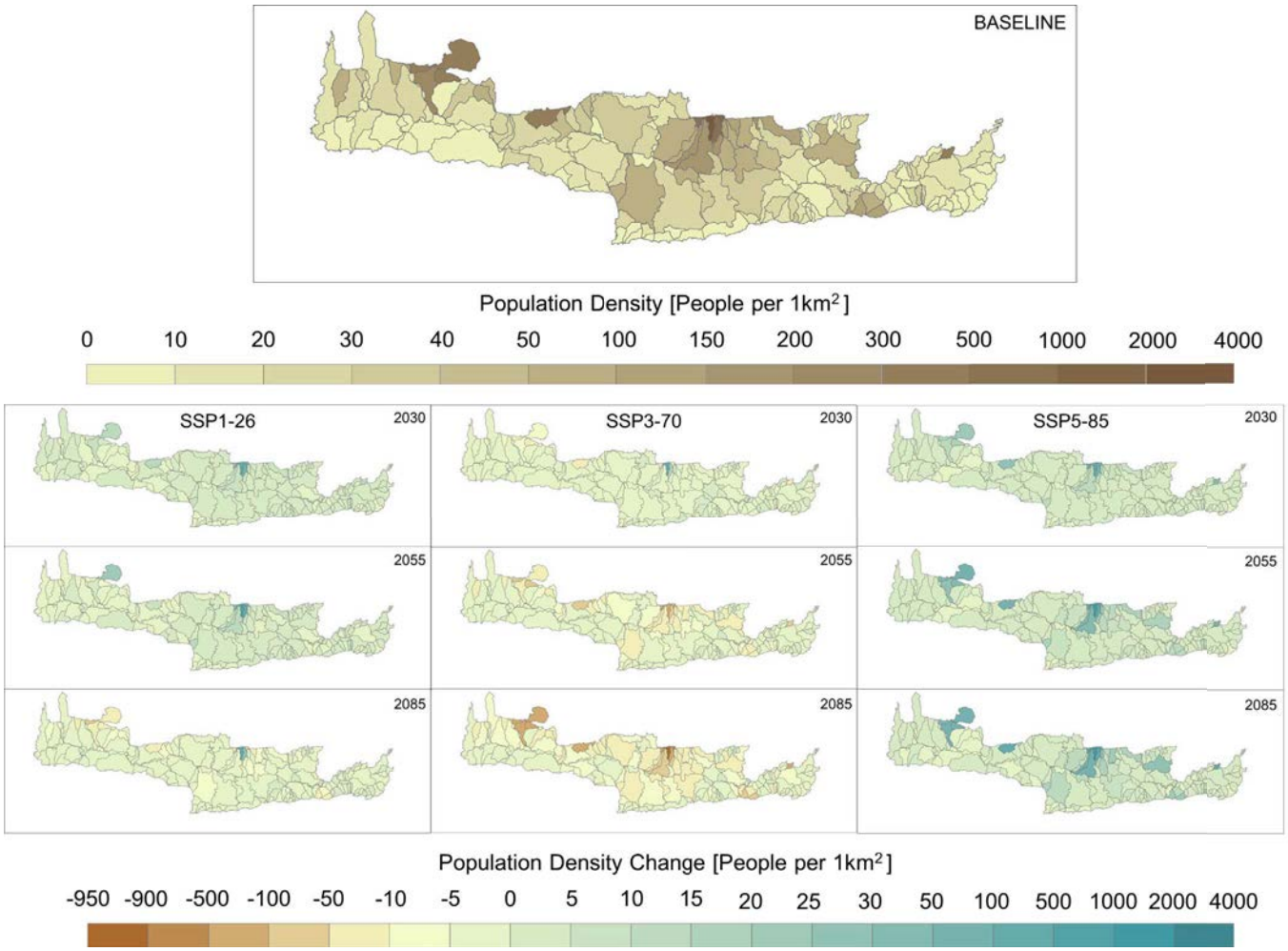

Figure 7-6: Population water-stress exposure sub-indicator. Baseline (2020) population-density-based exposure at sub-basin scale (top) and projected values for 2011–2040, 2041–2070 and 2071–2100 under SSP1-2.6, SSP3-7.0 and SSP5-8.5.

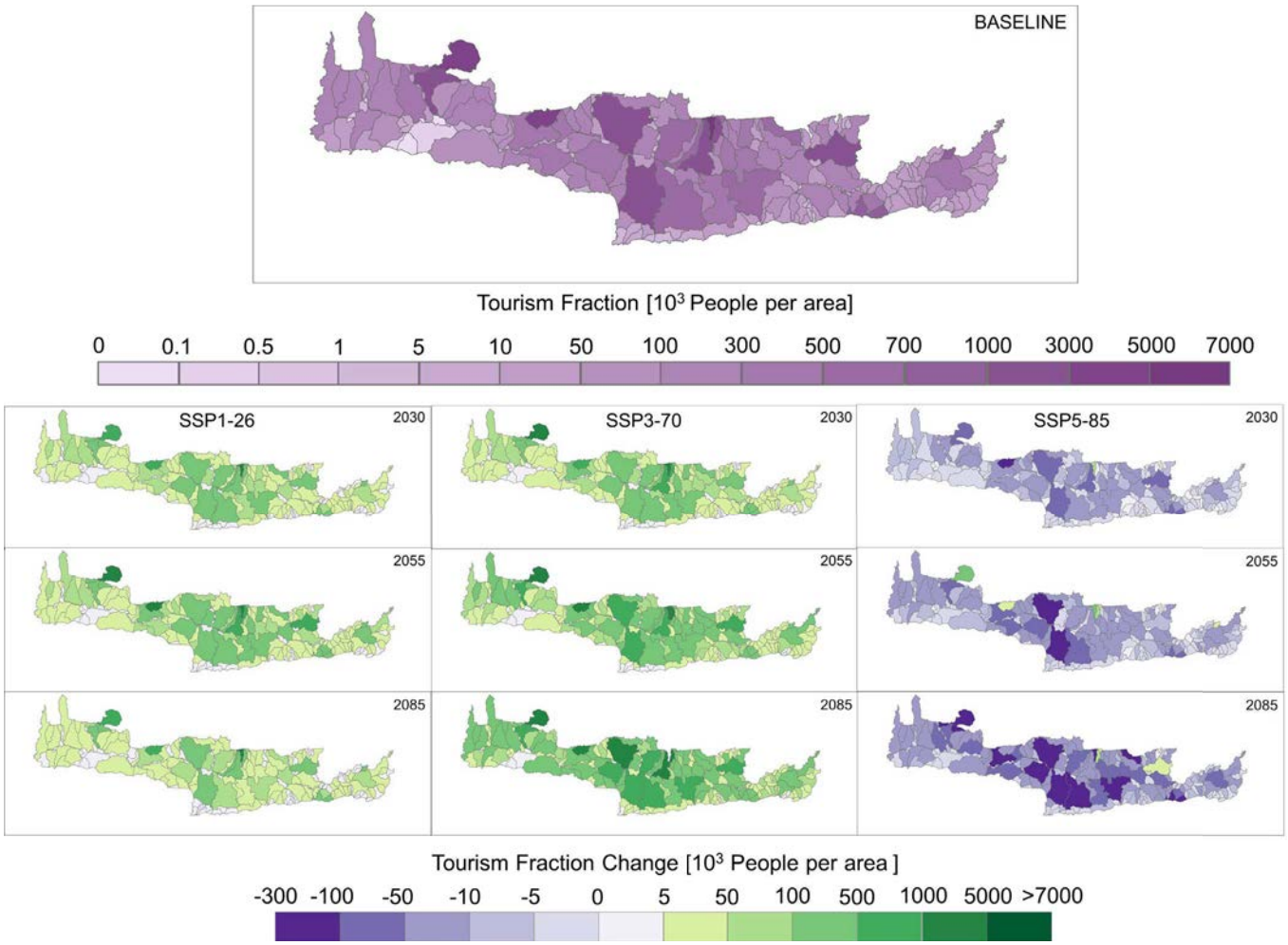

Figure 7-7: Tourism water-stress exposure sub-indicator. Baseline (2020) tourism-related exposure at sub-basin scale (top) and projected values for 2011–2040, 2041–2070 and 2071–2100 under SSP1-2.6, SSP3-7.0 and SSP5-8.5.

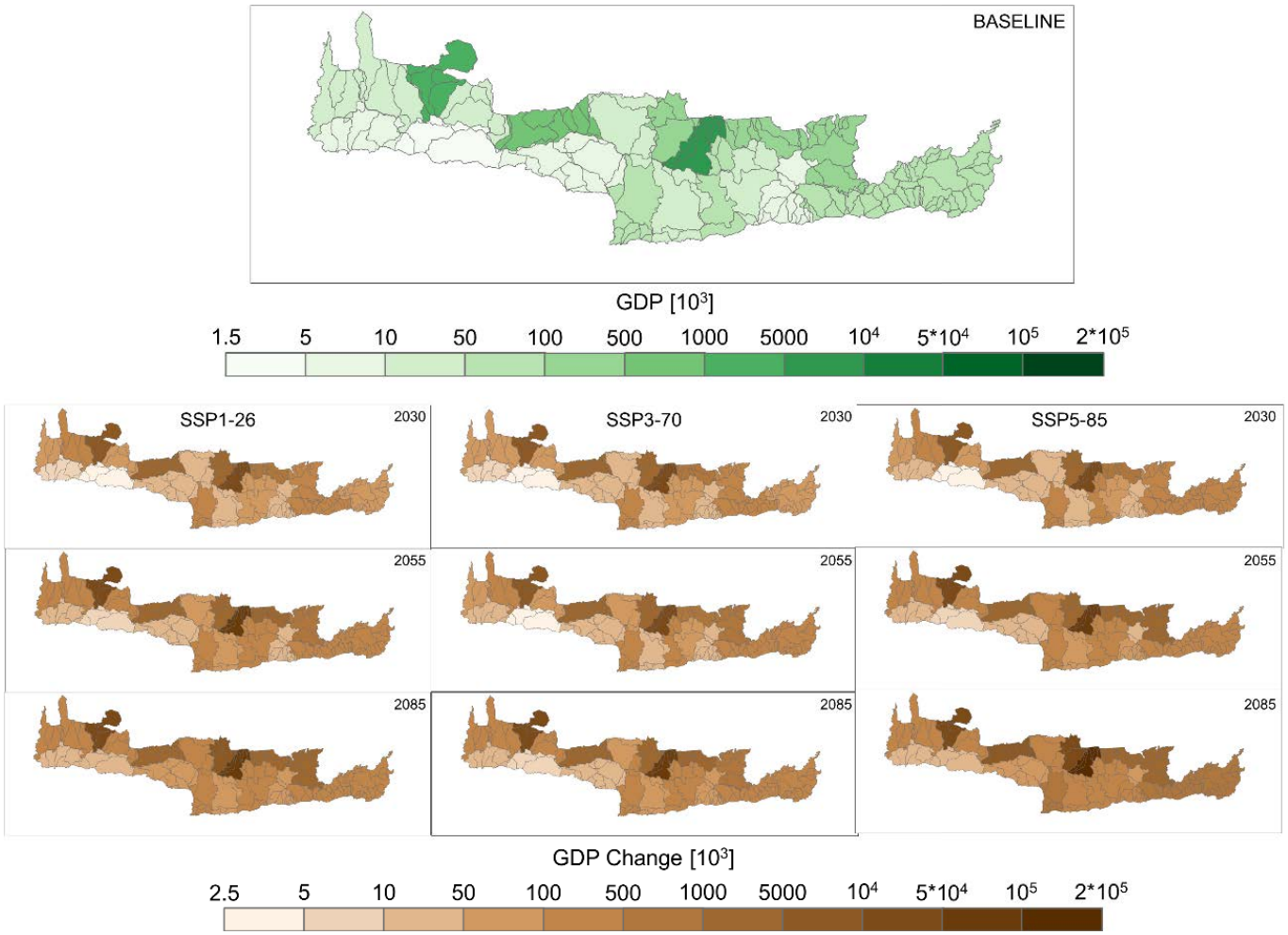

Figure 7-8: GDP per capita vulnerability sub-indicator at sub-basin scale. Baseline (2020) pattern (top) and projected changes for 2011–2040, 2041–2070 and 2071–2100 under SSP1-2.6, SSP3-7.0 and SSP5-8.5.

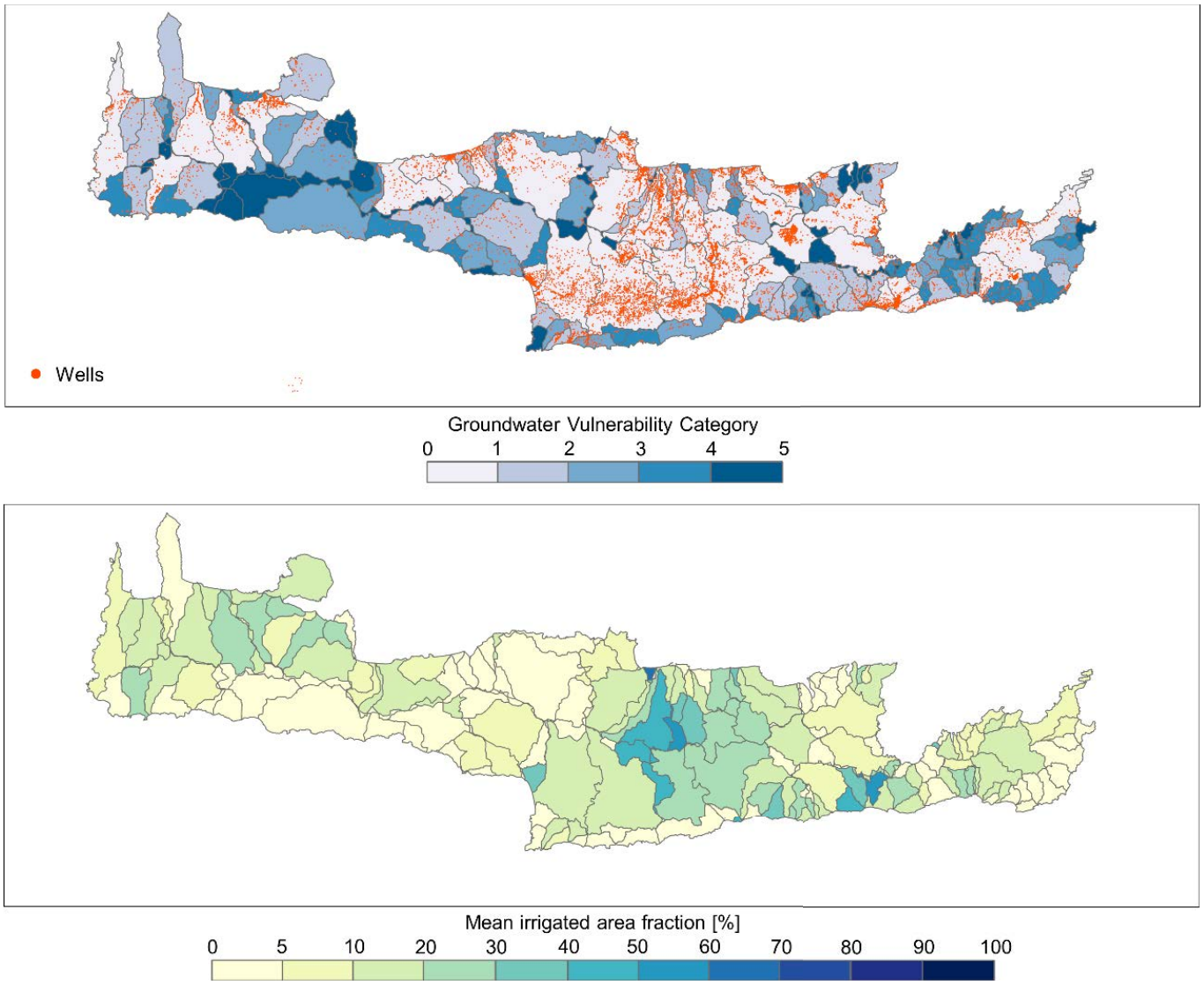

Figure 7-9: Groundwater-related vulnerability and access to irrigation sub-indicators. Top: spatial distribution of registered groundwater wells overlaid on sub-basin units. Bottom: aggregated groundwater-access vulnerability scores at sub-basin scale.

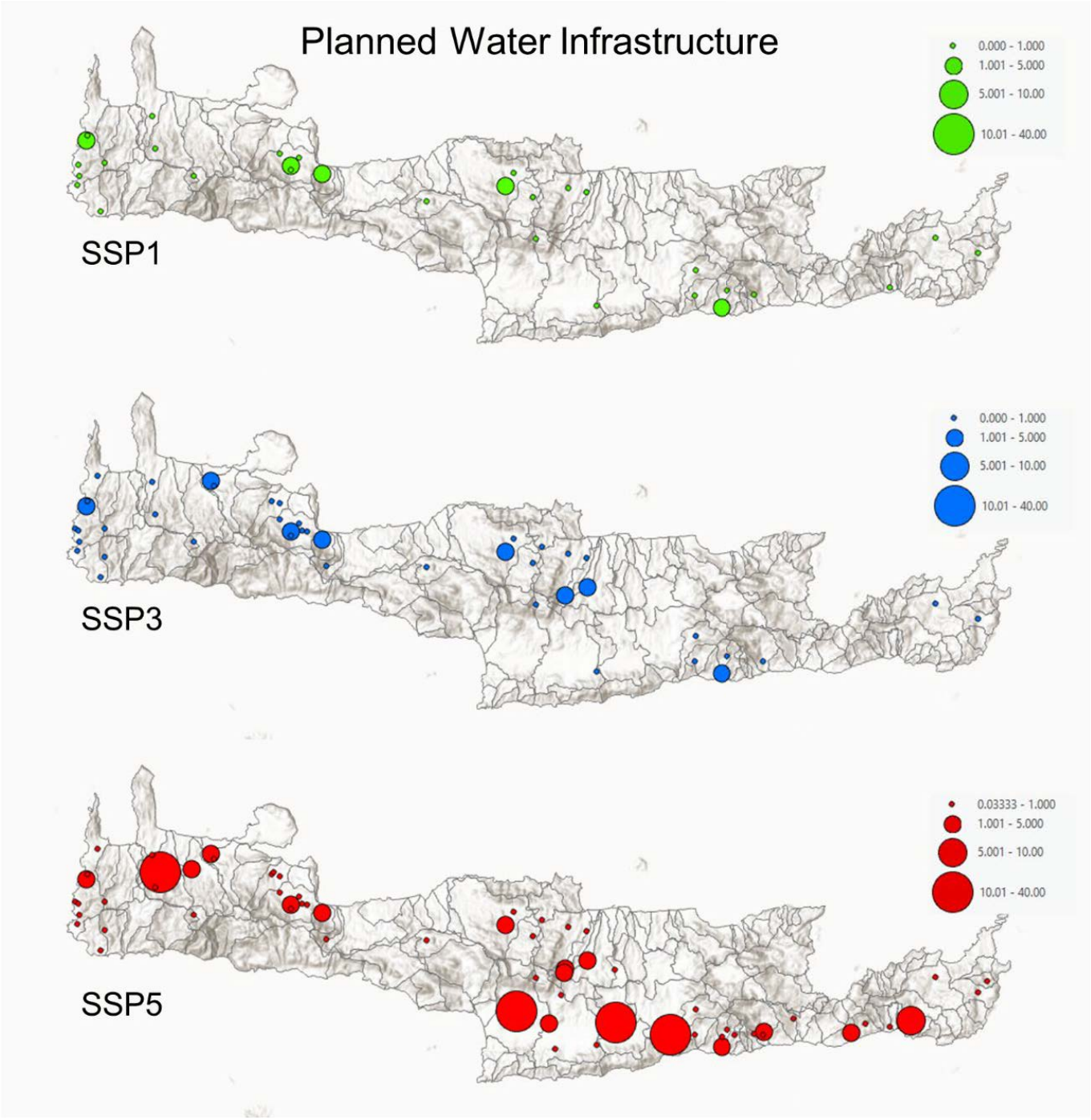

Figure 7-10: Spatial distribution and indicative storage capacity of planned water-infrastructure works under SSP1, SSP3 and SSP5. Circle size is proportional to project capacity (Mm³); colours distinguish the three SSP-consistent portfolios. The maps illustrate the contrasting extent and concentration of candidate works across scenarios.

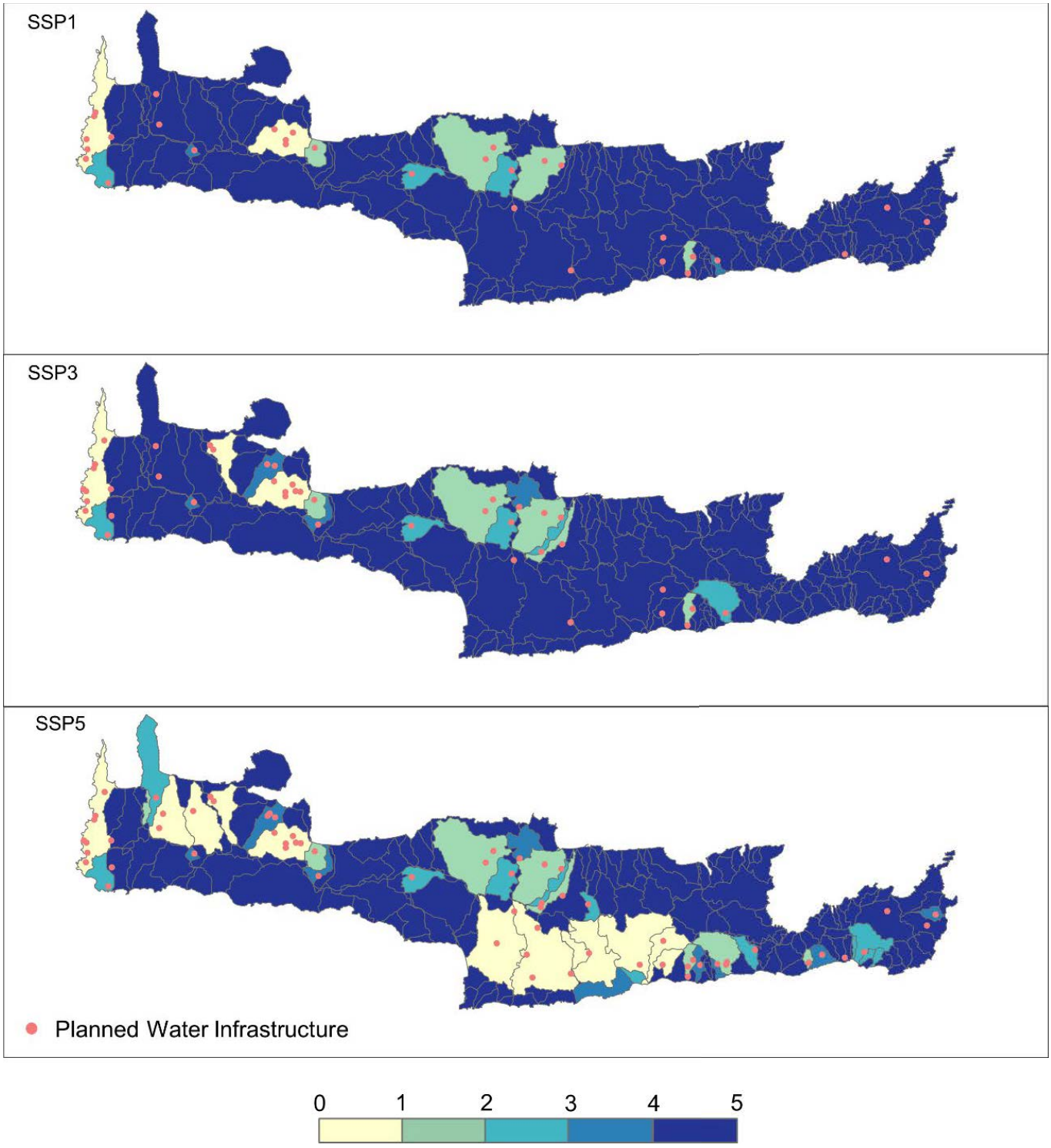

Figure 7-11: Planned water-infrastructure sub-indicator at sub-basin scale for SSP1, SSP3 and SSP5. Colours represent relative infrastructure capacity (from low – light yellow – to high – dark blue) resulting from the SSP-consistent screening of projects. Red dots mark the locations of the individual works included in each scenario portfolio.

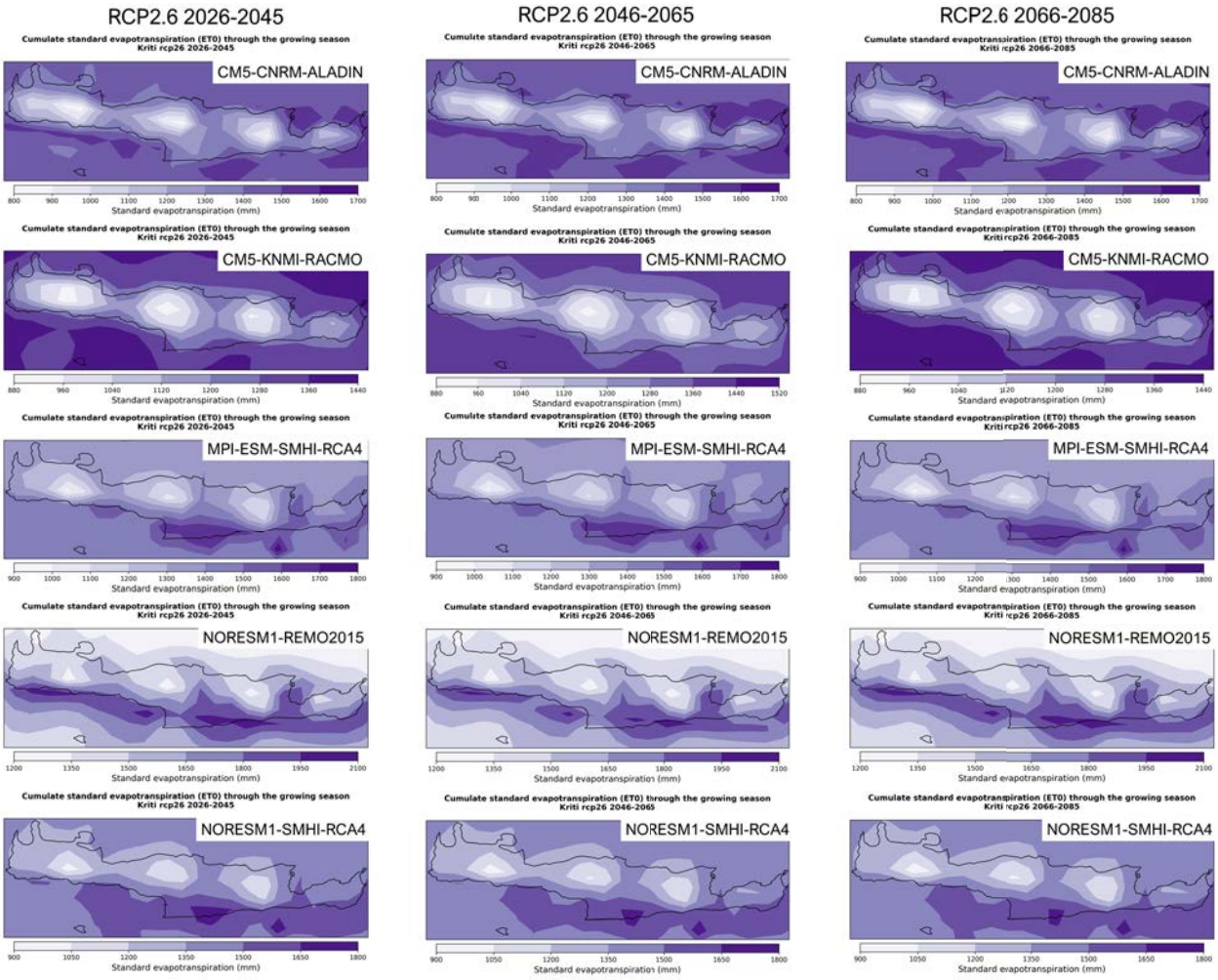

Figure 7-12: Cumulative standard evapotranspiration (ET_0) in Crete for RCP2.6, for three future periods (2026–2045, 2046–2065, 2066–2085) and five EURO-CORDEX RCMs.

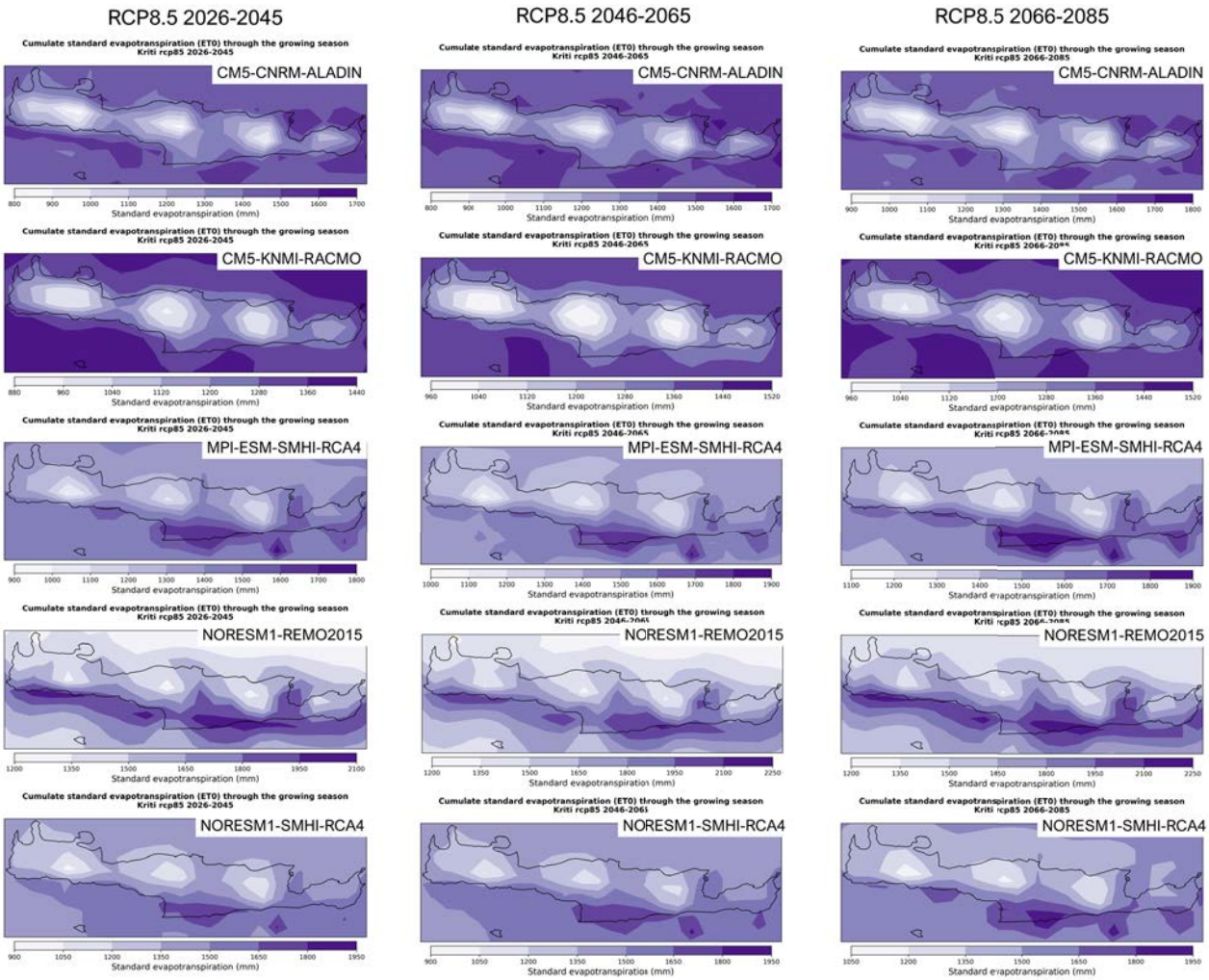

Figure 7-13: Cumulative standard evapotranspiration (ET_0) in Crete for RCP8.5, for three future periods (2026–2045, 2046–2065, 2066–2085) and five EURO-CORDEX RCMs.

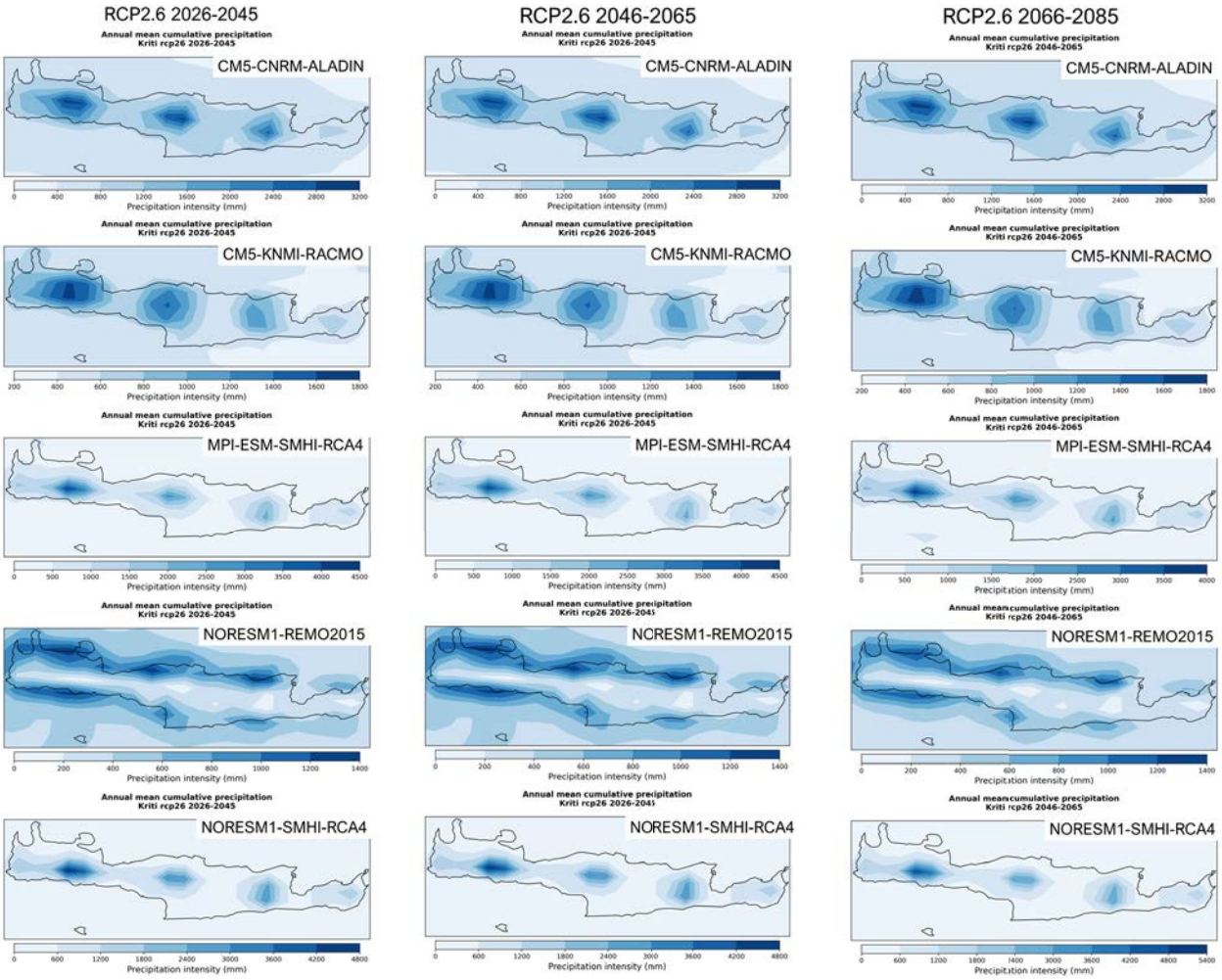

Figure 7-14: Annual mean cumulative precipitation in Crete for RCP2.6, for three future periods (2026–2045, 2046–2065, 2066–2085) and five EURO-CORDEX RCMs.

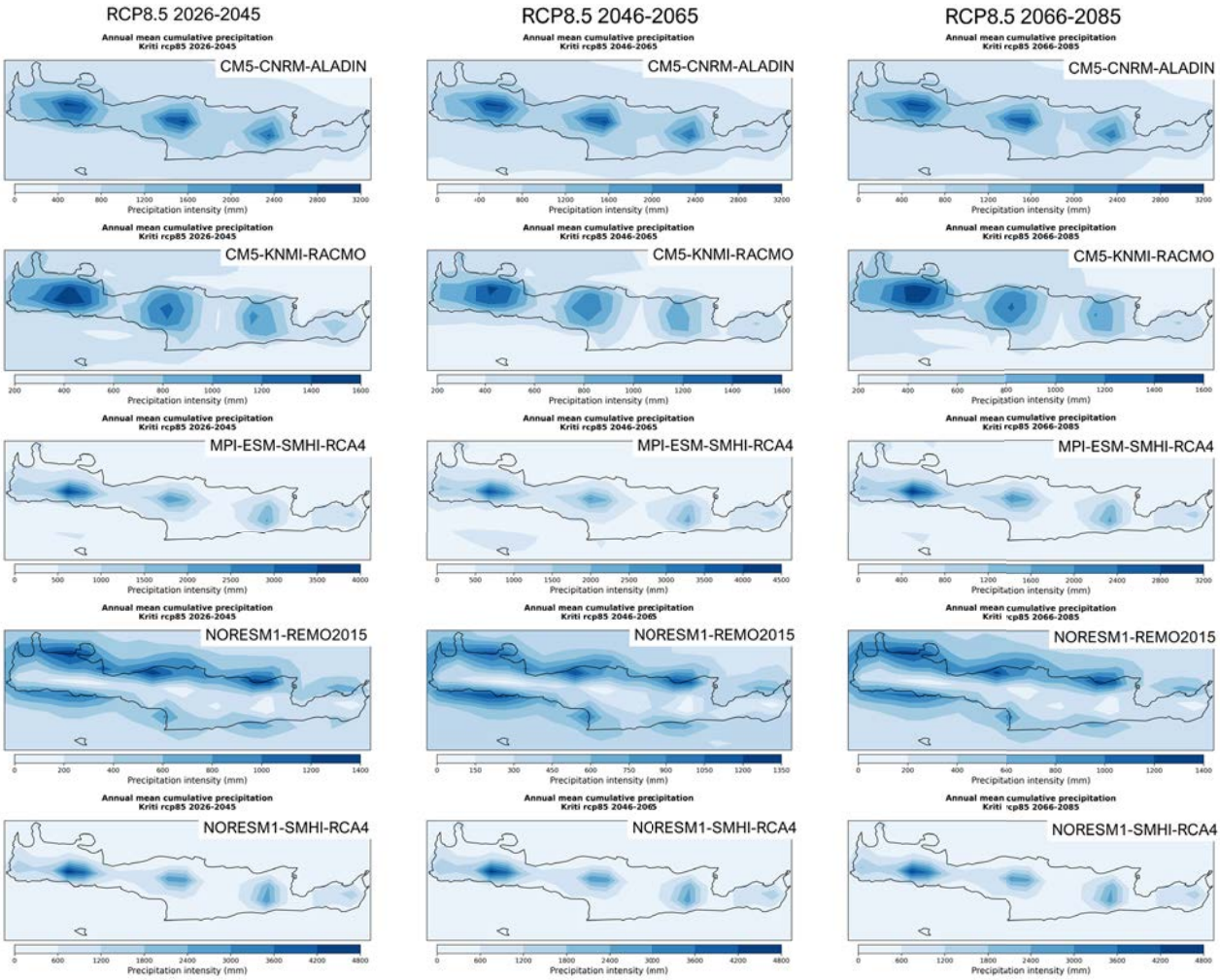

Figure 7-15: Annual mean cumulative precipitation in Crete for RCP8.5, for three future periods (2026–2045, 2046–2065, 2066–2085) and five EURO-CORDEX RCMs. Note that the colour ramps are of different scale among models.

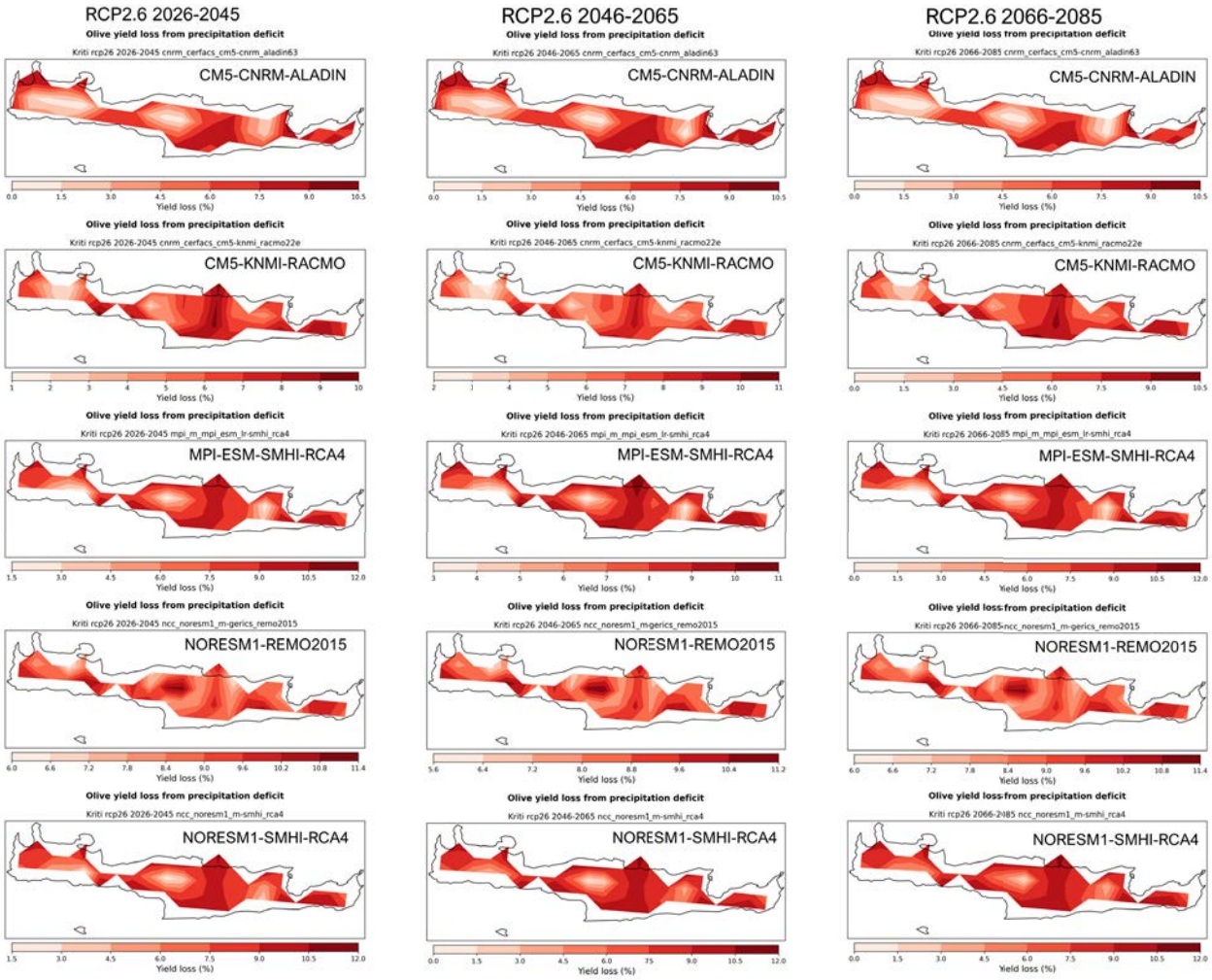

Figure 7-16: Olive yield loss (%) from precipitation deficit under rainfed conditions in Crete for RCP2.6, for three future periods (2026–2045, 2046–2065, 2066–2085) and five EURO-CORDEX RCMs, as computed by the CLIMAAX agricultural drought hazard workflow.

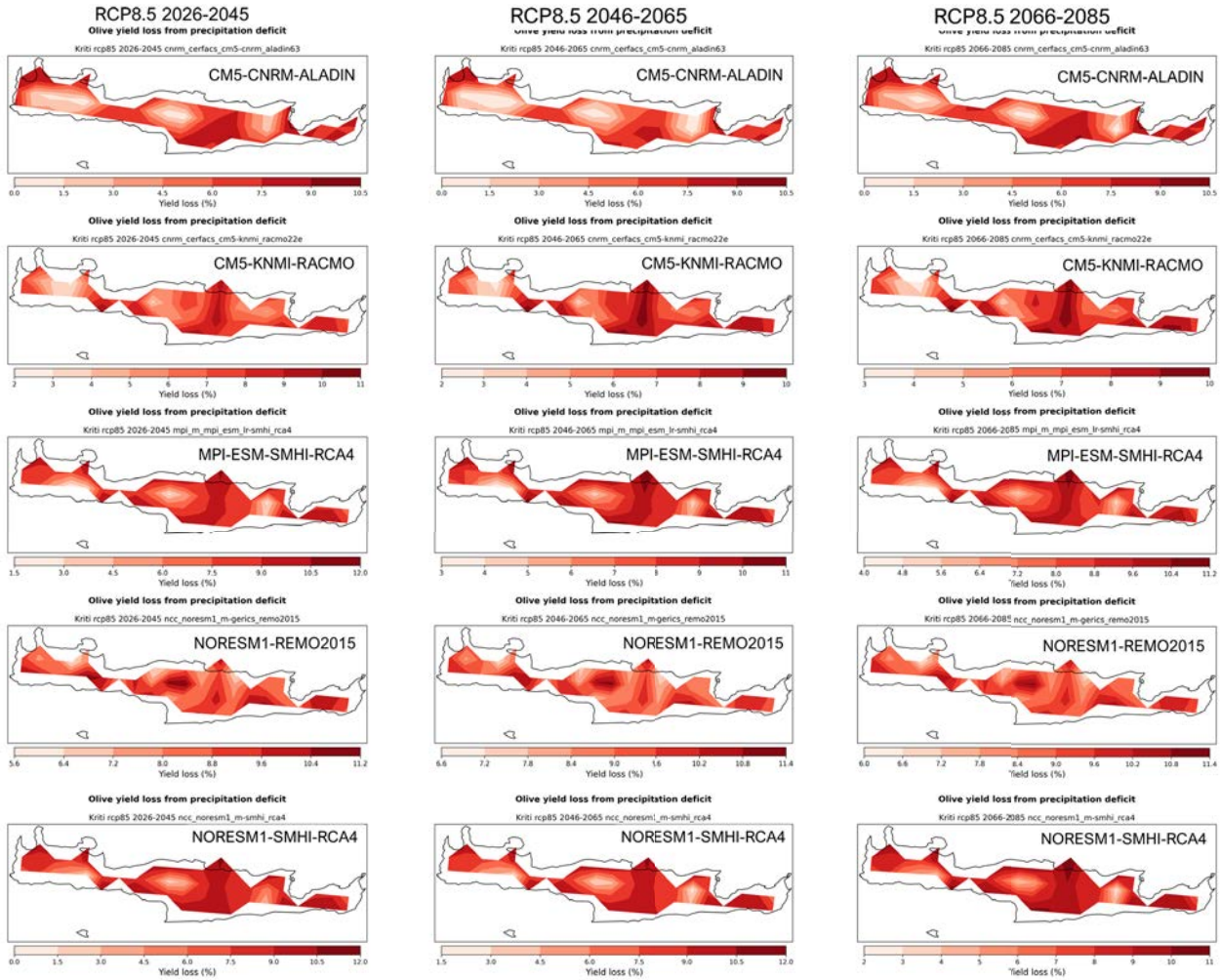

Figure 7-17: Olive yield loss (%) from precipitation deficit under rainfed conditions in Crete for RCP8.5, for three future periods (2026–2045, 2046–2065, 2066–2085) and five EURO-CORDEX RCMs, as computed by the CLIMAAX agricultural drought hazard workflow.

Funded by the European Union

CLIMAAX climate ready regions

Flood Hazard and Risk Assessment for Crete

2nd Phase

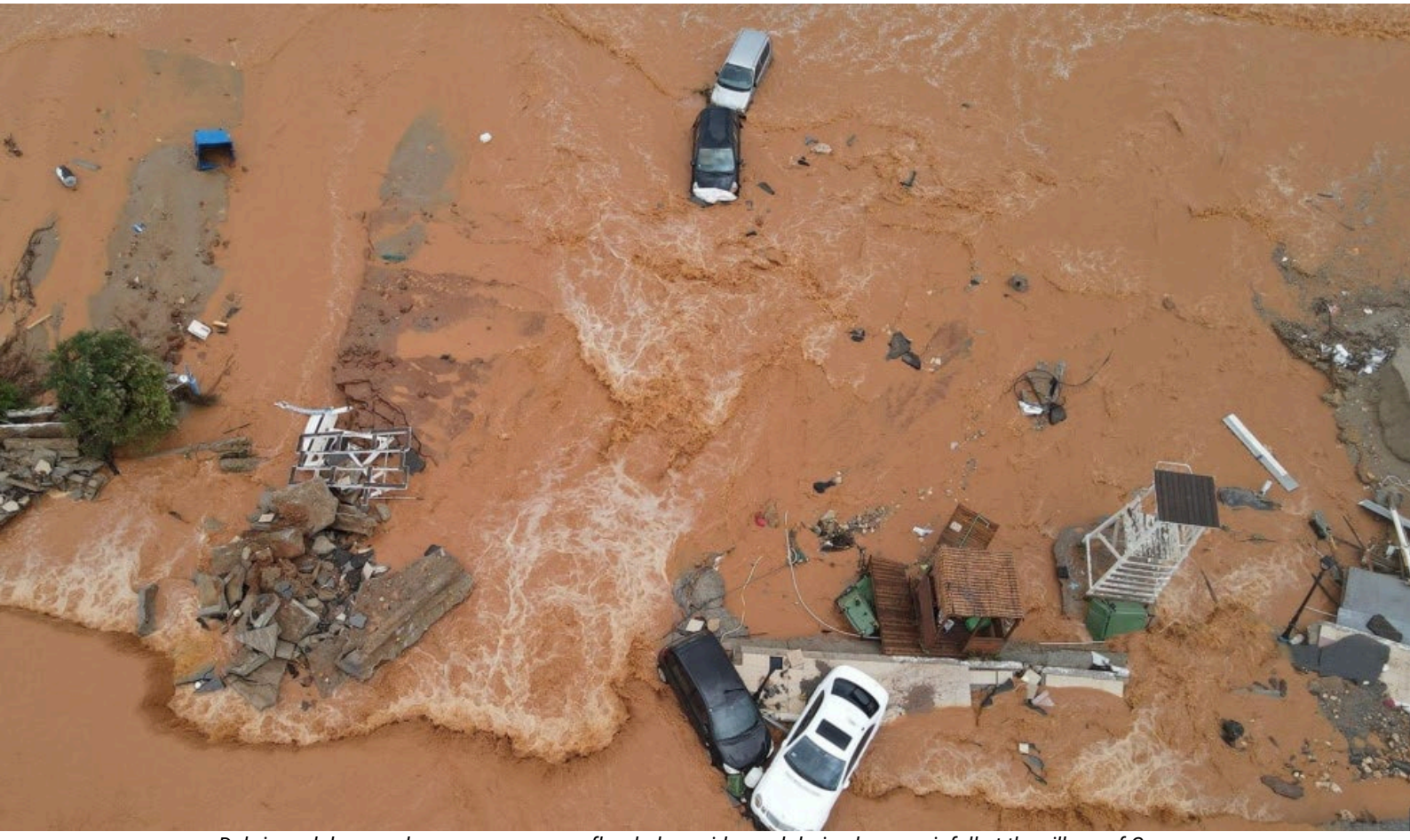

Debris and damaged cars are seen on a flooded seaside road during heavy rainfall at the village of Gournes on the island of Crete, Greece, Nov. 10, 2020. (photo: VOA News)

Authors: Aristeidis Koutroulis, Technical University of Crete
Mikaela Papa, Technical University of Crete

Prepared for: The Region of Crete
Project Title: Climate Resilient Crete (CRETE)
Cascade Funded by: The European Union's Horizon Europe Climate Programme
Grant Agreement No.: 101093864 – CLIMAAX

Contents

Contents 2
1 Executive Summary 4
2 Introduction 5
2.1 Background 5
2.2 Objectives of the second-phase assessment 5
2.3 Study area and hazard context 6
2.4 Structure of this report 7
3 Methodological Framework 7
3.1 Local 2m flood hazard maps (baseline period) 8
3.2 River Flood Exposure - Land-Use data 9
3.3 Vulnerability - damage curves for land use and linked economic damages 10
3.4 Building and Population Exposure data 11
3.5 Extreme Precipitation - Critical impact rainfall thresholds and local rainfall patterns 13
3.6 River Discharge workflow – Giofyros and Keritis basins 15
4 Results 16
4.1 River Flood 16
4.2 Hazard Assessment 16
4.3 River flood risk assessment based on land use type 17
4.4 Building Damage and Critical Infrastructure Exposure 19
4.5 Population Exposure and Displacement 24
4.6 Extreme Precipitation 27
4.6.1 Hazard Assessment 27

4.6.2 Risk Assessment 33
4.7 River Discharge 36
4.7.1 Hazard Assessment 36
5 Methodological limitations and uncertainties 42
6 Discussion and Conclusions 43
7 References 45
8 Appendix 47

Disclaimer: In the preparation of this work, generative Artificial Intelligence (ChatGPT) was used as an assisting tool in specific parts of the text, primarily to improve grammar, sentence structure, and overall clarity, and to help shorten certain sections.

1 Executive Summary

This Phase2 CLIMAAX assessment refines the understanding of flood risk in Crete by combining high-resolution national Flood Risk Management Plan (FRMP) flood maps (2m), Microsoft Global Building Footprints, a building-derived population layer, and CLIMAAX workflows for extreme precipitation and river discharge focusing on ten flood-prone areas are analysed in detail. Compared to the pan-European, coarser Phase1 assessment, this phase is better aligned with local topography, exposure and hazard patterns.

The updated river-flood hazard assessment confirms extensive floodplain inundation, especially in high depths in narrow urban torrents in Rethymno, Agios Nikolaos and Ierapetra Messara and the Lasithi Plateau, and. Combining FRMP depths with LUISA land use and CLIMAAX depth, damage curves yield large direct economic losses. In the RP1000 scenario, Messara reaches around €1.2 billion of damage and Heraklion roughly €0.6 billion, with several other basins in the €100–400 million range. Building-level calculations using ms-buildings and a universal damage function indicate an Expected Annual Damage (EAD) of about €7 million per year for Heraklion (with a plausible range of ~€4.5–9.3 million). Population exposure is estimated by assigning 4 residents per 100 m² of building footprint and intersecting with flood extents. In Heraklion, around 30,000 people are exposed in a 50-year event and more than 42,000 in a 1000-year event. Those in buildings with water depths above 1m (displaced population) increase from roughly 16,000 to more than 34,000. Aggregated across return periods, the Expected Annual Exposed Population (EAEP) is about 638 people and the Expected Annual Displaced Population (EADP) about 425 people per year. Other hotspots with substantial exposure include Ierapetra, Messara, Kladisos and Agios Nikolaos, where linear coastal development along torrents intersects with flood corridors.

Future hazard is explored through the Extreme Precipitation workflow, using bias-corrected EURO-CORDEX simulations and two impact-based 24-hour rainfall thresholds derived from recent damaging events (100 mm/day medium, 200 mm/day severe). Projections indicate more intense heavy rainfall and more frequent exceedances of these thresholds in central and eastern Crete, particularly under RCP8.5. River-discharge statistics for Giofyros and Keritis show corresponding increases in high flows, though with basin- and scenario-dependent strength and considerable model spread.

The Phase2 assessment provides a more realistic, spatially detailed picture of flood risk in Crete and clearly identifies Heraklion, Messara, Lasithi Plateau and several coastal basins as priority areas for adaptation. Key implications include the need for stricter land-use control in floodplains, targeted upgrades of flood and drainage infrastructure, and strengthened emergency planning under both current and future climate conditions.

2 Introduction

2.1 Background

The island of Crete is highly exposed to hydrometeorological extremes due to its complex topography, steep catchments, dense coastal settlements and rapidly growing urban areas (Diakakis et al., 2012; Flocas et al., 2017; Koutroulis et al., 2010). Floods in particular, ranging from mainly flash floods in small torrential streams to riverine flooding in larger basins, pose a recurring threat to people, critical infrastructure and economic activities (Sarchani and Tsanis, 2019). Recent flood events (Lagouvardos et al., 2020) have highlighted both the intensity of local phenomena and the need for robust, spatially explicit risk information to support planning, civil protection and climate adaptation decisions at regional and municipal level.

Within this context, the Region of Crete participates in the CLIMAAX project as a pilot case, using the CLIMAAX Risk and Resilience (CRR) framework and associated workflows to develop evidence-based climate risk assessments. During the first phase of the project, a preliminary flood risk assessment was carried out using pan-European datasets (e.g. JRC river flood hazard maps, GHS-POP, OSM buildings) and standard CLIMAAX workflows. This allowed the region to obtain an initial, harmonised picture of flood hazard, exposure and risk, and to test the CRR framework in practice.

However, the Phase1 assessment also revealed several important limitations for local decision-making in Crete, e.g. the coarse resolution of the hazard datasets, the incomplete representation of small and flash-flood prone catchments, and the limited reliability of exposure and population estimates based on global products (Schiavina et al., 2023). In addition, the available pan-European hazard datasets (Baugh et al., 2024) did not allow for a robust assessment of future flood risk under climate change (Ward et al., 2020) at the spatial scale relevant for regional planning.

2.2 Objectives of the second-phase assessment

The second phase of the CLIMAAX flood assessment for Crete has been designed to address some of these limitations by integrating higher-resolution, locally relevant datasets and additional CLIMAAX workflows. The overall objective is to produce a more realistic and operationally useful characterisation of current and future flood risk, aligned with the official Greek implementation of the EU Floods Directive (2007/60/EC) and the needs of regional and local stakeholders.

More specifically, this second-phase assessment aims to:

– Refine flood hazard characterisation by replacing coarse pan-European hazard maps with detailed 2 m flood hazard maps from the Flood Risk Management Plan (*EL13 Flood Risk Management Plan for Crete*, 2024) of the Region of Crete for the baseline period.

– Improve exposure and population estimates by using the Microsoft Global Building Footprints [1] dataset to represent the building stock and to derive population distributions, overcoming the spatial gaps of OpenStreetMap (OSM) and artefacts in global population grids.
– In the absence of high resolution flood hazard maps for future scenarios, to enhance the understanding of climate-related changes in flood-generating rainfall by applying the CLIMAAX extreme precipitation workflow, in combination with the national updated intensity-duration-frequency (IDF) curves [2] and to assess shifts in heavy precipitation statistics under future climate scenarios, as a proxy of exposure to future flood risk.
– Provide a hydrological perspective on flood hazard through the CLIMAAX river discharge statistics workflow, applied to a representative flood-prone basin in Crete (Giofiros).
– Update and refine flood risk metrics (e.g. exposed buildings, exposed and displaced population, expected annual damage) for selected high-risk areas, using consistent vulnerability and depth-damage functions together with the improved hazard and exposure datasets.

2.3 Study area and hazard context

The assessment gives particular attention to areas already identified as having significant flood risk in the national Flood Risk Management Plans, as well as urban and peri-urban zones where exposure is concentrated (Figure 2-1). Small, steep catchments with rapid hydrological response and limited storage dominate much of the island, so flash floods and urban floods are a central concern alongside more classical riverine flooding. Coastal and alluvial plains, such as those around Heraklion, Messara and parts of Chania, combine high exposure with complex hydraulic behaviour influenced by both river flows and local drainage conditions.

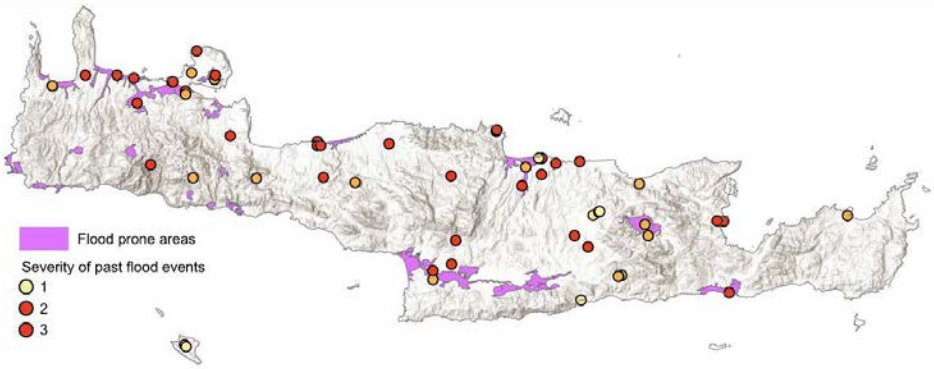

Figure 2-1: Flood-prone areas and past flood events in Crete.

[1] microsoft/GlobalMLBuildingFootprints. (2023, September 26). GitHub; Microsoft. https://github.com/microsoft/GlobalMLBuildingFootprints

[2] https://floods.ypeka.gr/sdkp-lap/omvries-2round/

2.4 Structure of this report

The remainder of this sub-deliverable is structured as follows:

- Section 3 presents the methodological framework of the second-phase assessment. It describes the 2 m FRMP flood hazard maps, LUISA land-use data, Microsoft Global Building Footprints and the derived population layer, as well as the CLIMAAX workflows used for land-use based risk, building and population exposure, extreme precipitation and river discharge. The section concludes with a short discussion of methodological limitations.
- Section 4 presents the results of the second-phase analysis for the ten areas of interest. It includes (i) river flood hazard and land-use based risk, (ii) building damage and critical infrastructure exposure, (iii) population exposure and displacement, (iv) extreme precipitation hazard and risk based on impact thresholds, and (v) river-discharge indicators for the Giofyros and Keritis basins.
- Section 5 provides a discussion of the main findings, comparing them with the Phase-1 assessment, interpreting the combined evidence from flood, exposure and climate projections, and highlighting implications for flood risk management and climate adaptation in Crete.
- Section 6 offers the conclusions and recommendations, summarising key messages for policymakers, practitioners and stakeholders in the Region of Crete and outlining priorities for further refinement of data, methods and adaptation planning.

3 Methodological Framework

This second-phase flood risk assessment builds on the Phase1 CLIMAAX analysis but integrates higher-resolution local datasets and additional CLIMAAX workflows. The study follows the standardized CLIMAAX workflows for river flooding, flood damage and population exposure, and complements them with (i) 2m flood hazard maps from the (Flood Risk Management Plan of the Region of Crete (*EL13 Flood Risk Management Plan for Crete*, 2024) for the baseline period, (ii) the Microsoft Global Building Footprints ("microsoft/GlobalMLBuildingFootprints," 2025) dataset for the representation of buildings and derivation of population, (iii) the Extreme Precipitation workflow based on EURO-CORDEX climate simulations and the updated national IDF curves, and (iv) the River Discharge Statistics workflow applied to the flood-prone Giofiros basin. The methodology is organised into three main components:

– Flood hazard assessment, using 2 m FRMP flood hazard maps for RP50, RP100 and RP1000 and complementing them with CLIMAAX extreme-precipitation and river-discharge indicators to characterise current and future flood-generating conditions.
– Exposure and vulnerability analysis, combining LUISA land-use data and ms-buildings to quantify exposed land-use classes, buildings and population (assuming 4 persons per 100 m² of footprint) and applying CLIMAAX/ Huizinga depth–damage functions (Universal class) to represent vulnerability.

– Flood risk assessment, estimating direct economic damages, Expected Annual Damage (EAD), and exposed and displaced population (EAEP, EADP) for selected return periods in ten areas of interest across Crete (Skoutelonas, Gerani, Kladisos, Koiliaris, Rethymno, Heraklio, Lasithi Plateau, Agios Nikolaos, Ierapetra and Messara; see Figure 3-1).

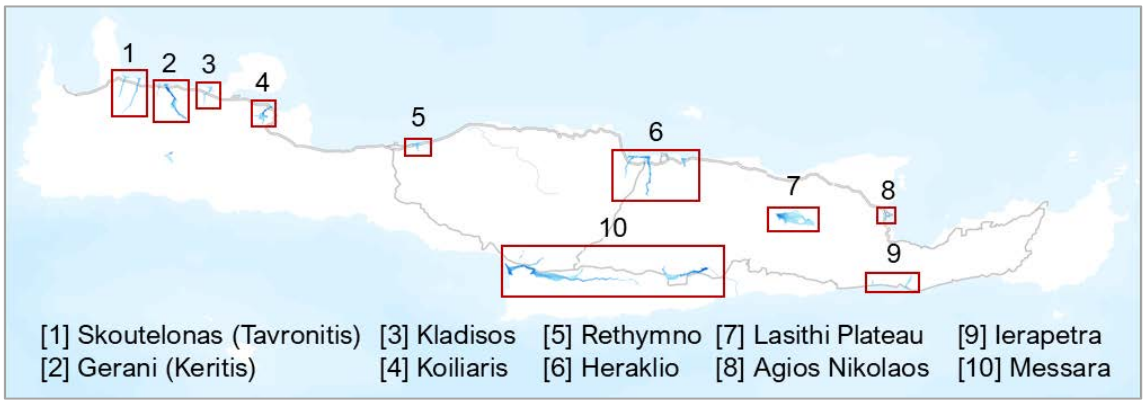

Figure 3-1: Location of the ten focus areas (1–10) used in the second-phase flood risk assessment in Crete.

3.1 Local 2m flood hazard maps (baseline period)

For the second-phase assessment, flood hazard for the baseline (present-day) climate is represented using 2 m resolution flood hazard maps produced in the framework of the 1st Revision of the Flood Risk Management Plan (*EL13 Flood Risk Management Plan for Crete*, 2024) for the Water District of Crete (EL13), in accordance with the EU Floods Directive 2007/60/EC.

These maps provide maximum inundation depth and flow velocity for design flood events with return periods of 50, 100 and 1000 years (RP50, RP100, RP1000) for riverine flooding and flooding in closed depressions. They were developed by the national contractors for the FRMP using a consistent hydrological-hydraulic modelling chain at the scale of the Zones of Potential Significant Flood Risk in Crete.

The main steps for the generation of the high resolution flood hazard maps can be summarised as follows:

Topographic basis and computational grid:

– The geometry of the terrain is derived from the Digital Elevation Model (DEM) of Ktimatologio A.E., with cell sizes of 2m (and locally 1m), which was used to construct the 2D hydraulic mesh.
– River channels and embankments were digitised explicitly, and the 2D mesh was defined to cover the low-lying floodplain and adjacent areas where overbank flow can occur.

Design rainfall and hydrological modelling

- Design storms for RP50, RP100 and RP1000 were derived from the updated national IDF curves, based on long series from 82 raingauges and 17 pluviographs across EL13 (Crete water district) and processed within the national SWICCA/C3S framework.
- Losses and runoff generation were estimated with the SCS-CN (Curve Number) method, using combined layers of CORINE 2018 land cover and soil type to assign Curve Numbers under average antecedent moisture conditions.
- Design hydrographs and peak discharges for each sub-basin were simulated with HEC-HMS, for the selected storm duration and return period, and summarised in terms of peak flow and effective rainfall for all basins in EL13.

Hydraulic routing and floodplain mapping

- Flood routing was carried out predominantly with the 2D unsteady flow module of HEC-RAS, which is recommended for extensive floodplains and complex flow patterns. 1D models were used only where appropriate for small, confined channels.
- Manning's roughness coefficients were spatially distributed according to CORINE land cover classes (urban, agricultural, natural areas, etc.).
- Model outputs (maximum water surface elevation, water depth and flow velocity) for RP50, RP100 and RP1000 were exported to GIS (ArcGIS) and converted into raster hazard layers at 2 m resolution for each examined region.

In this CLIMAAX 2nd phase study, these flood hazard rasters of the ten focus areas (Figure 3-1) were Used as the primary hazard input to the flood damage and exposure workflows, so that all risk metrics (exposed buildings, exposed and displaced population, expected damages) are directly linked to officially adopted, high-resolution hazard maps.

The resulting river flood potential for RP50, RP100 and RP1000 in each area of interest is illustrated in detail in the Appendix maps (Figures), which show the spatial pattern and depth of inundation at 2m resolution for the present-day climate.

3.2 River Flood Exposure - Land-Use data

River flood exposure is assessed with the CLIMAAX Risk Assessment for River Flooding workflow by overlaying the 2 m FRMP flood depth maps with the LUISA Land Cover dataset. LUISA (Figure 3-2) provides a harmonised classification of urban, agricultural, transport and natural areas for Crete. Each LUISA class is linked to a CLIMAAX damage category (e.g. residential, industrial, agricultural), allowing us to identify which assets are inundated and to assign a flood depth to each exposed land-use type for RP50, RP100 and RP1000 in the ten areas of interest.

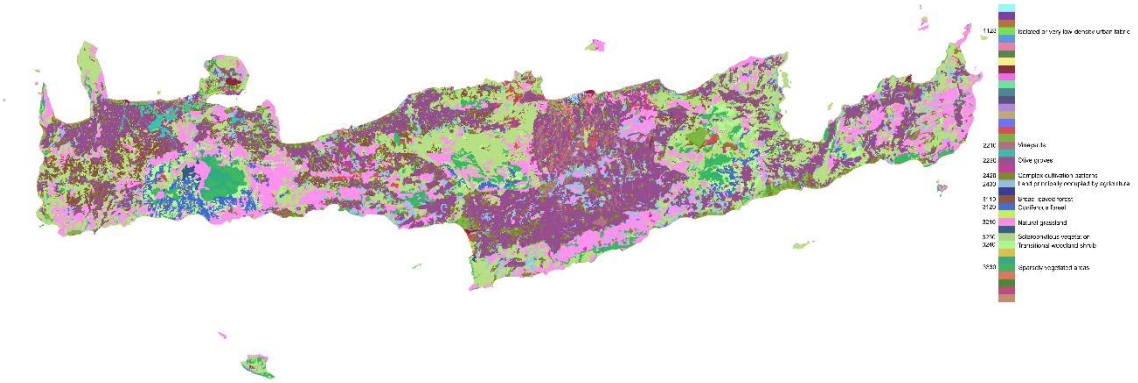

Figure 3-2: LUISA Land Cover Map of Crete, a high-resolution classification of land use types, essential for flood risk assessment. The dataset is available from the Copernicus Land Monitoring Service.

3.3 Vulnerability - damage curves for land use and linked economic damages

Vulnerability is represented through depth-damage curves embedded in the CLIMAAX workflow. For each damage category (residential, commercial, industrial, agricultural, transport, roads) the JRC/CLIMAAX curves (Figure 3-3) provide a damage ratio (%) as a function of flood depth. Additional curves are defined per LUISA land-cover class (Figure 3-4) including non-damageable categories where damage is zero.

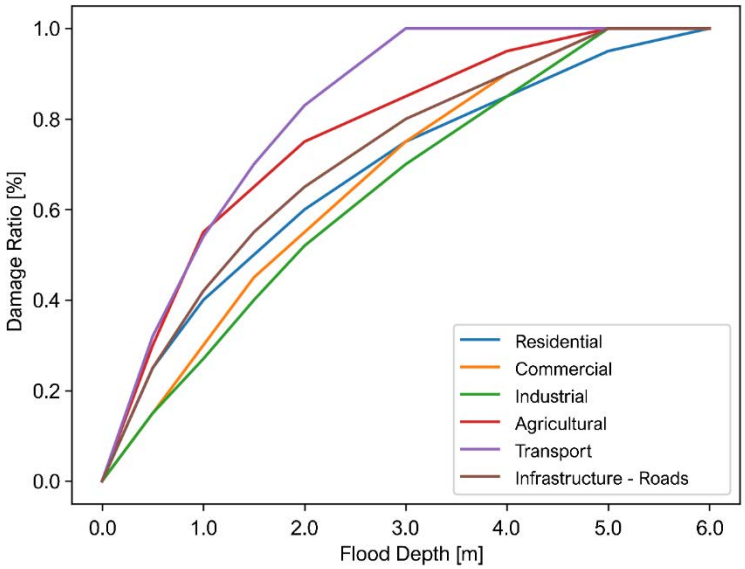

Figure 3-3: JRC Depth-Damage Curves for different damage classes indicating the relationship between flood depth (m) and damage ratio (%) for residential, commercial, industrial, agricultural, and infrastructure categories.

For every inundated cell, the workflow combines (i) flood depth from the 2m flood hazard maps, (ii) land use from LUISA, (iii) the relevant depth-damage curve, and (iv) country-

specific asset values from an external table to compute direct economic losses, which are then aggregated to derive damage and risk indicators.

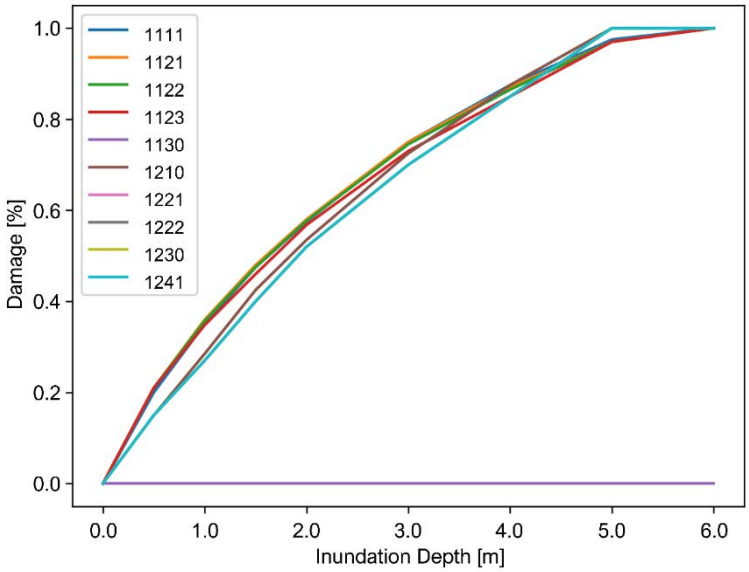

Figure 3-4: Vulnerability functions for selected LUISA land-cover classes, showing the damage ratio as a function of inundation depth.

3.4 Building and Population Exposure data

Building and population exposure are quantified with the CLIMAAX Risk Assessment for Buildings and Population Exposure workflow, using the Microsoft Global Building Footprints (ms-buildings) as the core exposure layer. The ms-buildings polygons (Figure 3-5) are intersected with the 2m flood depth maps to identify inundated structures for each return period and area of interest. The added value of the ms-buildings dataset over OpenStreetMap is illustrated in Figure 3-6.

Population is derived directly from building area, assuming a uniform residential density of 4 people per 100 m² of building footprint. For each building, the number of residents is obtained by multiplying its footprint area by this density. People living in buildings where flood depth exceeds the selected thresholds are counted as exposed and, for higher depths, as displaced. Aggregation across all buildings yields exposed and displaced population per return period and the related expected-annual indicators.

For damage calculations, all buildings are treated with the Universal damage class provided in the CLIMAAX code. Maximum damage values per square metre (reconstruction + contents) are derived from the global depth–damage database of Huizinga et al., (2017), adjusted from 2010 to 2022 using the national Consumer Price Index.

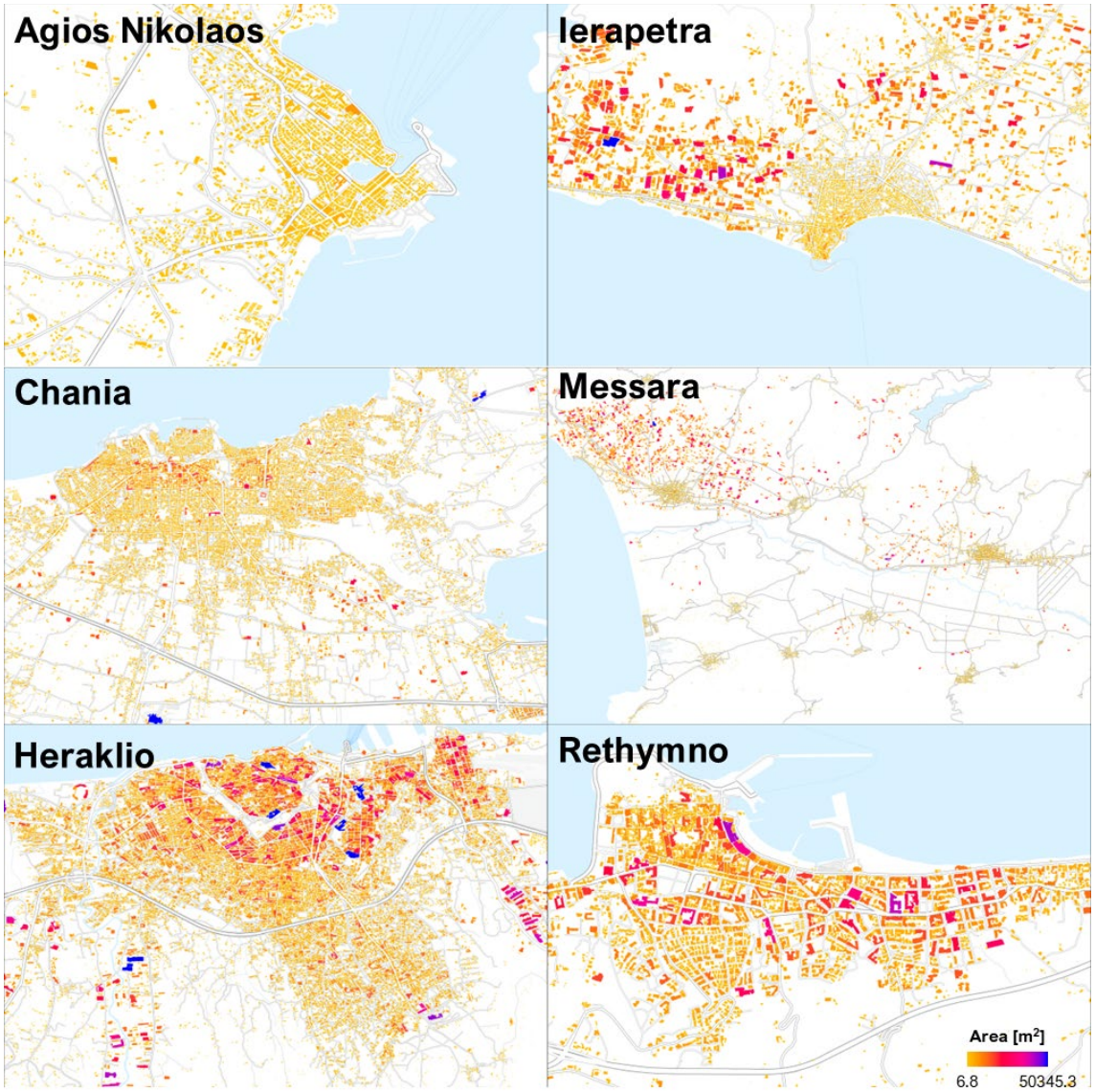

Figure 3-5: Microsoft Global Building Footprints (ms-buildings) in selected urban and peri-urban areas (Agios Nikolaos, Ierapetra, Chania, Messara, Heraklio, Rethymno), coloured by footprint area, used as the primary input for building and population exposure.

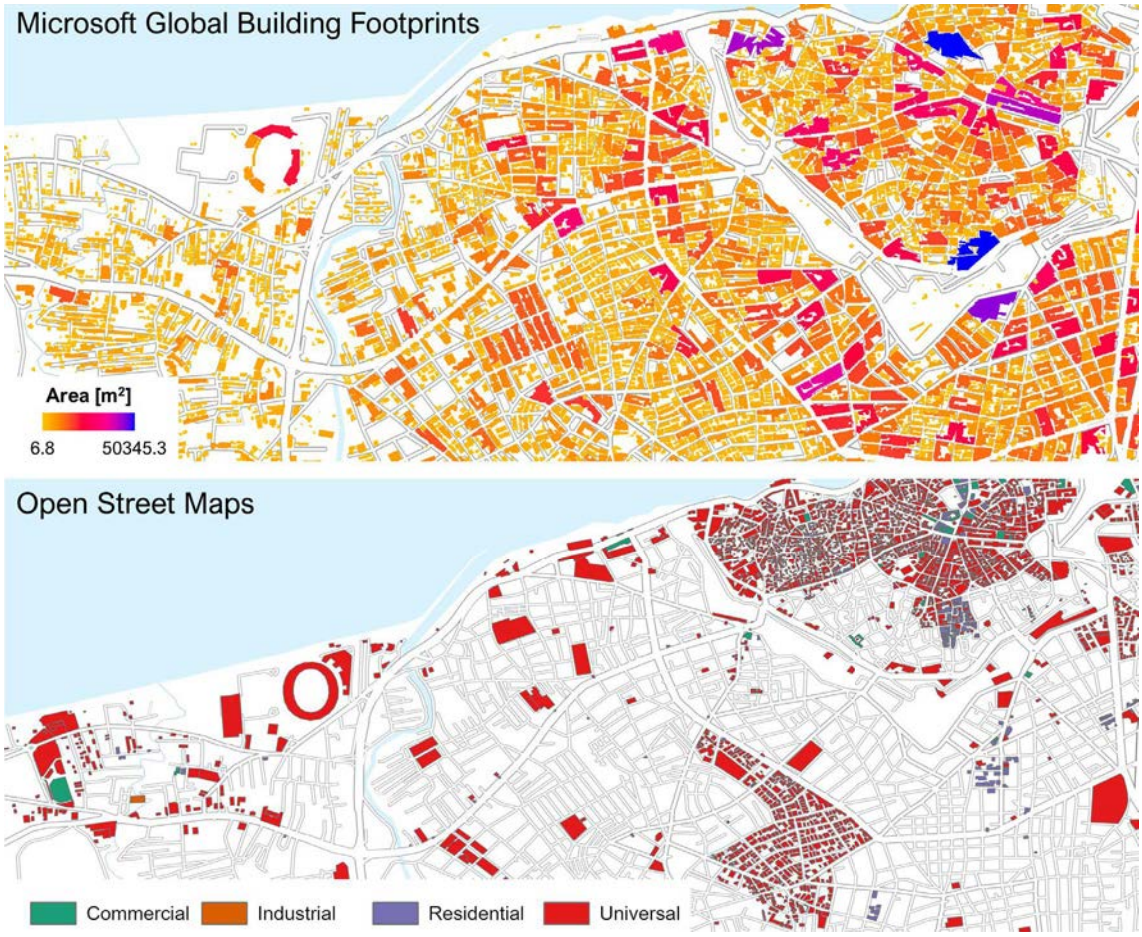

Figure 3-6: Comparison of exposure datasets for Heraklio. Top: Microsoft Global Building Footprints coloured by footprint area, showing almost complete coverage of the building stock. Bottom: OpenStreetMap building layer with damage classes (commercial, industrial, residential, universal), illustrating substantial gaps and inconsistent coverage relative to the ms-buildings dataset. Apparent geometric misalignments are due to the use of different map projection systems in the two maps.

3.5 Extreme Precipitation - Critical impact rainfall thresholds and local rainfall patterns

In the absence of reliable flood hazard maps for future climate scenarios, we complemented the river flood based risk assessment by applying the CLIMAAX Extreme Precipitation workflow. This workflow uses bias-corrected EURO-CORDEX simulations and extreme-value analysis to derive return levels of daily and sub-daily rainfall for the baseline and future periods.

To link modelled rainfall extremes with actual flood impacts in Crete, we compiled a flash-flood event database with date (Appendix Table 8-1 and Table 8-2), location, qualitative impact description and a three-class impact severity scale. Event locations

were compared with mapped flood-prone areas (Figure 3-7) and, where available, point gauge measurements were used to estimate 24-hour rainfall totals.

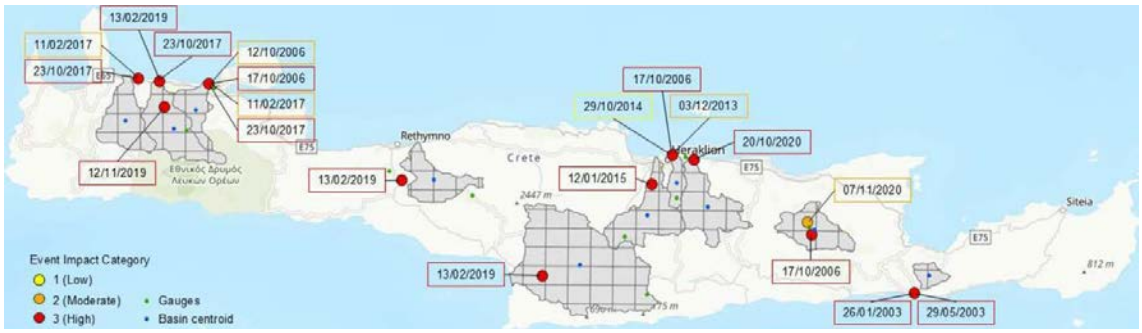

Figure 3-7 Major recent flood events in Crete, with dates and affected basins, used to define local impact rainfall thresholds and to select basins for detailed analysis.

Based on these observed events and impacts we defined two critical impact thresholds for Crete:

- 100 mm/day as medium-impact rainfall
- 200 mm/day as severe / high-impact rainfall

Using the official national IDF curves[3] we then derived basin-averaged IDF curve. IDF parameters were aggregated over each basin, and design depths and return periods were calculated for the 24-hour duration and the specific rainfall thresholds. These observationally based IDFs are used as a benchmark to compare with the EURO-CORDEX-based extreme precipitation statistics for the baseline period and to interpret projected changes in heavy rainfall under future scenarios. Figure 3-8 illustrates the spatial overlap between the EURO-CORDEX grid points used in the CLIMAAX datasets and the centres of the national IDF grid cells over Crete.

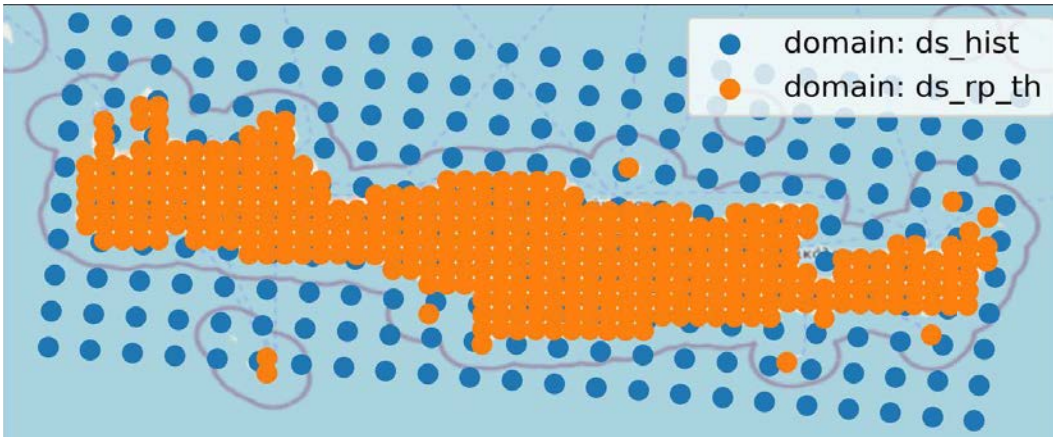

Figure 3-8 Spatial overlap of the EURO-CORDEX grid (blue points, ds_hist domain) with the centroids of the national IDF grid cells used to derive basin-averaged IDF parameters (orange points, ds_rp_th domain) over Crete.

[3] https://floods.ypeka.gr/sdkp-lap/omvries-2round/

3.6 River Discharge workflow – Giofyros and Keritis basins

To complement the map-based hazard assessment, we applied the CLIMAAX hazard assessment for river flooding using river discharge statistics workflow to two of the most flood-prone basins in Crete with high observed impacts: Giofyros (Heraklio) and Keritis (Gerani/Chania). The workflow uses the Hydrological Climate Impact Indicators (HCII) dataset produced by SMHI and distributed via the Copernicus Climate Data Store, which provides catchment-scale river discharge simulations from the E-HYPEcatch hydrological model forced by EURO-CORDEX climate projections at ~0.11° resolution.

For each of the two basins we:

- selected the corresponding E-HYPE catchment unit from the CLIMAAX mirror of the HCII dataset (Figure 3-10)
- extracted historical daily discharges to characterise variability and derive flow-duration curves
- analysed monthly mean discharges to describe the seasonal cycle
- obtained HCII indicators of extreme river discharges and their relative changes for multiple return periods (2, 5, 10, 50 years) and time slices (early-, mid-, end-century) under different RCP scenarios.

The discharge statistics were used to explore how climate change may alter high-flow regimes in Giofyros and Keritis, and to provide a hydrological context for the flood hazard information derived from the flood hazard maps and the extreme-precipitation workflow.

Figure 3-9: Location of the Giofyros (top) and Keritis (bottom) basins in Crete and the corresponding E-HYPEcatch units (shaded) used in the CLIMAAX river discharge workflow.

4 Results

4.1 River Flood

4.2 Hazard Assessment

Flood hazard in the second phase is described by the 2 m resolution flood hazard maps produced in the framework of the 1st Revision of the Flood Risk Management Plan (*EL13 Flood Risk Management Plan for Crete*, 2024) for the Water District of Crete, for return periods of 50, 100 and 1,000 years (RP50, RP100, RP1000). Table 4-1summarises, for each of the ten study areas, the inundated area by flood-depth class (0–1 m, 1–2 m, 2–3 m, 3–4 m, 4–5 m and >5 m). The total inundated area across all areas of interest increases from about 70 km² for RP50 to 72 km² for RP100 and 91 km² for RP1000, i.e. roughly a 30 % increase between RP50 and RP1000.

Table 4-1: Flood extent (km²) in each study area for different flood-depth classes (0–1 m, 1–2 m, 2–3 m, 3–4 m, 4–5 m and >5 m) and return periods (RP50, RP100, RP1000). The bottom row ("SUM") gives the total inundated area over all ten areas of interest.

		Flood depth (m)						
		0-1	**1-2**	**2-3**	**3-4**	**4-5**	**>5**	**SUM**
50yrRP	Agios Nikolaos	0.25	0.27	0.12	0.03	0.02	0.01	0.70
	Heraklion (Town)	2.60	3.06	1.71	0.56	0.23	0.12	8.28
	Ierapetra	1.51	0.35	0.09	0.01	0.00	0.00	1.95
	Keritis	1.54	1.39	1.34	0.49	0.23	0.23	5.22
	Kladisos	0.73	0.28	0.16	0.06	0.01	0.00	1.25
	Koiliaris	1.71	0.94	0.43	0.17	0.08	0.03	3.37
	Lasithi Plateau	12.97	2.89	0.69	0.21	0.07	0.03	16.86
	Messara	10.95	8.78	4.53	2.14	0.73	0.34	27.47
	Rethymno	0.94	0.48	0.11	0.03	0.02	0.02	1.61
	Tavronitis	2.16	0.94	0.24	0.17	0.11	0.05	3.68
	SUM	35.36	19.38	9.41	3.87	1.50	0.85	70.37
		0-1	**1-2**	**2-3**	**3-4**	**4-5**	**>5**	**SUM**
100yrRP	Agios Nikolaos	0.24	0.24	0.16	0.04	0.02	0.01	0.72
	Heraklion (Town)	2.18	3.00	2.11	0.86	0.32	0.19	8.66
	Ierapetra	1.57	0.41	0.10	0.01	0.00	0.00	2.10
	Keritis	1.94	1.60	1.52	0.70	0.29	0.31	6.35
	Kladisos	0.74	0.33	0.18	0.10	0.02	0.01	1.37
	Koiliaris	1.57	1.04	0.55	0.24	0.11	0.07	3.58
	Lasithi Plateau	12.83	2.77	0.88	0.26	0.09	0.04	16.86
	Messara	10.25	9.29	4.99	2.68	0.94	0.57	28.73
	Rethymno	0.95	0.60	0.19	0.04	0.02	0.03	1.83
	Tavronitis	1.97	1.34	0.35	0.18	0.15	0.09	4.08
	SUM	34.24	20.63	11.05	5.11	1.95	1.31	74.29
		0-1	**1-2**	**2-3**	**3-4**	**4-5**	**>5**	**SUM**
1000yrRP	Agios Nikolaos	0.20	0.19	0.20	0.20	0.09	0.05	0.93
	Heraklion (Town)	1.66	2.21	2.75	2.14	1.24	0.81	10.80
	Ierapetra	1.55	0.74	0.27	0.07	0.01	0.00	2.64
	Keritis	1.46	1.63	1.35	1.26	0.87	0.98	7.55

Kladisos	0.54	0.63	0.28	0.19	0.12	0.04	1.81
Koiliaris	1.04	1.21	0.78	0.54	0.33	0.35	4.25
Lasithi Plateau	10.10	4.72	1.71	1.30	0.46	0.20	18.51
Messara	8.22	10.35	8.01	4.47	3.29	2.83	37.17
Rethymno	0.62	0.74	0.59	0.32	0.06	0.05	2.39
Tavronitis	1.15	1.82	1.01	0.37	0.24	0.27	4.86
SUM	26.54	24.23	16.95	10.86	6.72	5.60	90.90

The largest inundated extents are found in the Messara plain and the Lasithi Plateau, each with roughly 16–25 km² of flooded area depending on the return period, mostly with depths below 3 m. In contrast, smaller basins such as Keritis, Kladisos, Koiliaris, Tavronitis and the urban torrents of Heraklio, Rethymno, Ierapetra and Agios Nikolaos have more limited floodplain area but show locally high depths, especially under RP1000.

The detailed maps in Appendix Figure 8-9 to Figure 8-18 illustrate these patterns. For each area, the RP50 and RP1000 depth maps and their difference highlight (i) the extension of inundation along river valleys and coastal plains, and (ii) the strong deepening of flows in confined channels and urban sections during very rare events. Overall, the FRMP outputs provide spatially coherent and physically plausible flood depth fields at 2m resolution, which form the basis for the subsequent risk analyses.

4.3 River flood risk assessment based on land use type

Flood risk by land use was quantified by overlaying the 2m flood-depth maps with the LUISA land-cover dataset and applying the depth–damage curves described in Section 3.3. For each inundated grid cell and return period (RP50, RP100, RP1000), land-use specific damage ratios were combined with maximum asset values to obtain direct economic losses, which were then aggregated per area of interest.

Figure 4-1 maps the spatial pattern of land-use based damage for RP100. High and very-high damage cells cluster in:

– coastal and river-mouth urban areas (Heraklion, Rethymno, Agios Nikolaos, Ierapetra), and
– intensively cultivated parts of Messara, the Lasithi Plateau and lower Keritis/Koiliaris.

Corresponding RP50 and RP100 maps illustrating the progression of damage severity with return period are provided in the Appendix (Figure 8-19 and Figure 8-20).

Table 4-2summarises the total direct damage per event for each of the ten areas. Across all areas combined, damages increase from about €1.95 billion for RP50 to €3.21 billion for RP1000 (2022 price level). The largest contributions come from Messara, Heraklion and the Lasithi Plateau, reflecting the combination of extensive floodplains with high concentrations of agricultural and urban assets. Messara alone accounts for roughly 34 % of total RP1000 damage, followed by Heraklion (~19 %) and Lasithi (~11 %).

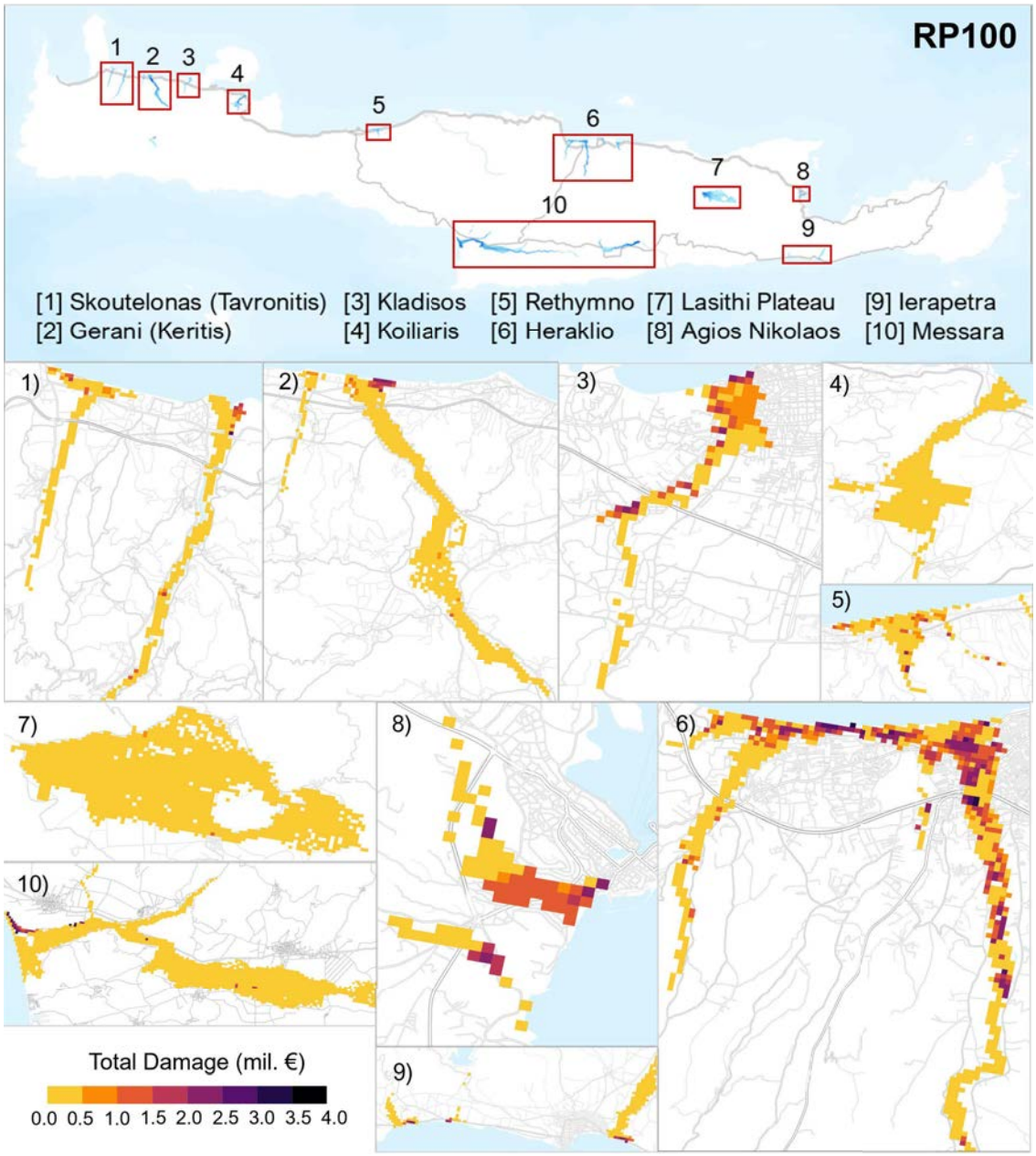

Figure 4-1 Spatial distribution of land-use based flood damage for RP100 in the ten areas of interest.

Most areas show a strong increase in losses with return period (roughly a factor of 1.7–2.5 between RP50 and RP1000), especially Rethymno, Kladisos, Keritis and Agios Nikolaos, where deeper flooding affects dense urban fabric. In Heraklion, damages rise only modestly between RP50 and RP1000, suggesting that highly exposed urban zones are already largely impacted for RP50–100.

Table 4-2. Total direct flood damage per return period (RP50, RP100, RP1000) in each of the ten study areas, expressed in million euro [10^6 €] at 2022 price level, based on LUISA land use and CLIMAAX depth–damage functions.

	Total damage [10^6€]		
Region	**RP50**	**RP100**	**RP1000**
[1] Skoutelonas Tavronitis	83.0	106.8	168.2
[2] Keritis Maleme	142.9	200.9	295.7
[3] Kladisos	63.8	79.1	142.2
[4] Koiliaris	67.2	78.7	118.9
[5] Rethymno	58.9	75.0	149.1
[6] Heraklion	523.5	615.1	615.1
[7] Lasithi Plateau	243.5	247.3	365.2
[8] Agios Nikolaos	50.3	55.3	92.6
[9] Ierapetra	48.2	53.6	81.0
[10] Messara	667.1	743.7	1178.1

4.4 Building Damage and Critical Infrastructure Exposure

Building-level damage was assessed by intersecting the flood-depth maps with the Microsoft Global Building Footprints and applying the Universal depth–damage function (Section 3.4). For each building and return period (RP50, RP100, RP1000), flood depth was converted to a damage ratio and multiplied by the maximum reconstruction-plus-content value; results were summarized as mean and maximum damage per area of interest (Table 4-3).

Table 4-3: Total mean and maximum damage to buildings per region, of a 50, 100, and 1000 return period flood event, based on current climatic conditions.

	Total maximum damage [10^6€]					
	RP50		**RP100**		**RP1000**	
Region	***Mean***	***Max***	***Mean***	***Max***	***Mean***	***Max***
Tavronitis Skoutelonas	22.8	19.0	31.2	23.0	85.3	35.6
Keritis Maleme	16.0	22.6	26.8	37.2	48.6	60.8
Kladisos	30.9	46.6	44.0	63.0	99.3	124.2
Koiliaris	7.6	9.8	9.7	12.4	19.3	23.2
Rethymno	60.2	34.2	87.6	46.3	176.0	105.7
Heraklion	265.4	378.9	313.8	427.5	589.2	731.5
Lasithi Plateau	8.5	12.9	8.6	13.0	14.2	19.8
Agios Nikolaos	26.0	36.1	31.1	41.8	55.2	66.2
Ierapetra	68.5	135.2	80.0	152.3	133.9	229.4
Messara	52.5	70.5	59.3	79.0	99.3	117.2

Across all areas, building damage increases strongly with return period. Heraklion clearly dominates total losses, with mean damages rising from €265 million (RP50) to almost €590 million (RP1000) and individual building losses exceeding €5 million in the most exposed industrial and commercial complexes. High mean damages are also obtained for Ierapetra, Rethymno, Kladisos and Messara, reflecting dense urban fabric or clusters of large industrial / greenhouse buildings in low-lying coastal zones. Smaller rural basins (Koiliaris, Tavronitis, Lasithi Plateau) show lower absolute losses but still experience a two- to three-fold increase in mean damage between RP50 and RP1000.

The spatial pattern of building impact is illustrated for Heraklion in Figure 4-2 and Figure 4-3. Figure 4-2 shows that, already for RP50, long stretches of the Giofyros and adjacent torrents inundate buildings with depths up to 1–5 m, mainly in the western and southern suburbs. With higher return periods the number of flooded buildings grows only moderately, but depths increase and more structures fall into the higher depth classes. Figure 4-3 maps the corresponding mean monetary damage per building. Damage hotspots align with commercial strips and dense urban blocks near the river mouths and bridge crossings, where individual buildings can incur losses well above €1–2 million for RP1000 events.

Beyond ordinary buildings, the analysis also examined the exposure of critical infrastructure in Heraklion (Figure 4-5), including helipads, designated shelters, healthcare units and fire stations. Most assets remain outside the core inundation zones, but several shelters and health facilities lie close to the flooded corridors and become surrounded or directly affected under RP100 and especially RP1000 conditions, showing potential access problems and the need to verify redundancy and emergency routes in future civil-protection planning.

Equivalent building-damage maps for the remaining nine areas of interest (Tavronitis/Skoutelonas, Keritis, Kladisos, Koiliaris, Rethymno, Lasithi Plateau, Agios Nikolaos, Ierapetra and Messara) are provided in the Appendix (Figure 8-21 to Figure 8-29). They confirm the strong concentration of building losses in coastal urban areas and intensively used floodplains, and the marked escalation of damage between the RP50 and RP1000 scenarios.

Compared to the Phase1 assessment, which relied on OpenStreetMap building data with significant gaps and under-representation of small structures, the Phase2 damage estimates based on ms-buildings are considered more realistic in terms of exposed building counts and spatial coverage. However, the ms-buildings dataset does not systematically provide building function (e.g. residential, commercial, industrial). As a result, all buildings are treated with the same Universal damage class, which limits the differentiation of damage by building type and introduces additional uncertainty in the absolute damage values and their sectoral breakdown.

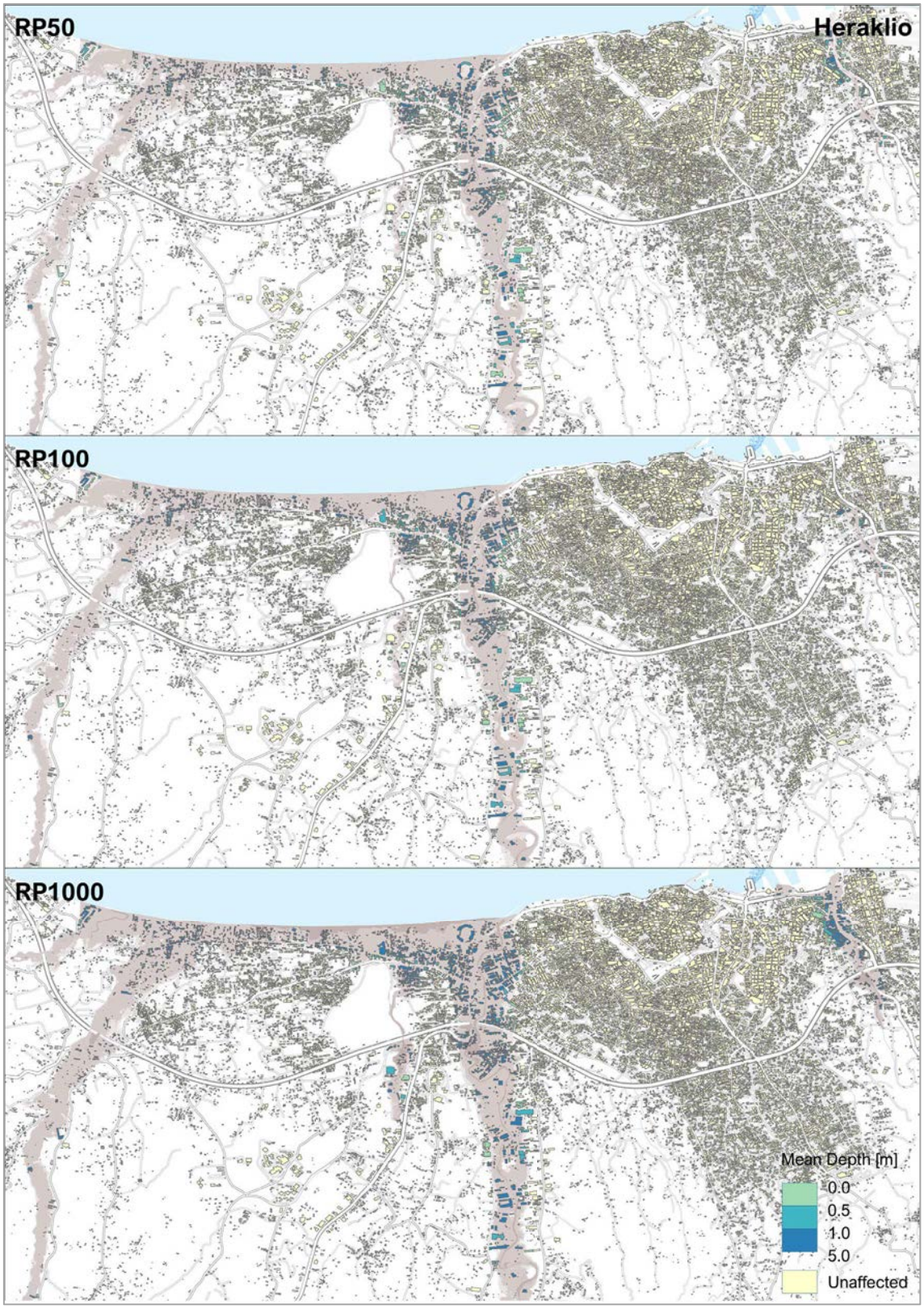

Figure 4-2 Mean flood depth at building locations in Heraklion for the 50, 100, and 1000-year return period Buildings are classified based on flood depth categories: 0.0–0.5m (light blue) and 0.5–1.0m (dark blue).

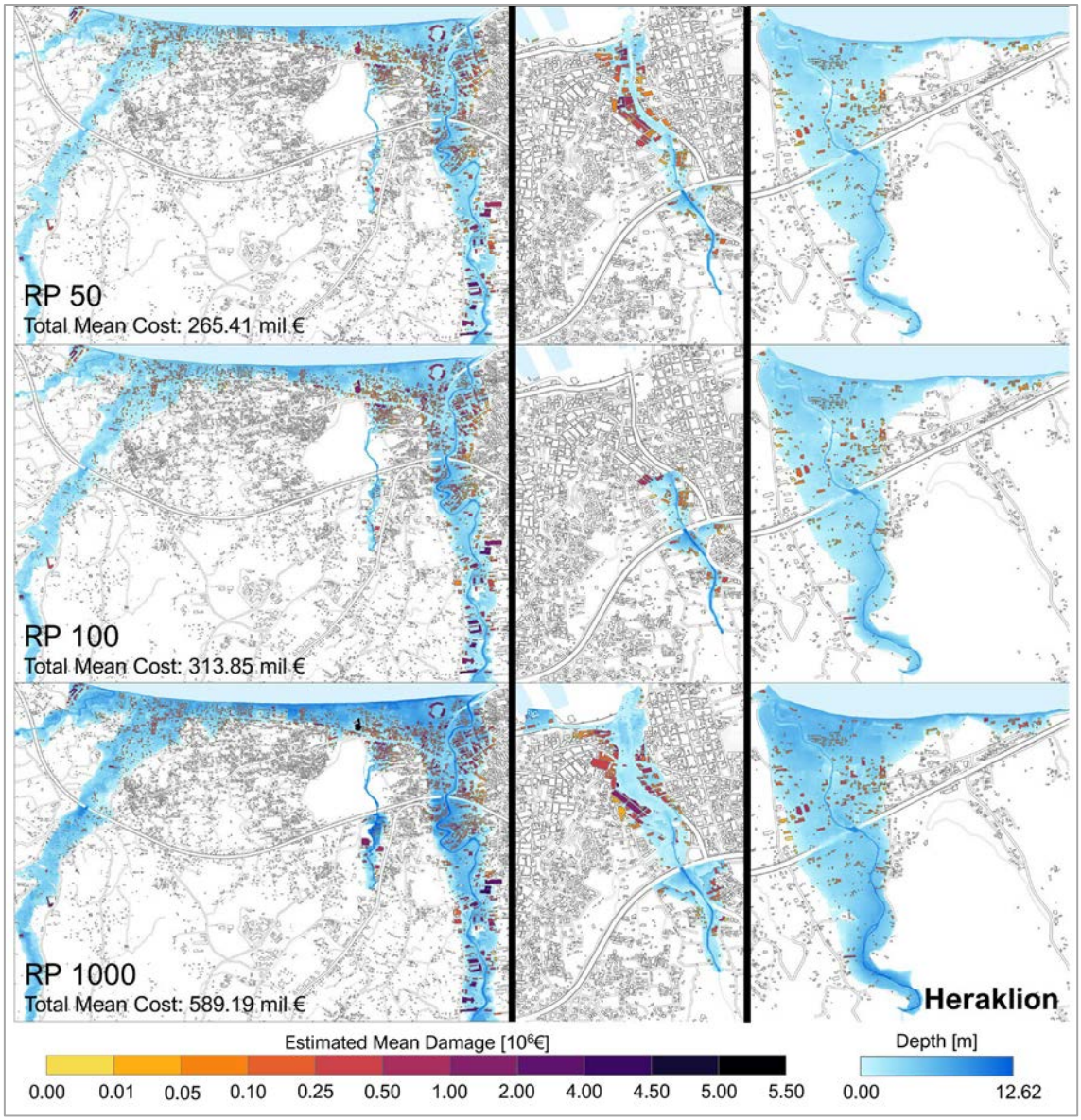

Figure 4-3 Estimated mean direct damage to individual buildings in Heraklion for RP50, RP100 and RP1000. Coloured polygons show the spatial distribution of mean damage per building (in 10^6 €), overlaid on the corresponding flood-depth maps; zoomed panels highlight critical hotspots along the main urban torrents.

The relationship between event return period and aggregated building losses in Heraklion is summarized in Figure 4-4. For each modelled return period, damages were computed using the minimum, mean and maximum flood depth at each building footprint in order to bracket the uncertainty associated with sub-grid depth variability. Scenario damages increase almost linearly with return period, ranging from roughly €150–200 million for the lowest depth assumption to more than €700 million for the highest depth assumption at the longest return period. Integrating these curves yields an Expected Annual Damage (EAD) of about €7 million for mean depths (with a range of approximately €4.5–9.3 million for minimum and maximum depth assumptions), providing a compact indicator of long-term flood risk to the building stock in Heraklion.

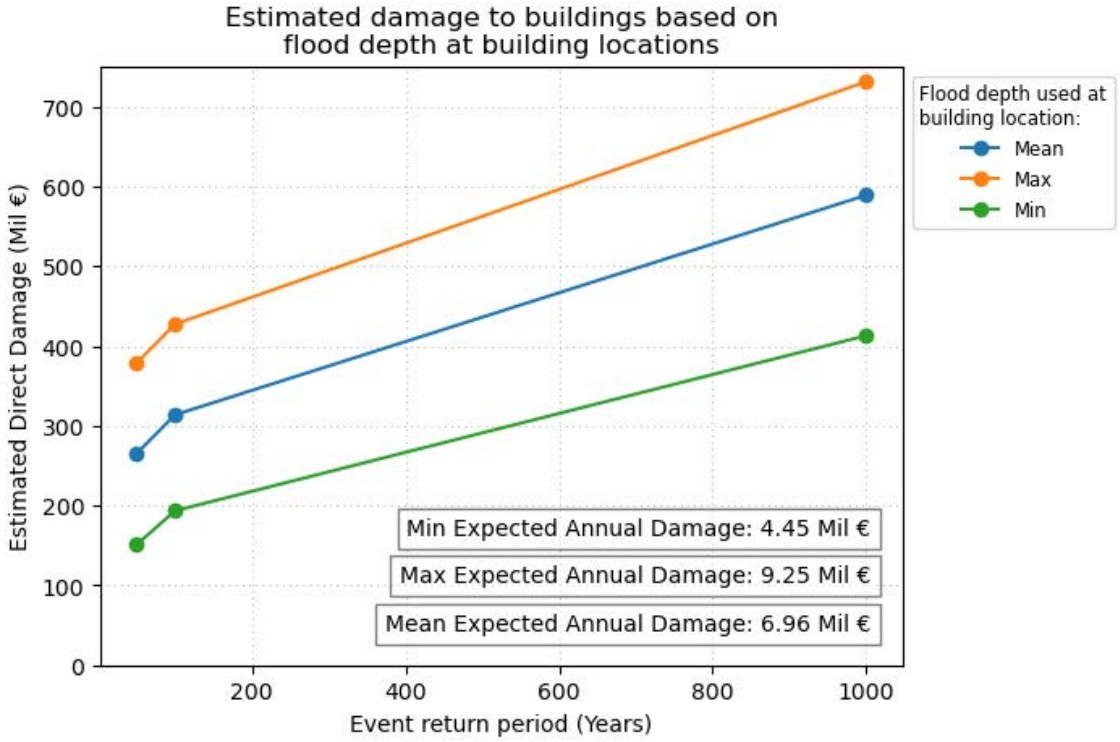

Figure 4-4: Estimated direct damage to buildings in Heraklion for different flood return periods (10, 50, 100, and 500 years)

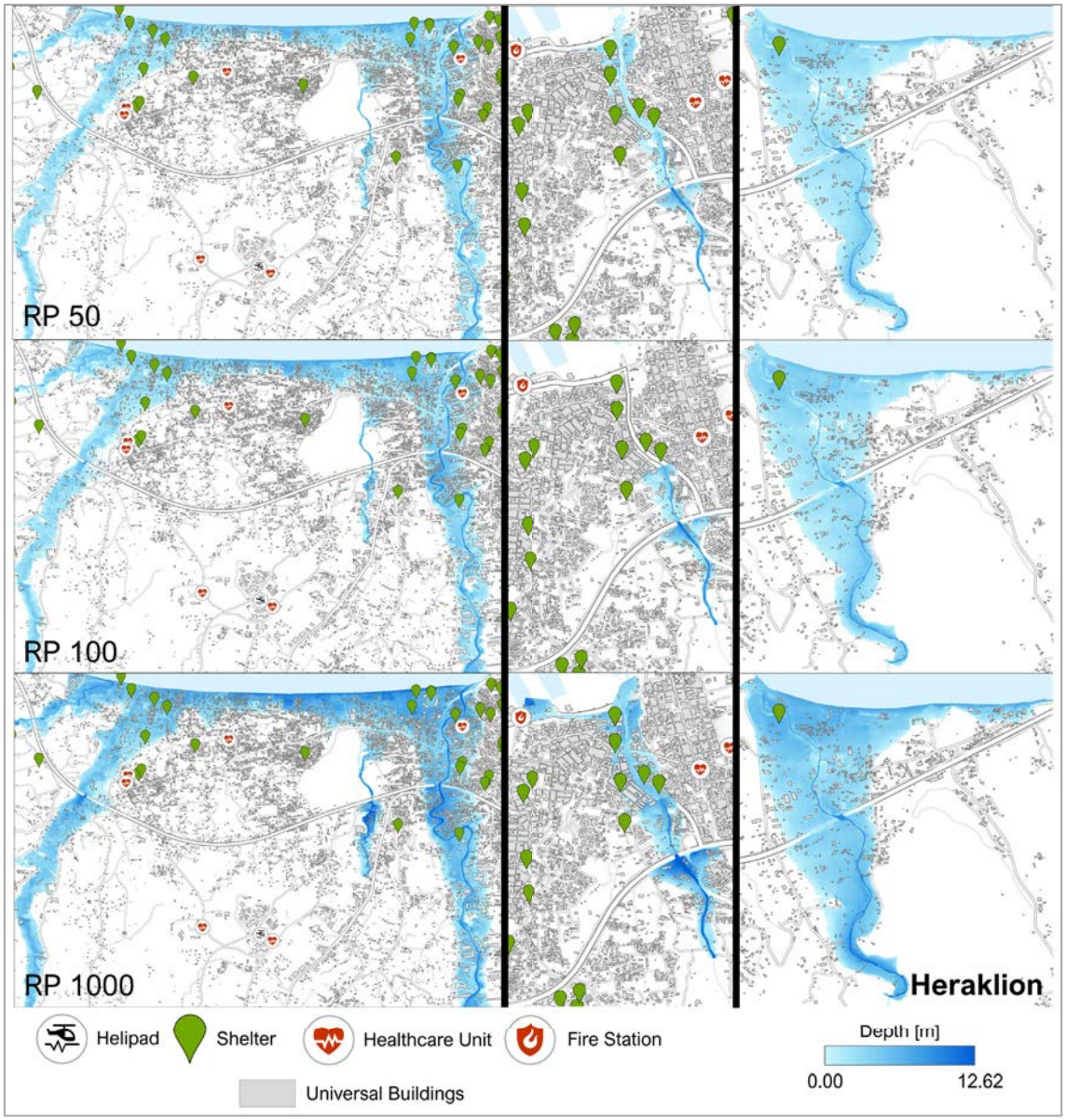

Figure 4-5 Exposure of selected critical infrastructure to river flooding in Heraklion for RP50, RP100 and RP1000. The maps provide an overview of exposed critical infrastructure across the area, including healthcare units, fire stations, shelters, and transportation hubs.

4.5 Population Exposure and Displacement

Population exposure and displacement were estimated by intersecting the 2m flood maps with the ms-buildings derived population layer (4 persons per 100 m² of footprint). People living in any inundated building were counted as exposed, while those in buildings experiencing flood depths > 1.0 m were classified as displaced.

For Heraklion, the number of exposed residents increases from roughly 30,000 people for RP50 to more than 42,000 people for RP1000 (Figure 4-6). The corresponding number of displaced residents rises from about 16,000 (RP50) to more than 34,000 (RP1000) (Figure 4-7), indicating that a large share of the exposed population is affected by damaging flood depths, particularly for the rarest events. Integrating over return periods yields an Expected Annual Exposed Population (EAEP) of about 638 people per year and an Expected Annual Displaced Population (EADP) of about 425 people per year, summarising the average annual human impact of river flooding in Heraklion under current conditions.

At the scale of all ten areas of interest (Table 4-4), Heraklion clearly dominates both exposure and displacement, accounting for around half of all exposed and displaced residents in each scenario. Other important hotspots include Ierapetra, Messara, Kladisos and Agios Nikolaos, where dense coastal settlements and linear development along torrents lead to thousands of people being exposed and several hundred to thousands displaced in the RP1000 event. In contrast, more rural catchments such as Koiliaris, Tavronitis and parts of the Lasithi Plateau show lower absolute numbers but still substantial displacement relative to their local population.

Table 4-4: Total estimated and exposed and displaced per region, of a 50, 100, and 1000 return period flood event, based on current climatic conditions.

	Total Exposed | Displaced Population					
Region	**RP50**		**RP100**		**RP1000**	
Tavronitis Skoutelonas	2274	591	2486	832	3050	1723
Keritis Maleme	2070	762	3301	1582	4360	2879
Kladisos	7205	897	8247	1545	11260	6877
Koiliaris	944	425	1073	575	1553	1098
Rethymno	3753	964	4933	1490	7956	5766
Heraklion Town	29947	16397	31306	19940	42490	34137
Lasithi Plateau	1750	252	1753	247	2228	659
Agios Nikolaos	2697	1711	2850	2112	3470	3020
Ierapetra	12253	2337	13257	2887	17033	6238
Messara	6976	3414	7472	3832	7314	5863

These estimates provide a first-order but spatially detailed picture of the human impacts of river flooding in Crete. They should, however, be interpreted as indicative, given the simplifying assumption of uniform population density per building and the absence of seasonal population variations (tourism) in the exposure calculation.

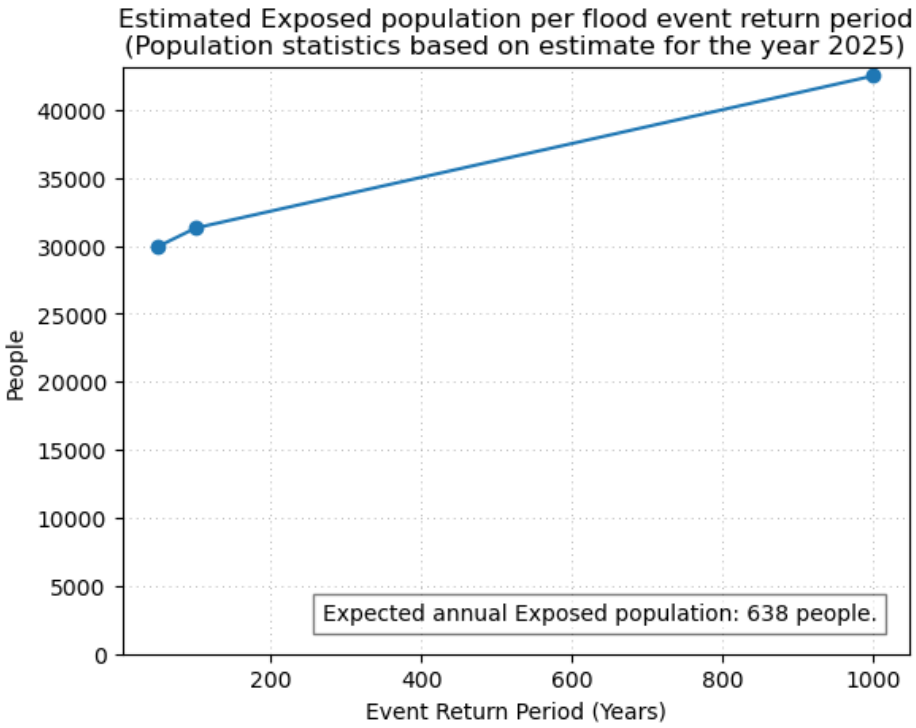

Figure 4-6: Estimated exposed population in Heraklion for different flood return periods (50, 100, and 1000 years), based on population estimates for the year 2025.

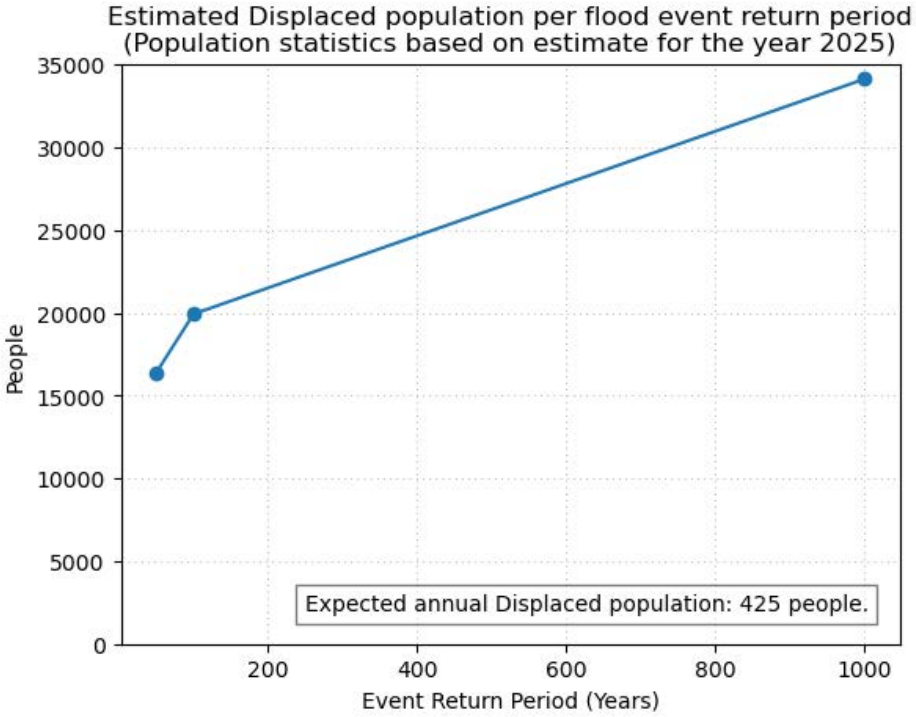

Figure 4-7: Estimated displaced population in Heraklion for different flood return periods (50, 100, and 1000 years), based on population estimates for the year 2025. Displacement is defined as exposure to flood depths exceeding 1.0 meters.

4.6 Extreme Precipitation

4.6.1 Hazard Assessment

In the absence of flood-hazard projections for future climate scenarios, heavy rainfall was analysed using the CLIMAAX Extreme Precipitation workflow and the bias-corrected EURO-CORDEX ensemble. The focus was on 24-hour rainfall extremes over Crete and, in particular, the Giofyros (Heraklion) and Keritis (Chania) basins where major flash-flood impacts have been recorded.

To relate modelled heavy rainfall to real impacts in Crete, we compiled a catalogue of recent damaging flood events (Table 8-1 and Table 8-2). The table lists 19 flash flood locations between 2003 and 2020 and, for each event, includes the date, location, reported precipitation from the nearest rain gauge, event duration and a qualitative impact description with a three-level impact severity (1 = low, 2 = moderate, 3 = high). For every case we extracted daily rainfall from multiple datasets CLIMADAT grid (Varotsos et al., 2025), MSWEP (Beck et al., 2019), E-OBS (E-OBS, 2020), ERA5-Land (Muñoz-Sabater et al., 2021) and local stations including stations of the NOANN network (Lagouvardos et al., 2017) for the event day as well as –1 and +1 day, in order to capture timing uncertainty and multi-day accumulations. We also report the corresponding RP50/RP100/RP1000 24-h depths from the official national IDF curves, scaled at the basin level of each event. Comparing observed impacts with these multi-source rainfall estimates confirmed that high-impact events are generally associated with 24-h totals above ~100 mm and often above 200 mm, supporting the choice of 100 mm/day and 200 mm/day as medium and severe impact rainfall thresholds for Crete.

Focusing on two highly impacted basins in Crete, Figure 4-8 and Figure 4-9 show the time series of annual maximum daily precipitation for Giofyros and Keritis, respectively. For Giofyros, historical annual maxima typically range between ~20–45 mm, with occasional years approaching 50 mm based on bias adjusted multi-model mean EUROCORDEX estimates, which can be considered moderate when compared to annual maxima based on local observations. Under both RCP4.5 and RCP8.5 scenarios, the spread of annual maxima increases noticeably, and events exceeding 60–80 mm become more frequent, especially in the late 21st century. Keritis exhibits higher historical maxima (often 60–120 mm) and future simulations indicate a shift towards even more intense events, with several years above 120 mm and a persistent high inter-annual variability under RCP8.5.

These changes are summarised in the IDF curves for Giofyros and Keritis (Figure 4-10). For both basins, the projected 24-hour return levels increase with time and are consistently higher for RCP8.5 than for RCP4.5. For Giofyros, the 50-year return level moves from well below the 100 mm/day medium-impact threshold to values approaching or exceeding it by the end of the century. In Keritis, where historical extremes are already high, both 50-year and 100-year return levels increase substantially, bringing a larger portion of the IDF curve into the “severe impact” range (≥200 mm/day) in the far-future RCP8.5 scenario. The widening gaps between the coloured curves and

the historical envelope also highlight the increasing modelled uncertainty for very long return periods.

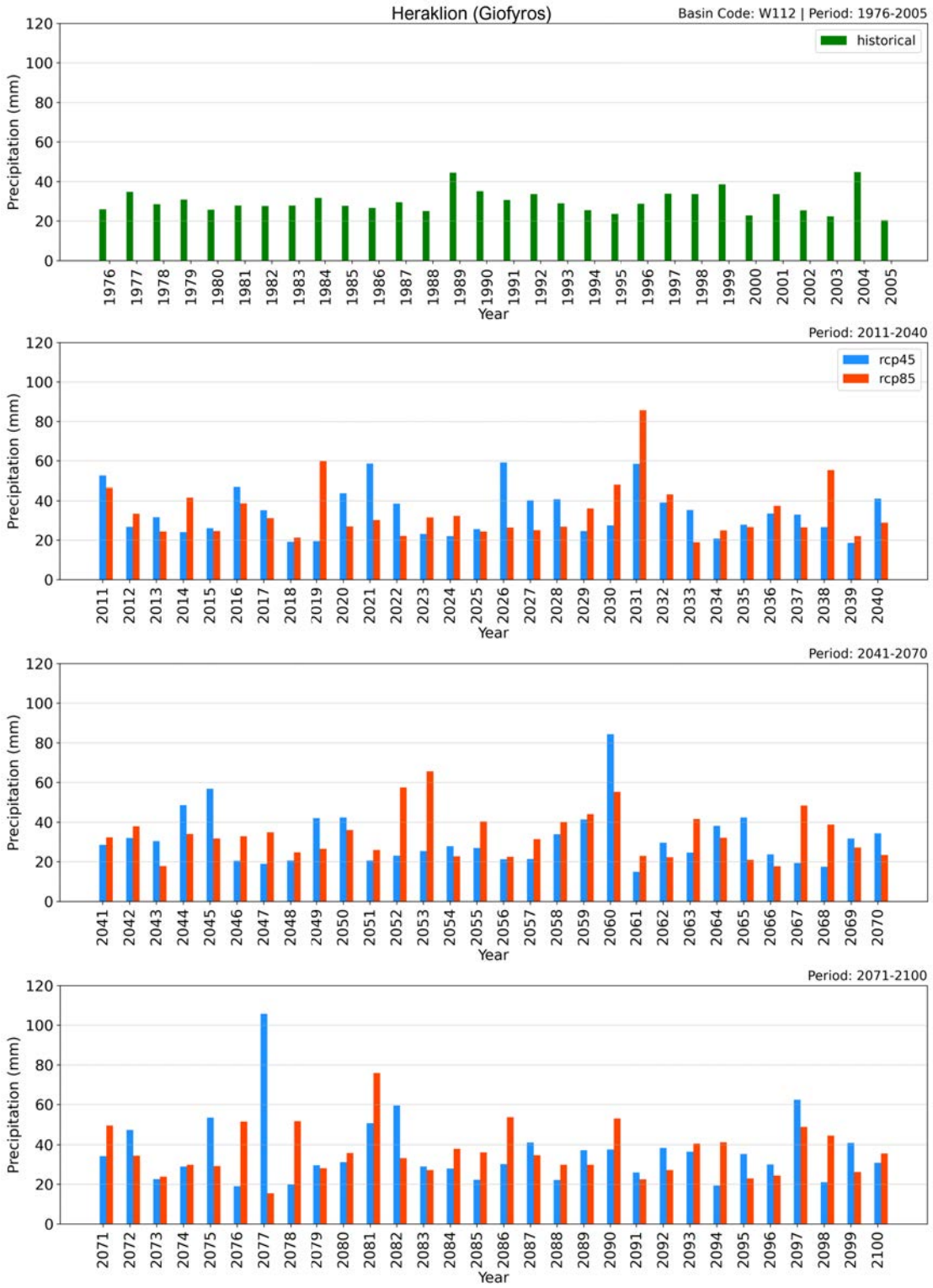

Figure 4-8 Annual maximum daily precipitation of the Giofyros river basin in Heraklion, as estimated from the multi-model mean baseline period (green bars) and RCP4.5 (blue)/ RCP8.5 (red) climate projections of 2011–2040, 2041–2070, 2071–2100 .

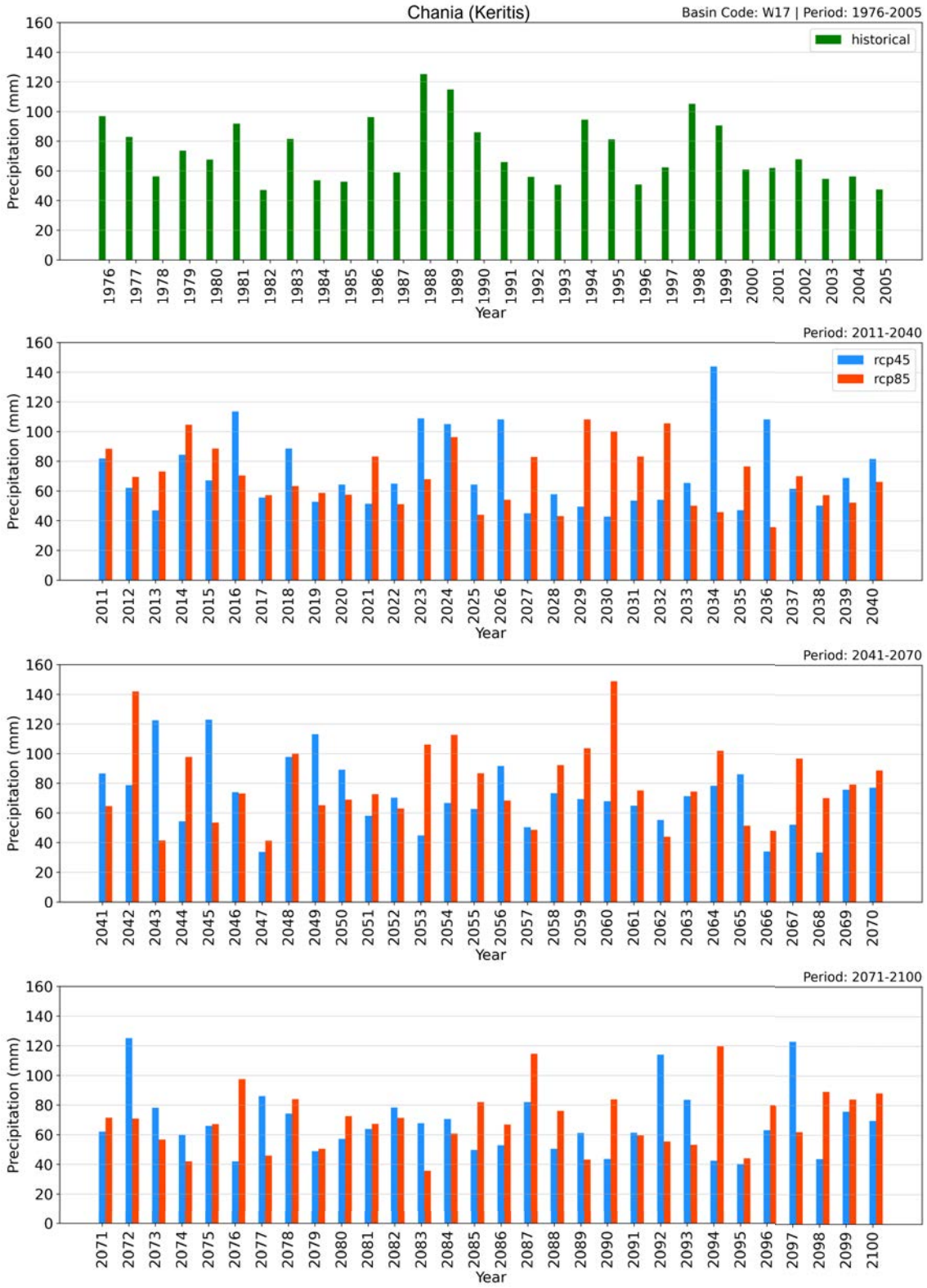

Figure 4-9 Annual maximum daily precipitation of the Keritis river basin in Chania, as estimated by the multi-model mean baseline period of 1976–2005 (green bars) and RCP4.5 (blue)/ RCP8.5 (red) climate projections of 2011–2040, 2041–2070, 2071–2100.

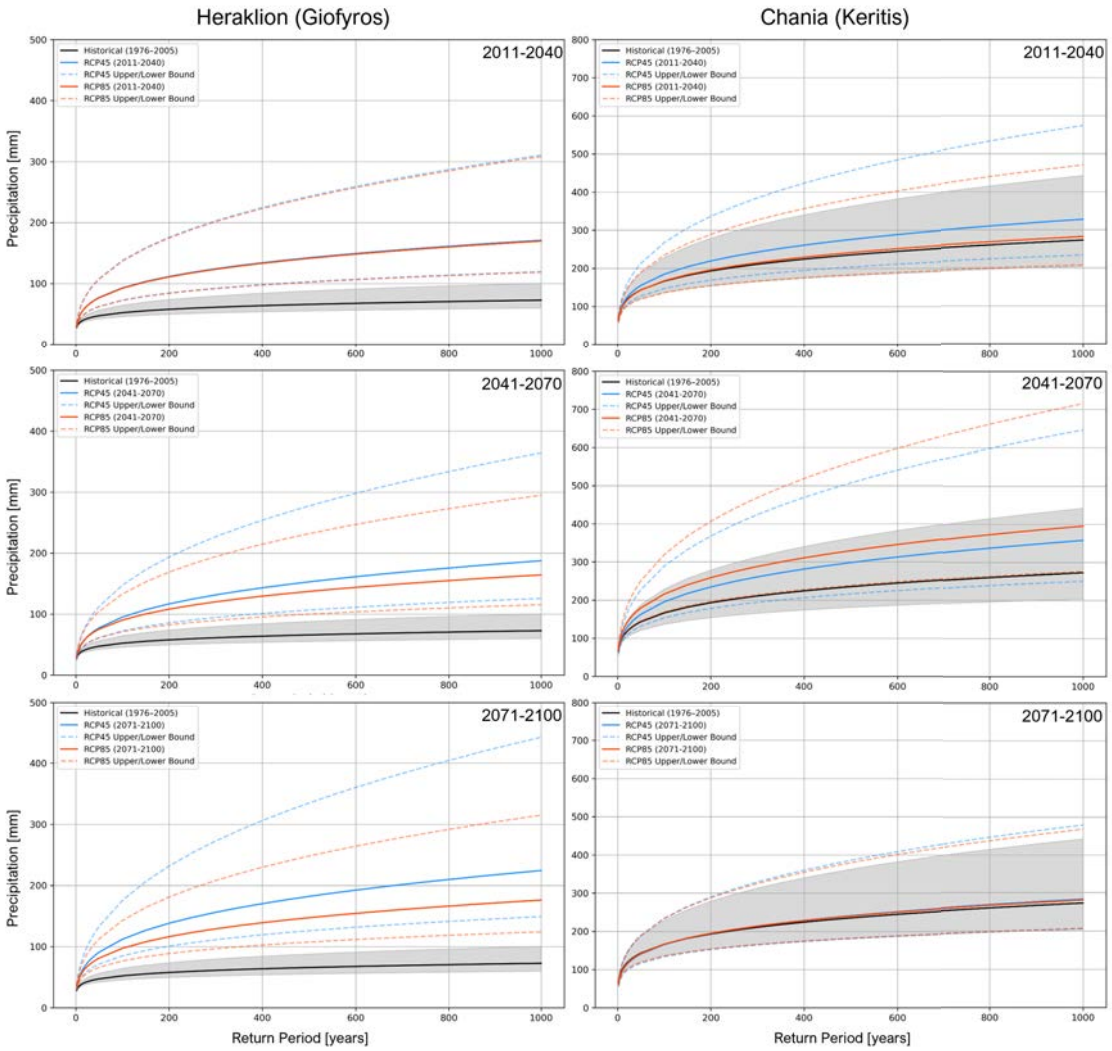

Figure 4-10 Projected IDF curves of Giofyros (left) and Keritis (right) river basins, estimated from multi-model annual daily precipitation maxima, for 2011–2040, 2041–2070, and 2071–2100. The blue and orange continuous lines represent RCP4.5 and RCP8.5 climate scenarios, respectively, whereas the dotted lines, of the same colour, their confidence intervals. The black line displays the historical IDF curve of 1976–2005, with the grey shaded area showing the historical confidence interval. Note that the two basins are presented at different scales.

At the island scale, Figure 4-11 presents multi-model IDF curves for Crete derived from three EURO-CORDEX GCM–RCM combinations and their ensemble mean. Across the three future periods, both scenarios show a gradual upward shift of the curves relative to the 1976–2005 baseline, with RCP8.5 yielding the strongest intensification of high-return-period rainfall. This supports the basin-scale findings for Giofyros and Keritis and suggests that heavier 24-hour rainfall events will become more frequent and more intense across much of the island.

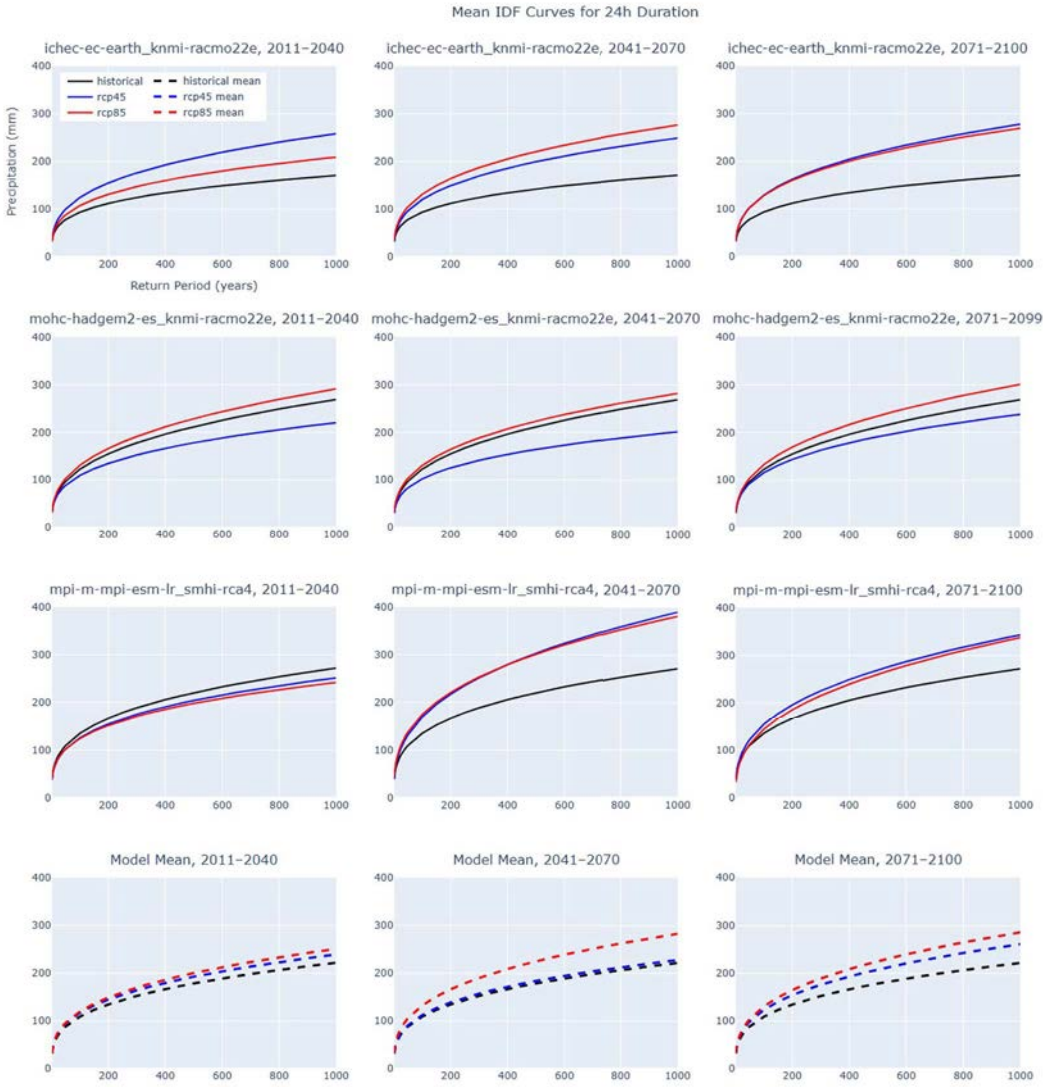

Figure 4-11 Multi-model IDF curves for 24-hour rainfall over Crete, derived from three EURO-CORDEX GCM–RCM combinations for the periods 2011–2040, 2041–2070, and 2071–2100. For each model, historical (1976–2005) IDF curves are shown in black, with RCP4.5 and RCP8.5 projections in blue and red, respectively. The bottom row displays the ensemble-mean IDF curves for each period and scenario.

The spatial pattern of these changes is illustrated in Figures 4-12 and 4-13, which map the multi-model mean 50-year 24-hour precipitation return level and its relative change compared to the baseline. Under RCP4.5 (Figure 4-12), modest increases in the 50-year return level are projected for central and eastern Crete in the near future, with more widespread and stronger increases by mid- and late century. Under RCP8.5 (Figure 4-13), the signal is amplified: central and eastern lowlands and several mountainous grid cells show pronounced increases (locally above +50–100% by 2071–2100), indicating a much higher likelihood that both the 100 mm and 200 mm impact thresholds will be exceeded during rare events.

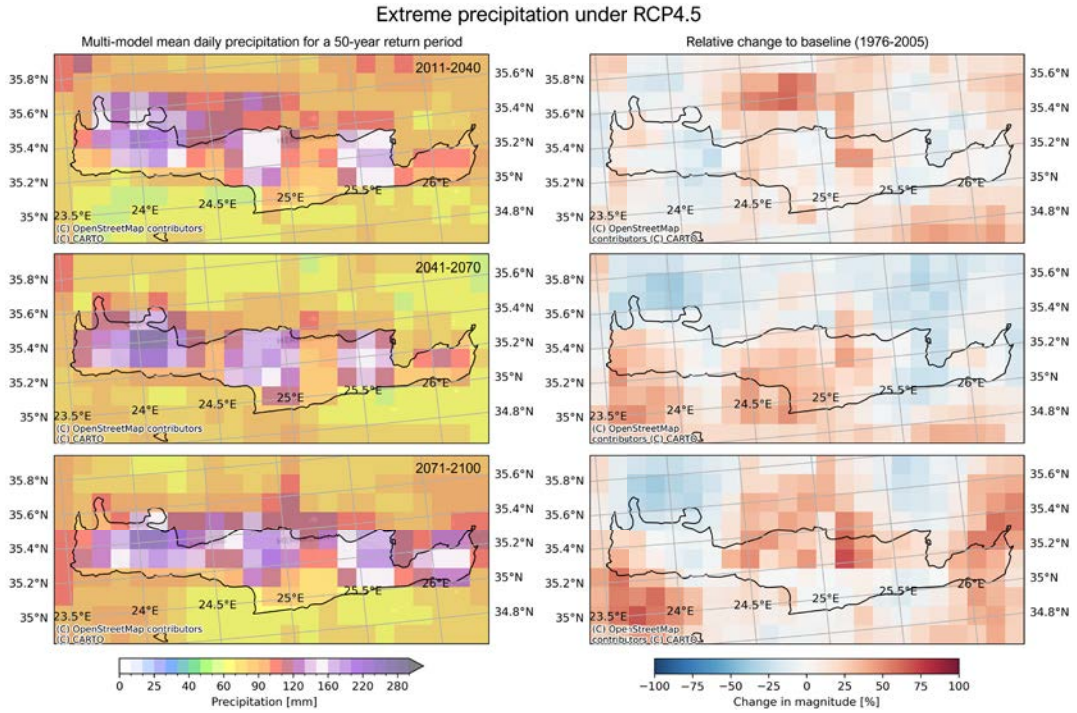

Figure 4-12 Spatial distribution of the multi-model mean 24-hour precipitation return level for a 50-year event (left) and its relative change with respect to the 1976–2005 baseline (right) under the RCP4.5 scenario for 2011–2040, 2041–2070, and 2071–2100. Warmer colours indicate higher return-level rainfall and positive percentage changes.

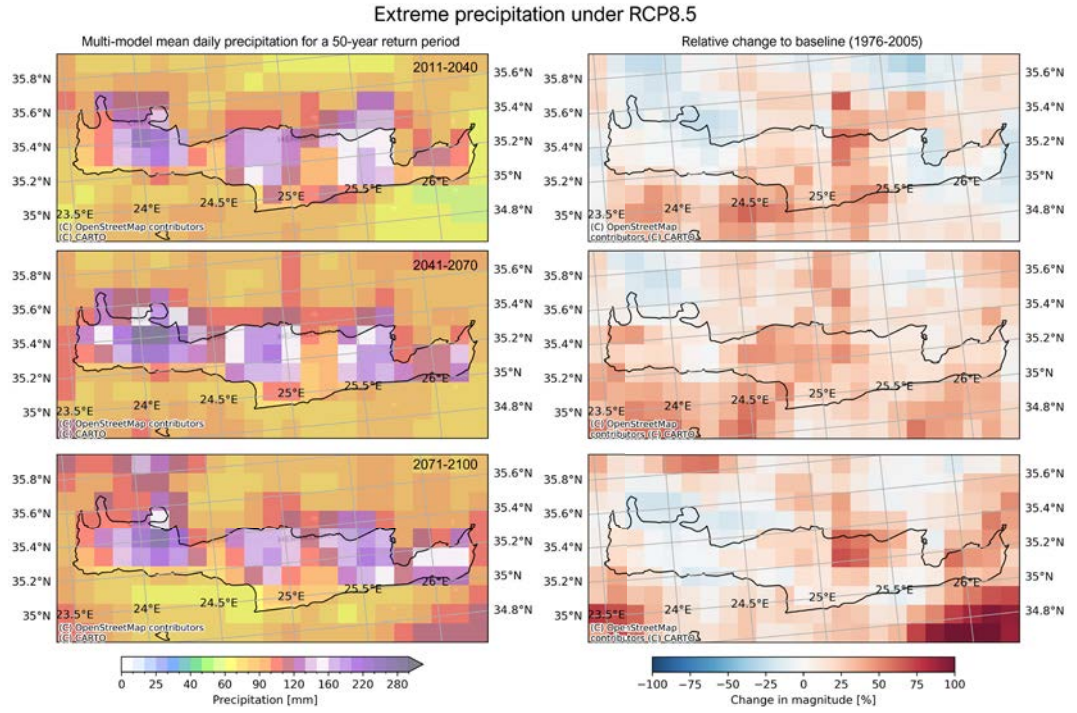

Figure 4-13 As in Figure 4-12, but for the RCP8.5 scenario. Compared to RCP4.5, RCP8.5 shows a stronger and more spatially extensive increase in 50-year 24-hour precipitation, particularly over central and eastern Crete by the end of the century.

Taken together, the basin-scale and island-scale analyses suggest that rainfall conditions capable of producing medium (≥100 mm/day) and severe (≥200 mm/day) impacts are projected to become more frequent in key flood-prone catchments and over large parts of Crete, particularly under the high-emissions pathway. These changes should be considered when interpreting the river-flood and building-damage results and when planning future flood-risk reduction measures.

4.6.2 Risk Assessment

To translate the extreme-precipitation projections into risk-relevant metrics, we focused on the two impact rainfall thresholds defined from past events in Crete: 100 mm/day (medium impact) and 200 mm/day (severe impact). For every EURO-CORDEX grid cell we used the fitted IDF curves to (i) quantify the relative change in the rainfall associated with these thresholds, and (ii) derive the equivalent return period of exceeding each threshold for the baseline (1976–2005) and the three future periods under RCP4.5 and RCP8.5.

Figure 4-14 and Figure 4-15 map the percentage change in 24-h rainfall associated with the 100 mm/day and 200 mm/day thresholds, respectively. For the medium-impact threshold, changes are modest and spatially heterogeneous in 2011–2040, but both scenarios show a gradual intensification of threshold-level rainfall towards mid- and late-century, especially over central and eastern Crete. The signal is much stronger for the severe-impact threshold under RCP8.5. Large parts of western and central Crete experience increases exceeding several tens of percent by 2071–2100, indicating that storm totals comparable to past high-impact events are projected to become substantially more intense.

Figure 4-16 and Figure 4-17 express the same information in terms of return period. For the 100 mm/day threshold, much of Crete currently experiences return periods of roughly 5–20 years, with shorter return periods over the windward slopes in the west. Under RCP4.5, these return periods generally shorten by one class (e.g. from 10–20 years to 5–10 years) by mid-century, while under RCP8.5 they shorten further and the area affected expands eastwards by the end of the century. For the 200 mm/day threshold, which is a rare but highly damaging rainfall amount in the historical climate, return periods in several western and central grid cells decrease from >50–100 years to the order of 10–20 years under late-century RCP8.5. This implies a several-fold increase in the likelihood of rainfall capable of triggering severe flash-flood impacts in the most exposed basins.

Overall, the risk-oriented indicators confirm that even if mean rainfall changes are moderate, the frequency and intensity of impact-relevant daily extremes are projected to increase, particularly under the high-emissions scenario and in western-central Crete. These results should still be interpreted cautiously, as they inherit the uncertainties of the EURO-CORDEX simulations, the bias-correction and extreme-value fitting, and do not explicitly account for local hydrological or drainage responses.

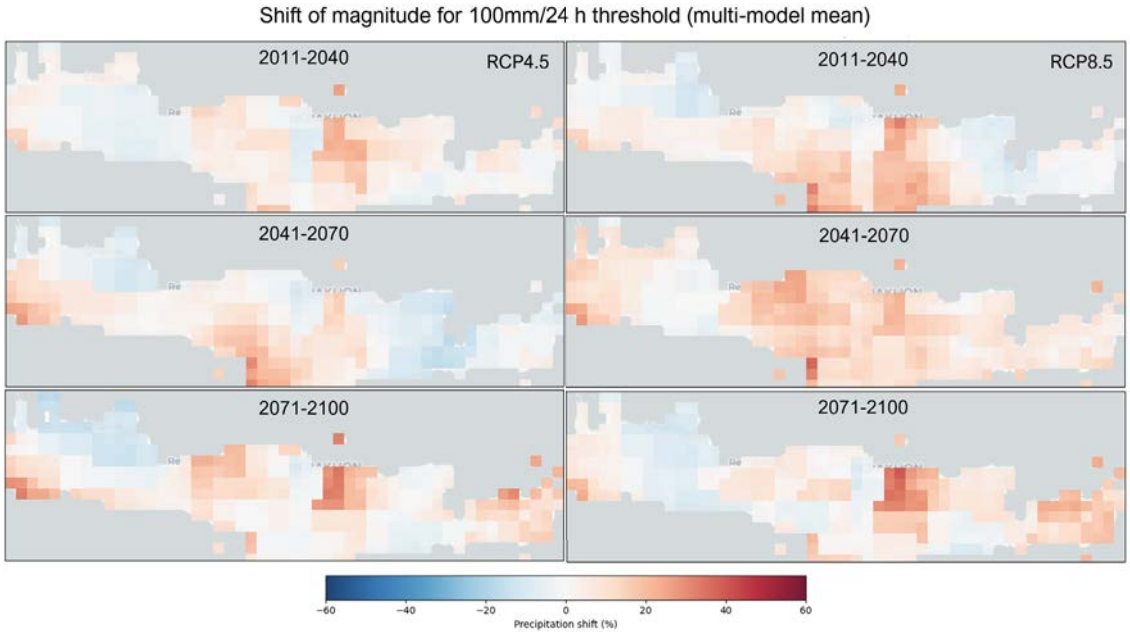

Figure 4-14 Relative change (%) in 24-hour precipitation associated with the medium-impact rainfall threshold of 100 mm/day over Crete, for three future periods (2011–2040, 2041–2070, 2071–2100) under RCP4.5 (left column) and RCP8.5 (right column), expressed as a percentage shift with respect to the 1976–2005 baseline.

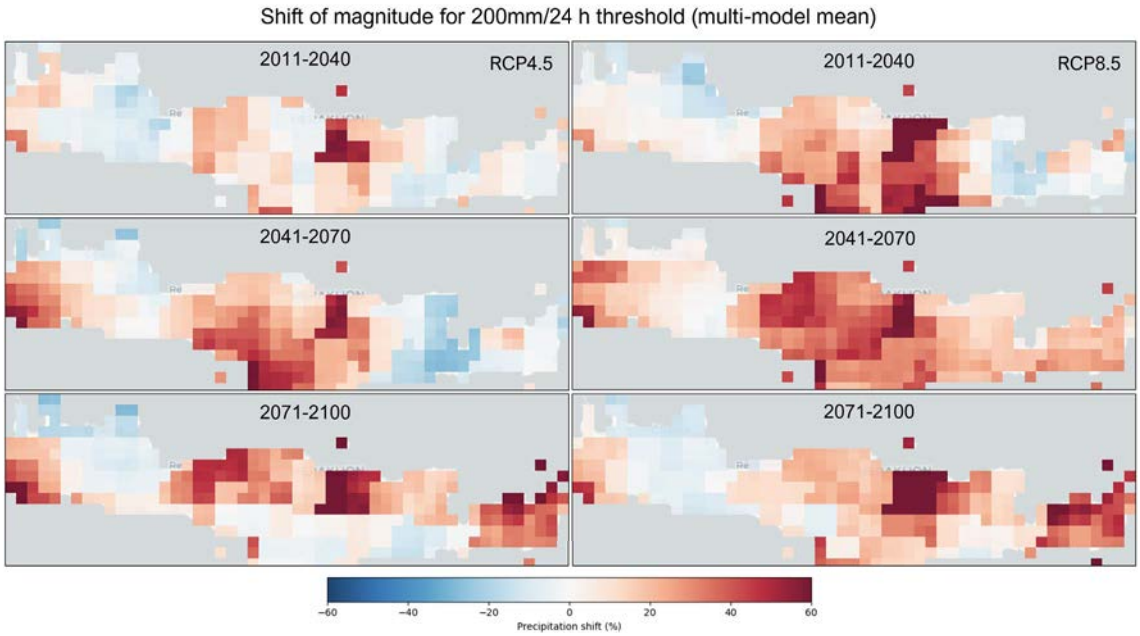

Figure 4-15 Same as Figure 4-14 but for the severe-impact rainfall threshold of 200 mm/day, showing the projected percentage change in 24-hour rainfall intensity relative to the 1976–2005 baseline.

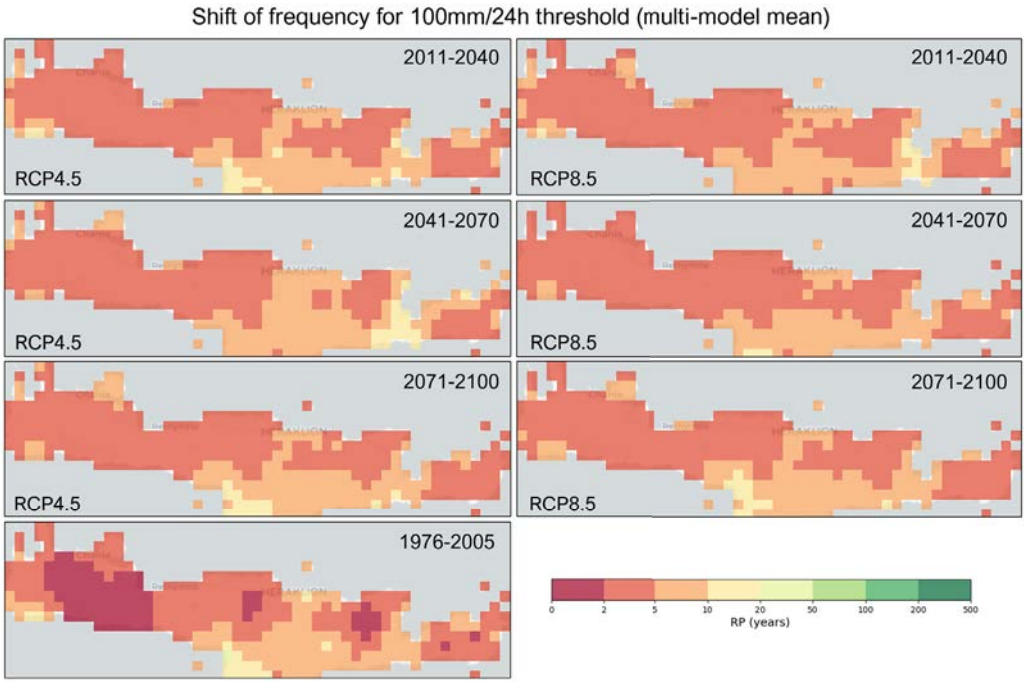

Figure 4-16 Equivalent return period (years) of exceeding the 100 mm/day medium-impact rainfall threshold over Crete, derived from EURO-CORDEX IDF curves for 2011–2040, 2041–2070, and 2071–2100 under RCP4.5 (left column) and RCP8.5 (right column), with the historical (1976–2005) return period map shown in the bottom panel for comparison.

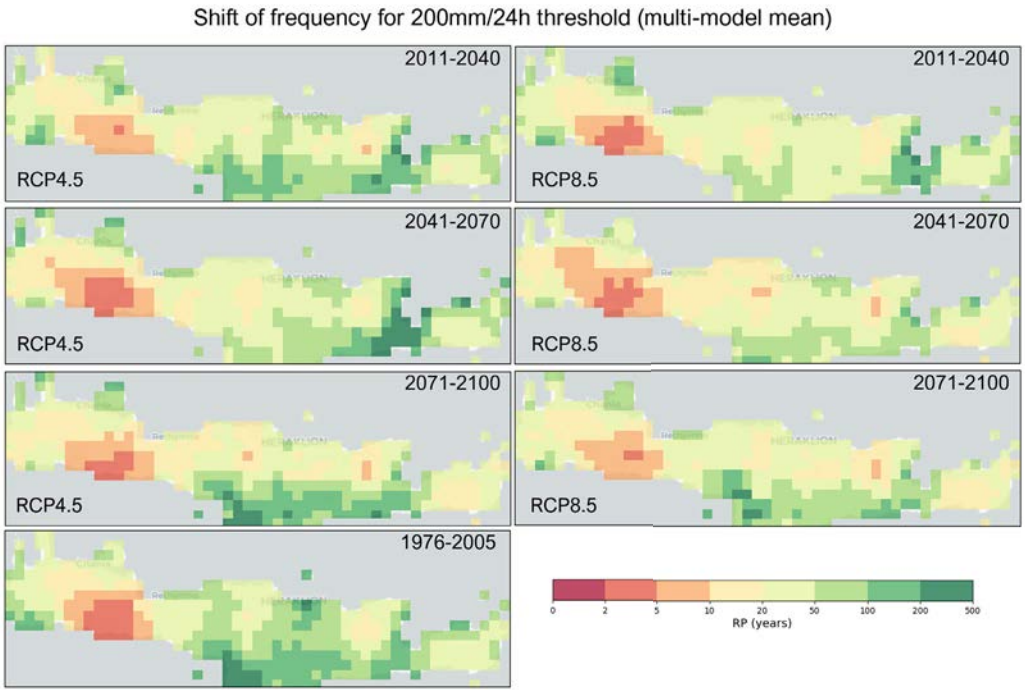

Figure 4-17 Equivalent return period (years) of exceeding the 200 mm/day severe-impact rainfall threshold over Crete, for the same periods and scenarios as Figure 4-16, with the baseline (1976–2005) map shown in the bottom panel.

4.7 River Discharge

4.7.1 Hazard Assessment

The River Discharge workflow was applied to the two basins with the highest observed flood impacts in Crete, the Giofyros (Heraklion) and Keritis (Chania) catchments. Using bias-corrected EURO-CORDEX simulations as meteorological input, a small ensemble of catchment models was run for the historical period (1971–2000) and for three future time slices (2011–2040, 2041–2070, 2071–2100) under RCP4.5 and RCP8.5.

Figure 4-18 and Figure 4-19 show daily discharge time series for the historical period. Individual GCM–RCM combinations (Figure 4-18) reproduce a strongly intermittent, flash-flood regime in both basins, with long periods of very low flow interrupted by sharp flood peaks. When all combinations are overlaid (Figure 4-19), the ensemble spread in peak magnitudes becomes evident, but the timing of high-flow episodes is broadly consistent across models. Peak simulated discharges are generally higher in Keritis than in Giofyros, reflecting the larger and steeper upstream area.

Seasonal patterns and projected changes in mean flows are summarised in Figure 4-20. In the historical period, both basins display a pronounced winter peak (December–February) and negligible flows during summer, typical of Mediterranean ephemeral rivers. Under both RCP4.5 and RCP8.5, ensemble medians suggest modest increases in winter and early-spring mean discharges towards the end of the century, especially in Giofyros, while summer flows remain close to zero. However, individual model trajectories diverge, with some combinations indicating reduced winter flows, highlighting substantial uncertainty in the magnitude of seasonal changes.

Projected changes in flood-relevant high flows are presented in Figure 4-21 and Figure 4-22.Figure 4-21 shows ensemble estimates of 10-year (RP10) and 50-year (RP50) peak discharges. In both basins, RP10 and RP50 flows generally increase from the historical period to mid- and late-century, with larger changes under RCP8.5. Giofyros exhibits particularly strong increases in RP50 flows in the long term, while Keritis shows more moderate but still positive changes. Figure 4-22 expresses these changes as percentages relative to the historical baseline and emphasises the large spread between individual GCM–RCM combinations: some members suggest near-stationary or even slightly reduced extremes in the near term, whereas others project increases exceeding 100% for specific horizons and return periods. Overall, the ensemble points to an intensification of river-discharge extremes in both basins, but with considerable model uncertainty that needs to be acknowledged in risk-management applications.

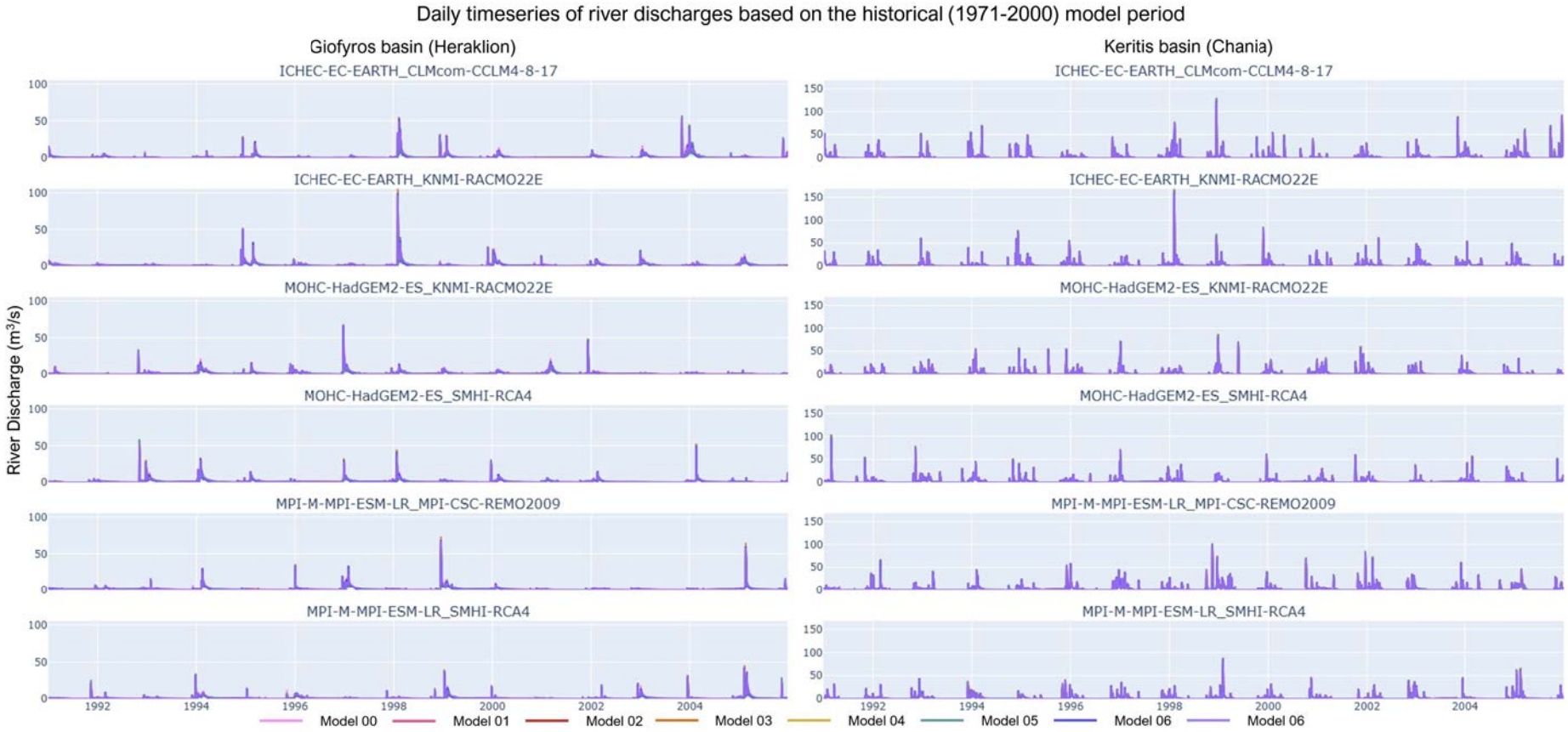

Figure 4-18 Daily river-discharge time series simulated for the historical period (1971–2000) for each individual GCM–RCM combination and the catchment-model ensemble mean, for the Giofyros basin (left) and Keritis basin (right).

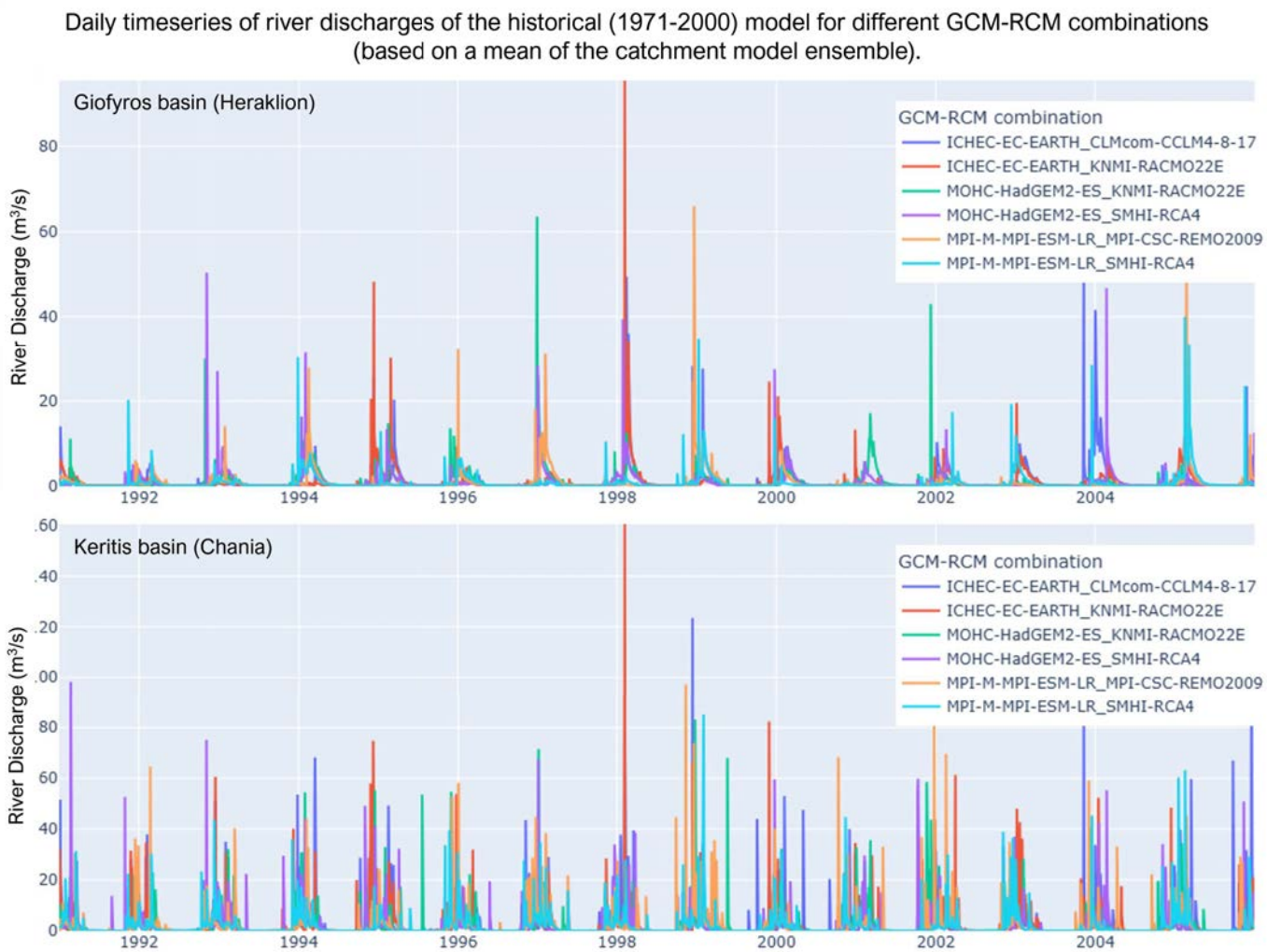

Figure 4-19 Comparison of daily river-discharge time series for the historical period (1971–2000) showing all GCM–RCM combinations (coloured lines) for Giofyros (top) and Keritis (bottom); peaks illustrate the spread in simulated flood magnitudes among models.

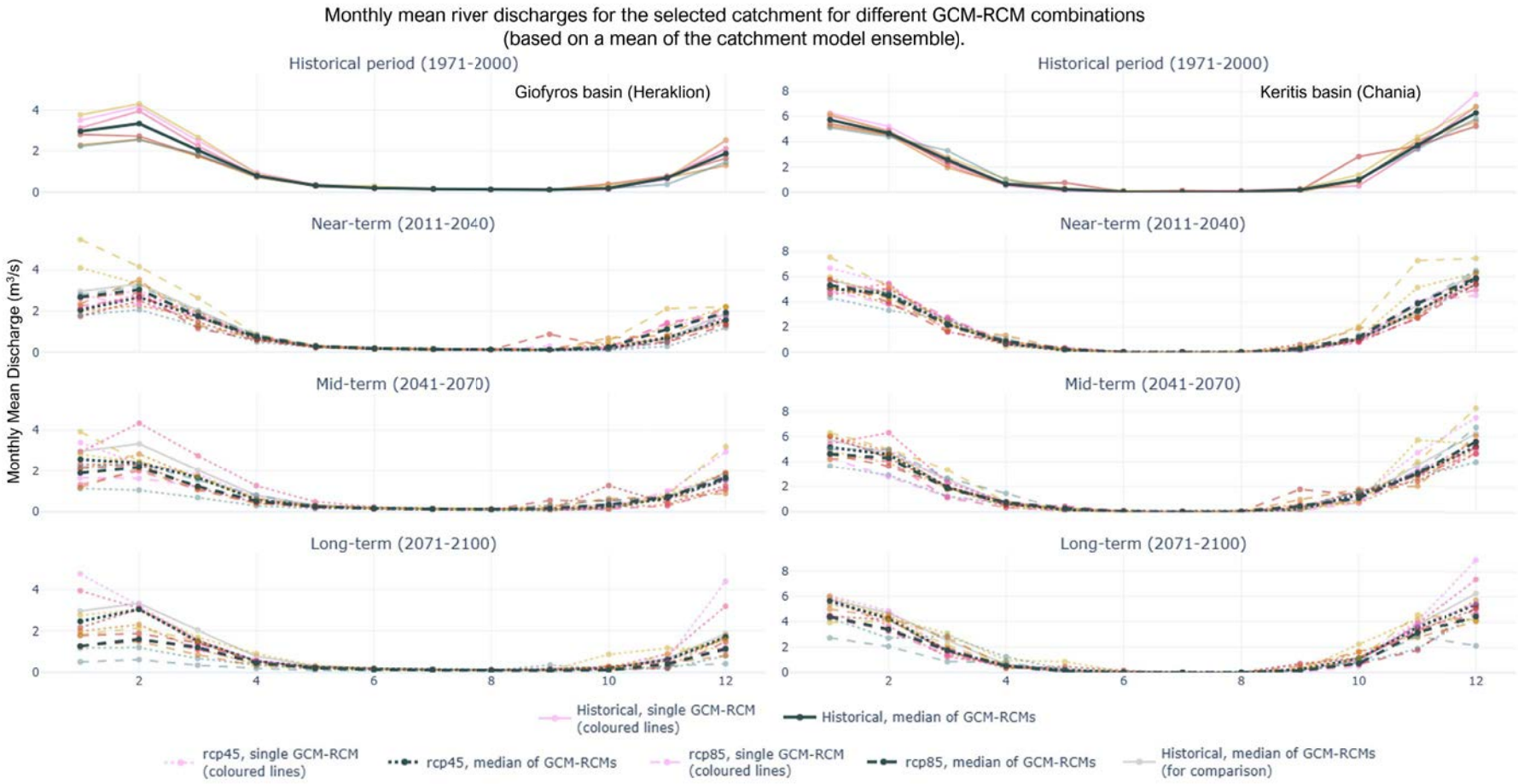

Figure 4-20 Monthly mean river discharges for Giofyros (left) and Keritis (right) for the historical period and for the near- (2011–2040), mid- (2041–2070) and long-term (2071–2100) future under RCP4.5 and RCP8.5; coloured lines show individual GCM–RCM combinations and bold lines the ensemble medians.

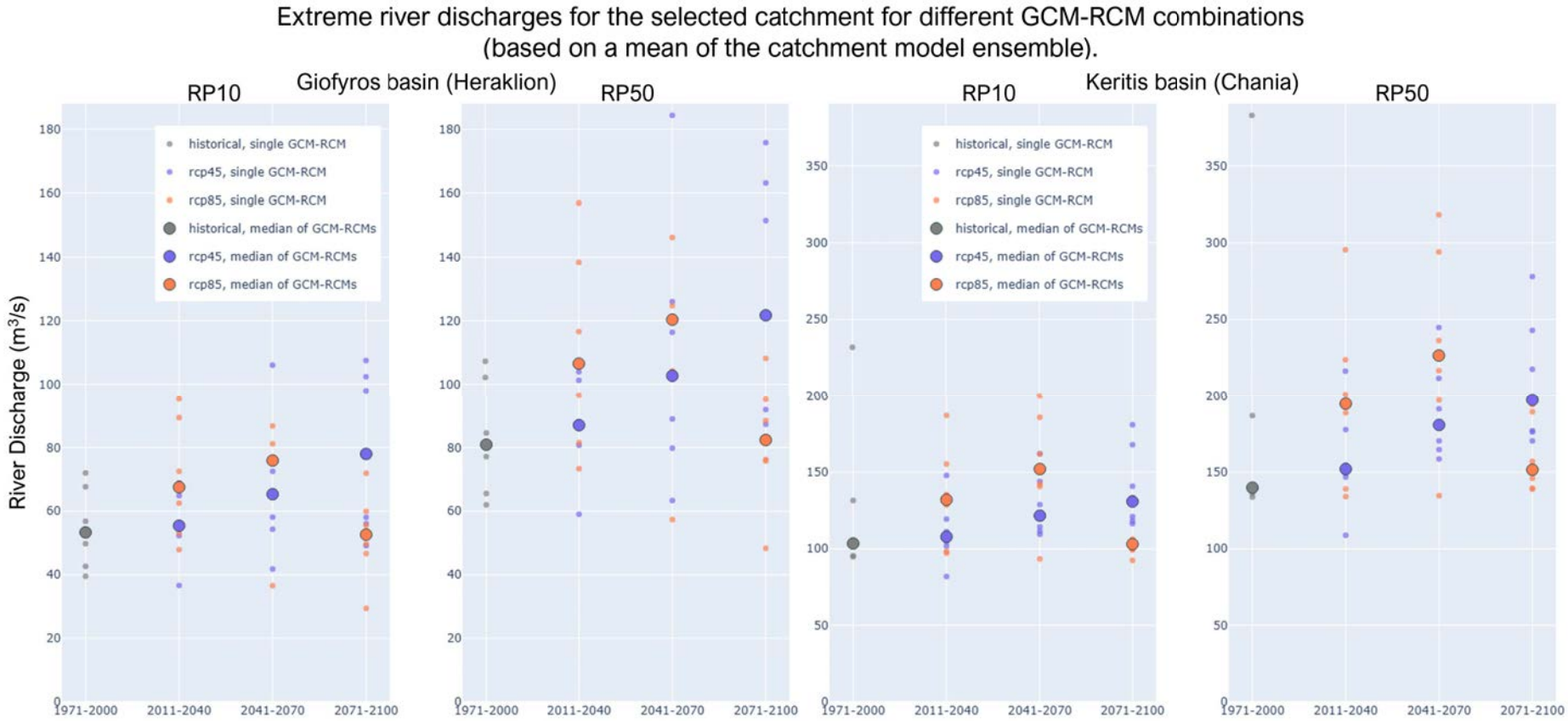

Figure 4-21 Extreme river-discharge estimates (10-year and 50-year return period flows) for Giofyros (left panels) and Keritis (right panels) for the historical baseline and future time slices under RCP4.5 and RCP8.5, derived from the catchment-model ensemble driven by different GCM–RCM combinations.

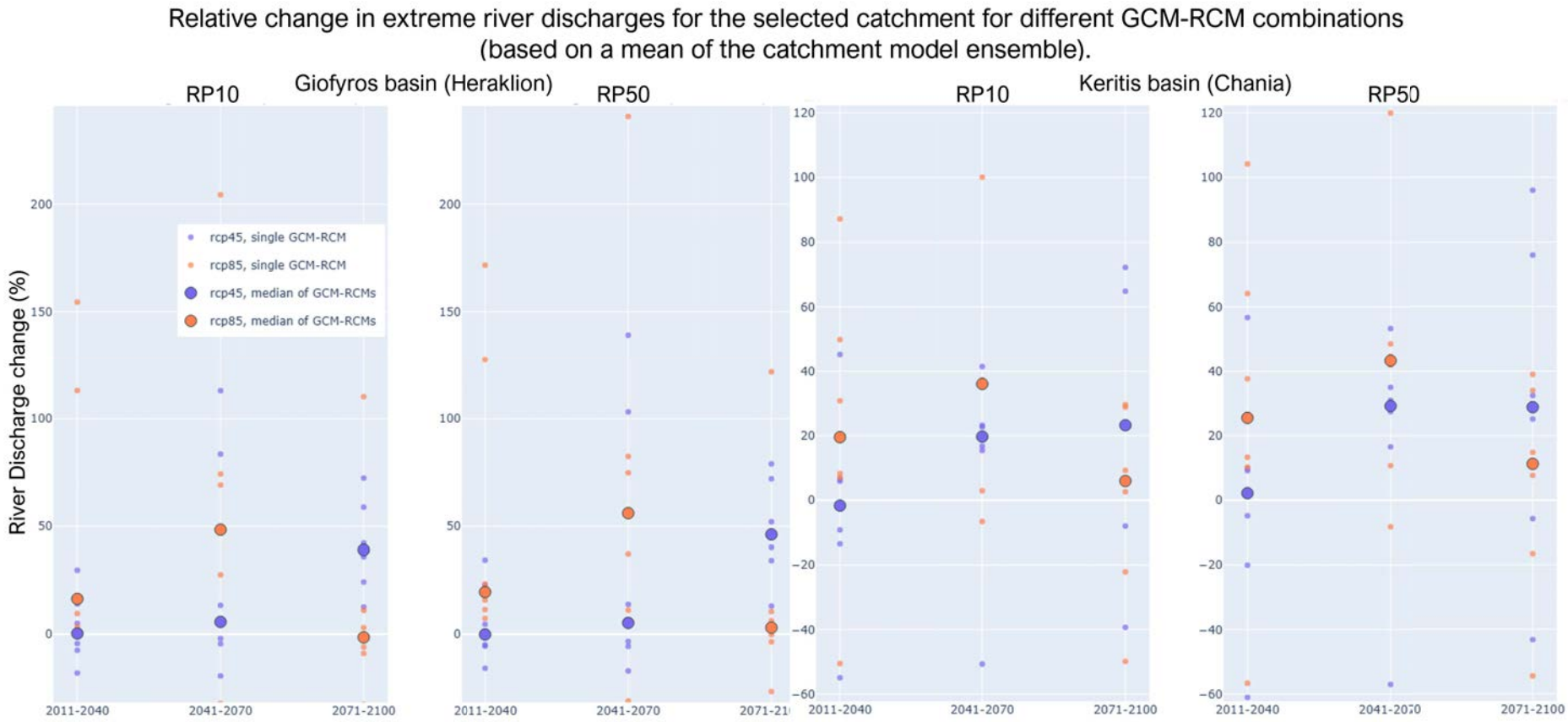

Figure 4-22 Relative change (%) in 10-year and 50-year extreme river discharges for Giofyros (left) and Keritis (right) for the future periods 2011–2040, 2041–2070 and 2071–2100 under RCP4.5 and RCP8.5, compared to the historical baseline; dots show individual GCM–RCM combinations and large symbols the ensemble medians.

The comparison between the extreme-precipitation and river-discharge results reveals a clear spatial contrast between the Giofyros and Keritis basins (Figure 3-10). Giofyros, located in central-northern Crete, lies within the area where the multi-model projections show the strongest increase in heavy 24-hour rainfall, particularly for the 200 mm/day threshold and under RCP8.5, and this is reflected in consistently positive and often large increases in extreme river discharges for both RP10 and RP50 in all future periods. In contrast, Keritis, situated in western Crete where projected changes in extreme rainfall are weaker and more mixed (with patches of near-zero or even negative shifts, especially under RCP4.5), shows a much less robust hydrological response: changes in extreme discharges are smaller, and under RCP4.5 some periods even exhibit negative or near-zero median changes. Across scenarios and time slices, this leads to a divergent signal, with Giofyros emerging as a clear hotspot of increasing flood potential, most pronounced in the mid- and late-century RCP8.5 projections, while Keritis displays a more subdued and scenario-dependent response that mirrors the more heterogeneous precipitation changes over western Crete.

5 Methodological limitations and uncertainties

Although the Phase2 assessment improves substantially on Phase1, several limitations remain:

Flood hazard maps

- Represent a specific baseline situation; they do not explicitly account for future changes in land use, drainage systems or defence works.
- Local uncertainties arise from DEM quality, roughness parameterisation and design hydrology used in the national modelling.

Building footprints and population

- Microsoft Global Building Footprints do not systematically distinguish building use; all buildings are treated with the same Universal damage class.
- Population is estimated from footprint area assuming a uniform density of 4 persons per 100 m².

Vulnerability and damage functions

- Maximum damage values and depth–damage relations are based on Huizinga et al. (2017) global functions and national CPI adjustments, not on Cretan-specific empirical loss data.

Extreme-precipitation analysis

- The CLIMAAX products rely on bias-corrected EURO-CORDEX simulations at ~12 km resolution; local convective extremes and small orographic effects may be smoothed.

– Impact thresholds (100 and 200 mm/day) are derived from a limited set of documented events and available gauges and should be seen as indicative ranges rather than strict limits.

River discharge indicators (Giofyros and Keritis)

– HCII/E-HYPEcatch discharges represent aggregated catchment responses at coarse resolution and may not reproduce local channel modifications, abstractions or regulation.

These limitations are considered when interpreting the results in the following sections and underline the need for continued refinement with additional local data and stakeholder input.

6 Discussion and Conclusions

The Phase2 CLIMAAX assessment for Crete provides a much more detailed and internally consistent picture of flood hazard and risk than the preliminary Phase1 study. By combining 2m hazard maps, the Microsoft building footprints, land-use data, and dedicated CLIMAAX workflows for extreme precipitation and river discharge, the analysis links physical drivers, exposure and impacts across multiple spatial scales and time horizons. The results emphasise three main points: (i) the concentration of present-day river-flood risk in a limited number of coastal plains and urbanised torrents, (ii) the large potential for high-impact rainfall and discharge extremes to intensify under climate change, especially in central and eastern Crete, and (iii) the importance of using locally relevant datasets to avoid under- or mis-representation of risk hotspots that appears in coarser, pan-European products.

At the baseline, the FRMP hazard maps show that the largest inundated extents occur in the Messara plain and the Lasithi Plateau, while the most hazardous depths are often found in narrow urban torrents in Heraklion, Rethymno, Agios Nikolaos and Ierapetra. When combined with LUISA land use, these patterns translate into very high direct damage potential: for RP1000, Messara, Heraklion and Lasithi together account for roughly two-thirds of the total land-use-based losses across all ten areas. Building-level results sharpen this picture. Heraklion, in particular, emerges as the dominant hotspot of structural damage and human exposure, with mean building losses exceeding €0.5 billion in RP1000 and around 42,000 residents exposed and 34,000 displaced in that scenario. Even for more moderate return periods, thousands of people are already living in buildings subject to damaging flood depths, underlining the need for risk-reduction measures that go beyond very rare design events.

The extreme-precipitation analysis adds a forward-looking perspective. Modelled changes in annual maximum 24-hour rainfall and IDF curves indicate that, in much of central and eastern Crete, rainfall capable of generating the historically defined “medium” (≥100 mm/day) and “severe” (≥200 mm/day) impacts is projected to become both more frequent and more intense, particularly under RCP8.5. Giofyros, which drains

a heavily urbanised part of Heraklion, lies within the zone of strongest projected intensification; its 50-year return level moves into or above the 100 mm threshold in far-future scenarios. In contrast, Keritis in western Crete is located where modelled precipitation changes are weaker and more heterogeneous, leading to a less robust signal. This west–central contrast is echoed by the river-discharge statistics: extreme flows (RP10, RP50) in Giofyros increase in almost all scenarios and time slices, while changes in Keritis are smaller and sometimes near-stationary, especially under RCP4.5.

Taken together, the hazard, damage and population-exposure results suggest that existing high-risk areas such as Heraklion, Messara, Ierapetra and parts of Chania are likely to face increasing pressure from both more intense local rainfall and higher river discharges. In these locations, present-day risk is already high: densely built floodplains, limited space for conveyance and storage, and critical infrastructure sites close to inundation corridors leave little margin for error in emergency planning. The projected intensification of heavy rainfall and river floods therefore strengthens the case for anticipatory adaptation, including stricter land-use control in flood-prone zones, upgrading of drainage and protection works, and targeted preparedness plans for neighbourhoods where large numbers of people may become displaced in rare events. At the same time, the more mixed climate signal over western Crete does not imply an absence of risk: historical extremes there are already severe, and even modest percentage increases can translate into substantial additional damage where exposure is high.

The Phase2 assessment also demonstrates the value of replacing pan-European datasets with local information. Using the 2m hazard maps eliminates many of the inconsistencies and omissions identified in Phase1, particularly for small flash-flood-prone catchments that were poorly represented in continental river-flood products. Likewise, switching from OpenStreetMap to Microsoft's building footprints greatly improves the completeness of the building inventory and therefore the plausibility of exposure counts and damage estimates. The use of a building-based population layer, rather than coarse population grids, enables more nuanced estimates of exposed and displaced residents and more realistic computation of expected-annual indicators such as Expected Annual Damage, Expected Annual Exposed Population and Expected Annual Displaced Population for Heraklion.

At the same time, this enhanced realism comes with new challenges. The local hazard maps are themselves the outcome of complex national modelling assumptions (design storms, runoff coefficients, roughness values) that are outside the scope of this report to validate. They also describe present-day conditions only and do not yet reflect potential future changes in land use, urban drainage or defence measures. The building-based approach to population exposure, although spatially detailed, assumes constant occupancy and a uniform density across all buildings. It does not capture seasonal tourism peaks, the presence of basements, nor socially differentiated vulnerability that may strongly influence actual impacts and recovery.

This Phase2 CLIMAAX application confirms that Crete is already experiencing substantial river-flood risk and that, without additional adaptation, this risk is likely to grow, particularly in central and eastern parts of the island. The results provide a solid technical foundation for dialogue with local and regional authorities, helping to identify priority basins, cities and infrastructure systems for detailed studies and early action. Future work should focus on refining local hydraulic modelling in key areas, enriching exposure and vulnerability data, and exploring adaptation pathways that can keep flood risk at acceptable levels under a changing climate.

7 References

Baugh, C., Colonese, J., D'Angelo, C., Dottori, F., Neal, J., Prudhomme, C., Salamon, P., 2024. Global river flood hazard maps. European Commission, Joint Research Centre (JRC).

Beck, H.E., Wood, E.F., Pan, M., Fisher, C.K., Miralles, D.G., Dijk, A.I.J.M. van, McVicar, T.R., Adler, R.F., 2019. MSWEP V2 Global 3-Hourly 0.1° Precipitation: Methodology and Quantitative Assessment. Bull. Am. Meteorol. Soc. 100, 473–500. https://doi.org/10.1175/BAMS-D-17-0138.1

Diakakis, M., Mavroulis, S., Deligiannakis, G., 2012. Floods in Greece, a statistical and spatial approach. Nat. Hazards 62, 485–500. https://doi.org/10.1007/s11069-012-0090-z

EL13 Flood Risk Management Plan for Crete, 2024.

E-OBS, 2020. E-OBS daily gridded meteorological data for Europe from 1950 to present derived from in-situ observations [WWW Document]. https://doi.org/10.24381/cds.151d3ec6

Flocas, H.A., Tsanis, I.K., Katavoutas, G., Kouroutzoglou, J., Iordanidou, V., Alexakis, D.D., 2017. Climatological aspects of cyclonic tracks associated with flood events in Crete, Greece. Theor. Appl. Climatol. 130, 1163–1174. https://doi.org/10.1007/s00704-016-1946-z

Huizinga, J., De, M.H., Szewczyk, W., 2017. Global flood depth-damage functions: Methodology and the database with guidelines [WWW Document]. JRC Publ. Repos. https://doi.org/10.2760/16510

Koutroulis, A.G., Tsanis, I.K., Daliakopoulos, I.N., 2010. Seasonality of floods and their hydrometeorologic characteristics in the island of Crete. J. Hydrol. 394, 90–100. https://doi.org/10.1016/J.JHYDROL.2010.04.025

Lagouvardos, K., Dafis, S., Giannaros, C., Karagiannidis, A., Kotroni, V., 2020. Investigating the Role of Extreme Synoptic Patterns and Complex Topography During Two Heavy Rainfall Events in Crete in February 2019. Climate 8, 87. https://doi.org/10.3390/cli8070087

Lagouvardos, K., Kotroni, V., Bezes, A., Koletsis, I., Kopania, T., Lykoudis, S., Mazarakis, N., Papagiannaki, K., Vougioukas, S., 2017. The automatic weather stations NOANN network of the National Observatory of Athens: operation and database. Geosci. Data J. 4, 4–16. https://doi.org/10.1002/gdj3.44

microsoft/GlobalMLBuildingFootprints, 2025.

Muñoz-Sabater, J., Dutra, E., Agustí-Panareda, A., Albergel, C., Arduini, G., Balsamo, G., Boussetta, S., Choulga, M., Harrigan, S., Hersbach, H., Martens, B., Miralles, D.G., Piles, M., Rodríguez-Fernández, N.J., Zsoter, E., Buontempo, C., Thépaut, J.-N., 2021. ERA5-Land: a state-of-the-art global reanalysis dataset for land applications. Earth Syst. Sci. Data 13, 4349–4383. https://doi.org/10.5194/essd-13-4349-2021

Sarchani, S., Tsanis, I., 2019. Analysis of a Flash Flood in a Small Basin in Crete. Water 11, 2253. https://doi.org/10.3390/w11112253

Schiavina, M., Freire, S., Carioli, A., MacManus, K., 2023. GHS-POP R2023A - GHS population grid multitemporal (1975-2030). European Commission, Joint Research Centre (JRC). https://doi.org/10.2905/2FF68A52-5B5B-4A22-8F40-C41DA8332CFE

Varotsos, K.V., Katavoutas, G., Kitsara, G., Karali, A., Lemesios, I., Patlakas, P., Hatzaki, M., Tenentes, V., Sarantopoulos, A., Psiloglou, B., Koutroulis, A.G., Grillakis, M.G., Giannakopoulos, C., 2025. CLIMADAT-GRid: a high-resolution daily gridded precipitation and temperature dataset for Greece. Earth Syst. Sci. Data 17, 4455–4477. https://doi.org/10.5194/essd-17-4455-2025

Ward, P.J., Winsemius, H.C., Kuzma, S., Bierkens, M.F.P., Bouwman, A., Moel, H.D., Loaiza, A.D., Eilander, D., Englhardt, J., Erkens, G., Gebremedhin, E.T., Iceland, C., Kooi, H., Ligtvoet, W., Muis, S., Scussolini, P., Sutanudjaja, E.H., Beek, R.V., Bemmel, B.V., Huijstee, J.V., Rijn, F.V., Wesenbeeck, B.V., Vatvani, D., Verlaan, M., Tiggeloven, T., Luo, T., 2020. Aqueduct Floods Methodology.

8 Appendix

Flood Hazard maps of the ten focus areas (1–10 in Figure 3-1) used in the second-phase flood risk assessment in Crete.

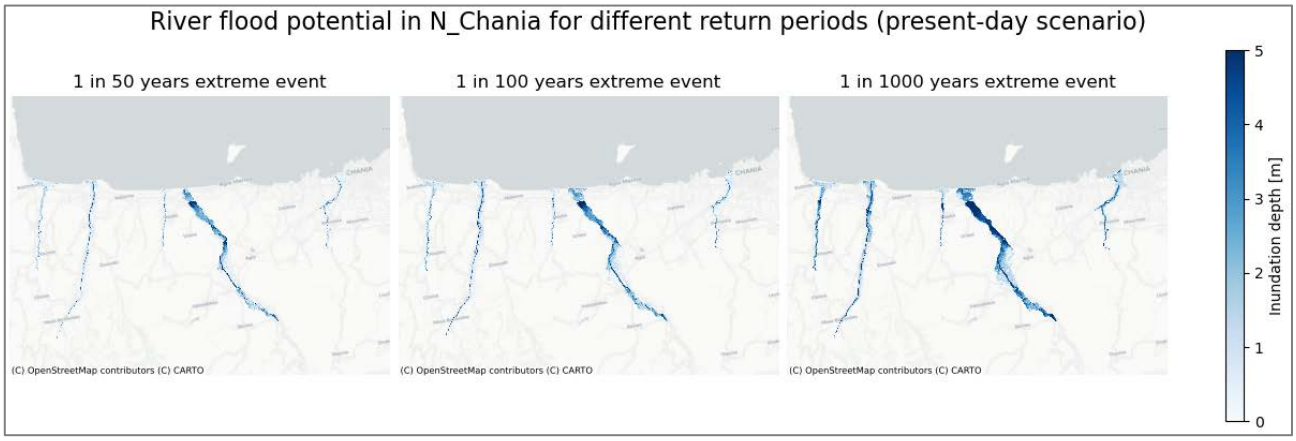

Figure 8-1 River flood potential in [1] Skoutelonas (Tavronitis), [2] Gerani (Keritis), [3] Kladisos, for different return periods (present-day scenario).

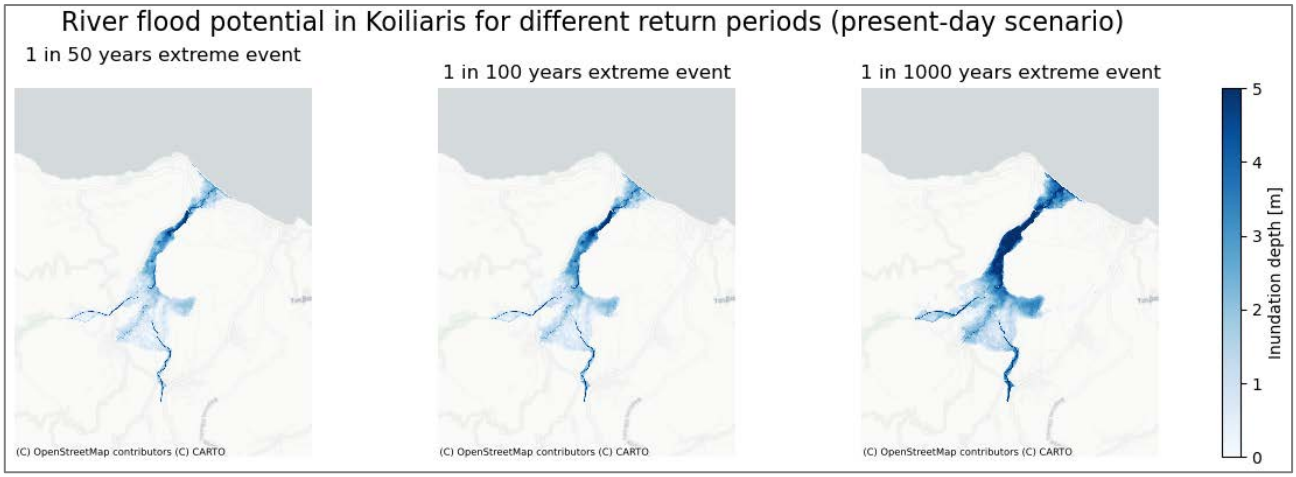

Figure 8-2 River flood potential in [4] Koiliaris, for different return periods (present-day scenario).

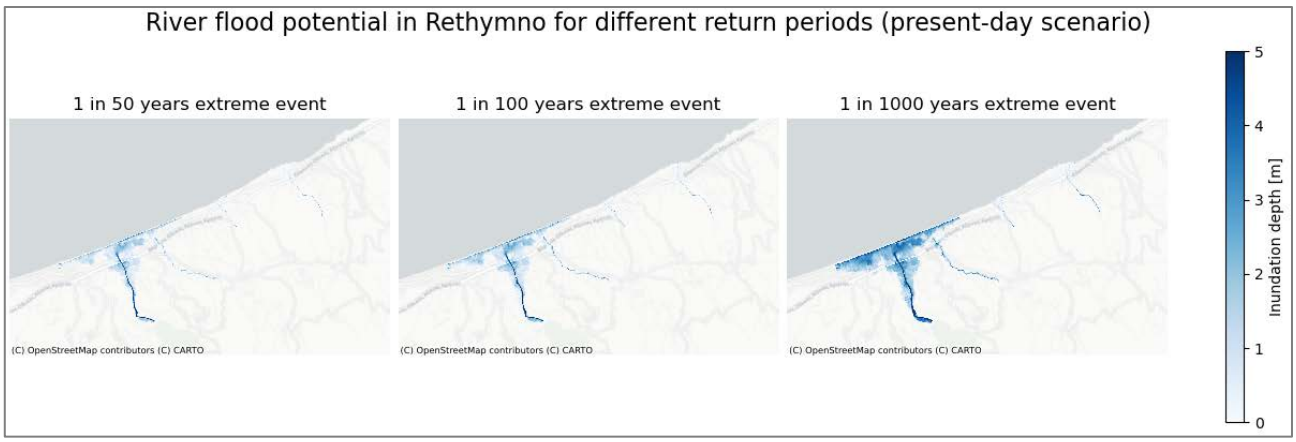

Figure 8-3 River flood potential in [5] Rethymno, for different return periods (present-day scenario).

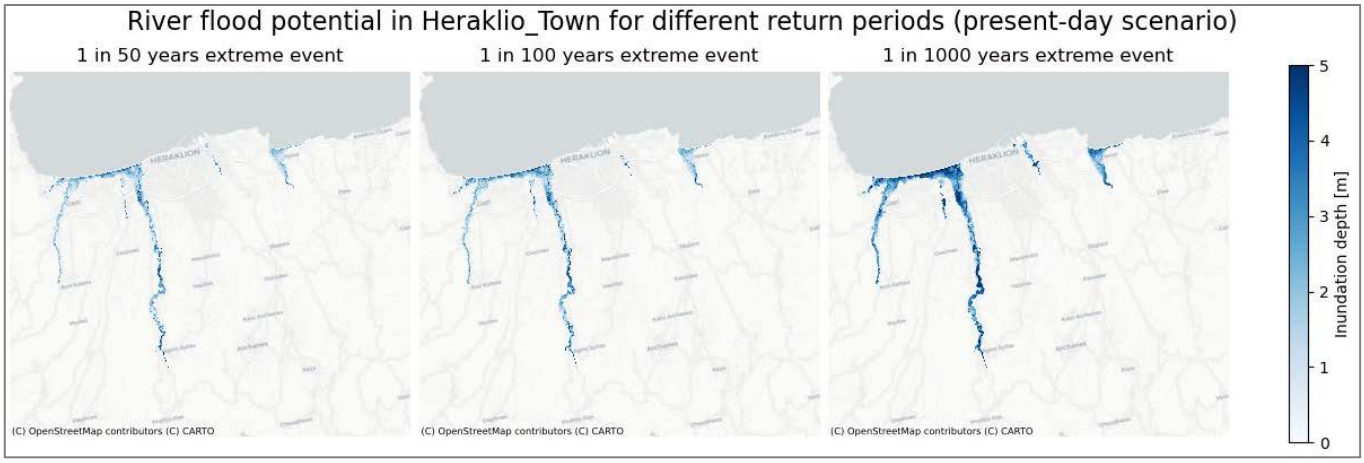

Figure 8-4 River flood potential in [6] Heraklio, for different return periods (present-day scenario).

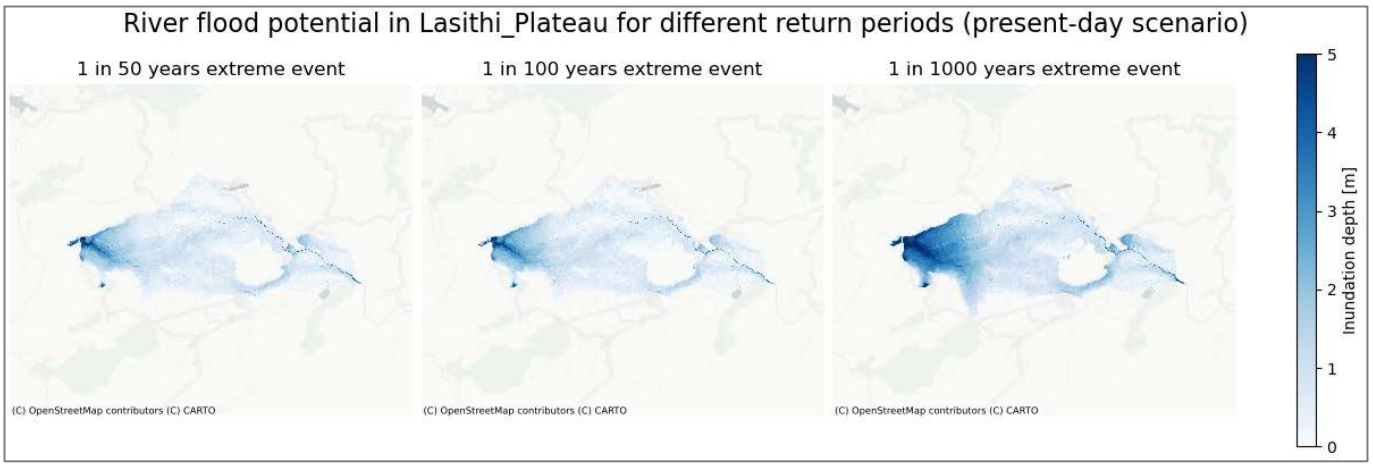

Figure 8-5 River flood potential in [7] Lasithi Plateau, for different return periods (present-day scenario).

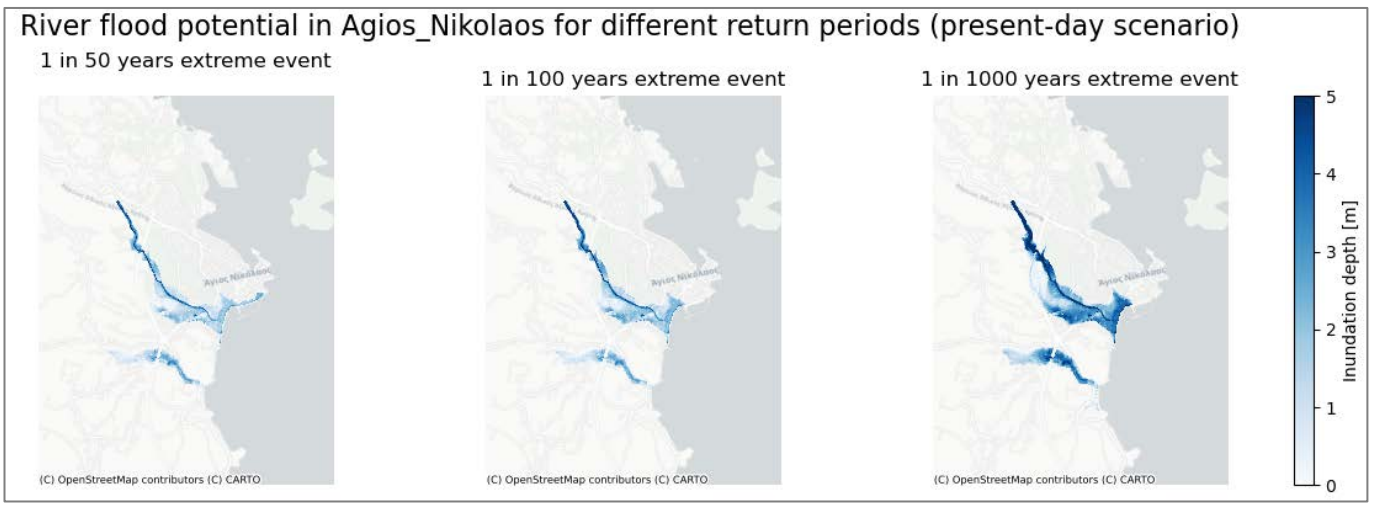

Figure 8-6 River flood potential in [8] Agios Nikolaos, for different return periods (present-day scenario).

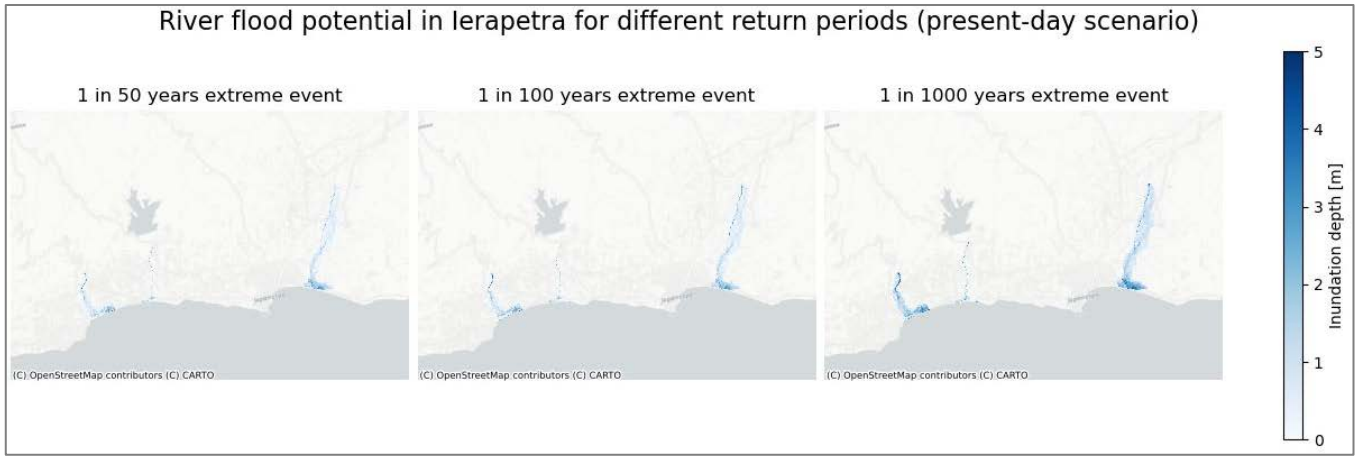

Figure 8-7 River flood potential in [9] Ierapetra, for different return periods (present-day scenario).

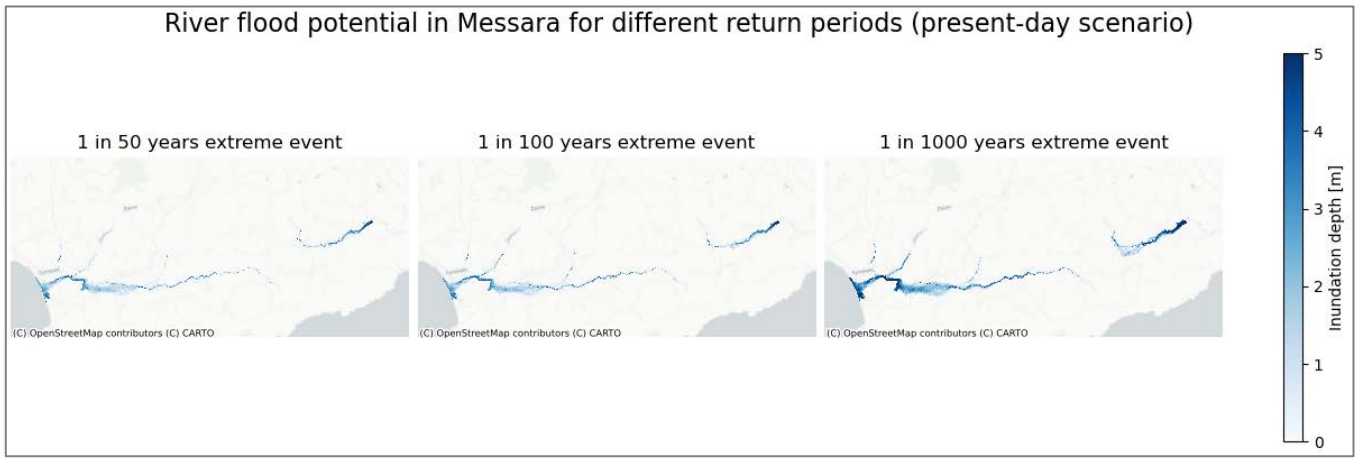

Figure 8-8 River flood potential in [10] Messara, for different return periods (present-day scenario).

Table 8-1 Catalogue of selected flood events in Crete used to define impact rainfall thresholds and to support the extreme precipitation analysis. For each event the table reports date, location, reported precipitation and duration, daily rainfall from CLIMADAT grid, MSWEP, E-OBS, ERA5-Land and local stations for the event day and the surrounding days (−1, +1), estimated RP50/RP100/RP1000 24-h rainfall from national IDF curves, impact severity class, and a brief description of observed impacts.

					CLIMADATGRid			MSWEP			EOBS			ERA5L			Station based			Official national IDF curves scaled at basin		
No	Date	Location	Precipitation (reports for closest stations of NOANN network)	Duration of event (d)	-1	0	1	-1	0	1	-1	0	1	-1	0	1	-1	0	1	RP50	RP100	RP1000
1	26/1/2003	Ierapetra	57 (3h)	2	2.0	13.8	27.6	0.6	58.7	3.7	1.4	41.4	5.5	0.0	12.4	0.0	-	-	-	157.6	185.9	309.8
2	29/5/2003	Ierapetra	113 (12h)	1	4.6	21.0	36.1	2.4	90.4	0.0	0.0	76.6	0.0	0.1	7.7	1.0	-	-	-	157.6	185.9	309.8
3	12/10/2006	Chania	168	1	28.5	20.9	11.8	98.2	52.9	3.8	-	-	-	4.0	19.4	9.9	-	-	-	241.8	284.6	472.0
4	17/10/2006	Chania	151	2	8.0	150.3	48.7	1.8	133.1	73.9	-	-	-	0.0	52.5	10.5				241.8	284.6	472.0
5	17/10/2006	Heraklio		0	7.7	46.6	19.3	1.4	39.8	37.8	-	-	-	0.1	24.8	4.2	10.0	63.0	45.5	146.6	172.2	284.2
6	17/10/2006	Oropedio		0	17.0	36.0	15.7	1.8	47.2	44.8	0.0	7.3	61.6	0.0	23.1	1.3				204.1	240.5	399.7
7	3/12/2013	Heraklio	50.8 (Knossos), 46.2 (W Heraklio)	2	5.1	20.3	12.0	0.2	33.6	18.1	-	-	-	0.4	10.2	2.2	0.0	82.0	39.5	146.6	172.2	284.2
8	29/10/2014	Heraklio	31.6 (0.5h)	1	13.0	5.4	4.4	8.8	17.3	15.5	-	-	-	1.2	6.3	3.1	18.0	9.5	1.0	146.6	172.2	284.2
9	12/1/2015	Profitis Ilias	101.2 (Stavrakia)	2	1.4	19.2	44.9	0.3	9.1	73.7	-	-	-	0.0	0.8	11.0	0.0	25.5	72.3	146.2	171.7	283.2
10	11/2/2017	Chania	92.2 (Kentro)	1	12.7	21.0	2.9	44.8	46.2	1.1	-	-	-	2.0	16.7	1.3	-	-	-	241.8	284.6	472.0
11	11/2/2017	Chania	105 (Kolymvari)	1	12.7	21.0	2.9	44.8	46.2	1.1	-	-	-	2.0	16.7	1.3	-	-	-	241.8	284.6	472.0
12	23/10/2017	Chania	192 (Kentro)	4	0.0	14.5	10.3	0.0	5.9	2.4	-	-	-	0.0	0.0	1.6	-	-	-	240.9	283.8	471.5
13	23/10/2017	Platanias	242	4	0.0	14.5	10.3	0.0	5.9	2.4	-	-	-	0.0	0.0	1.6	-	-	-	240.9	283.8	471.5
14	13/2/2019	Platanias	88.2	4	23.0	99.8	47.9	1.8	79.6	52.1	-	-	-	1.3	15.0	14.1	0.0	180.0	50.0	270.9	318.9	529.3
15	13/2/2019	Moires		0	22.2	26.4	25.4	4.6	19.8	18.9	-	-	-	0.1	9.2	4.1	8.5	4.0	7.0	133.0	156.2	257.7
16	13/2/2019	Kare	243.6 (Fourfouras)	4	22.6	50.7	34.0	2.4	71.6	47.3	-	-	-	0.1	16.4	9.1	28.0	46.6	65.4	182.4	214.1	353.1
17	12/11/2019	Alikianos	87	3	0.0	3.4	91.8	0.0	2.5	54.8	-	-	-	0.4	0.0	26.0	-	-	-	270.9	318.9	529.3
18	20/10/2020	Karteros	205.8	3	-	-	-	11.8	55.9	78.1	-	-	-	5.1	20.3	2.1	0.6	95.3	164.3	143.3	168.6	279.0
19	7/11/2020	Oropedio	314 (Tzermiado), 169 (Potamoi)	1	-	-	-	44.3	19.9	0.0	-	-	-	2.4	1.1	0.0	-	-	-	204.1	240.5	399.7

Table 8-2 Catalogue of selected flood events in Crete used to define impact rainfall thresholds (from Table 8-1). For each event the table reports impact severity class, and a brief description of observed impacts.

No	Date	Location	Fatalities	Impact intensity	Description
1	26/1/2003	Ierapetra	0	3	Flash-floods and windstorms caused damages in Ierapetra, where many greenhouses were destroyed. Three people drowned due to seagale in the port of Kasteli, Chania.
2	29/5/2003	Ierapetra	1	3	Intense thunderstorms in Ierapetra, where a person drowned when a stream overflowed.
3	12/10/2006	Chania	0	2	Storms along with flash-floods were noted in Chania.
4	17/10/2006	Chania	0	3	Storms caused severe damage in Crete and the Dodecanese islands.
5	17/10/2006	Heraklio	0	3	Storms caused severe damage in Crete and the Dodecanese islands.
6	17/10/2006	Oropedio	0	3	Storms caused severe damage in Crete and the Dodecanese islands.
7	3/12/2013	Heraklio	0	2	Flash-floods and windstorms caused landslides in Kissamos, Chania and Heraclion.
8	29/10/2014	Heraklio	0	1	Over 70 calls for flooding in buildings in Heraclion induced by intense storm.
9	12/1/2015	Profitis Ilias	0	3	15 people were rescued and 45 freed in Heraclion during intense thunderstorm. Landslides, flash-floods, falling trees and power outages in Crete.
10	11/2/2017	Chania	0	2	Rainstorm caused flash floods in Chania city and the cavalier of the venetian bastion collapse. A car was destroyed. Landslides at the provincial road in Kolympari, Chania.
11	11/2/2017	Chania	0	2	Rainstorm caused flash floods in Chania city and the cavalier of the venetian bastion collapse. A car was destroyed. Landslides at the provincial road in Kolympari, Chania.
12	23/10/2017	Chania	0	3	The low pressure system called 'Daedalus' causes severe flash-floods and landslides in Chania. Greenhouses ruined in Vaenia (Ierapetra).
13	23/10/2017	Platanias	0	3	The low pressure system called 'Daedalus' causes severe flash-floods and landslides in Chania. Greenhouses ruined in Vaenia (Ierapetra).
14	13/2/2019	Platanias	0	3	Storm 'Chioni': Four people were killed when swept away by the torrent of Geropotamos in Messara, Heraklion. Flooding and damage to local roads in the municipality Platanias, Chania. Landslides in Rethymno.
15	13/2/2019	Moires	4	3	Storm 'Chioni': Four people were killed when swept away by the torrent of Geropotamos in Messara, Heraklion. Flooding and damage to local roads in the municipality Platanias, Chania. Landslides in Rethymno.
16	13/2/2019	Kare	0	3	Storm 'Chioni': Four people were killed when swept away by the torrent of Geropotamos in Messara, Heraklion. Flooding and damage to local roads in the municipality Platanias, Chania. Landslides in Rethymno.
17	12/11/2019	Alikianos	0	3	Storm 'Victoria': Rainfall and strong winds cause problems in Corfu, Kefalonia, Chania, Attica and Rhodes. Flooded homes and shops, road network damage, landslides, power and water outages among the problems.
18	20/10/2020	Karteros	0	3	Rapid rains caused floods, landslides, debris flow and problems in infrastructure and electricity in the northern parts of the prefectures of Heraklion and Chania. People were endangered in Karteros, Heraklion and Souda.
19	7/11/2020	Oropedio	0	2	Heavy rains caused floods and landslides in the Lassithi Plateau and in areas of Kasteli Pediados.

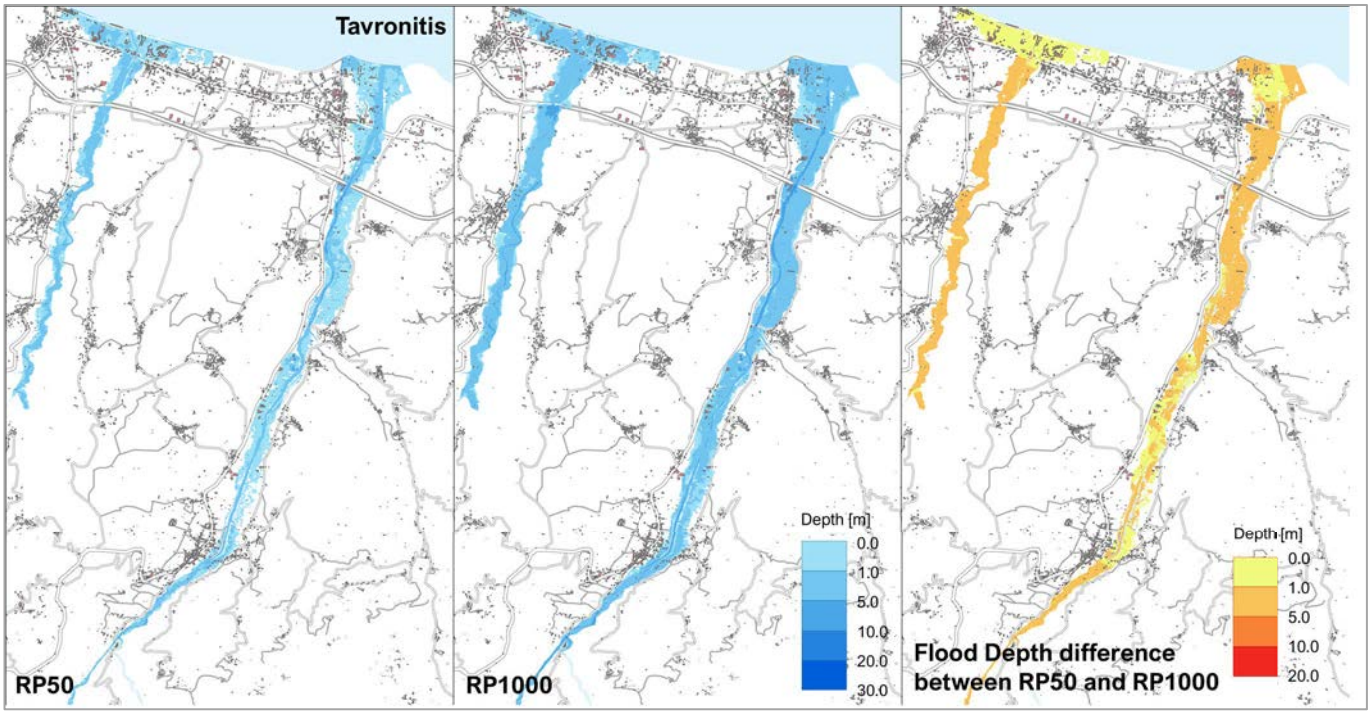

Figure 8-9 River flood hazard in [1] Tavronitis for the present-day climate. The left and middle panels show inundation depth (m) for RP50 and RP1000 events from the 2m flood hazard maps; the right panel presents the difference in water depth between RP50 and RP1000.

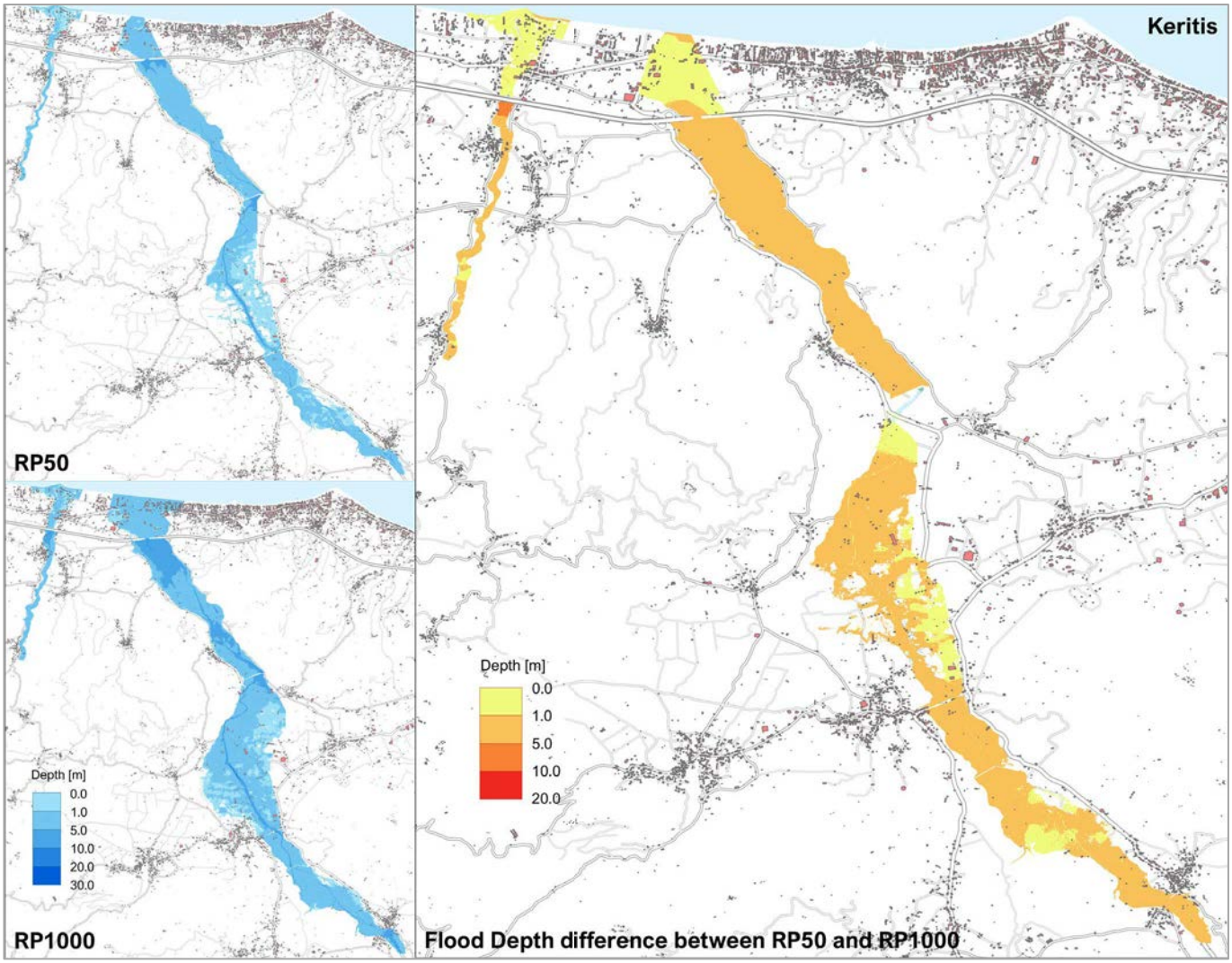

Figure 8-10 River flood hazard in [2] Keritis for the present-day climate. The left and middle panels show inundation depth (m) for RP50 and RP1000 events from the 2m flood hazard maps; the right panel presents the difference in water depth between RP50 and RP1000.

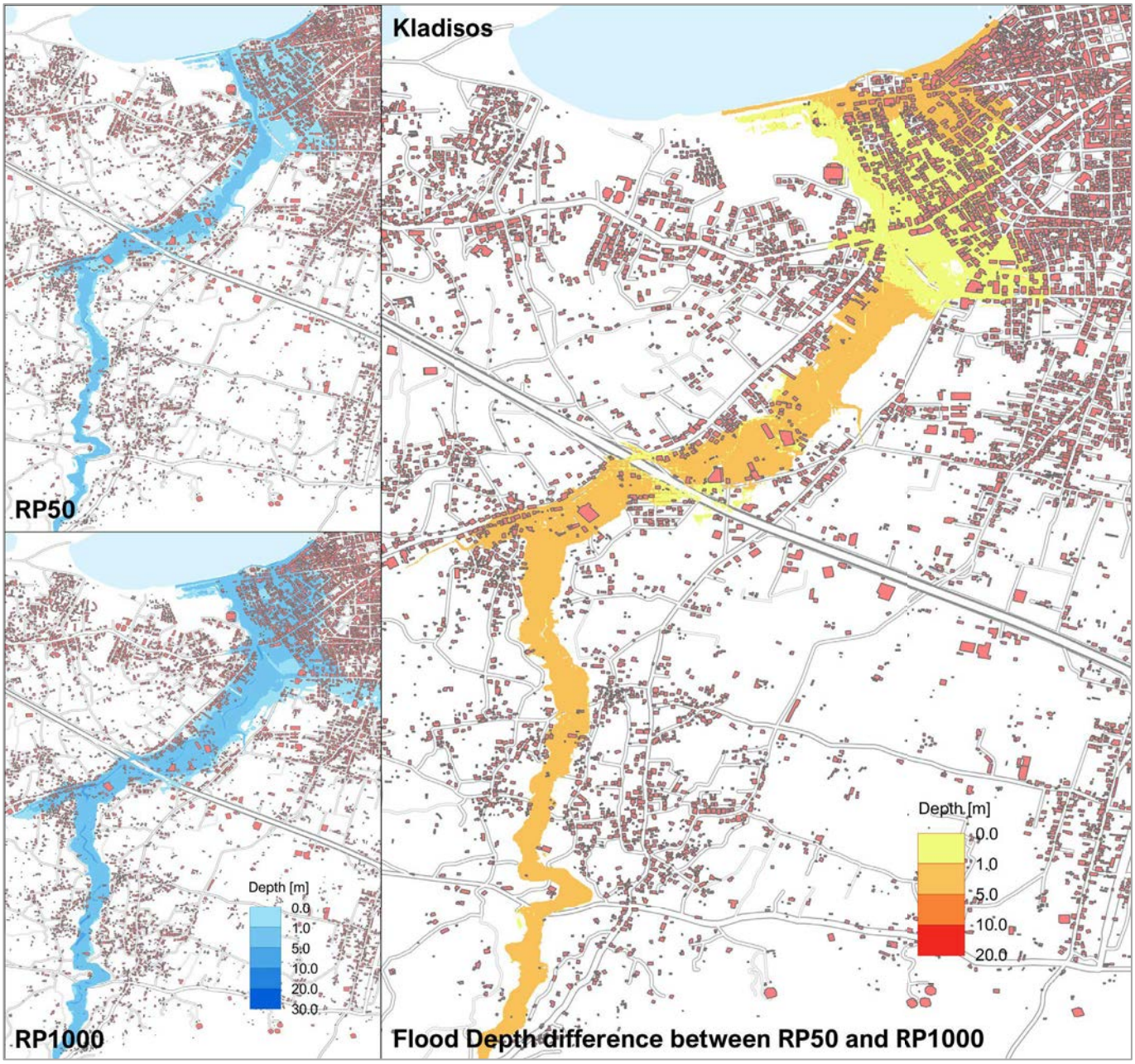

Figure 8-11 River flood hazard in [3] Kladisos for the present-day climate. The left and middle panels show inundation depth (m) for RP50 and RP1000 events from the 2m flood hazard maps; the right panel presents the difference in water depth between RP50 and RP1000.

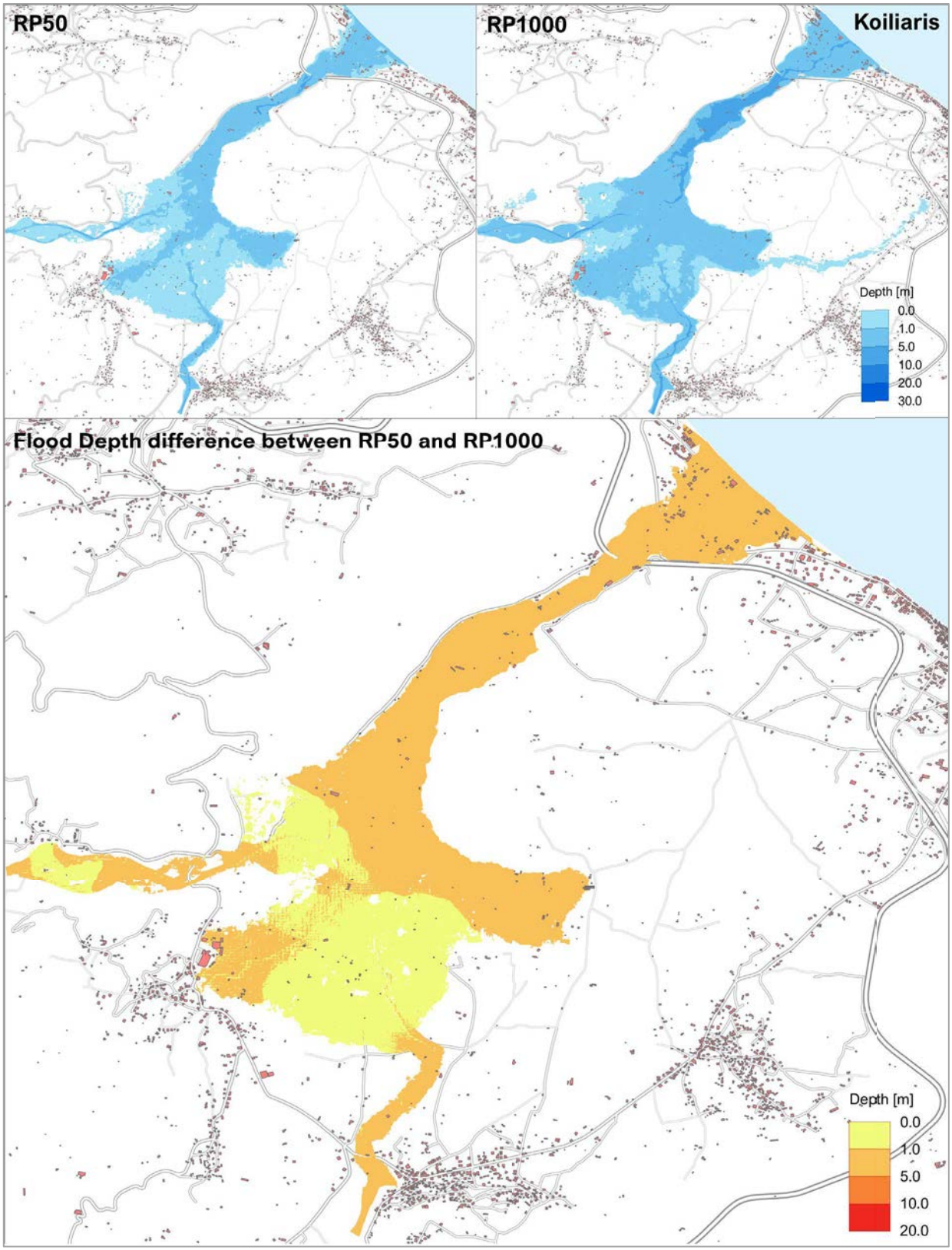

Figure 8-12 River flood hazard in [4] Koiliaris for the present-day climate. The left and middle panels show inundation depth (m) for RP50 and RP1000 events from the 2m flood hazard maps s; the right panel presents the difference in water depth between RP50 and RP1000.

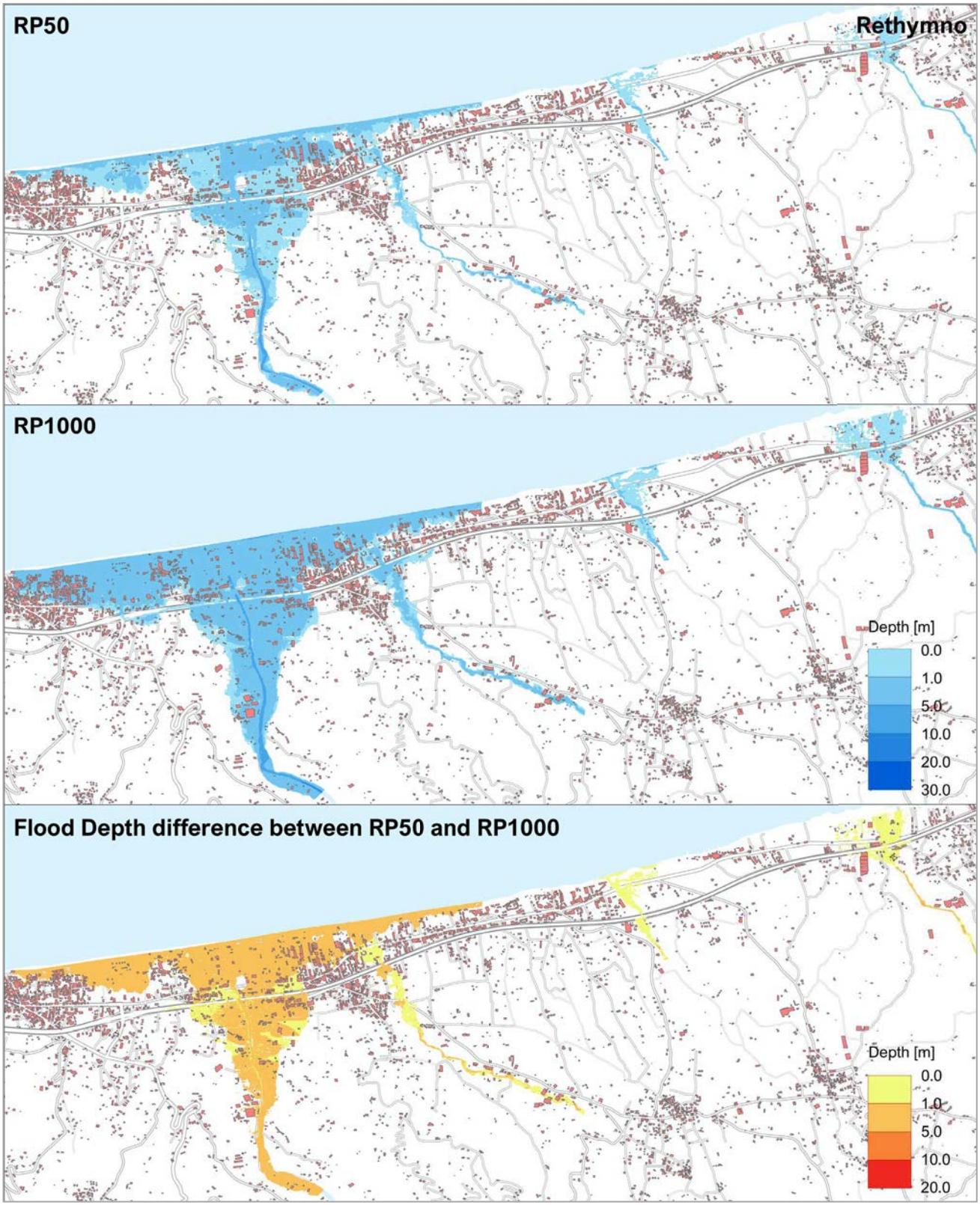

Figure 8-13 River flood hazard in [5] Rethymno for the present-day climate. The left and middle panels show inundation depth (m) for RP50 and RP1000 events from the 2m flood hazard maps; the right panel presents the difference in water depth between RP50 and RP1000.

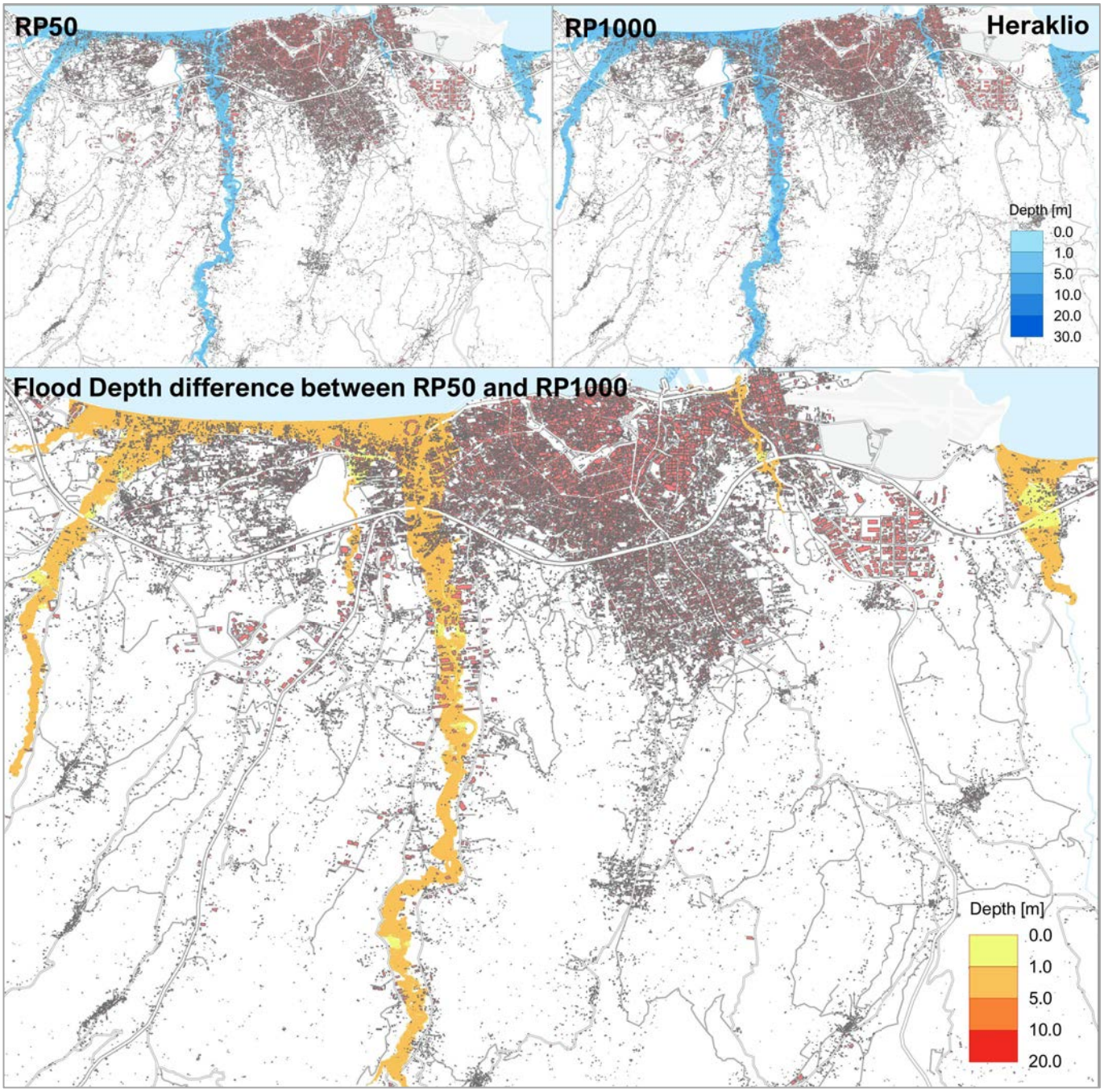

Figure 8-14 River flood hazard in [6] Heraklio for the present-day climate. The left and middle panels show inundation depth (m) for RP50 and RP1000 events from the 2m flood hazard maps; the right panel presents the difference in water depth between RP50 and RP1000.

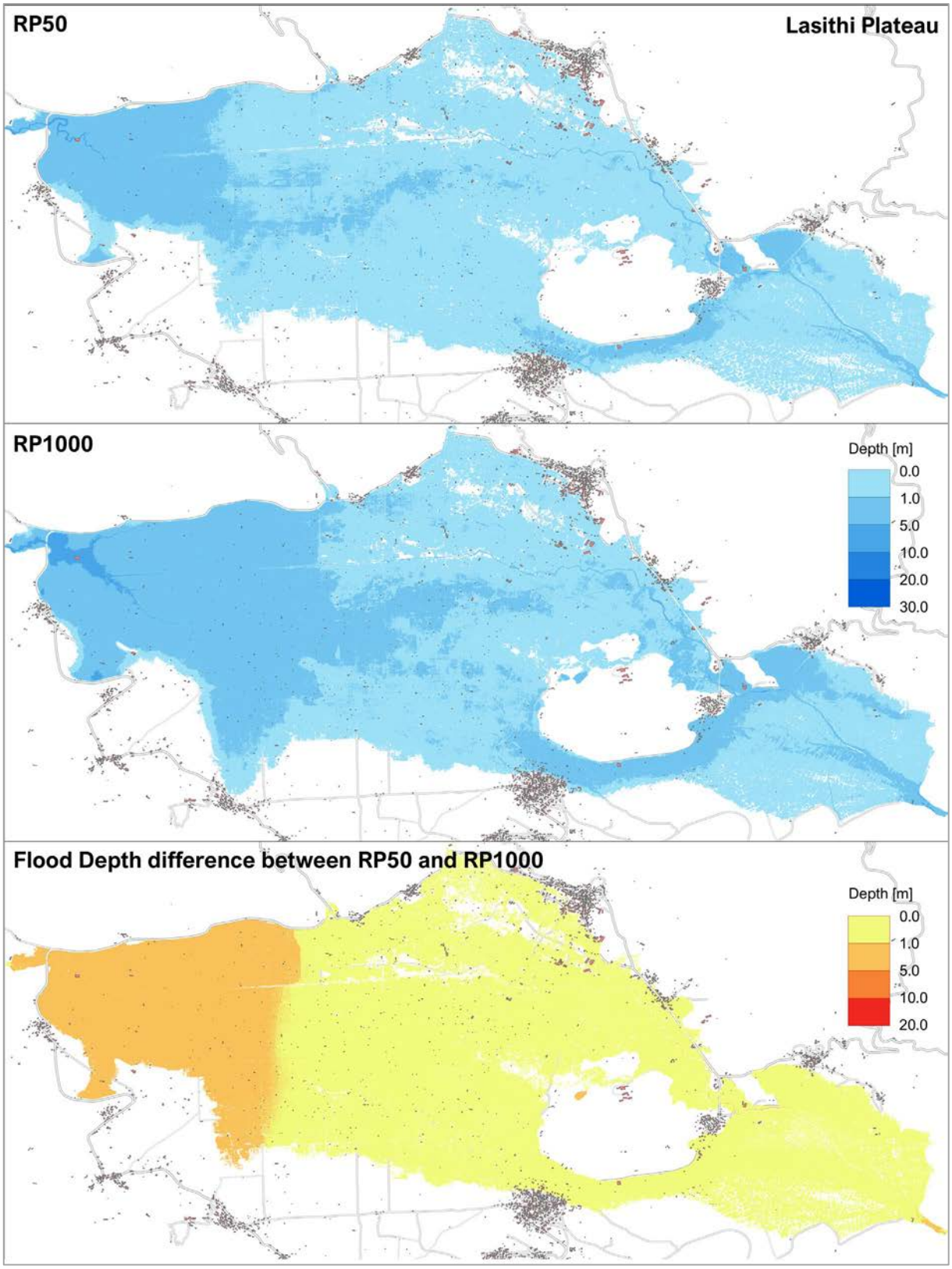

Figure 8-15 River flood hazard in [7] Lasithi Plateau for the present-day climate. The left and middle panels show inundation depth (m) for RP50 and RP1000 events from the 2m flood hazard maps; the right panel presents the difference in water depth between RP50 and RP1000.

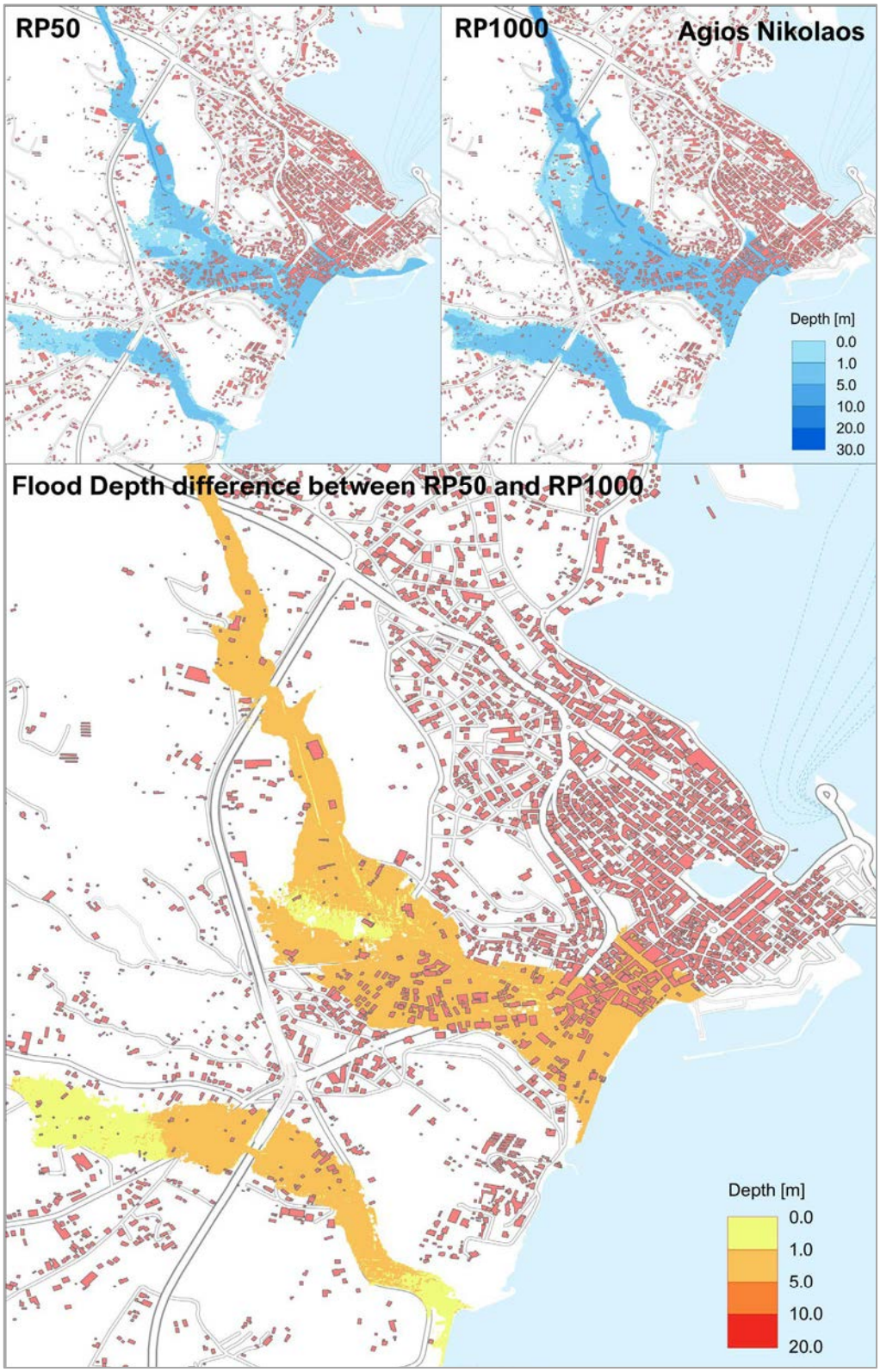

Figure 8-16 River flood hazard in [8] Ag. Nikolaos for the present-day climate. The left and middle panels show inundation depth (m) for RP50 and RP1000 events from the 2m flood hazard maps; the right panel presents the difference in water depth between RP50 and RP1000

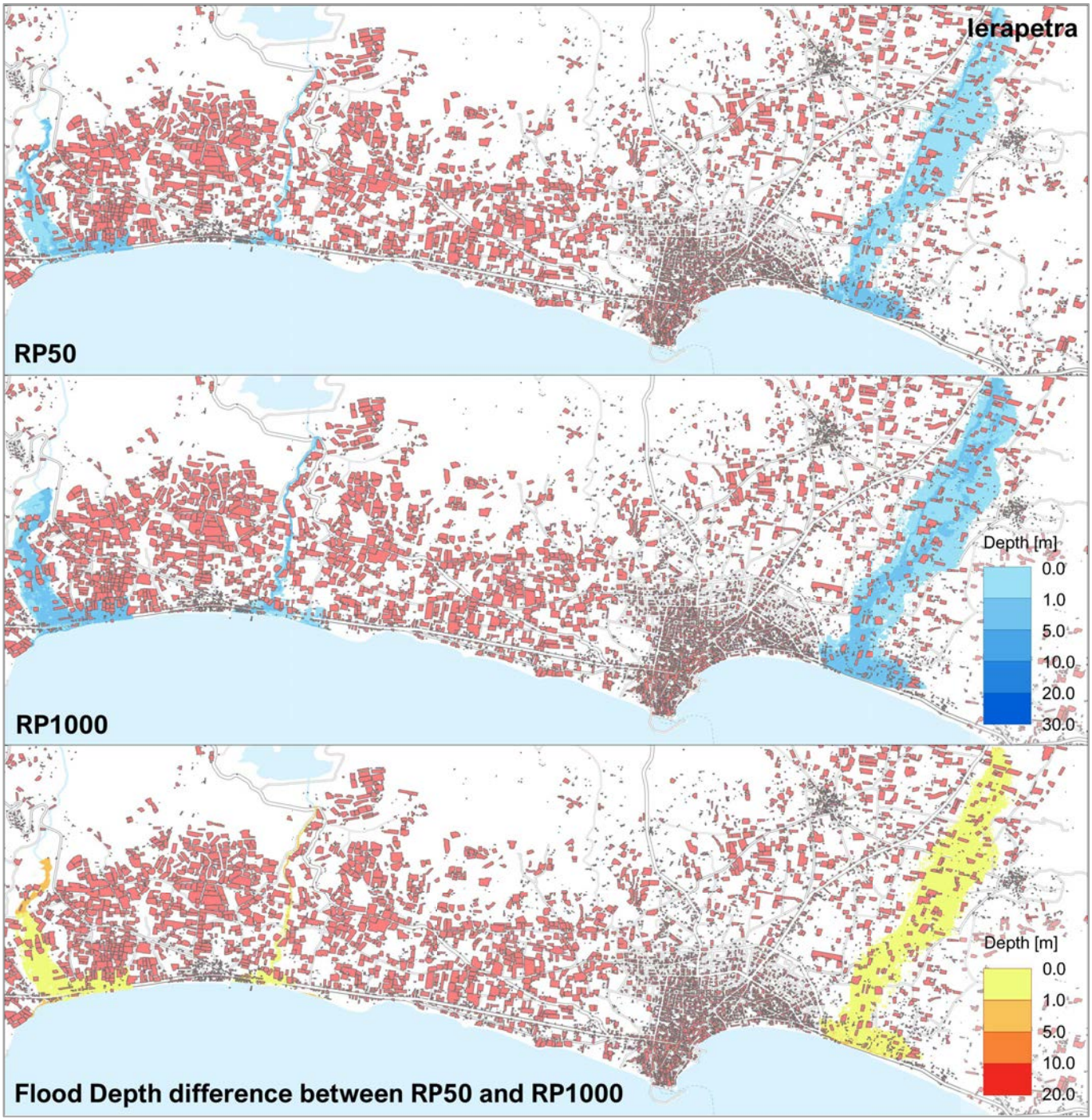

Figure 8-17 River flood hazard in [9] Ierapetra for the present-day climate. The left and middle panels show inundation depth (m) for RP50 and RP1000 events from the 2m flood hazard maps; the right panel presents the difference in water depth between RP50 and RP1000.

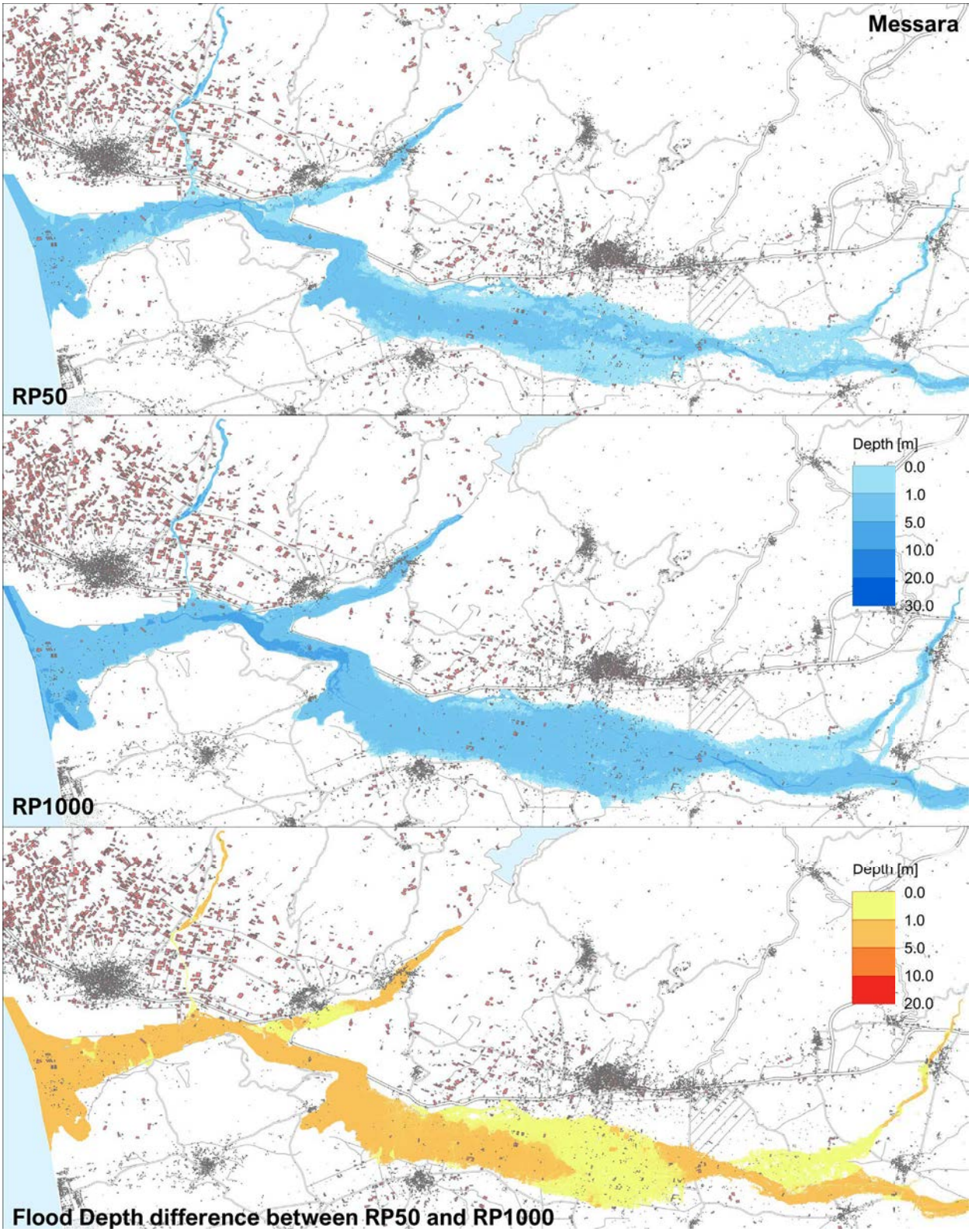

Figure 8-18 River flood hazard in [10] Messara for the present-day climate. The left and middle panels show inundation depth (m) for RP50 and RP1000 events from the 2m flood hazard maps; the right panel presents the difference in water depth between RP50 and RP1000.

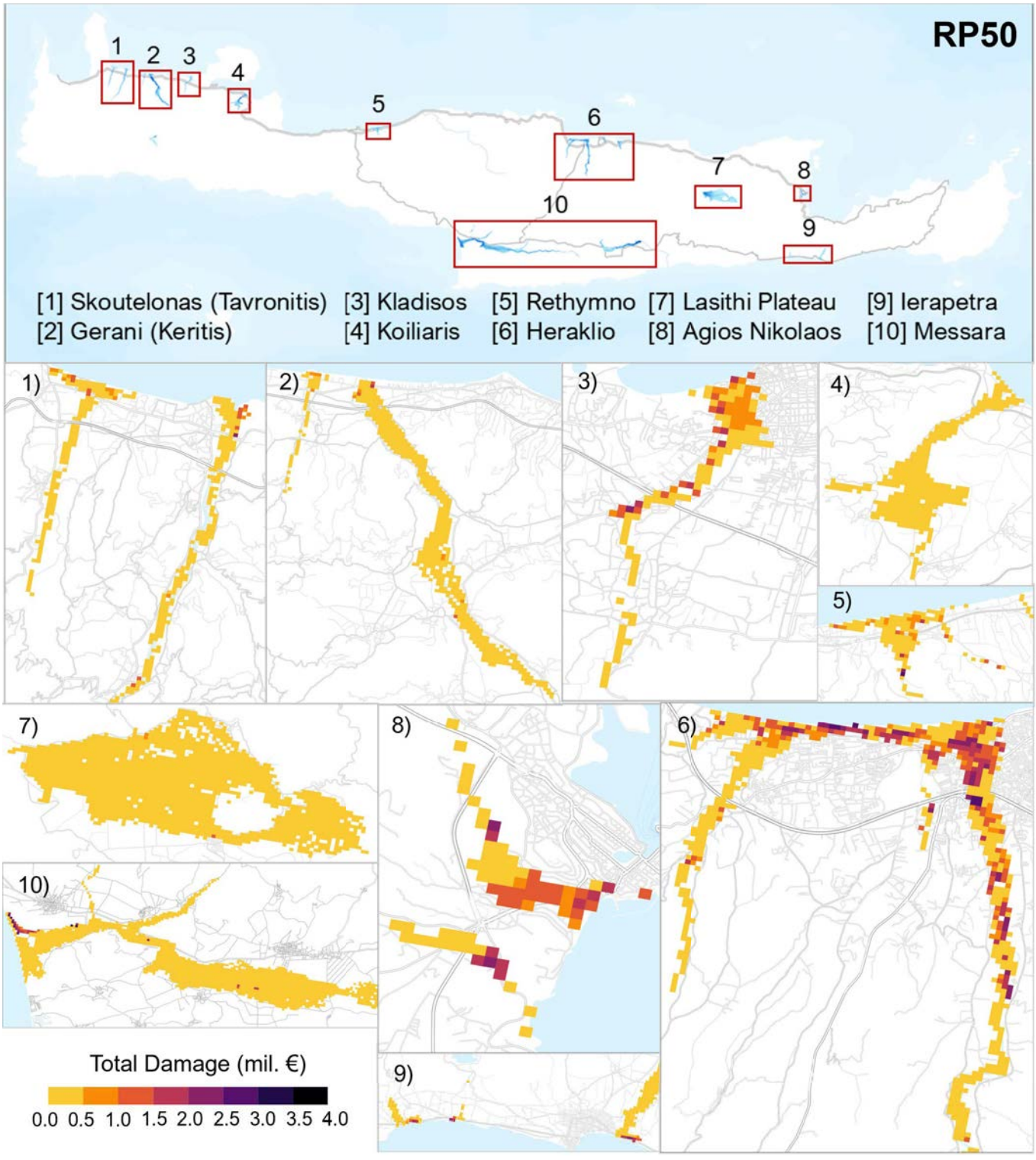

Figure 8-19 Spatial distribution of land-use based flood damage for RP50 in the ten areas of interest.

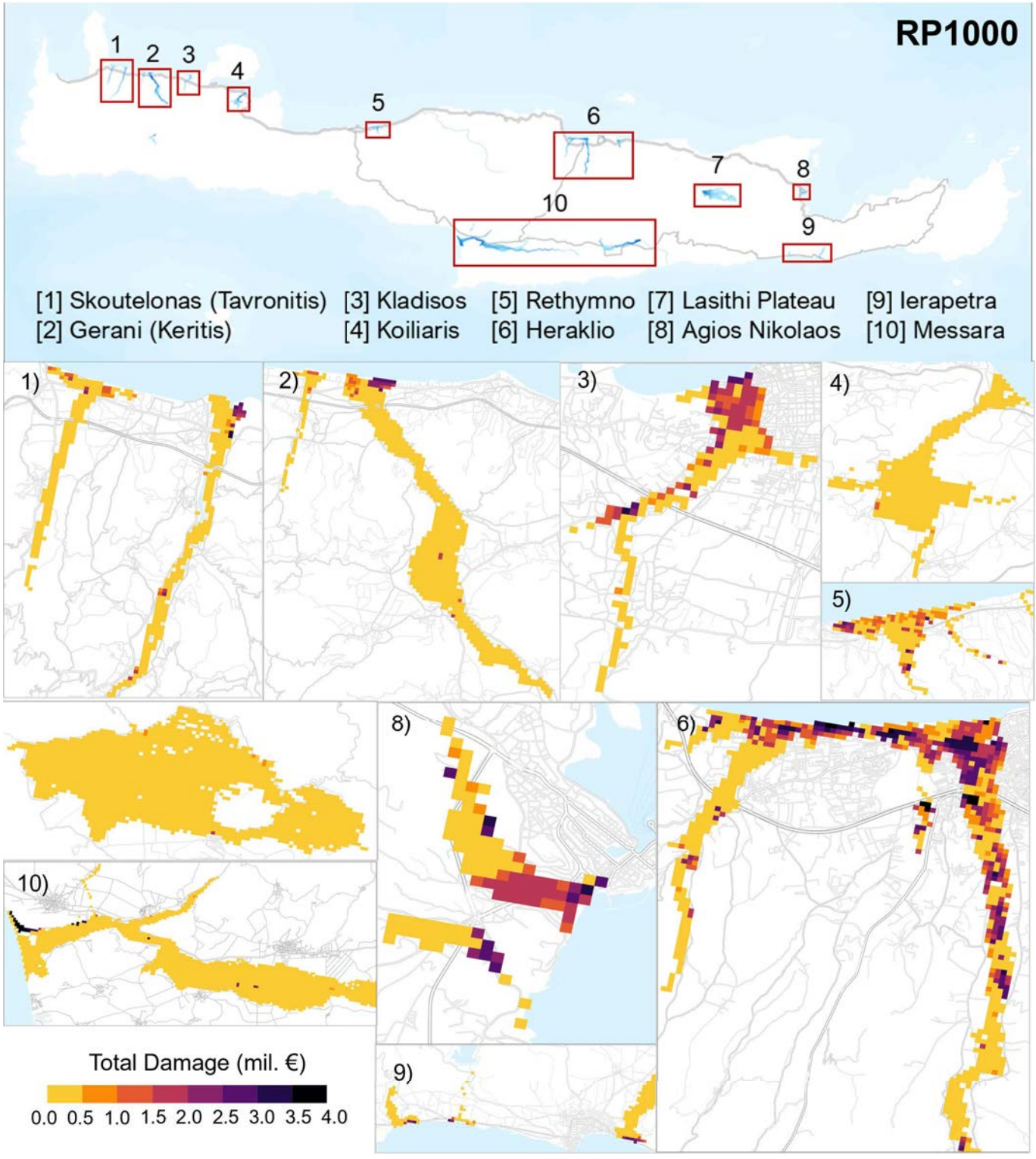

Figure 8-20 Spatial distribution of land-use based flood damage for RP1000 in the ten areas of interest.

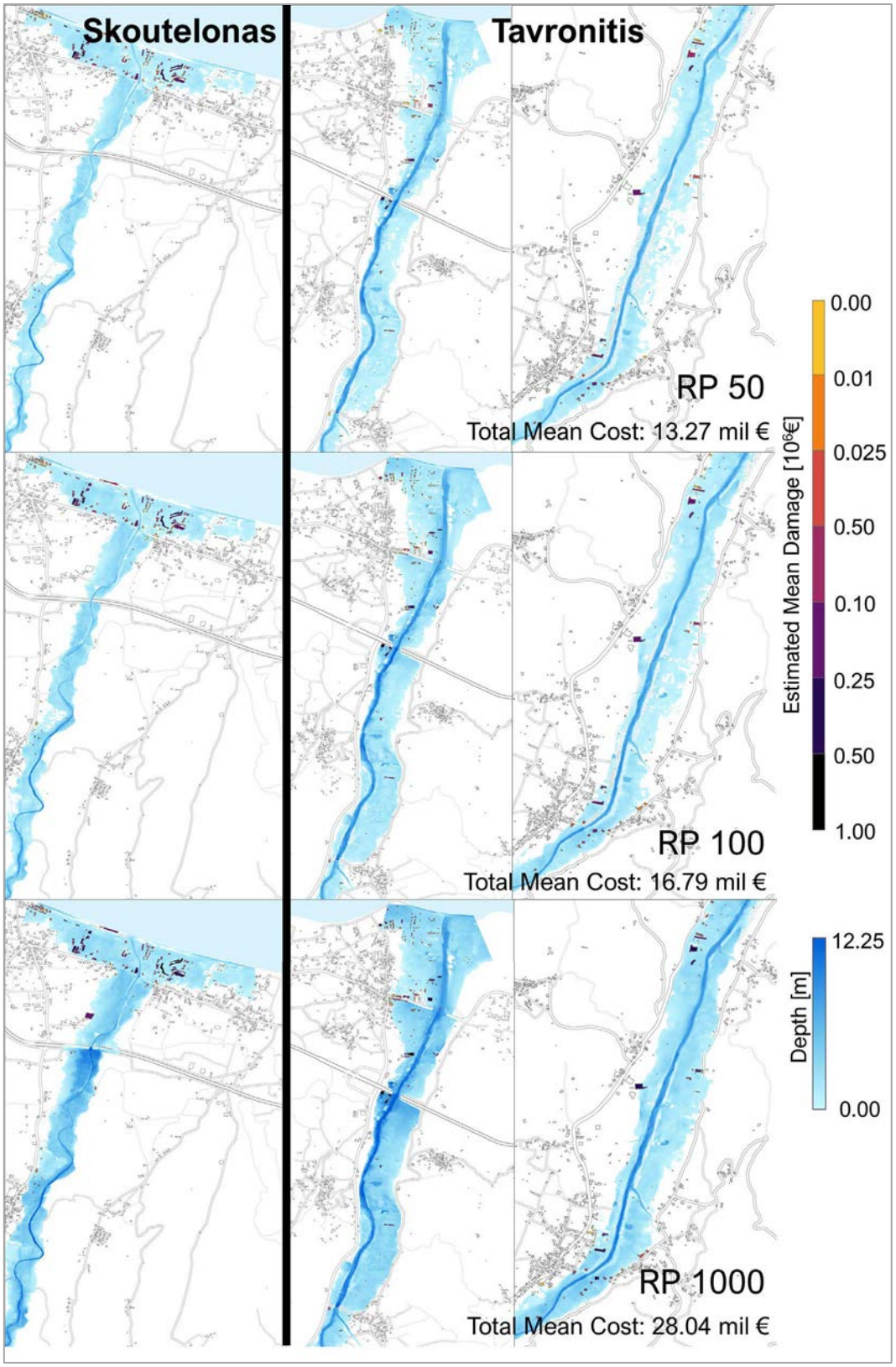

Figure 8-21 Estimated mean direct damage to buildings in Skoutelonas and Tavronitis for RP50, RP100 and RP1000. The figure distinguishes the two neighbouring river corridors, where exposed buildings along the valley floors experience steadily increasing damage with return period.

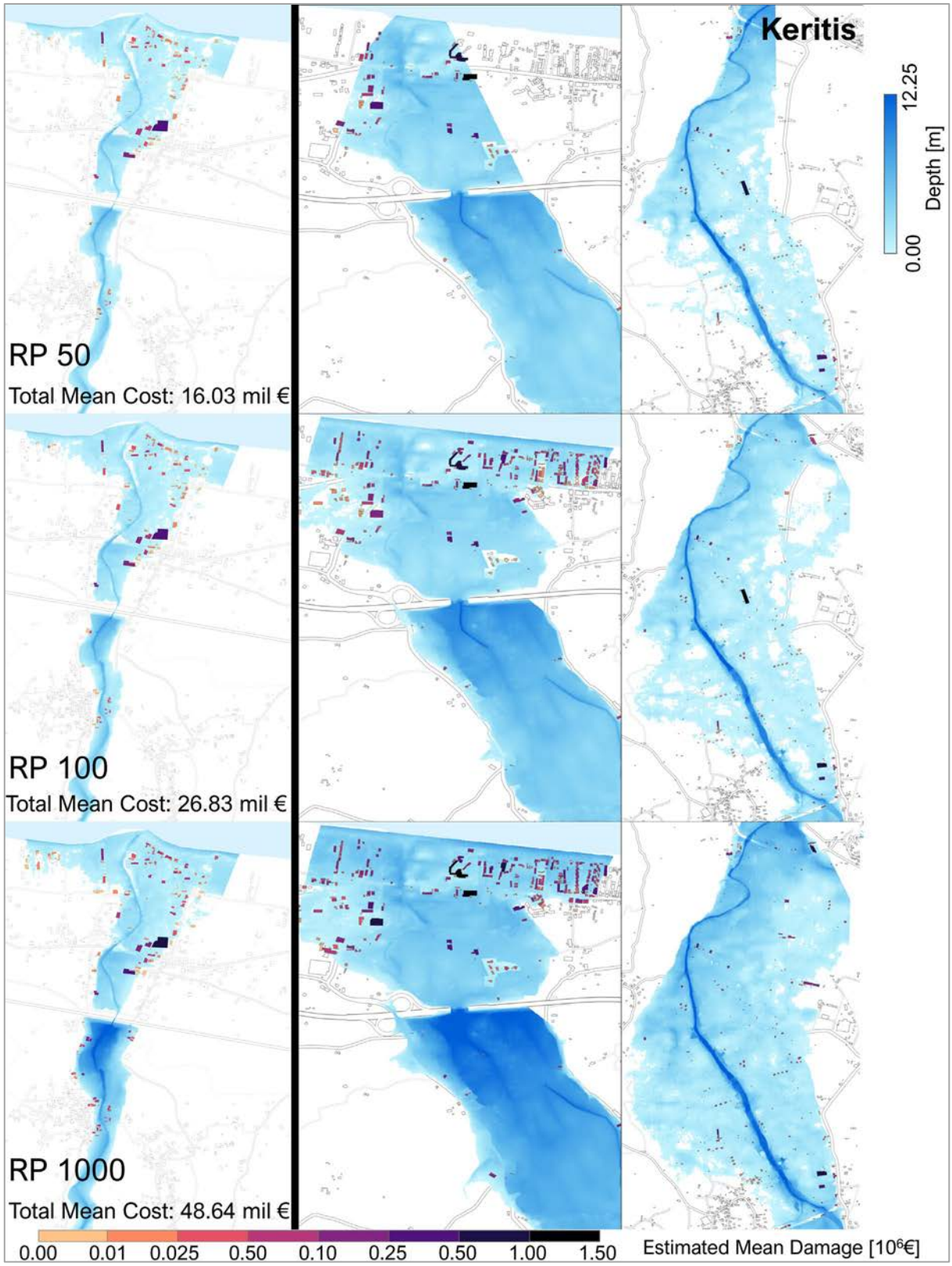

Figure 8-22 Estimated mean direct damage to buildings in the Keritis (Gerani) basin for RP50, RP100 and RP1000. High losses are concentrated near the river mouth and in upstream clusters.

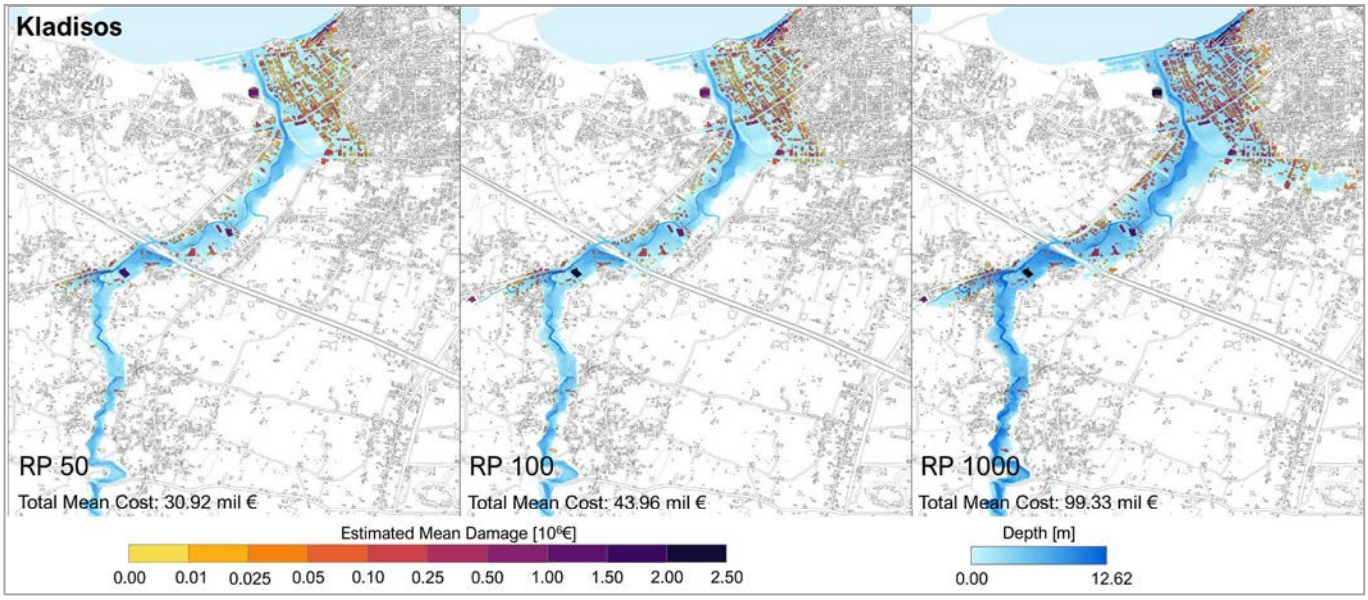

Figure 8-23 Estimated mean direct damage to buildings along the Kladisos river for RP50, RP100 and RP1000. Damage hotspots are located in the urbanised lower reach and near key crossings, with several buildings exceeding €1–2 million of mean damage under RP1000.

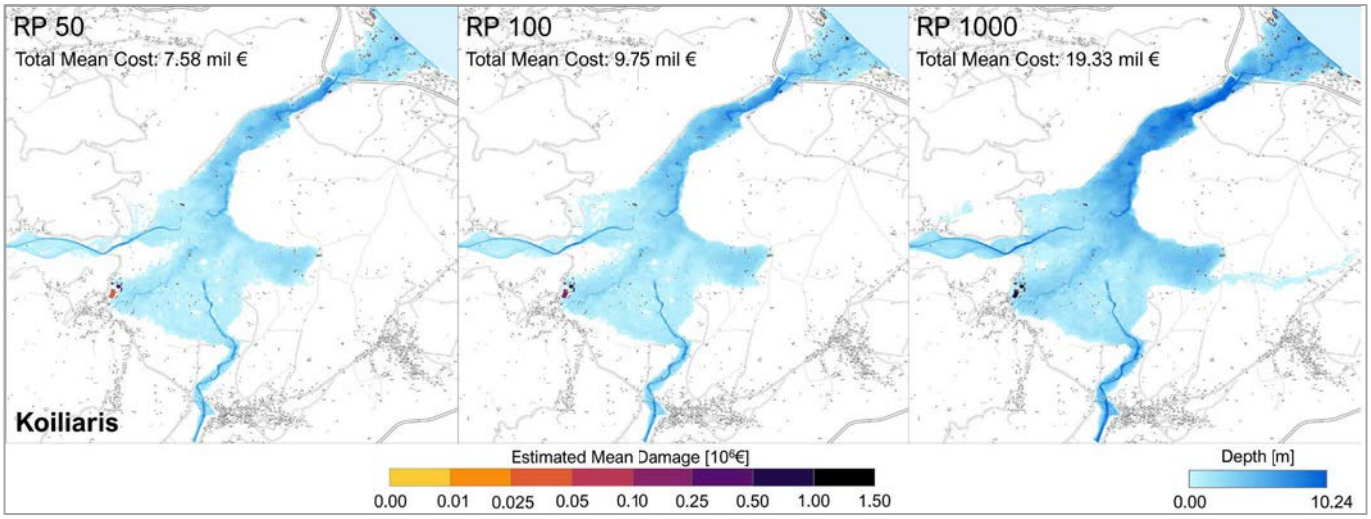

Figure 8-24 stimated mean direct damage to buildings in the Koiliaris basin for RP50, RP100 and RP1000. Although the number of exposed buildings is relatively small, a subset of structures in the lower basin and near the coast show significant damages under RP1000 conditions.

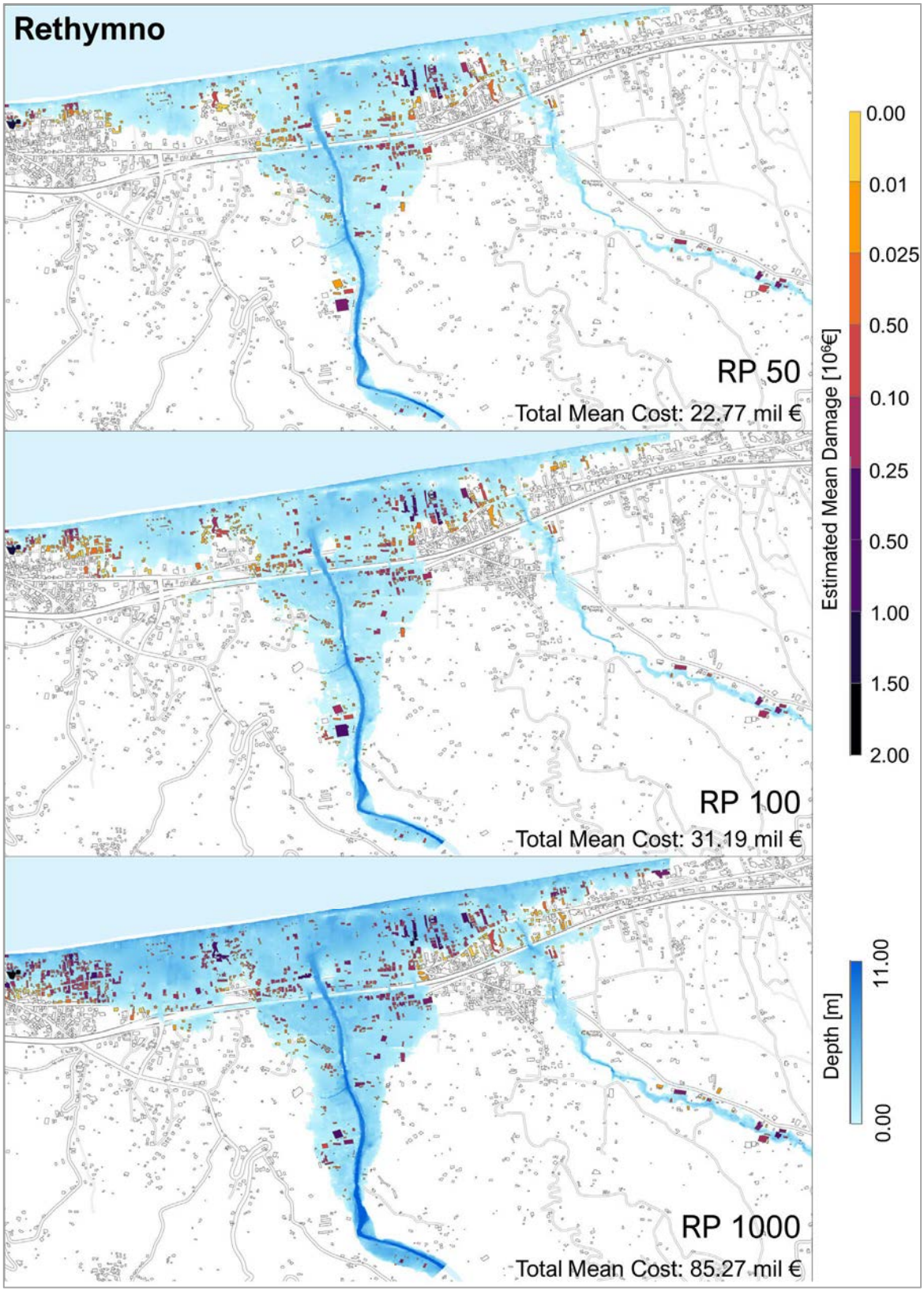

Figure 8-25 Estimated mean direct damage to buildings in Rethymno for RP50, RP100 and RP1000. The maps highlight progressive intensification of damage along the main torrent and adjacent coastal urban area.

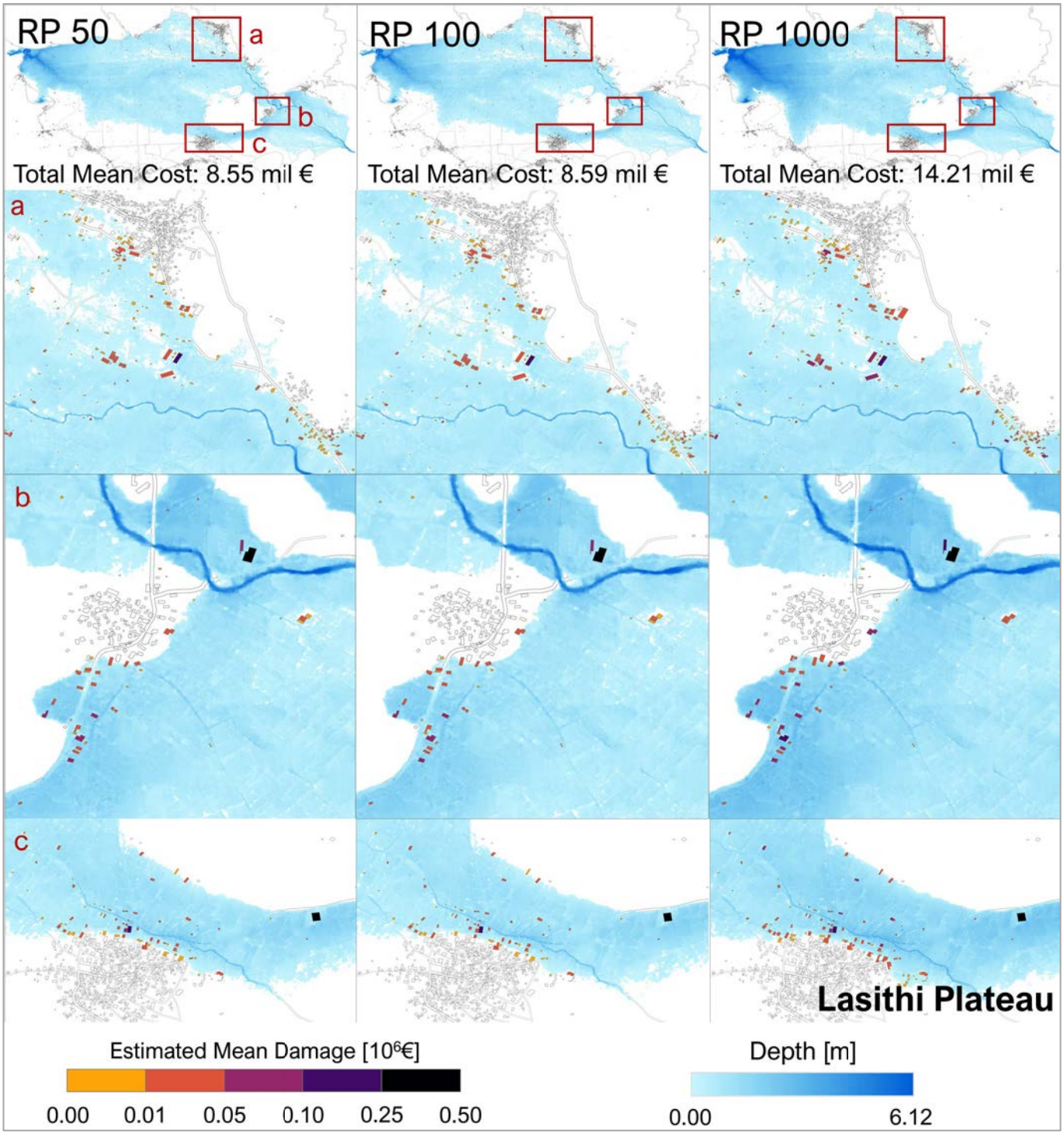

Figure 8-26 Estimated mean direct damage to buildings in the Lasithi Plateau for RP50, RP100 and RP1000. Panels a–c highlights local hotspots.

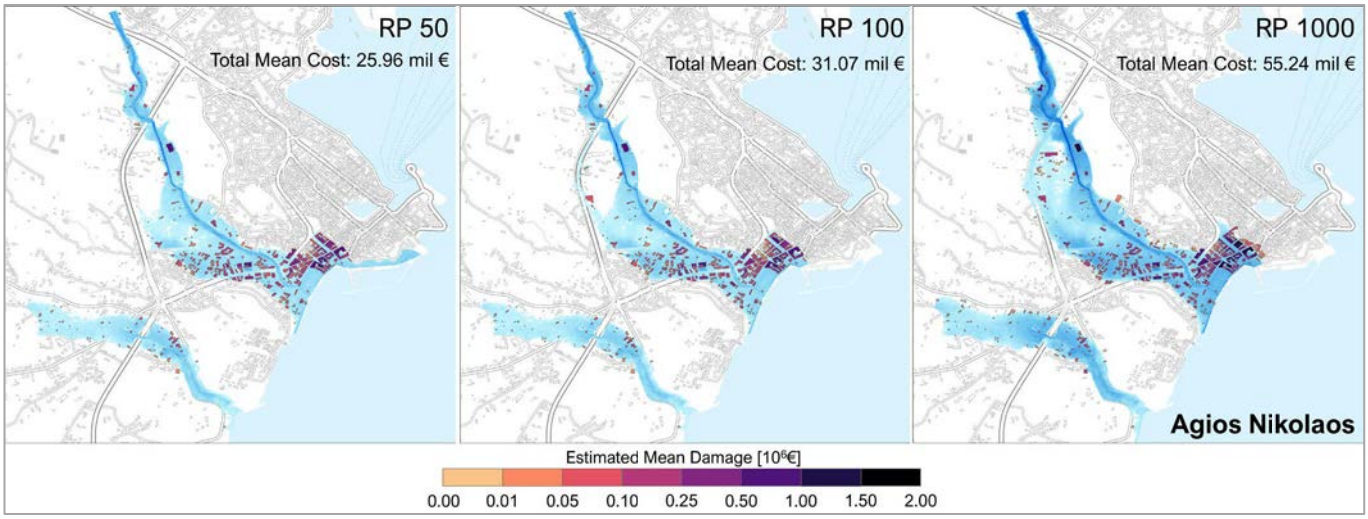

Figure 8-27 Estimated mean direct damage to buildings in Agios Nikolaos for RP50, RP100 and RP1000. Building-level losses increase markedly along the urban waterfront and lower stream corridor, with total mean damage more than doubling between RP50 and RP1000.

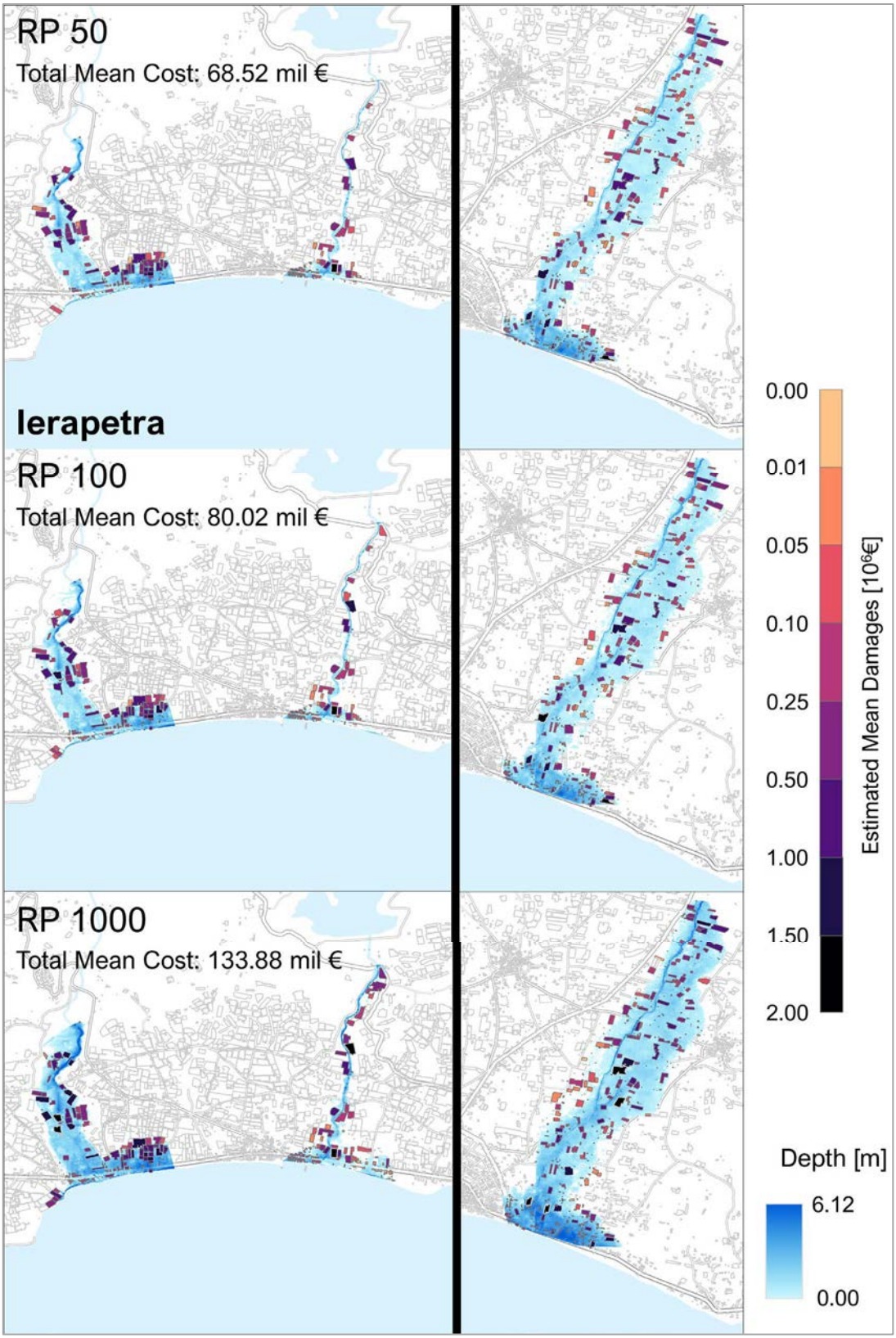

Figure 8-28 Estimated mean direct damage to buildings in Ierapetra for RP50, RP100 and RP1000. Damage hotspots occur along the coastal strip and along the torrent upstream of the town.

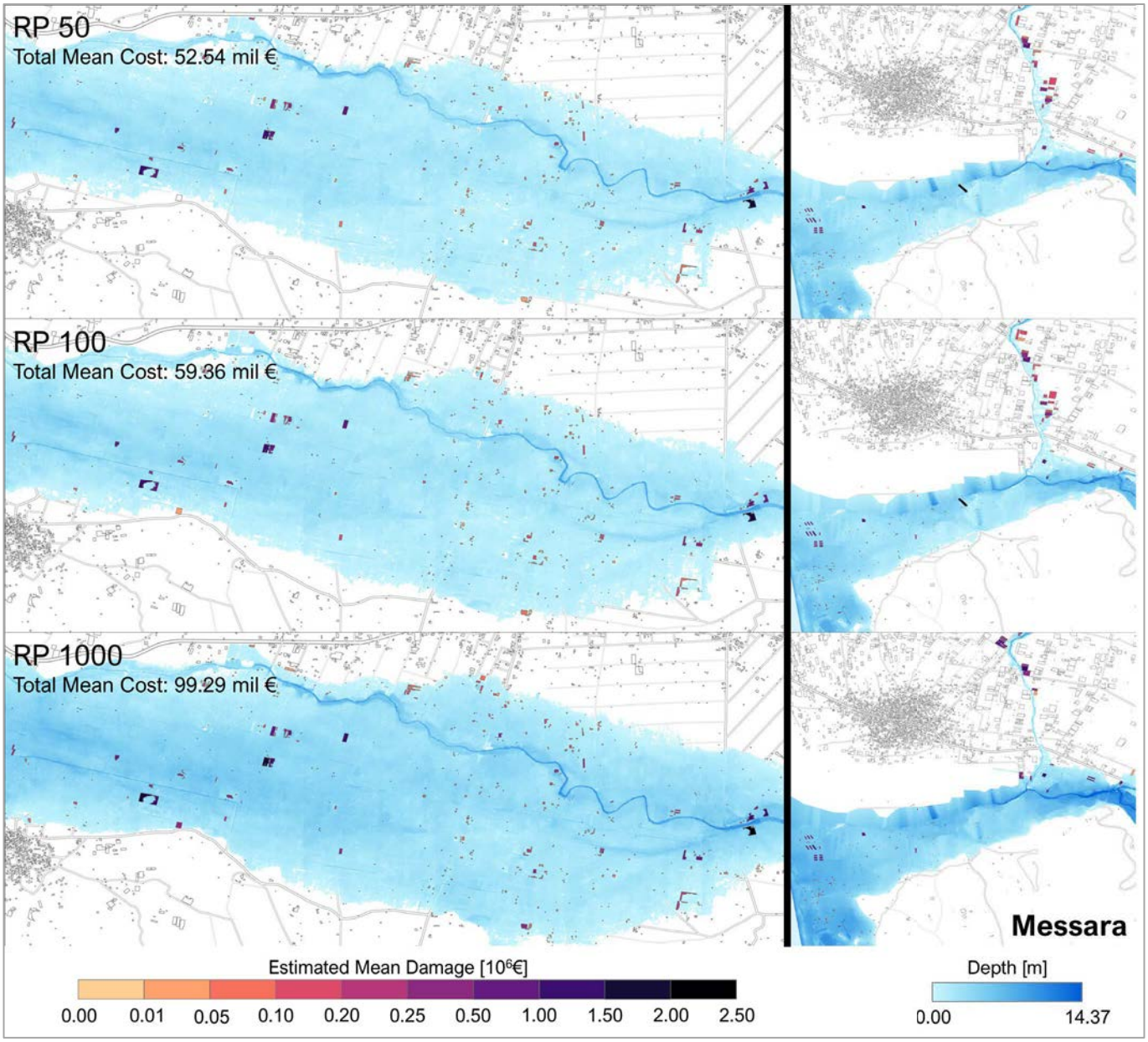

Figure 8-29 Estimated mean direct damage to buildings in the Messara plain for RP50, RP100 and RP1000. Maps show losses in both the central agricultural floodplain and the Tymbaki urban area.

Funded by the European Union

CLIMAAX climate ready regions

C&D Outputs of CRETE-CLIMAAX project

Press Releases, Media Coverage and Dissemination

Authors: Aristeidis Koutroulis, Technical University of Crete
Mikaela Papa, Technical University of Crete
Marinos Kritsotakis, Region of Crete
Eleni Kargaki, Region of Crete

Project Title: Climate Resilient Crete (CRETE)
Cascade Funded by: The European Union's Horizon Europe Climate Programme
Grant Agreement No.: 101093864 – CLIMAAX

1 Official institutional press releases / announcements local news media coverage

1. **Region of Crete – CLIMAAX-CRETE working meeting**
   Phase: 1
   Type: Official regional press release
   URL: https://www.crete.gov.gr/synantisi-ergasias-tis-omadas-toy-eyropaikoy-ergoy-climaax-crete/
2. **Region of Crete – "Horizon Europe & Crete: Climate-resilient Crete"**
   Phase: 1
   Type: Official regional press release / project framing
   URL: https://www.crete.gov.gr/horizon-2020-crete-climate-resilient-crete-quot-klimatika-anthektiki-kriti/
3. **Cretalive – CLIMAAX-CRETE working meeting (Crete)**
   Phase: 1
   Type: Online news article
   URL: https://www.cretalive.gr/kriti/synantisi-ergasias-tis-omadas-toy-eyropaikoy-ergoy-climaax-crete
4. **Technical University of Crete – cooperation with Region of Crete for climate resilience**
   Phase: 1
   Type: University press release
   URL: https://www.tuc.gr/el/to-polytechneio/symbainei-sto-polytechneio/item/polytechneio-kritis-kai-perifereia-kritis-enonoyn-dynameis-gia-tin-klimatiki-anthektikotita-toy-nisioy
5. **Haniotika Nea – CLIMAAX-CRETE working meeting**
   Phase: 1
   Type: Regional newspaper article
   URL: https://www.haniotika-nea.gr/synantisi-ergasias-tis-omadas-toy-eyropaikoy-ergoy-climaax-crete/
6. **Flashnews – CLIMAAX-CRETE & Region of Crete (tag page)**
   Phase: 1
   Type: Series of online news items (tag aggregator)
   URL: https://flashnews.gr/tag/climaax-crete-perifereia-kritis/
7. **Candiadoc – CLIMAAX-CRETE (tag page)**
   Phase: 1
   Type: Series of online news items (tag aggregator)
   URL: https://www.candiadoc.gr/tag/climaax-crete/
8. **Rethnea – CLIMAAX-CRETE working meeting**
   Phase: 1
   Type: Regional newspaper article
   URL: https://rethnea.gr/synantisi-ergasias-tis-omadas-tou-evropaikou-ergou-climaax-crete/
9. **Nea Kriti – "Alarm for Crete's water resources – reservoirs are drying up"**
   Phase: 2
   Type: Thematic article on water scarcity referencing project context
   URL: https://www.neakriti.gr/kriti/2154016_synagermos-gia-ta-nera-tis-kritis-stereyoyn-ta-fragmata-agonas-dromoy-mehri-ton

10. **Kriti360 – "Crete and Western Greece join forces for climate resilience"**
    Phase: 2
    Type: Regional news article on inter-regional collaboration
    URL: https://kriti360.gr/kriti-kai-dytiki-ellada-enonoyn-dynameis-gia-tin-klimatiki-anthektikotita/
11. **Region of Western Greece – press release on cooperation with Region of Crete**
    Phase: 2
    Type: Official regional press release (legacy site)
    URL: https://legacy.pde.gov.gr/gr/enimerosi/deltia-tupou/item/23849-synergasia-perifereion-dytikis-elladas-kai-kritis-se-themata-draseon-klimatikis-anthektikotitas.html?tmpl=component&print=1
12. **Parakritika – Working meeting of the Regions of Western Greece and Crete for climate-resilience actions**
    Phase: 2
    Type: Online news article
    URL: https://www.parakritika.gr/24/10/2025/para-kritika/synantisi-ergasias-ton-perifereion-dytikis-elladas-kai-kritis-gia-draseis-klimatikis-anthektikotitas/
13. **Ekriti – Region of Crete & Regions of Western Greece working meeting on climate-resilience actions**
    Phase: 2
    Type: Online news article
    URL: https://www.ekriti.gr/kriti/perifereia-kritis-synantisi-ergasias-me-tis-perifereies-dytikis-elladas-gia-draseis-klimatikis-anthektikotitas
14. **PATH4PDE Living Lab – Cooperation of Western Greece and Crete on climate-resilience actions**
    Phase: 2
    Type: Institutional / project portal article
    URL: https://path4pde.living-lab.gr/index.php/el/component/content/article/317-synergasia-periphereion-dytikes-elladas-kai-kretes-se-themata-draseon-klimatikes-anthektikotetas?catid=8
15. **Agrinionews – Cooperation of Western Greece and Crete on climate-resilience actions**
    Phase: 2
    Type: Regional news article
    URL: https://www.agrinionews.gr/synergasia-perifereion-dytikis-elladas-kai-kritis-se-themata-draseon-klimatikis-anthektikotitas/
16. **CNA – Working meeting of the Regions of Western Greece and Crete for climate-resilience actions**
    Phase: 2
    Type: Online news article
    URL: https://www.cna.gr/crete-all/synantisi-ergasias-ton-perifereion-dytikis-elladas-kai-kritis-gia-draseis-klimatikis-anthektikotitas/
17. **Agrinioculture – Cooperation of Western Greece and Crete on climate-resilience actions**
    Phase: 2
    Type: Online news article / blog
    URL: https://www.agrinioculture.gr/2025/10/27/synergasia-perifereion-dytikis-elladas-kai-kritis-se-themata-draseon-klimatikis-anthektikotitas/

18. **Sinidisi – Joint event of Regions of Western Greece and Crete on climate resilience**
    Phase: 2
    Type: Online news article
    URL: https://sinidisi.gr/perifereies-dytikis-elladas-kritis-imerida-gia-tin-klimatiki-anthektikotita/
19. **Agriniopress – Cooperation of Western Greece and Crete on climate-resilience actions**
    Phase: 2
    Type: Online news article
    URL: https://www.agriniopress.gr/synergasia-perifereion-dytikis-elladas-kai-kritis-se-themata-draseon-klimatikis-anthektikotitas/
20. **Rethnea – CLIMAAX-CRETE working meeting / inter-regional collaboration**
    Phase: 2 (re-use of same outlet link as in Phase 1, counted once)
    Type: Regional newspaper article
    URL: https://rethnea.gr/synantisi-ergasias-tis-omadas-tou-evropaikou-ergou-climaax-crete/
21. **Region of Western Greece – Information note on cooperation with Crete (new site)**
    Phase: 2
    Type: Official regional press release
    URL: https://pde.gov.gr/el/enimerotika-deltia/%CF%83%CF%85%CE%BD%CE%B5%CF%81%CE%B3%CE%B1%CF%83%CE%AF%CE%B1-%CF%80%CE%B5%CF%81%CE%B9%CF%86%CE%B5%CF%81%CE%B5%CE%B9%CF%8E%CE%BD-%CE%B4%CF%85%CF%84%CE%B9%CE%BA%CE%AE%CF%82-%CE%B5%CE%BB%CE%BB%CE%AC/
22. **Cretalive – "Climate resilience: Working meeting of the Regions of Crete and Western Greece"**
    Phase: 2
    Type: Online news article
    URL: https://www.cretalive.gr/kriti/klimatiki-anthektikotita-synantisi-ergasias-ton-perifereion-kritis-kai-dytikis-elladas
23. **Instagram – CLIMAAX-CRETE / Region of Crete post**
    Phase: 2
    Type: Social media post (visual summary of joint meeting)
    URL: https://www.instagram.com/p/DGD-Me6sj8s/

2 Scientific dissemination activities and conference outputs

(A) SafeHeraklion 2025 – Conference Paper & Poster

Event: SafeHeraklion 2025 – 11th International Conference on Civil Protection & New Technologies, 22–24 October 2025, Heraklion, Crete
Phase: 2
Type: Peer-reviewed conference paper and poster
Title: *Assessing Flood Risk and Extreme Precipitation in Crete*
Authors: M. Papa, M. Kritsotakis, E. Kargaki, E. Stylianou, A. Koutroulis
Outlet: *SafeHeraklion 2025 Proceedings* (ISSN 2654-1823) and conference poster session
URL:
https://safegreece.org/safeheraklion2025/images/docs/safeheraklion2025_proceedings.pdf

(B) FutureMed Workshop & Training School – Poster Presentation

Event: 1st FutureMed Workshop & Training School, 29 September – 3 October 2025, Chania, Crete
Phase: 2
Type: Scientific poster presentation (Book of Abstracts)
Title: *Implications of applying a common Climate Risk Assessment Framework at the regional scale: Insights from the CLIMAAX implementation in Crete*
Authors: M. Papa, M. Kritsotakis, E. Kargaki, E. Stylianou, A. Koutroulis
Outlet: FutureMed Book of Abstracts
URL: https://futuremedaction.eu/wp-content/uploads/2025/09/BookOfAbstract.pdf

(C) Conference poster – CLIMAAX Barcelona Workshop 2025

Event: CLIMAAX Workshop “Success Highlights from CLIMAAX Implementations”, 10–11 June 2025, Barcelona
Phase: 2
Type: Scientific poster presentation
Title: Climate Resilient Crete (CRETE) – Climate Risk Assessment Phase 1
Authors: M. Papa, M. Kritsotakis, E. Kargaki, E. Stylianou, A. Koutroulis
Outlet: CLIMAAX internal workshop poster session, CosmoCaixa Science Museum, Barcelona

Funded by the European Union

CLIMAAX climate ready regions

SafeGreece Conference Proceedings

ISSN 2654-1823

SafeGreece new technologies & civil protection

Hellenic Mediterranean University

SafeHeraklion 2025 new technologies & civil protection

Hellenic Mediterranean University
Events Amphitheater of the School of Health Sciences

22-24.10

proceedings

Sponsored by: satways, planetek hellas, totalview

Supported by: Regional Development Fund of Crete, Περιφέρεια Κρήτης Region of Crete, E.P.P.O Earthquake Planning & Protection Organisation

Funded by the European Union

CLIMAAX climate ready regions

SafeHeraklion 2025 Proceedings | ISSN 2654-1823

ASSESSING FLOOD RISK AND EXTREME PRECIPITATION IN CRETE

Mikaela Papa[1], Marinos Kritsotakis[2], Eleni Kargaki[3], Evgenia Stylianou[4], Aristeidis Koutroulis[5]
[1,5]*School of Chemical and Environmental Engineering, Technical University of Crete (Greece),*
(E-mail: kpapa@tuc.gr, akoutroulis@tuc.gr)
[2,3,4]*Directorate-General for Sustainable Development, Region of Crete, (Greece).*
(E-mail: kritsotakis@crete.gov.gr, kargaki@crete.gov.gr, stylianou@crete.gov.gr)

ABSTRACT

This study presents a flood hazard and risk assessment for Crete, conducted as part of the CLIMAAX project using refined local data and standardised workflows. The analysis focuses on ten flood-prone regions across the island, integrating high-resolution hazard maps, socio-economic exposure layers, and vulnerability indicators. High resolution flood hazard maps for return periods of 50, 100, and 1000 years supported the analysis. Exposure and risk metrics were calculated using land use classifications and building footprint datasets. Results indicate substantial variation in flood damage potential across the island, with Heraklion, Messara, and Northern Chania showing the highest estimated losses. In Heraklion alone, building damage under the 1000-year scenario is estimated at €589.2 million, with over 1,000 individuals exposed and more than 550 likely to be displaced. Future climate projections, based on EURO-CORDEX simulations, suggest an upward shift in the intensity and frequency of extreme precipitation events. These trends underline the growing urgency for adaptation planning. The assessment outputs provide evidence to support regional decision-making and prioritisation of flood resilience investments, while demonstrating the value of localised data integration within harmonised risk assessment frameworks.

Keywords: Flood risk, climate change, Crete, hazard assessment, exposure analysis

1. INTRODUCTION

Floods are a significant hazard in Crete, threatening human safety, infrastructure, and economic activities, accentuated by the varying topography and Mediterranean climate of the island, which facilitate both riverine and flash flooding. Climate change has intensified these risks, with studies projecting more frequent and severe extreme precipitation events [1]. As demonstrated by the destructive floods of February 2019 in Chania and Rethymno, which caused widespread infrastructure damage and disruptions to transportation networks, Crete is experiencing shifts towards localised, high-intensity storms in autumn and winter, thus increasing rapid runoff and overwhelming drainage systems [2]. Additionally, urbanisation and land-use changes have amplified flood risks by reducing infiltration and increasing surface runoff [3]. Expanding settlements along riverbanks, floodplains, and low-lying areas, combined with inadequate drainage in dense urban centres, such as Heraklion, Chania, and Rethymno, have heightened vulnerability, underscoring the combined impact of climatic and anthropogenic drivers on flood risk. This study applies the CLIMAAX project methodology to deliver a comprehensive flood risk assessment for Crete, integrating hydrological and meteorological data, flood hazard modelling, and socio-economic indicators, such as population density, infrastructure, and land use. By analysing historical and projected precipitation patterns, mapping hazard zones, and evaluating exposure and vulnerability, the study provides evidence to support regional flood risk management and adaptation planning. Aligned with the European Floods Directive (2007/60/EC) and the 1st Revision of the Flood Risk Management Plan for Crete (EL13), the findings aim to enhance policymaking, disaster preparedness, and long-term resilience strategies. The assessment follows standardised CLIMAAX workflows, focusing on economic damages and population exposure from river flooding through three main components: hazard assessment, risk assessment, and exposure analysis.

2. METHODOLOGICAL FRAMEWORK

2.1. Flood and Extreme Precipitation Hazard Assessment

The flood and extreme precipitation hazard assessment relies on a high-resolution (2 m × 2 m) flood hazard dataset covering ten subregions of Crete under current climate conditions, derived from the 1st Revision of the Flood Risk Management Plan (FRMP) for the Water District of Crete (EL13). This dataset provides detailed maps of flood extents and depths for three return periods (50, 100, and 1000 years), though it does not account for man-made flood protection measures, which may lead to overestimations in certain areas. To evaluate hazards linked to extreme precipitation, the study incorporates EURO-CORDEX daily precipitation flux data at 12 km spatial resolution for both historical simulations (1976–2005) and future climate projections (2011–2040, 2041–2070, 2071–2100) under RCP4.5 and RCP8.5 scenarios. Applying the General Extreme Value (GEV) probability distribution to annual maximum precipitation, the analysis estimates expected precipitation for different return periods and quantifies shifts in precipitation magnitudes relative to the historical baseline (1976–2005).

2.2. Flood and Extreme Precipitation Risk Assessment

The second part of the assessment combines hazard data with exposure and vulnerability indicators to quantify potential flood damages. Flood risk is estimated by evaluating the probability of different flood depths affecting buildings, infrastructure, and economic assets, using predefined depth-damage functions that reflect how impacts vary across land use categories. Land use information derives from the LUISA Land Cover dataset [4], which provides high-resolution classifications of urban, agricultural, and natural areas, while the Global ML Building Footprints [5] supplies building contours for the entire island. Built-up zones show higher vulnerability due to greater economic exposure, whereas natural landscapes provide greater water absorption capacity. Depth-damage curves and vulnerability functions link land cover types to expected damage ratios at varying flood depths, with transport and agricultural areas identified as the most sensitive. Economic damage estimates are based on country-specific data, ensuring a comprehensive evaluation of flood impacts. Since the workflow is built on precomputed datasets and standardised functions, no external hydrological modelling or GIS-based mapping is required. In parallel, the extreme precipitation risk assessment applies critical rainfall thresholds, estimated from past flood events in Crete, to evaluate how the frequency of fixed precipitation magnitudes is projected to shift under future climate conditions (RCP4.5 and RCP8.5).

3. RESULTS AND DISCUSSION

Flood hazard and risk analyses across the flood-prone regions of Crete revealed considerable variability in exposure, economic damage, and vulnerability patterns under current climatic conditions. Results are presented of the ten hydrological regions, with a focus on the Heraklion area, where refined outputs illustrate both current and potential future impacts. **Figure 2a** shows the flood depth and extent in Heraklion under 50-year and 1000-year return period events, alongside their depth difference. Substantial increases in flood depth and extend are observed between the two scenarios, particularly in low-lying urban and peri-urban areas of northern Heraklion, which highlight the effect of increased event severity on densely built environments. **Figure 3** further details the population and asset exposure within Heraklion. The estimated number of residents exposed to flooding increases significantly with the return period, from approximately 445 under RP50 to over 1,000 under RP1000, while the number of potentially displaced individuals reaches over 550. **Figure 3c** shows spatially explicit building damage estimates in Heraklion, with highest losses in coastal zones and drainage basins intersecting urban cores.

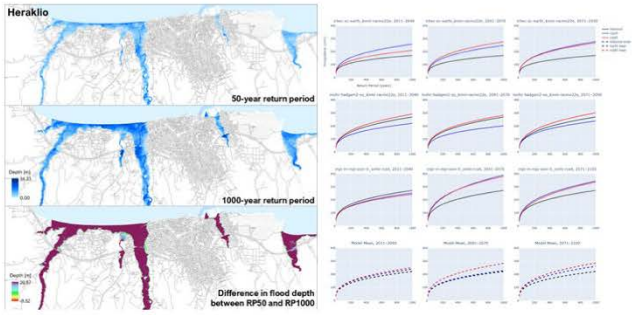

(a) (b)

Figure 1. (a) Flood depth and extent of a 50- and 1000-year return period, in Heraklion, and the changes in depth between the two return periods. (b) Mean Intensity-Duration-Frequency curves, of three EUROCORDEX models, from three assessment periods and the RCP4.5 and RCP8.5 climate scenarios, over Crete, as well as the calculated mean of the models.

Economic losses by region are summarised in **Table 1**. Heraklion consistently shows the highest mean expected damages across all return periods, with building damage estimates reaching €265.4 million under the 50-year event, increasing to €589.2 million under the 1000-year scenario. Similarly high damage values are observed in Messara and Northern Chania.

Table 1. Total estimated economic damage to land types and total mean economic damage to buildings per region, of a 50, 100, and 1000 return period (RP), based on current climatic conditions.

	Total damage [10^6€]		
Region	**RP50**	**RP100**	**RP1000**
Agios Nikolaos	50.3/26.0	55.3/31.1	92.6/55.2
Heraklio Town	523.5/265.4	615.1/313.8	615.1/589.2
Ierapetra	48.2/68.5	53.6/80.0	81.0/133.9
Keritis (Maleme)	142.9/16.0	200.9/26.8	295.7/48.6
Kladisos	63.8/30.9	79.1/44.0	142.2/99.3
Koiliaris	67.2/7.6	78.7/9.7	118.9/19.3
Lasithi Plateau	243.5/8.5	247.3/8.6	365.2/14.2
Messara	667.1/52.5	743.7/59.3	1178.1/99.3
Northern Chania	290.3/60.2	389.5/87.6	607.3/176.0
Rethymno	58.9/22.8	75.0/31.2	149.1/85.3
Tavronitis (Skoutelonas)	83.0/13.3	106.8/16.8	168.2/28.0

Extreme precipitation analysis using EURO-CORDEX simulations (**Figure 2b**) reveals a projected upward shift in the intensity-duration-frequency (IDF) curves of northern Heraklion. Across all three future periods and under both RCP4.5 and RCP8.5 scenarios, increases in maximum daily precipitation are evident, particularly in short-duration extremes. The ensemble mean of three EURO-CORDEX models suggests that by 2100, rainfall events currently classified as 50-year storms may occur with significantly higher frequency. These shifts imply not only more frequent high-intensity storms but also a shortening of the return period for damaging events, both critical factors in flood preparedness and infrastructure planning.

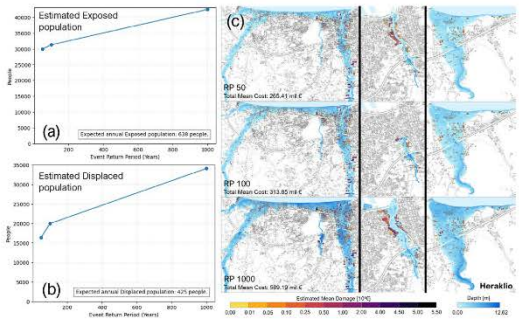

Figure 2. (a), (b) Estimated exposed and displaced population per flood event return period, respectively. (c) Estimated economic damage to buildings in Heraklion, based on mean flood depth for a 50-year (top), 100-year (middle) and 500-year return period (bottom).

4. CONCLUSION

The flood risk assessment carried out for Crete highlights the differentiated vulnerability of its flood-prone regions, with Heraklion emerging as a critical hotspot for both current and future flood impacts. The use of high-resolution hazard data, combined with updated socio-economic indicators, allowed for accurate spatial representation of damage potential and population exposure under varying return periods. Key findings indicate that increasing event severity is strongly correlated with expanded inundation areas and economic losses, particularly in urban and agricultural zones with limited natural drainage. In Heraklion, the concentration of exposure and built infrastructure near river systems significantly amplifies risk. Across the island, regions such as Messara and Northern Chania also exhibit elevated damages, driven by both land use patterns and topographic characteristics. Climate projections indicates that the intensity and recurrence of extreme rainfall events are expected to rise, further reducing return periods for damaging floods. These insights reinforce the need for anticipatory adaptation strategies, including land-use regulation, investment in flood protection infrastructure, and incorporation of climate resilience criteria into urban development planning.

ACKNOWLEDGMENTS

The work was supported by the European Union's Horizon Europe research and innovation programme under Grant Agreement No. 101093864 (project CLIMAAX).

REFERENCES

1. Tsanis, I. K., Koutroulis, A. G., Daliakopoulos, I. N., & Jacob, D. (2011). Severe climate-induced water shortage and extremes in Crete: A letter. Climatic Change, 106(4), 667–677. doi:10.1007/s10584-011-0048-2
2. Koutroulis, A. G., Tsanis, I. K., & Daliakopoulos, I. N. (2010). Seasonality of floods and their hydrometeorologic characteristics in the island of Crete. Journal of Hydrology, 394(1), 90–100. doi:10.1016/j.jhydrol.2010.04.025
3. Angelakis, A. N., Antoniou, G., Voudouris, K., Kazakis, N., Dalezios, N., & Dercas, N. (2020). History of floods in Greece: Causes and measures for protection. Natural Hazards, 101(3), 833–852. doi:10.1007/s11069-020-03898-w
4. European Commission. Joint Research Centre. (2021). The LUISA base map 2018: A geospatial data fusion approach to increase the detail of European land use/land cover data. Publications Office. https://data.europa.eu/doi/10.2760/503006
5. microsoft/GlobalMLBuildingFootprints. (2023, September 26). GitHub; Microsoft. https://github.com/microsoft/GlobalMLBuildingFootprints

Funded by the European Union

CLIMAAX climate ready regions

Assessing Flood Risk and Extreme Precipitation in Crete

Mikaela Papa[1], Marinos Kritsotakis[2], Eleni Kargaki[2], Evgenia Stylianou[2], Aris Koutroulis[1]
[1]School of Chemical and Environmental Engineering, Technical University of Crete,
[2]Directorate-General for Sustainable Development, Region of Crete

This study presents a flood hazard and risk assessment for Crete, conducted as part of the CLIMAAX project using refined local data and standardised workflows. The analysis focuses on ten flood-prone regions across the island, integrating high-resolution hazard maps, socio-economic exposure layers, and vulnerability indicators. High resolution flood hazard maps for return periods of 50, 100, and 1000 years supported the analysis. Exposure and risk metrics were calculated using land use classifications and building footprint datasets. Results indicate substantial variation in flood damage potential across the island, with Heraklion, Messara, and Northern Chania showing the highest estimated losses. In Heraklion alone, building damage under the 1000-year scenario is estimated at a maximum of €732 million, with over 40000 individuals exposed and more than 30000 likely to be displaced. Future climate projections, based on EURO-CORDEX simulations, suggest an upward shift in the intensity and frequency of extreme precipitation events. These trends underline the growing urgency for adaptation planning. The assessment outputs provide evidence to support regional decision-making and prioritisation of flood resilience investments, while demonstrating the value of localised data integration within harmonised risk assessment frameworks.

Flood Hazard and Risk Assessment

Figure 1. Flood Hazard maps of the riverine system in the town of Heraklion, of 50, 100, and 1000 return periods (RP).

Hazard

- 10 subregions of Crete
- 2m x 2m hazard flood maps (RP50, RP100, RP1000) of present-day climate.

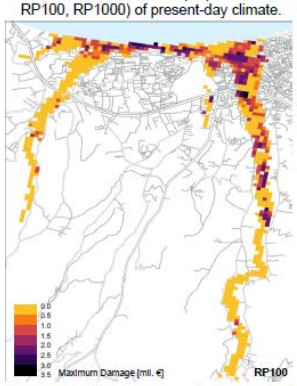

Figure 2. Potential maximum economic damage to land types in Heraklion (Giofyros river), caused by a 100-year flood event.

Risk

- LUISA landcover 2018 basemap [1]
- Global ML Building Footprints [2]
- Damage-Depth functions by JRC
- To estimate the flood exposure of the population we allocated 25m² of living area per person and assumed a one-to-one correlation of population to buildings.
- Affected areas and potential maximum flood damage to land use types and buildings

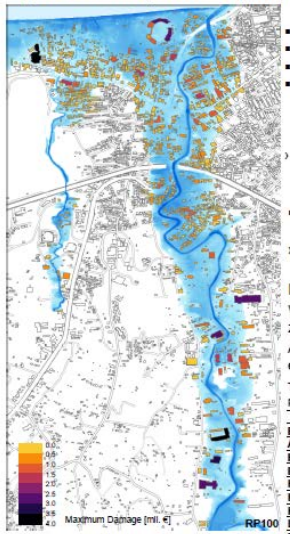

Figure 3. Potential maximum economic damage to buildings in Heraklion (Giofyros river), caused by a 100-year flood event.

Conclusions

- Heraklion presents as a critical hotspot for both current and future flood impacts.
- The concentration of exposure near river systems significantly amplifies risk

Increasing event severity is strongly correlated with expanded inundation areas and economic losses, particularly in urban and agricultural zones with limited natural drainage.

Across the island, regions such as Messara and Northern Chania also exhibit elevated damages, driven by both land use patterns and topographic characteristics.

Table 1. Total potential maximum damage to buildings and land types and total exposed and displaced (>1m depth) population for RP50, RP100, RP1000. (Results are presented as regional sums).

	Total economic damage to **Buildings	Land Use** (10^6 €)					Total **Exposed	Displaced** Population				
Region	**RP50**		**RP100**		**RP1000**		**RP50**		**RP100**		**RP1000**	
Agios Nikolaos	36.1	50.3	41.8	55.3	66.2	92.6	2697	1711	2850	2112	3470	3020
Heraklion (Town)	378.9	523.5	427.8	615.1	731.6	615.1	29947	16397	31308	19940	42490	34137
Ierapetra	135.2	48.2	152.3	53.6	229.4	81.0	12253	2337	13257	2887	17033	6238
Keritis (Maleme)	22.6	142.9	37.2	200.9	60.8	295.7	2070	762	3301	1582	4360	2879
Kladissos (Chania)	46.6	63.8	63.0	79.1	124.2	142.2	7205	897	8247	1545	11260	6877
Koiliaris (Kalyves)	9.8	67.2	12.4	78.7	23.2	118.9	944	425	1073	575	1563	1098
Lasithi Plateau	12.9	243.5	13.0	247.3	19.8	365.2	1750	252	1753	247	2228	659
Messara (Tymbaki, Moires)	70.5	667.1	79.0	743.7	117.2	1178.1	6976	3414	7472	3832	7314	5863
Rethymno	34.2	58.9	46.3	75.0	105.7	149.1	3753	964	4933	1490	7956	5766
Tavronitis (Skoutelonas)	19.0	83.0	23.0	106.8	35.6	168.2	2274	591	2486	832	3050	1723

Extreme Precipitation Hazard and Risk Assessment

Figure 4. Reported flood events and their impact category. The grey areas (grid) show the basins under consideration for the application of the Intensity-Duration-Frequency (IDF) function.

Hazard

- Bias corrected EUROCORDEX datasets at 12km spatial resolution (historical, RCP4.5, RCP8.5)
- General Extreme Value (GEV) probability distribution of annual maximum precipitation to estimate the expected precipitation for different return periods and quantify shifts in magnitudes relative to the historical baseline (1976–2005).

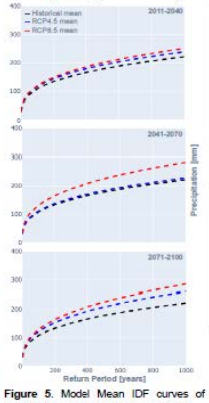

Figure 5. Model Mean IDF curves of 2011-2040, 2041-2070, and 2071-2100.

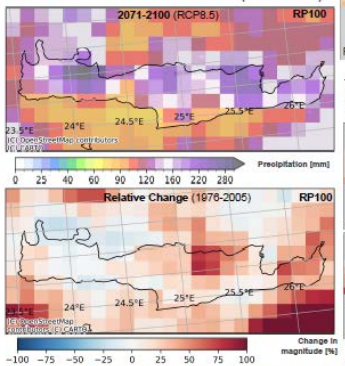

Figure 6. Mean precipitation of 100 RP in Crete for 2071-2100, under RCP8.5 (left) and the change of precipitation compared to the 1976-2005 baseline period (right).

Risk

- Critical rainfall thresholds are prompted by past flood events in Crete
- Shift of frequency of fixed precipitation magnitude under future scenarios

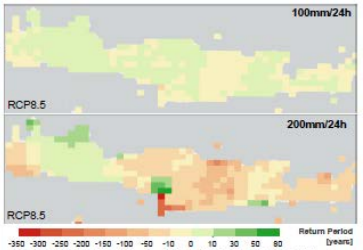

Figure 7. Shift of frequency for 100 and 200mm/24h threshold between 1976-2005 and 2017-2100, under RCP8.5 (model mean).

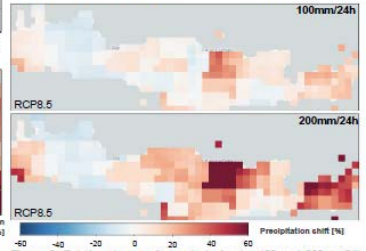

Figure 8. Relative change of magnitude for the 100 and 200mm/24h threshold in 2071-2100, under RCP8.5 (model mean).

Conclusions

- Climate projections indicate that the intensity and recurrence of extreme rainfall events are expected to rise, potentially causing damaging floods.
- These insights reinforce the need for anticipatory adaptation strategies, including land-use regulation, investment in flood protection infrastructure, and incorporation of climate resilience criteria into urban development planning.

1. European Commission. Joint Research Centre. (2021). The LUISA base map 2018: A geospatial data fusion approach to increase the detail of European land use/land cover data. Publications Office. https://data.europa.eu/doi/10.2760/503006
2. microsoft/GlobalMLBuildingFootprints. (2023, September 26). GitHub; Microsoft. https://github.com/microsoft/GlobalMLBuildingFootprints

BOOK OF ABSTRACT

P1.15 - Implications of applying a common Climate Risk Assessment Framework at the regional scale: Insights from the CLIMAAX implementation in Crete

Mikaela Papa[1], Marinos Kritsotakis[2], Eleni Kargaki[2], Evgenia Stylianou[2], Aristeidis Koutroulis[1]

[1]*Technical University of Crete*

[2]*Region of Crete*

The increasing frequency and intensity of climate-related hazards across Europe highlights the pressing need for a harmonised approach to climate risk assessment (CRA). In response, the CLIMAAX project introduces a common methodology for Climate Risk Assessment (CRA) across Europe, supporting regional authorities in evaluating key climate-related hazards. This paper presents findings from the first implementation phase in Crete, where the Region applied the standardised CRA framework to assess drought and flood risks using openly available datasets and workflows.

The results identified high-risk areas across the island, particularly in water-stressed agricultural zones. Under a high-emissions scenario, eastern Crete shows a substantial increase in drought severity, with projected revenue losses for olive cultivation exceeding €500/ha. Simultaneously, flood exposure is pronounced in urban centers where natural drainage systems have been disrupted by land use changes.

The application of the common CRA framework revealed several methodological limitations. Coarse-resolution datasets did not adequately capture local hydrological features, particularly flash floods in small catchments. Furthermore, vulnerability assessments lacked critical information on intersectoral water competition and local infrastructure exposure. These constraints limited the ability to fully tailor adaptation strategies to local conditions.

Despite these challenges, the process enabled regional stakeholders to establish a baseline risk profile and inform future adaptation planning. Stakeholder engagement was central to the process, highlighting the importance of inclusive risk communication and local data integration.

The case of Crete demonstrates the potential of the CLIMAAX framework to support evidence-based adaptation, while underscoring the need for methodological refinement to reflect local complexity and planning needs.

Climate Resilient crETE (CRETE)

Climate Risk Assessment – Phase 1

Mikaela Papa[1], Marinos Kritsotakis[2], Eleni Kargaki[2], Evgenia Stylianou[2], Aris Koutroulis[1],

[1]School of Chemical and Environmental Engineering, Technical University of Crete
[2]Directorate-General for Sustainable Development, Region of Crete

Crete, with 630,000 residents and over 4 million annual tourists, faces increasing climate risks affecting its water-dependent economy. Agriculture, especially olive cultivation, and tourism are both highly vulnerable to drought and competing for limited water resources. Seasonal tourism surges during dry months, intensifying urban water demand and straining infrastructure. At the same time, rapid coastal development and tourism expansion in flood-prone areas have significantly raised flood exposure, especially from flash floods, hazards not well captured by existing large-scale models. This Phase 1 assessment under the CLIMAAX framework applies standardized workflows to evaluate drought and flood risks, highlighting key vulnerabilities and data limitations. The findings support future adaptation planning and call for more localized models and integrated water management strategies in Crete.

Relative Drought Risk

Relative drought risk was mapped using long-term precipitation deficits and socio-economic vulnerability indicators. The analysis revealed spatial disparities in exposure, with Heraklion and Lasithi emerging as high-risk areas under multiple future scenarios (SSP126, SSP370, SSP585)

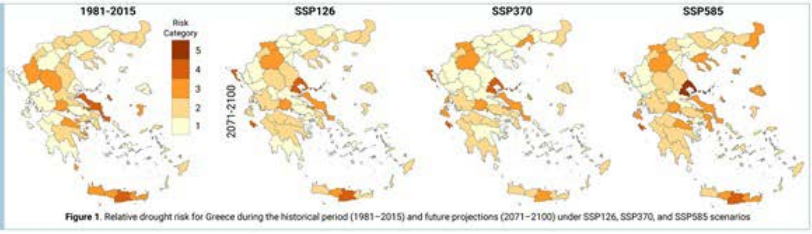

Figure 1. Relative drought risk for Greece during the historical period (1981–2015) and future projections (2071–2100) under SSP126, SSP370, and SSP585 scenarios

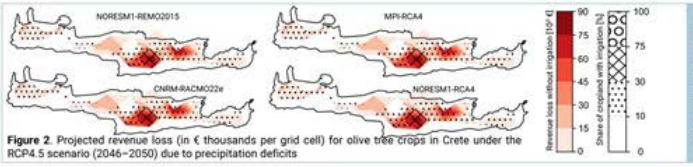

Figure 2. Projected revenue loss (in € thousands per grid cell) for olive tree crops in Crete under the RCP4.5 scenario (2046–2050) due to precipitation deficits

Agricultural Drought Risk

Agricultural drought risk focused on projected irrigation-related losses, particularly for olive groves—Crete's dominant crop. Under RCP4.5 (2046–2050), central and eastern Crete are expected to experience the highest economic losses due to reduced precipitation and elevated evapotranspiration.

River Flooding

River flood risk assessment used JRC maps combined with land use and damage functions. Results show highest risk in urbanized floodplains, especially around Heraklion, with total damages reaching €515 million under the 500-year scenario. Flash floods is the major hazard type in Crete and are not captured in these models, limiting their local relevance.

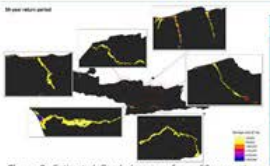

Figure 3: Estimated flood damages for a 50-year return period in Crete.

Figure 4: Flood depth maps for a 250RP from the Aqueduct Floods dataset.

Flood Damage and Population Exposure

Figure 4. Estimated building damage in Heraklion based on mean flood depth for the 500-year return period.

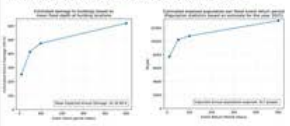

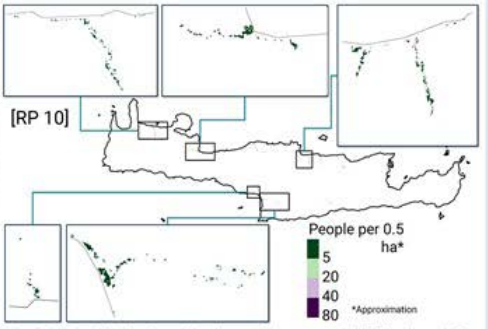

Figure 6. Estimated displaced population due to a 10-year return period (RP) flood event in Crete.

Building and population exposure were assessed using OpenStreetMap and GHS-POP data. Key urban centers show significant vulnerability, with damage concentrated along riverbanks and low-lying coastal areas.
Mean Expected Annual Damage (EAD) is estimated at €35.38 million/year, though likely underestimated due to incomplete building data.
The Expected Annual Population Exposed (EAPE) is 917 people, while the Expected Annual Population Displaced (EAPD) due to depths >1m is 484 people.

Limitations This first-phase assessment applied standardized, which provide a useful baseline but also introduce constraints that limit local applicability:

- Averaging across global climate models smooths extremes, underestimating drought severity and frequency.
- Socio-economic indicators (e.g. GDP per capita) show implausible projections under some SSPs, affecting risk mapping validity.
- The JRC river flood maps exclude small basins (<150 km²), overlooking flash floods, Crete's dominant flood hazard.
- Flood risk analysis is limited to historical return periods, with no projections under climate change scenarios.
- Incomplete OpenStreetMap coverage and resolution issues in population datasets led to misplaced infrastructure and population estimates.

Recommendations The next phase will focus on enhancing the assessment methodologies by incorporating local datasets, refining drought and flood risk models, and addressing identified data gaps. Additionally, stakeholder engagement will be expanded to ensure that risk assessment results align with regional adaptation planning and policy development. These improvements will be critical for the upcoming revision of the Regional Climate Change Adaptation Plan (2026+) and for developing more targeted climate resilience strategies for Crete.

Τοποθεσία: Αίθουσα Συνεδριάσεων Περιφέρειας Κρήτης Ηρακλείου

Ημερομηνία: Τετάρτη 22 Οκτωβρίου 2025

Ώρα: 08.30

ΗΜΕΡΙΔΑ

«Κοινή Συνάντηση Εργασίας
Περιφέρειας Δυτικής Ελλάδας & Περιφέρειας Κρήτης
σε θέματα δράσεων Κλιματικής Ανθεκτικότητας»

στο πλαίσιο υλοποίησης των Ευρωπαϊκών Έργων

"Climate Resilient crETE" – «Κλιματικά Ανθεκτική Κρήτη»
του προγράμματος «CLIMAAX Horizon Europe»
&
"Region of Western Greece moving towards climate resilience - Path4PDE
"Η Περιφέρεια Δυτικής Ελλάδας στον δρόμο προς την κλιματική ανθεκτικότητα",
Horizon 2020 - Pathways2Resilience

Τοποθεσία: Αίθουσα Συνεδριάσεων Περιφέρειας Κρήτης Ηρακλείου

Ημερομηνία: Τετάρτη 22 Οκτωβρίου 2025

Ώρα: 08.30

ΠΡΟΓΡΑΜΜΑ 22/10/2025

Ώρα	Τίτλος	Ομιλητές
8.30-9.00	**Προσέλευση**	
9.00-9.30	**Καλωσόρισμα - Γνωριμία Συμμετεχόντων**	
9.30-10.00	**Χαιρετισμοί**	**Στυλιανός Μπλέτσας,** Αντιπεριφερειάρχης Βιώσιμης Ανάπτυξης, Ενέργειας, Χωροταξίας και Περιβάλλοντος Π.Δ.Ε. **Ιωάννης Αναστασάκης,** Αντιπεριφερειάρχης Κλιματικής Αλλαγής&Βιώσιμης ΚινητικότηταςΠ.Κ. **Νικόλαος Ξυλούρης,** Αντιπεριφερειάρχης Περιβάλλοντος Π.Κ.
10.00-11.00	**Παρουσίαση έργου Climate Resilient crETE (ΠΚ)**	Δρ. **Μαρίνος Κριτσωτάκης** Καθ. **Αριστείδης Κουτρούλης** Δρ. **Μαρία Στρατηγάκη** **Μικαέλα Παπά**
11.00-12.00	**Παρουσίαση έργου Path4PDE (ΠΔΕ), Περιγραφή σημαντικών τομέων τρωτότητας και χρηματοδοτικών εργαλείων δράσεων ΠΔΕ**	Δρ. **Στέφανος Παπαζησίμου,** Πρ. Τμ. Κλιματικής Ανθεκτικότητας, Διεύθυνση Περιβάλλοντος, Κλιματικής Ανθεκτικότητας και Χωρικού Σχεδιασμού, Π.Δ.Ε.
12.00-12.30	**Διάλειμμα**	
12.30-13.00	**Η Συμβολή της Αρχικής Αξιολόγησης και των Ενδιαφερόμενων Μερών στη Διαμόρφωση Κοινού Οράματος στην ΠΔΕ**	Δρ**. Βαρβάρα Συγγούνη,** Διεύθυνση Περιβάλλοντος, Κλιματικής Ανθεκτικότητας και Χωρικού Σχεδιασμού, Π.Δ.Ε. Δρ**. Μαρίνα Κούτα,** Τμ. Πολιτικών Μηχανικών Π.Π.
13.00-13.30	**Δομή σχεδίου ανθεκτικότητας ΠΔΕ (προτάσεις, απόψεις, ανταλλαγή ιδεών)**	**(Συντονιστής:** Δρ**. Στέφανος Παπαζησίμου)** **Όλοι οι συμμετέχοντες**
13.30-14.00	**Παρατηρητήριο Κλιματικής Αλλαγής ΠΚ**	**Ευγενία Στυλιανού** **Ελένη Καργάκη**
14.00-14.30	**Διερεύνηση συνέργειας με οργανικές μονάδες ΠΚ - ΠΔΕ**	**(Συντονιστής:** Δρ. **Μαρίνος Κριτσωτάκης)** **Όλοι οι συμμετέχοντες**
14.30-15.00	**Κλείσιμο Συνάντησης-Συζήτηση**	**Όλοι οι συμμετέχοντες**

ΠΡΟΣΚΛΗΣΗ

Σας προσκαλούμε σε Ημερίδα που συνδιοργανώνει η Περιφέρεια Κρήτης και η Περιφέρεια Δυτικής Ελλάδας με θέμα:

«Κοινή Συνάντηση Εργασίας Περιφέρειας Δυτικής Ελλάδας & Περιφέρειας Κρήτης σε θέματα δράσεων Κλιματικής Ανθεκτικότητας»

που θα πραγματοποιηθεί την Τετάρτη 22 Οκτωβρίου 2025, και ώρα 10:00
στην Αίθουσα Συνεδριάσεων της Περιφέρειας Κρήτης Ηρακλείου

στο πλαίσιο υλοποίησης των Ευρωπαϊκών Έργων

"Climate Resilient crETE" – «Κλιματικά Ανθεκτική Κρήτη»
του προγράμματος «CLIMAAX Horizon Europe»
&
"Region of Western Greece moving towards climate resilience - Path4PDE
"Η Περιφέρεια Δυτικής Ελλάδας στον δρόμο προς την κλιματική ανθεκτικότητα",
Horizon 2020 - Pathways2Resilience

ΗΜΕΡΙΔΑ

Κοινή Συνάντηση Εργασίας Περιφέρειας Δυτικής Ελλάδας & Περιφέρειας Κρήτης
σε θέματα δράσεων Κλιματικής Ανθεκτικότητας
Τετάρτη 22/10/2025

ΠΕΡΙΦΕΡΕΙΑ ΚΡΗΤΗΣ
REGION OF CRETE

Ονοματεπώνυμο	Φορέας	Ιδιότητα	E-mail	Υπογραφή
Βρύνια Αγγελική	Περιφέρεια Δυτικής Ελλάδος	Επιστημονική Συνεργάτης Path4PDE	ac.vrinia@pde.gov.gr	
Νακρή Μαρία	Περιφέρεια Δυτ. Ελλάδας	Προϊσταμένη τμήματος Ενεργ. Σχεδ. ΠΔΕ	m.makri@pde.gov.gr	
Παπαοίκη Γεωργία	Περιφέρεια Δυτικής Ελλάδος	Προϊσταμένη Τμήματος Επαγγέλματος	g.papoutsi@pde.gov.gr	
Συγγούνη Βαρβάρα	Επ. Συνεργ. Περιφέρεια Δυτικής Ελλάδας	Επιστημονική Συνεργάτης	v.siggouri@pde.gov.gr	
Πλέγα Χρυσίνα	Περιφέρεια Δυτ. Ελλάδος	Χαράλαμπος Τμ. Κλιματικής Ανθεκτικότητας P.M. Path4PDE	ch.plega@pde.gov.gr	
Αδαμοπούλου Μαρία	Περιφέρεια Δυτικής Ελλάδας	Υπάλληλος Δ/νσης Περιβάλλοντος - F.M. Path4PDE	m.adamopoulou@pde.gov.gr	
ΣΤΡΑΤΗΓΑΚΗ ΜΑΡΙΑ	ΠΕΡΙΦΕΡΕΙΑ ΚΡΗΤΗΣ	ΣΥΝΕΡΓΑΤΗΣ ΕΥΡΩΠ. ΕΡΓΟΥ CLIMPACT	stratigaki@crete region.gr	
ΜΑΡΙΝΟΣ ΕΡΙΤΣΟΤΑΚΗΣ	Π. Κ.	ΓΕΝ. Δ/ΝΤΗΣ	kritsotakis@crete.gov.gr	
ΓΙΑΝΝΗΣ ΑΝΑΣΤΑΣΑΚΗΣ	Π Κ	Διπεριφερειάρχης	anastasakis@crete.gov.gr	
Ευφροσύνη Σπυλιανού	Π.Κ	Υπηρεσιακή Περιοδεύουσα Επιθ. Περιφ. Μηχ.	spyliano@crete.gov.gr	
Ελένη Καρδάκη	Π. Κ.	Τμ. Διαχειριστικής Αλλαγής	karg@crete.gov.gr	
Μαρία Αποστολάκη	Περ. Κρήτης	Τμ Κλιματικής Αλλαγής & Ενεργ. Σχεδιασμού	mapostolaki@crete.gov.gr	
Αριστείδης Κουτρούλης	Πολυτεχνείο Κρήτης	Αν. Καθηγητής	akoutroulis@tuc.gr	
Παύλος Μιχαηλάκης	Πολυτεχνείο Κρήτης	Μηχ. Περιβάλλοντος	kpapa@tuc.gr	
Μαρία Αικατερίνη	Περιφέρεια Κρήτης	Ειδική Συνεργάτης Αντιπερ. Περ/ρειας	s.perivaloutos@creteregion.gr	

ΗΜΕΡΙΔΑ

Κοινή Συνάντηση Εργασίας Περιφέρειας Δυτικής Ελλάδας & Περιφέρειας Κρήτης
σε θέματα δράσεων Κλιματικής Ανθεκτικότητας
Τετάρτη 22/10/2025

ΠΕΡΙΦΕΡΕΙΑ ΚΡΗΤΗΣ
REGION OF CRETE

Ονοματεπώνυμο	Φορέας	Ιδιότητα	E-mail	Υπογραφή
Μαυράκη Στέλλα	Περιφέρεια Κρήτης	Γεωλόγος // Συνεργάτης Transcend	stmauraki@crete region.gr	
Δαφνομήλη Δήμητρα	>>	Δημ. Υπ. / Δ/νση ΠΕΧΩΣ	dafnomili@crete.gov.gr	
Πανταζόγλου Φώτης	-11-	Γεωλόγος / Δ/νση ΠΕΧΩΣ	fpantazoglou@crete.gov.gr	
Παπαδημητρίου Στεφ	Περιφ. Δυτ. Ελλάδας	Πρ. Τμ. Κοιν. Ανάπτ. Γεωλόγος.	s.papadimitriou@pde.gov.gr	
Ξυλούρης Νικόλαος	ΠΕΡ. ΚΡΗΤΗΣ	ΑΝΤΙΠΕΡΙΦ. ΠΕΡΙΒΑΛΛΟΝΤΟΣ	nξylou@crete.gov.gr	
Καλλιγερινάκη Μαρία	Περ. Κρήτης	Βοηθ. Δ/ντρια Ανάπτυξης Ενέργειας & Φυσικών Πόρων	mkaliger@crete.gov.gr	
Στεφανάκη Μαρία	ΠΕΡ. ΚΡΗΤΗΣ	Πολιτικός Μηχαν. ΤΕ / Δ/ΝΣΗ ΠΕΧΩΣ	mstefanaki@crete.gov.gr	
Καθωταάκη Μαρία	Περ. Κρήτης	ΠΕ Περιβάλλοντος Δασολόγος	mkasotaki@crete.gov.gr	
Κατσαβέλη Αικ.	Περ. Κρήτης	ΠΕ Περιβ./ντος	KKatsaveli@crete.gov.gr	
Αγαπάκης Εμμ.	Περ. Κρήτης	Γεν. Δ/ντής Υγιεινής	agapakis@crete.gov.gr	
ΑΝΝΑ ΚΑΓΙΑΜΠΑΚΗ	ΠΕΡ. ΚΡΗΤΗΣ	ΠΕΡΙΒΑΛΛΟΝΤΟΣ ΧΩΡ. ΣΧΕΔΙΑΣΜΟΥ.	kagiampaki@crete.gov.gr	ΣΡΑΧ.
ΣΤΕΦΑΝΙΔΗΣ Γ.	ΠΑΝ. ΜΗΧ. Π.Π.	ΟΜ. ΚΑΘΗΓΗΤΗΣ	ΥΓΙΣΤΕ@upatras.gr	ΓΣ.

ΠΕΡΙΦΕΡΕΙΑ ΚΡΗΤΗΣ
REGION OF CRETE

INVITATION TO STAKEHOLDERS WORKSHOP MEETING

THURSDAY 18/12/2025

Teams TELECONFERENCE

Climate Resilient crETE (CRETE) / CLIMAAX Horizon Europe

AGENDA

09:00 – 09:15	**WELCOME & GREETINGS** **Nikolaos Xylouris** Deputy Regional Governor for Environment | RoC **Ioannis Anastasakis** Deputy Regional Governor for Climate Change & Sustainable Urban Mobility | RoC
	Coordinator Dr. Marinos Kritsotakis Director General for Sustainable Development | RoC
09:15 – 09:45	**FLOOD RISK ASSESSMENT IN CRETE / Refined Workflow - Local Data**
09:45 – 10:15	**DROUGHT RISK ASSESSMENT IN CRETE / Refined Workflow - Local Data** **Prof. Aristeidis Koutroulis & Mikaela Papa** Technical University of Crete | School of Chemical and Environmental Engineering
10:15 – 11:45	**DISCUSSION | SUGGESTIONS & PROPOSALS FROM STAKEHOLDERS**
11:45 – 12:00	**KEY POINTS, NEXT STEPS & WRAP UP** **Dr. Maria Stratigaki** Project Manager CLIMAAX Horizon Europe | RoC

Funded by the European Union

This project has received funding from the European Union's Horizon Europe research and innovation programme under grant agreement No 101093864. Views and opinions expressed are however those of the author(s) only and do not necessarily reflect those of the European Union or the European Climate, Infrastructure and Environment Executive Agency (CINEA). Neither the European Union nor the granting authority can be held responsible for them.

STAKEHOLDERS LIST

AGAPAKIS GEORGIOS DASKALAKI CHRYSOULA FOTAKIS KONSTANTINOS	DIRECTOR GENERAL
AVRAMAKI CHRYSOULA APOSTOLAKI MARIA VAVADAKI AIKATERINI VEGLIRIS EMMANOUIL DAFNOMILI DIMITRA KAGIAMPAKI ANNA KASOTAKI MARIA KATSAVELI AIKATERINI KALOGIANNAKIS NIKOLAOS KOUTANTOU MARIA NIKOLOUDAKIS EMMANOUIL PANTAZOGLOU FOTIOS ROUKOUNAKIS EMMANOUIL STEFANAKI MARIA STYLIANOU EVGENIA	DIRECTORATE OF ENVIRONMENT AND SPATIAL PLANNING
PLOUMIDI ELENI SFAKIANAKI GEORGIA	INDEPENDENT CIVIL PROTECTION DIRECTORATE
VYTINIOTOU EIRINI ZIDIANAKIS IOANNIS MYLONAKI MARIA FOUNTI MARIA	RURAL DEVELOPMENT DIRECTORATE
TZAGKARAKI ELENI TRIAMATAKI HARA MALANDRAKIS CHRISTOPHOROS RANOUTSAKI ELENI GERONTI MARIA CHRISTINAKI CHRYSOULA	TECHNICAL PROJECTS
BARTOLOZZI JIULIA SGOURO MARGETA PSAROUDAKIS MICHAIL	TECHNICAL PROJECTS CRETE

Funded by the European Union

This project has received funding from the European Union's Horizon Europe research and innovation programme under grant agreement No 101093864. Views and opinions expressed are however those of the author(s) only and do not necessarily reflect those of the European Union or the European Climate, Infrastructure and Environment Executive Agency (CINEA). Neither the European Union nor the granting authority can be held responsible for them.